GEOCHEMISTRY AND PETROGRAPHY OF A LOWER CARBONIFEROUS, LACUSTRINE, HOT SPRING DEPOSIT: EAST KIRKTON, BATHGATE, SCOTLAND.

A thesis submitted for the degree of
Doctor of Philosophy.

by Rona Ann Richardson McGill.
BSc. Edinburgh University.

Department of Geology and Applied Geology.
University of Glasgow.

January 1994.

ACKNOWLEDGEMENTS

This research project was funded by NERC, and was a CASE studentship with the National Museums of Scotland; jointly supervised by Dr W.D.I Rolfe (of the NMS) and Dr A.J. Hall of the Department of Geology and Applied Geology, at the University of Glasgow.

It is unlikely that this thesis would ever have been completed without the help of Dr Allan Hall and Dr Tony Fallick, from SURRC, for pointing me in the right directions and plenty of good advice. I am also grateful to Dr Iain Rolfe for his guidance, and for contacts through the East Kirkton Project; it was helpful to be part of a large scale, multidisciplinary project. Other academic staff, from Glasgow Geology department, that have been actively involved in this project include Dr B. Bell, Dr C. J. Braithwaite, Dr G. Bowes, Dr J.J. Doody, Dr J. Harris, Prof. M. J. Russell, and Prof. D. K. Smythe; Dr A. Boyce and Dr G. Jenkin, from SURRC; I would like to thank them for all their help, and Gordon Walkden for making my work more controversial.

The technical assistance that I have received whilst pursuing this project, has been exceptional. Staff at the Chambers Street Museum, Edinburgh prepared thin sections and were very helpful and co-operative with information about the quarry, and access to museum samples; particularly Colin Chaplin, Bob Reekie, Bill Baird and Bobbie Paton. Technicians at the University of Glasgow were also brilliant: Dugald and Murdoch, with XRD analyses (and general moral advice); Dougie for the time he put into the photographs for the thesis and numerous presentations; Roddy and Eddie, lots of help; Jim Gallagher for the geochemistry techniques; Peter Ainsworth with SEM analyses; Alan and Erchie for thin sections, and cut rocks; John, Jimmy and Alec the jannies, for being cheerful and helpful; Jeanette, Mary and Irene in the office. Thanks, also to all the SURRC staff, in Block C: Terry, Alison, wee Julie, Elspeth, Gary and Chris; and to Fred, the glass blower, and Julian Jocelyn for references and his interest in the project.

For my friends in the Geology Department; especially Gaz and John for sharing a flat with me for the last year; Carolyn, Mark, Joe, Allison, Susan, Mehmet, Huseyin, Veysel, Helen, Dave D, Campbell, Chris, Richard, Tim, Lynda, John, Simon, Orla, Fish, Morgan, Clark, Peter, Maggie, Janey and her Feldspars. Friends outside of geology; Davy, Jane, Anne, Kirst and Stef, Jean Bell, Marnie, Sandra, Jennifer, Ann and Gordon. Family: especially Mum, Dad, Aunt Ann, Uncle Bill and Dusty. Also to all the people who helped me in the month I spent in New Zealand, especially at the DSIR in Taupo, and Rotorua; Moira Johnstone, Norma & Geoff, and Mr & Mrs Thane, for digs.

Lower Carboniferous palaeolatitude being close to the equator.

$\delta^{34}S$ analyses were made for pyrite samples, collected from a wide variety of lithological associations at East Kirkton. A large range of results was obtained, +8 to -34‰ with no strong mode, which is consistent with the potential variety of sulphur sources available within a lacustrine environment. The lowest values were obtained for pyrite associated with fossil wood, and for these samples bacterial involvement in sulphate reduction is inferred. Values of +6 to -2‰ are observed for pyrite extracted from chert samples, and this may possibly reflect a direct magmatic/hydrothermal source for the sulphur. It is thought that the East Kirkton $\delta^{34}S$ results are not consistent with sulphur originating from closed-system marine sulphate reduction

Whole rock analyses, by XRD and XRF, were obtained for thirty-one samples, collected from the five main lithological groups of the East Kirkton succession: Group I are stromatiform carbonate samples; Group II are shales and tuffs; Group III are carbonate-rich tuff samples; Group IV are shaley laminites; and Group V are carbonate-rich laminites. The results of these analyses show that the majority of elements which are found in East Kirkton samples (major and trace elements), are derived from the contemporary volcanic activity in the Bathgate Hills.

SiO_2 and CaO are anomalously enriched in the East Kirkton lithologies, relative to the Bathgate basalts (Smedley, 1986, for basalt analyses). It is thought that a second source from which both elements could be derived, are the Tyninghame or Gullane Formations, carbonate-rich sediments which occur at depth, beneath the East Kirkton Limestone. It is proposed that the elements were remobilised from these sediments via hydrothermal fluids, associated with the volcanic activity. Silica could be precipitated by the mixing of cooler lake waters with these fluids, but the CaO, forming calcite, could have been precipitated via biogenic mediation.

Group II samples have the highest concentrations of trace elements. These shales contain clay minerals, on which trace elements may be adsorbed; or trace elements may become concentrated in slowly deposited sediment. Sr values are high in all East Kirkton samples, and it is thought that the Sr-enriched basalts are a likely source. The highest values were obtained for samples containing biogenic carbonate features, like spherules. It would appear that biogenic precipitation mechanisms may also increase concentrations of Sr.

CONTENTS

Page

CHAPTER 3 - THE EAST KIRKTON PALAEOENVIRONMENT: STABLE ISOTOPE EVIDENCE FROM SILICATES AND SULPHIDES.

CHAPTER 4 - THE INFLUENCE OF VOLCANIC MATERIAL ON THE EAST KIRKTON GEOCHEMICAL SIGNATURE.

1. INTRODUCTION.

1.1 Background.

In 1984 Mr. Stan Wood, a commercial fossil-collector, discovered the fossilised remains of a tetrapod amphibian in one of the walls of Limefield Farm, a farm close to the town of Bathgate, in West Lothian. The source of this fossil was found to be a disused limestone quarry; the lithology was called the East Kirkton Limestone (Figure 1a and 1b). Vigorous excavation of this site, and study of the farm walls, revealed many other unique fossils (Wood *et al*, 1985), "including the earliest known complete amphibian ancestors of frogs and salamanders, and of reptiles" (Rolfe *et al*, 1990).

The fossil biota appeared to be a mixture of aquatic and terrestrial lifeforms. Some of the amphibians were fully land-going (Figure 2) and many of the other fossils preserved here, were indicative of preservation of a rare, early, terrestrial biota (e.g. the harvestman "spider", millipedes, scorpions and tree-fern-type plants). It was felt that this site could yield the earliest known fossil reptiles. One particular specimen (Figure 3), discovered by Stan Wood, seemed to fit many of the criteria which would distinguish amniotes (reptiles, birds and mammals) from non-amniote tetrapods (amphibians) (Smithson, 1989). *Westlothiana* , as it was named, ultimately fetched a price of £180,000, and resides in the collection of the National Museums of Scotland, bought from the proceeds of a high-profile, fund raising campaign, that prevented it from being sold outside the country.

These discoveries prompted the formation of the East Kirkton Research Group (in 1987); co-ordinated by Dr W. D. I. Rolfe of the National Museums of Scotland, and mainly comprised of palaeontologists studying the fauna and flora of the East Kirkton Limestone. The site has also been designated a Site of Special Scientific Interest (SSSI) due to the importance of these discoveries.

This Ph.D. thesis forms a significant part of the geochemical investigation of the lithology, focussing on silica phases. Work has been done on the carbonate phases by Dr. G. Walkden and Mr. R. Irwin, at Aberdeen University (Walkden *et al*, 1993), and the volcanic material has been studied by Dr. G. Durant of the Hunterian Museum, University of Glasgow (Durant, 1993).

1.2 Aims.

This thesis contains the results of a geochemical study of the East Kirkton Limestone (EKL). It began in October 1989, with the objectives of characterising the chemistry of this palaeontologically important lithology and to determine the extent to which the formation of the lacustrine limestone, and its chemistry, had been influenced by local hot-spring activity. Other directions which this project has taken include: producing a model of the palaeoenvironment to be updated as new data was obtained; assessing the lithology's potential for precious metal mineralisation; and to identify any lithologies that were possible lateral equivalents (contemporary and of similar origin) of East Kirkton, in the Lower Carboniferous of Scotland (Appendix B).

1.3 Background Geology

The East Kirkton Limestone (EKL) is of Visean age (Figure 1a), and is situated in the south of the Bathgate Hills, occurring only at the one locality, next to Limefield Farm (Figure 1b). The Bathgate Hills are high topographically and stratigraphically, in relation to the surrounding areas. They are one of many focuses for Carboniferous volcanic activity, and are at the margin of a major oil shale basin, stretching to the east, in the Midland Valley of Scotland.

To the east, pre-dating the EKL, are oil-shale deposits from a large fresh water lake, Lake Cadell (Figure 4). The maximum extent of this lake, an estimated 70km, is defined by outcrops of the Burdiehouse Limestone (Loftus and Greensmith, 1988). The EKL is possibly an isolated remnant of this larger lake, remaining after the main body of water had receded. On the western side of the Bathgate Hills, the sequences which pre-date the EKL are generally thick piles of lava; covered by the sediments of the Coal Measures, the Westphalian succession.

The dominant lithologies of the Bathgate Hills are of volcanic origin, alkaline basic lavas and ashes (Macdonald *et al*, 1977; Smedley, 1986). The focus of volcanic activity in this area is a crater located a few kilometers to the north of East Kirkton (near Linlithgow, Figure 5). The lava flows are thickest here; they taper to the south at East Kirkton, and are

commonly interspersed with tuffaceous material.

Locally, to the east of the EKL, separated by a sequence of ashes and basalts, are outcrops of the Strathclyde Group, while to the west, and overlying the EKL, are fully marine limestones, the West Kirkton Limestone and the Petershill Limestone. The EKL has no apparent features suggesting marine deposition; it has proximal terrestrial input (fauna and flora) and its fine scale laminations indicate a calm lacustrine environment. It is thought to be a fresh water limestone from the top of the West Lothian Oil-Shale Formation (Visean series, lower Brigantian stage, figure 1), pre-dating the marine incursion of the Lower Limestone Group. The base of the Lower Limestone Group in the Midland Valley of Scotland is generally defined by the Hurlet Limestone, the first of the marine sequence. The local equivalent of the Hurlet Limestone in the Bathgate Hills is the West Kirkton Limestone (Geological Survey of Great Britain, 1949).

The EKL was quarried (until early 1830's), and this excavation is the only exposure of this lithology (see also Appendix B). The area is mostly farmland, and rock outcrops are seldom exposed. The full extent of the EKL is not known, but attempts have been made to determine this through geophysical means (see appended paper Doody *et al*, 1993).

1.4 Description of the East Kirkton Limestone.

The East Kirkton Limestone is a very impure limestone. The sequence is comprised of (i) mixed shales and tuffs; (ii) thick tuffaceous horizons, which are often cemented by carbonate; (iii) laminites which can be shaley, carbonate-rich or cherty; (iv) lenses of massive limestone, often with stromatiform textures, and with voids filled by silica phases, calcite and occasionally bitumen.

The massive limestone lenses are possibly subaqueous, biogenic carbonate mounds focussed around hydrothermal seeps or small vents, as evidenced by the pervasive, multi-phase veining and vug fillings. The cherty laminae may represent primary silica deposits, sourced from hydrothermal fluids (Chapters 2 and 3). Full detailed descriptions of lithologies are given in Appendix C, and in Rolfe *et al* (1993).

1.5 Rationale of the project.

Dr A. J. Hall, supervisor of this project, sensed the potential for research into the geochemistry of the lithology. It has a valid contribution to make to the characterisation of the East Kirkton Limestone and it has provided evidence about the palaeoenvironment, in particular to the on-going debate concerning the presence or absence of hot-springs. In close proximity to the Hilderstone Silver Mine (Stephenson, 1983) and at a time when interest in the EKL, palaeontologically, coincided with renewed interest in gold exploration, which was focussing on fossil hot-springs, the EKL was considered to be a potential target for mineralisation. It was thought that the EKL might be similar to the Lower Devonian, Rhynie Chert (Aberdeenshire), where enrichments of gold and other heavy metals were discovered (Rice and Trewin, 1988).

Preliminary analyses were carried out as part of an Undergraduate, 4th year Applied Geology project, at Strathclyde University, by David Large (BSc thesis 1989, Strathclyde). The results of this isotope analyses and petrographic study were included in an early paper, summarising the work completed at this point by various members of the East Kirkton Project (W.D.I. Rolfe *et al*, 1990). This was not the first published work on East Kirkton; it had been observed in geological papers as early as the 1820's - 30's (Fleming, 1825; Hibbert, 1836), already the subject of hot-springs was mentioned in association with this lithology. These earlier interpretations and papers are discussed at the start of Chapter 3, and in Rolfe *et al*, 1993.

1.6 On the origin and sources of silica in lacustrine deposits.

The occurrence of silica in laminae, as at East Kirkton, can be due to several agencies: (i) biogenic silica from sponge spicules, radiolarian tests or diatoms, often diagenetically remobilised resulting in nodular chert formation; (ii) silica from hot-spring fluids, precipitated due to fluids cooling or a change in pH, sourced by country rocks, volcanogenic material or siliceous sediments; (iii) chert laminae with sodium silicate precursor e.g. magadiite, in an evaporitic type of environment, with hot-spring fluids and volcanogenic material as silica sources; and (iv) as a later replacive feature, due to veining, alteration, replacement or diagenesis.

The discussion below compares features of cherts with magadiite precursors and chertified lithologies where silica is derived from a

biogenic source or from volcanogenic material. It is intended to show why the hot-spring source of silica is favoured for the East Kirkton laminae, and that other models have been considered, but do not appear to be closely analogous to the East Kirkton chert laminae.

Discussion of textures that occur at East Kirkton, and how they have been interpreted are to be found in Chapters 2 and 3. These chapters also contain the evidence by which the chert laminae are considered to primary, and not replacive.

1.6.1 Magadiite precursor to chert.

Magadiite ($NaSi_7O_{13}(OH)_3 \cdot 3H_2O$) precursors to chert can produce irregular nodules or widespread thin chert laminae (Hay, 1968; Eugster, 1969; Sheppard and Gude, 1986). The change from the sodium silicate precursor to chert is thought to occur in early diagenesis and may produce syn-sedimentary deformation, as the magadiite has a putty-like consistency (Eugster, 1969). Often the chert laminae and nodules have a white coating - quartzose porcellanite (O'Neil and Hay, 1973) - which has often a reticulate surface pattern, and in which can be found preserved moulds of evaporite crystals, e.g. trona. The surface reticulation is due to the volume reduction which occurs on removal of Na^+ and water from the magadiite as it changes to chert.

"The occurrence of Magadi-type chert in sedimentary rock is indicative of an alkaline, lacustrine depositional environment..." and it is "useful as a prospecting tool for locating evaporites, zeolites and fluorite in continental sedimentary deposits", Sheppard and Gude (1986). These cherts have high $\delta^{18}O$ contents, as they precipitate from brines "a solution undergoing evaporation, as in the formation of a brine, will in general increase in ^{18}O content, with an increase in salinity" ... "Chert from high-salinity deposits of Lake Magadi have $\delta^{18}O$ 38.9 - 44.1‰ (average 42.1‰). Chert from moderate-salinity deposits have $\delta^{18}O$ values of 34.7 - 40.9‰ (average 38.0‰). Cherts of low-salinity deposits range from 32.1 to 34.6‰ (average 33.6‰)." The white rinds were lightest, isotopically, 31-32‰ and were considered to have grown after meteoric water was added, O'Neil and Hay (1973).

Mineral assemblages commonly associated with this type of silica occurrence include trona $Na_3H(CO_3)_2 \cdot 2H_2O$, gaylussite $Na_2Ca(CO_3)_2 \cdot 2H_2O$ or pirssonite $Na_2Ca(CO_3)_2 \cdot 5H_2O$, indicative of sodium carbonate brines, and siliceous zeolites clinoptilolite $(Na,K)_6[Al_6Si_{30}O_{72}] \cdot 24H_2O$, and less

commonly erionite $NaK_2MgCa_{1.5}[Al_8Si_{28}O_{72}]\cdot 28H_2O$. "Where direct evidence of sodium-carbonate brine is lacking, authigenic zeolites and K-feldspar provide an indirect line of evidence that the beds were deposited in saline, alkaline lake water." from Hay (1968). It has also been observed, Folk and Pittman (1971), that fibrous chalcedony associated with evaporitic environments has a tendency to be length-slow, this is relatively uncommon in any other environment, and occurs when the fluid precipitating the silica is in contact with brines or sulphate-rich fluids.

East Kirkton cherts have a $\delta^{18}O$ and δD isotopic signature consistent with formation from meteoric waters of a moderate temperature, 60°C ($\delta^{18}O$ = 21-27‰, see Chapters 2 and 3), which appears to discount formation of the cherts from brine solutions. There are isolated occurrences of pseudomorphs after gypsum noted from East Kirkton (Parnell, 1988), but it is possible that the gypsum formed biogenically (Thompson and Ferris, 1990) rather than by evaporation, and this evidence alone does not confirm this as a sabkha or playa environment. It is also noted that the fluids involved in the precipitation of the Magadi-type chert do not form mineral assemblages that include gypsum. Vug infilling chalcedony in the East Kirkton "mound" is observed to be length fast.

The white rinds in some East Kirkton laminae are not considered to be analogous to the "quartzose porcellanite" of the Magadi-type cherts, because the East Kirkton samples lack the surface reticulation features and evaporite moulds, that characterise magadiite cherts. Shales and laminites of the East Kirkton succession do not generally show any features associated with desiccation, i.e. mud cracks, which would be expected if periodic drying out of the lake had occurred. Cracks, filled by calcite veins, in the chert laminae (Chapter 2) do not have the distribution or morphology expected of desiccation cracks.

It is uncertain what the white rinds in the East Kirkton samples represent. They appear only to occur in the upper part of the sequence (above Unit 53/54) and are often associated with shale and carbonate, rather that chert. XRD analyses of samples with these coatings gave no indication of an unusual mineral assemblage i.e. XRD results were quartz, calcite and clays. The thin rind was very difficult to separate from the lithologies it coated and no pure samples were extracted for analyses.

Some of the vug infillings for mound samples also consisted of porous, white silica (EK 2.69 vug, results in Chapter 3, Table 1), and $\delta^{18}O$ values were inconsistent from one analyses to the next (it was repeated three times), although the sample had undergone standard processing to

ensure homogenisation. This was the only sample which behaved in this manner and the variation has been interpreted as a feature of oxygen exchange with later fluids, which have affected this porous sample after lithification. It is, therefore, suggested that porosity and oxygen exchange might be factors which also affect the "quartzose porcellanite" of the Magadi-type cherts resulting in the lighter isotopic results (O'Neil and Hay, 1973), with the $\delta^{18}O$ re-equilibrating with later, possibly meteoric fluids.

1.6.2 Chertification associated with biogenic and volcanogenic silica.

Chert as a replacement generally occurs in nodules and is considered to be a diagenetic feature. The main sources considered for the silica which forms these chert nodules are (i) a volcanogenic silica source (Cummings *et al* , 1989), or (ii) sponge spicules and/or radiolarian tests (Meyers, 1977; Maliva and Siever, 1989).

In basaltic volcanic material interstitial glass can release silica when converted to smectite (Cummings *et al*, 1989). At East Kirkton smectite is present in tuff samples, but as a mixed layer illite-smectite phase. Other minerals that are associated with the conversion of volcanic glass to smectite are celadonite, opal-CT and clinoptilolite, and these are not present at East Kirkton. In Cummings *et al* (1989), it is also stated that the conversion from the metastable assemblage (smectite, celadonite, opal-CT and clinoptilolite) to quartz, requires elevated temperatures (probably in excess of 150°C), or hydrothermal conditions with water as a solvent. There is no evidence that such temperatures were reached in the East Kirkton environment, or that the secondary, metastable mineral assemblage had occurred. If the chert was derived *in situ* , from alteration of volcanic material, then it would contain more impurities than are actually observed.

In the Kenyan-rift setting volcanic material is also considered as one of the sources of silica (Hay, 1968; Renaut and Owen, 1988). The associated volcanics are trachytic tuffs in Hay (1968), and they contain siliceous zeolites; clinoptilolite and erionite (or phillipsite in chert-free sequences). At Lake Bogoria (Renaut and Owen, 1988) the volcanics are phonolitic trachytes, and analcime is associated with removal of silica from clasts of this material. At East Kirkton local volcanics could have provided hydrothermal silica, produced by similar processes of alteration of volcanic material (Hall, 1989). The assemblages of secondary minerals, produced by

this alteration, are not found within the East Kirkton tuffs. It is also thought that $\delta^{18}O$ values associated with silica from the volcanic source might preserve a relict signature of volcanic $\delta^{18}O$, this is not observed for East Kirkton samples.

Chert which has formed from the skeletons of organisms will generally have remains of these skeletons preserved, or in associated lithologies which are not silica-rich, moulds of the silica skeletons will be observed where the silica has been removed to be reprecipitated in the chert-rich area (Renaut and Owen, 1988; Meyers, 1977; Maliva and Siever, 1989). A biogenic silica source is not considered very likely for East Kirkton as there are no moulds or calcitised grains resembling siliceous biogenic tests.

1.7 Format of the Thesis.

The main bulk of the research involved in this thesis is presented in three papers, Chapters 2 to 4, which comprise results from petrographic observation, stable isotope analyses ($\delta^{18}O$ and δD of silicates, and $\delta^{34}S$ of pyrite), XRD and XRF whole rock analyses. Chapter 5 is a summary of the conclusions drawn from these analyses, and a summary of the research project. Results of other work that was completed as part of this project, but which are (i) less relevant to the main aim of the research, i.e. geochemical characterisation of the East Kirkton Limestone, and (ii) not suitable for publication, are included in Appendices A - E.

Chapters 2 and 3 are concerned with the isotopic analyses and how evidence from these results relate to the observed petrographic textures. Chapter 2 was published after the first year of research in the proceedings of The 12th New Zealand Geothermal Workshop (1990), pp 203- 208. It provides an introduction to petrographic features of the East Kirkton lithologies; a discussion on evidence for the palaeoenvironment model that is proposed; and preliminary results from isotopic analyses with brief interpretation.

In Chapter 3, there is a further discussion of petrographic evidence, by which the silica phases are designated primary or secondary, and petrographic details of varieties of pyrite are described. The evidence provided by stable isotope analyses of silicates ($\delta^{18}O$ and δD) and pyrite ($\delta^{34}S$), for the East Kirkton palaeoenvironment, are presented as the bulk of the discussion of this paper. It has been published in the Transactions of

the Royal Society of Edinburgh: Earth Science, volume 84, a special East Kirkton publication with contributions from all the members of the East Kirkton Research Project.

There is still heated debate about the interpretation of silica phases (Walkden *et al*, 1993), but the interpretation of textural details and isotopic analyses presented in these chapters is considered to be the simplest explanation of the evidence that is presented.

Fluid temperatures obtained from $\delta^{18}O$ of carbonates (Walkden *et al*, 1993) indicate temperatures lower than those obtained from $\delta^{18}O$ of the silica. What is represented by the temperature obtained from $\delta^{18}O$ of the silica, is discussed in Chapter 3, but it should also be noted that two different values for $\delta^{18}O$ of Lower Carboniferous waters were used to calculate the quoted temperatures. That which is used in Chapter 3 ($\delta^{18}O$ water = -4‰, which gives silica temperatures of 40-60°C) was estimated from the East Kirkton data and if it is used to calculate temperatures for the fluids which deposited the carbonate, it gives higher values than those presented in Walkden *et al* (1993) (quoted temperature of 20°C, becomes 30-50°C). Carbonate phases would be precipitated biogenically from cool lake waters, while periodic influxes of warmer siliceous fluid would result in silica precipitation, on mixing of the two fluids. This need not cause a significant rise in the overall lake temperature.

Recent work on step heating of samples for $\delta^{18}O$ analyses, suggested that $\delta^{18}O$ results might be strongly influenced by oxygen in bound water within silica, as much as oxygen in Si-O bonds (Matheney and Knauth, 1993), but this was for samples where high water contents were observed and where water yield correlated with the $\delta^{18}O$ results (unlike East Kirkton samples, see Chapter 3).

Chapter 4 contains work that has not been published. It contains the results of the XRD and XRF bulk rock analyses. The results are related to specific rock types, and mineralogy (XRD) is compared with elemental analyses. The aim of the analyses in this chapter was to constrain which elements were sourced in the local volcanic material, and which required an additional hydrothermal source.

1.8 Bibliography.

Cummings, M. L., Trone, P. M. and Pollock, J. M. 1989. Geochemistry of colloidal silica precipitates in altered Grande Ronde Basalt,

northeastern Oregon, U. S. A. Chemical Geology, **75**, pp 61-79.

Doody, J. J., McGill, R. A. R., Darby, D. and Smythe, D. K. 1993. Geophysical surveys of the East Kirkton Limestone, Visean, West Lothian, Scotland. Trans. R. Soc. Edinburgh: Earth Science, **84**, pp 197-202.

Durant, G. P. 1993. Volcanogenic sediments of the East Kirkton Limestone (Visean) of West Lothian, Scotland. Trans. R. Soc. Edinburgh: Earth Science, **84**, pp 203-208.

Eugster, H. P. 1969. Inorganic bedded cherts from the Magadi area, Kenya. Contributions to Mineralogy and Petrology, **22**, pp 1-31.

Fleming, J. 1825. On the Neptunian formation of siliceous stalactites. Edinburgh J. of Science, **2**, pp 307-312.

Folk, R. L. and Pittman, J. S. 1971. Length slow chalcedony: a new testament for vanished evaporites. Journal of Sedimentary Petrology, **41**, p 1045.

Hall, A. J., Banks, D., Fallick, A. E. and Hamilton, P. J. 1989. An hydrothermal origin for copper-impregnated prehnite and analcime from Boylestone Quarry, Barrhead, Scotland. Journal of the Geological Society, London, 146, pp 701-713.

Hay, R. L. 1968. Chert and its sodium-silicate precursors in sodium-carbonate lakes of East Africa. Contributions to Mineralogy and Petrology, **17**, pp 255-274.

Hibbert, S. 1836. On the fresh-water limestone of Burdiehouse. Trans. R. Soc. Edinburgh: Earth Science, **13**, pp 169-282.

Geological Survey of Great Britain, NERC. 1949. *The Limestones of Scotland* . Aberdeen, Scotland: HMSO.

Large, D. J. 1989. The East Kirkton Limestone; a hot spring siliceous sinter [B.Sc. thesis]: Glasgow, University of Strathclyde, 22p.

Loftus, G. W. F. and Greensmith, J. T. 1988. The lacustrine Burdiehouse Limestone Formation - a key to the deposition of the Dinantian Oil Shales of Scotland. *In* Fleet, A. J., Kelts, K. and Talbot, M. R. (Eds.) *Lacustrine Petroleum Source Rocks* , pp 219-34. London: Geol. Soc Spec. Publ. **40**.

Macdonald, R., Thomas, J. E. and Rizzello, S. A. 1977. Variations in basalt chemistry with time in the Midland Valley province during the Carboniferous and Permian. Scottish J. of Geology, **13**, (I), pp 11-22.

Maliva, R. G. and Siever, R. 1989. Chertification histories of some Late Mesozoic and Middle Palaeozoic platform carbonates. Sedimentology, **36**, pp 907-926.

Matheney, R.K. and Knauth, L. P. 1993. New isotopic temperature

estimates for early silca diagenesis in bedded cherts. Geology, 21, pp 519-522.

Meyers, W. J. 1977. Chertification in the Mississippian Lake Valley Formation, Sacramento Mountains, New Mexico. Sedimentology, **24**, pp 75-105.

O'Neil, J. R. and Hay, R. L. 1973. ^{18}O and ^{16}O ratios in cherts associated with the saline lake deposits of East Africa. Earth and Planetary Science Letters, **19**, pp 257-266.

Parnell, J. 1988. Lacustrine petroleum source rocks in the Dinantian Oil Shale Group, Scotland: a review. *In* Fleet, A. J., Kelts, K. and Talbot, M. R. (Eds.) *Lacustrine Petroleum Source Rocks* , pp 235-46. London: Geol. Soc Spec. Publ. **40**.

Renaut, R. W. and Owen, R. B. 1988. Opaline cherts associated with sublacustrine hydrothermal springs at Lake Bogoria, Kenya Rift valley. Geology, **16**, pp 699-702.

Rice, C. M. and Trewin, N. H. 1988. A Lower Devonian gold-bearing hot spring system, Rhynie, Scotland. Trans. Institute of Mining and Metallurgy, **97**, B141-B144.

Rolfe, W. D. I., Durant, G. P., Fallick, A. E., Hall, A. J., Large, D. J., Scott, A. C., Smithson, T. R. and Walkden, G. M. 1990. An early terrestrial boita preserved by Visean vulcanicity in Scotland. *In* Lockley, M. G. and Rice, A. (Eds.) *Volcanism and fossil biotas* . pp 13-24. Boulder, California: Geol. Soc. of America, Special Paper **244**.

Rolfe, W. D. I., Durant, G. P., Baird, W. J., Chaplin, C., Paton, R. L. and Reekie, R. J. 1993. The East Kirkton Limestone, Visean, of West Lothian, Scotland: introduction and stratigraphy. Trans. R. Soc. Edinburgh: Earth Science, **84**, pp 177-188.

Scott, A. C. 1990. Preservation, evolution and extinction of plants in Lower Carboniferous volcanic sequences in Scotland. *In* Lockley, M. G. and Rice, A. (Eds.) *Volcanism and fossil biotas* . pp 25-38.Boulder, California: Geol. Soc. of America, Special Paper **244**.

Sheppard, R. A. and Gude, A. J. 1986. Magadi-type chert - A distinctive diagenetic variaty from lacustrine deposits. *In* Mumpton, F. A. (Ed.) *Studies in diagenesis* . U. S. Geological Survey Bulletin, Report **B1578**, pp 335-345.

Smedley, P. L. 1986. The relationship between calc-alkaline volcanism and within-plate continental rift volcanism: evidence from Scottish Palaeozoic lavas. Earth and Planetary Science Letters, **76**, pp 113-128.

Smithson, T. R. 1989. The earliest known reptile. Nature, **342**, pp 676-678.

Stephenson, D. 1983. Hilderston Mine, West Lothian: mining history and the nature of the vein mineralisation as deduced from old records. British Geological Survey, Report NL 83/4 (NERC copyright).

Thompson, J. B. and Ferris, F. G. 1990. Cyanobacterial precipitation of gypsum, calcite and magnesite from natural alkaline lake water. Geology, **18**, pp 995-998.

Walkden, G. M., Irwin, R. and Fallick, A.E. 1993. Carbonate spherules and botryoids as lake floor sediments. Trans. R. Soc. Edinburgh: Earth Science, **84**, pp 213-222.

Wood, S. P., Panchen, A. L. and Smithson, T. R. 1985. A terrestrial fauna from the Scottish lower Carboniferous. Nature, **314**, pp 355-356.

1.9 Figure Captions.

Figure 1a The geographical locality of the East Kirkton Quarry, in the Midland Valley of Scotland. It also shows the stratigraphic position of the East Kirkton Limestone within the lower Carboniferous, Visean Series.

Figure 1b East Kirkton is found at locality 1, on a map of the local geology of the Bathgate Hills. This figure is taken from an excursion guide, by Stephenson and Munro, in McAdam and Clarkson, 1986).

Figure 2 A fossil of a temnospondyl amphibian, which was found in the East Kirkton Limestone. The reconstruction of the living form is by Michael Coates.

Figure 3 A fossil of what was believed to be the oldest reptile, Westlothiana Lizziae. Found by Stan Wood, at East Kirkton.

Figure 4 A palaeoenvironmental reconstruction of the Midland Valley of Scotland, in Calciferous Sandstone Times. To the eastern side of the valley the extent of Lake Cadell is shown and the position of East Kirkton, which was deposited after the margins of Lake Cadell had begun to recede, and volcanic activity had begun in the Bathgate Hills.

Figure 5 The main focus of volcanic activity in the Bathgate Hills was at Linlithgow, and the lava flows taper to the south where the East Kirkton Limestone is found. The other limestones shown interfingered with the lava flows, lie stratigraphically above the EKL and are all marine.

Figure 1a

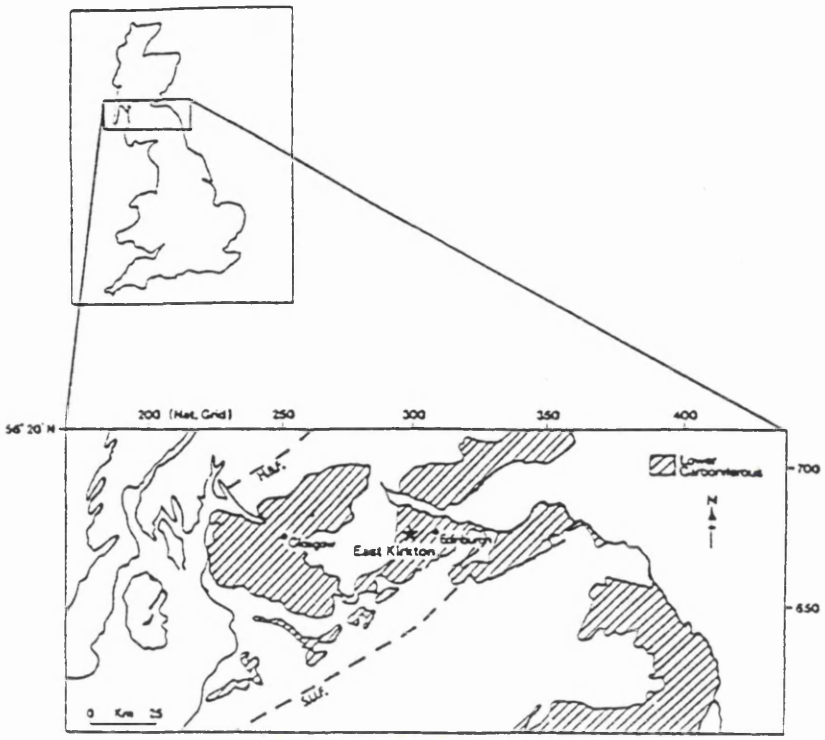

SERIES	STAGE	SPORE ZONE	WEST SCOTLAND	EAST SCOTLAND
VISEAN	BRIGANTIAN	NC	LOWER LIMESTONE GROUP	LOWER LIME-STONE GROUP
		VF		
	ASBIAN	NM	UPPER SEDIMENTARY GROUP	UPPER OIL SHALE GROUP
		TC	CLYDE PLATEAU LAVAS	LOWER OIL SHALE GROUP
	HOLKERIAN	TS		
	ARUNDIAN	Pu		
	CHADIAN			
TOURNAISIAN	COURCEYAN	CM	CEMENTSTONE GROUP	CEMENTSTONE GROUP

(after Scott, 1990).

Figure 1b

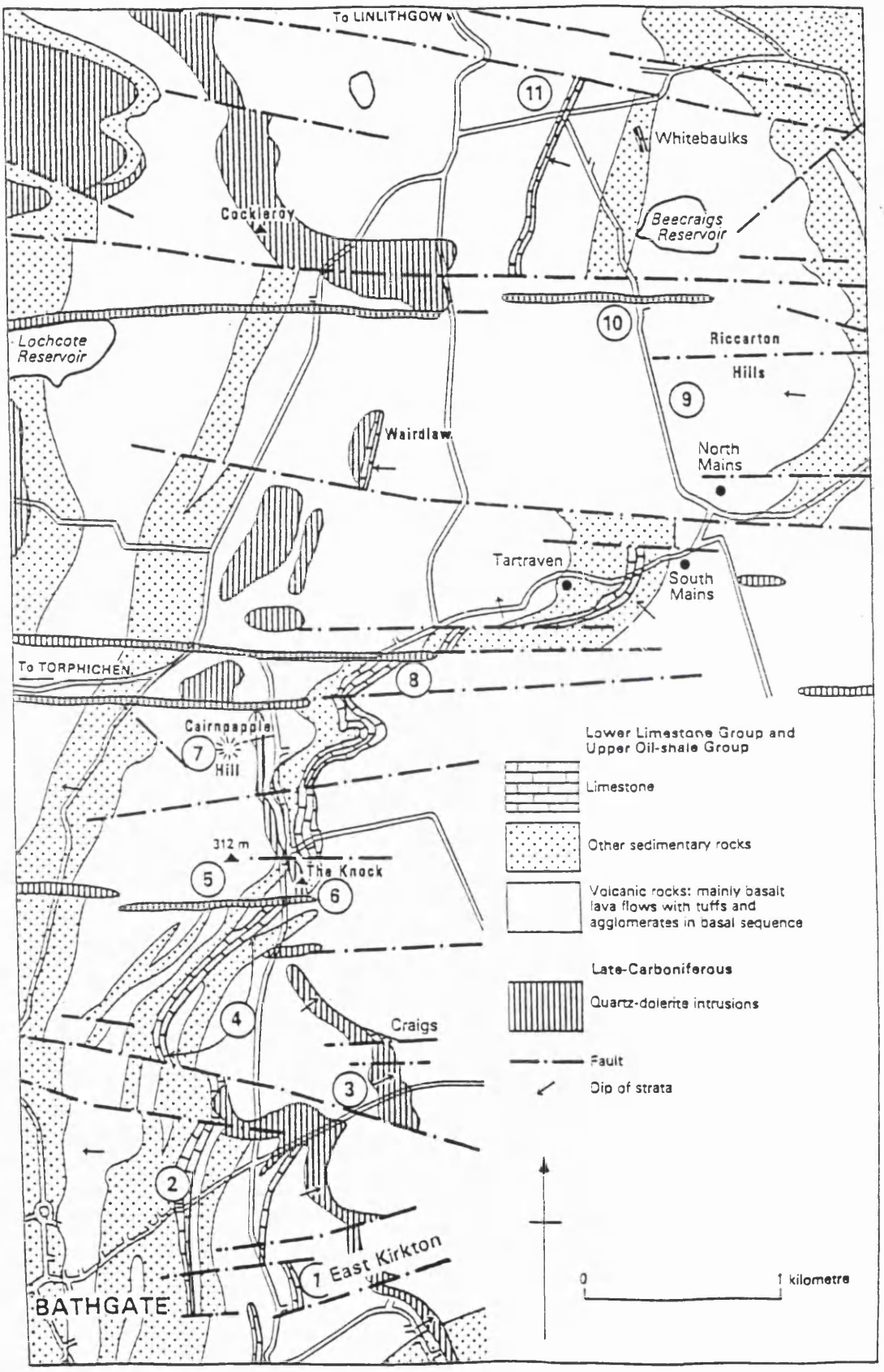
To LINLITHGOW
11
Whitebaulks
Cockleroy
Beecraigs Reservoir
10
Riccarton Hills
Lochcote Reservoir
9
Wairdlaw
North Mains
Tartraven
South Mains
To TORPHICHEN
8
Cairngapple Hill
7
312 m
The Knock
5
6
4
Craigs
3
2
1 East Kirkton
BATHGATE
Lower Limestone Group and Upper Oil-shale Group
Limestone
Other sedimentary rocks
Volcanic rocks: mainly basalt lava flows with tuffs and agglomerates in basal sequence
Late-Carboniferous
Quartz-dolerite intrusions
Fault
Dip of strata
0
1 kilometre

Figure 2

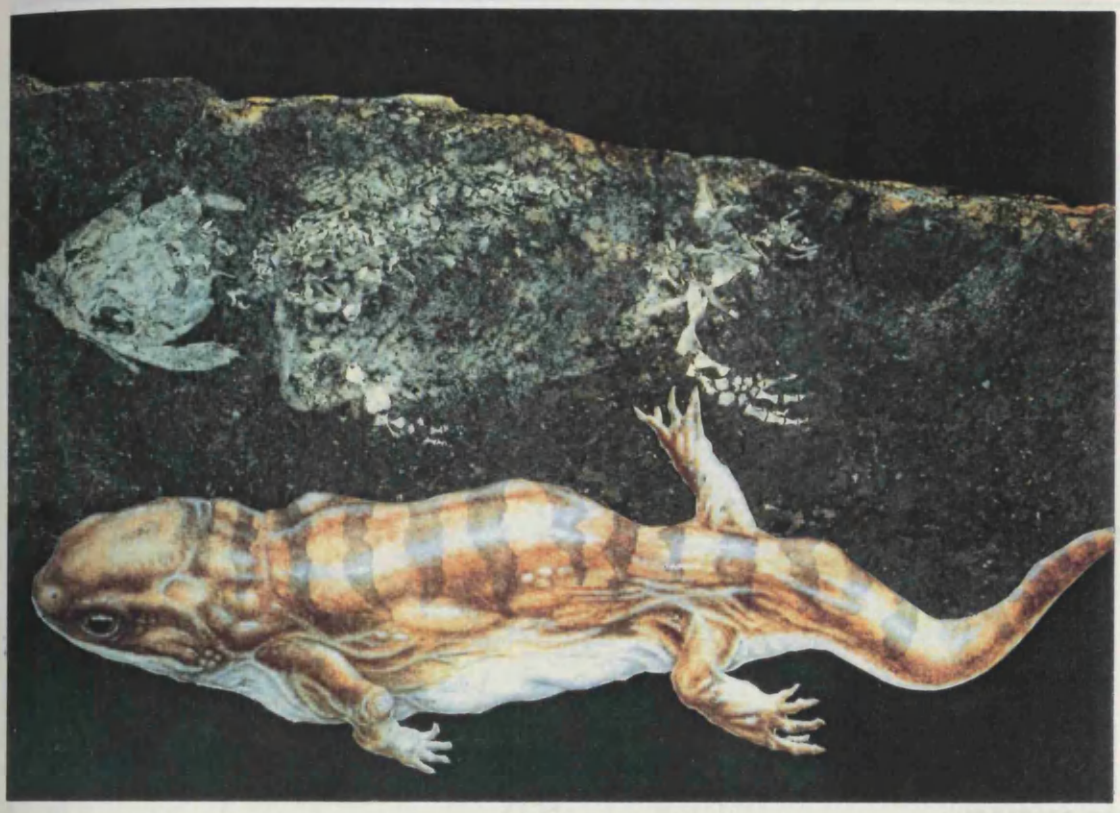

Figure 3

Figure 4

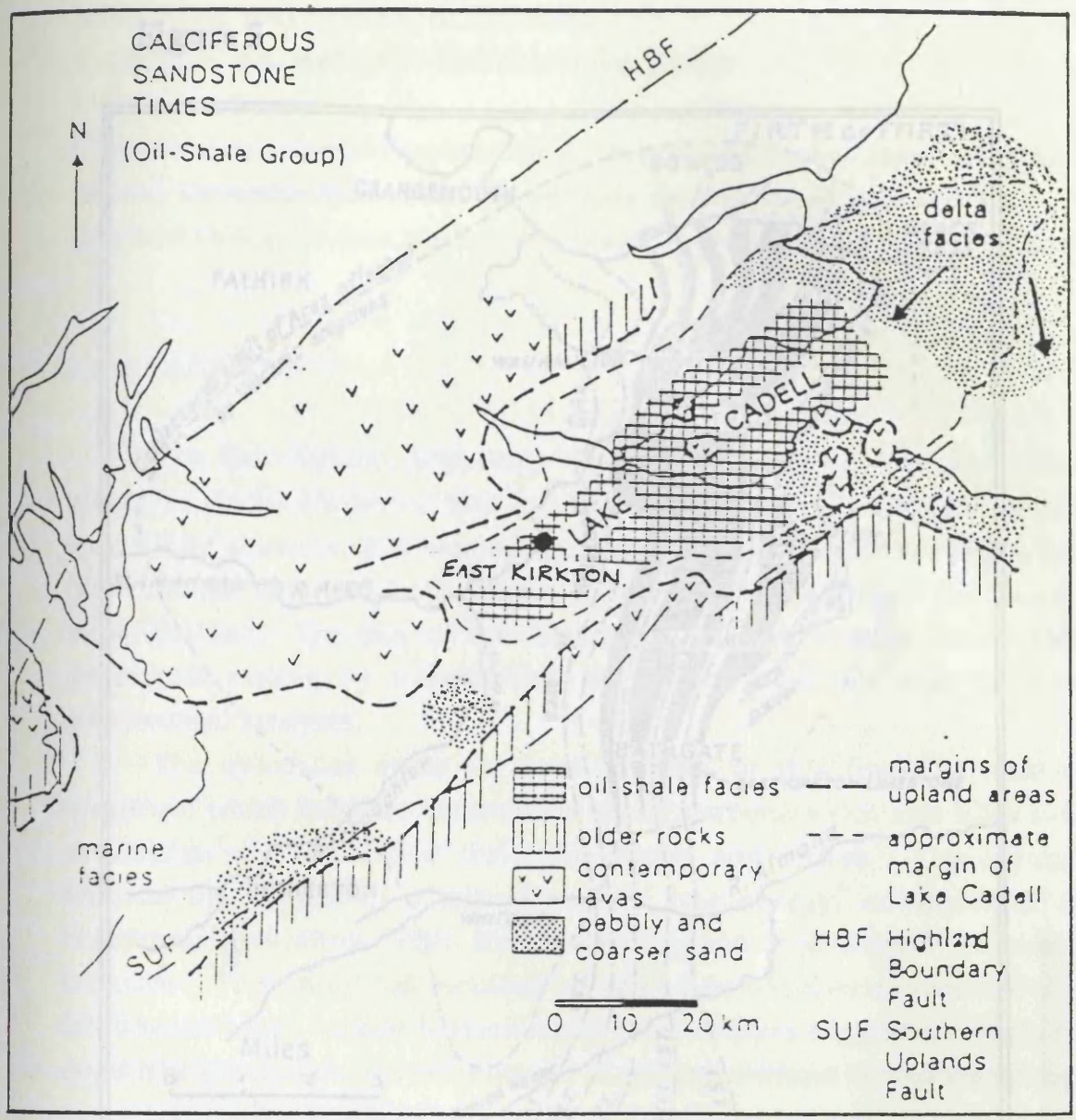
CALCIFEROUS
SANDSTONE
TIMES
(Oil-Shale Group)
N
HBF
delta
facies
CADELL
LAKE
EAST KIRKTON
marine
facies
SUF
oil-shale facies
older rocks
contemporary
lavas
pebbly and
coarser sand
0 10 20 km
margins of
upland areas
approximate
margin of
Lake Cadell
HBF Highland
Boundary
Fault
SUF Southern
Uplands
Fault

Figure 5

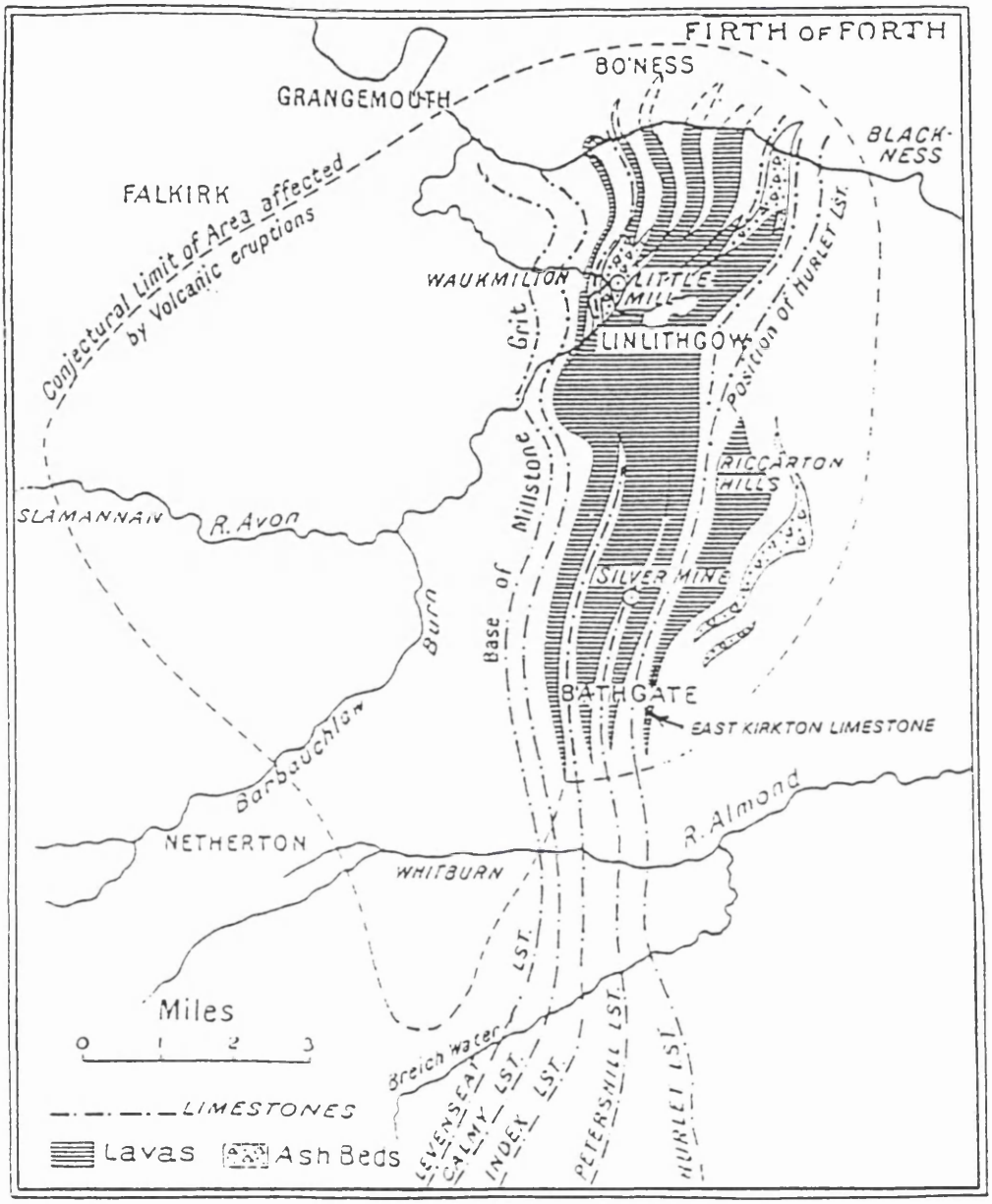
FIRTH OF FORTH
BO'NESS
GRANGEMOUTH
BLACK-NESS
FALKIRK
Conjectural Limit of Area affected by Volcanic eruptions
WAUKMILTON
LITTLE MILL
LINLITHGOW
Grit
Position of Hurlet Lst.
RICCARTON HILLS
SLAMANNAN
R. Avon
Base of Millstone Grit
SILVER MINE
Burn
BATHGATE
EAST KIRKTON LIMESTONE
Barbauchlan
NETHERTON
R. Almond
WHITBURN
Lst.
Miles
0 1 2 3
Breich Water
LIMESTONES
Lavas
Ash Beds

2. PETROGRAPHY AND GEOCHEMISTRY OF A LOWER CARBONIFEROUS, LACUSTRINE HOT-SPRING DEPOSIT: EAST KIRKTON, BATHGATE, SCOTLAND.

R. McGill[1], A.J. Hall[1], A.E. Fallick[2], W.D.I. Rolfe[3].

1Department of Geology and Applied Geology, University of Glasgow, Glasgow G12 8QQ.
2Scottish Universities Research and Reactor Centre, East Kilbride, Glasgow G75 0QU.
3Keeper of Geology, National Museums of Scotland, Chambers Street, Edinburgh EH1 1JF.

2.0 ABSTRACT.

The East Kirkton, Brigantian "limestone" was thought to be of hot-spring origin by Hibbert, (1836) due to the occurrence of numerous, small, spherulitic growths, this was supported by Cadell, (1925) following his observations of active hot-springs in Yellowstone National Park and in New Zealand. The aim of the continuing research is to constrain this geological setting by examination of textural evidence and detailed geochemical analyses.

The spherules occur in most horizons of this finely laminated sequence, which includes: bituminous shales; carbonate rich and silica rich sediments; and occasional limestone bands and lenses. The regular laminae are typical of a lake deposit, a low energy, environment of restricted circulation, with freshwater organisms preserved in many horizons. This study has focussed on the silicic sediments, unusual in a fresh water lake. At East Kirkton many chert textures suggest an origin as a gel-like precipitate: synsedimentary slumping without brittle fracturing indicates a silica precipitate capable of ductile movement. Cracks have formed perpendicular to bedding, without continuing from the chert into surrounding layers and these may be the shrinkage cracks of a cooled silica gel. Both silica and carbonate form primary precipitates, though both also form several replacive phases. Cathodoluminescence (CL), UV fluorescence and SEM were used to identify the presence of both carbonate and silica spherules,and also to differentiate a variety of carbonate phases, principally calcite and dolomite.

Isotopic analysis of $\delta^{18}O$ and δD are presented showing that the origins of the siliceous fluids can be constrained for the East Kirkton environment. The analyses ($\delta^{18}O$ = 21.3 to 26.9‰, n=18; δD = -52.2 to -90.7‰, n=13) fall close to the "agate line" of Fallick et al (1986) and

are consistent with equilibration of the cherts at 40 to 90°C with L. Carboniferous meteoric water of $\delta^{18}O$ = -4‰ and δD = -2‰. Fluids in equilibrium with this silica "gel" may have been trapped only as the "gel" cooled and hardened, upon mixing with the lake waters, to result in fine, laminae of chert.

2.1 INTRODUCTION.

2.1.1 General Background.

The East Kirkton "limestone" quarry is situated in an area of poor exposure in the Bathgate Hills, towards the eastern side of the Midland Valley of Scotland (Figure 1, locality 3). The limestone is located stratigraphically at the top of the Upper Oil Shale Group (Stephenson and Monro, 1986). The other localities indicated (Figure 1) across the Midland Valley, are seven other Carboniferous outcrops where well preserved and permineralised plant specimens have been found, often within volcanogenic sediments (Scott, 1990). Localities 4-7 on the east coast are also associated with lake deposits. The East Kirkton sequence is 12m at its thickest, and is an alternation of finely laminated, lacustrine sediments, in which are preserved freshwater brachiopods and evidence of considerable biological activity within the lake; and ash horizons which are only poorly bedded and show little lateral continuity. The aim of the petrographic study and geochemical analyses is to constrain the geological setting of this deposit allowing for evidence of low temperature origins as indicated by the biological activity, and high temperature input as indicated by the silica gel textures. Future research must also include using a soil geochemical survey to explore for associated mineralisation.

This small, disused quarry has become famous for its unusual fossil biota, including several unique, species of plant and animal. The fossil of the earliest reptile, nicknamed "Lizzie", is particulary well known since it has been featured in scientific journals (Wood et al, 1985 and Gee, 1988), on television, and was even discussed by the British Parliament when it was to be sold abroad. The sale of this fossil eventually realised £200,000 and it is now exhibited in the National Museum of Scotland (NMS) in Edinburgh. It is hoped that by study of the flora and fauna of this quarry, much may be learned about the evolution of early terrestrial life. The research reported here forms part of the East Kirkton Project co-ordinated

by W.D.I. Rolfe, (NMS). A review of studies under-taken up to 1989 has been published by Rolfe et al, (1990).

2.1.2 Palaeoenvironment.

Current interpretations suggest that the finely laminated sediments of which the succession is largely comprised, indicate a low energy, lacustrine environment which is disrupted by periodic volcanic eruptions depositing ash horizons of varying thickness (1m to 5cm). The volcanic centre identified by Cadell, (1925) was situated 8 km to the north of the quarry. There has been slumping within the sequence triggered either by the volcanic activity or by syn-sedimentary faults (Figure 2).

The preserved fossil plants and animals have been washed into the lake from their terrestrial habitat and since some of the plant remains are preserved as fusain they may have been burnt by forest fires sparked by volcanic activity. Other sediments, including the carbonate spherules and slumped chert horizons appear to have been derived from a hot-spring. There were also laminae comprised of pellets that could have been the faecal pellets of some animal living in or beside the lake. Delicate plant spores are often preserved in these laminae and this combined with small cubes of pyrite indicate a reducing environment. The thermal energy for the hydrothermal system could well have been high level intrusives such as alkali dolerites (teschenites) (Francis, 1983) associated with Lower Carboniferous volcanism in the Midland Valley of Scotland. The siliceous fluids are a possible product when meteoric water reacts with hot, alkaline basalt to produce hydrated alumino silicates such as prehnite and zeolites (Hall et al, 1989).

Within the quarry are two well defined massive lenses of carbonate. The lower of these was thought (Rolfe et al, 1990) to represent a carbonated sinter deposit but an altenative hypothesis for its origin is a low, mound grown around an active fluid conduit with both major carbonate and minor silica as chemical precipitates caused by the fluids expelled from the vent or by algal growth. The carbonate commonly forms in a stromatiform habit and distinct stromatolites are observed above the level of the sediments blanketing the lower parts of the lens; silica in the stromatolites may be replacement of the carbonate or could be fixed by the algae from a supersaturated silica solution. The second, higher, lens is possibly a channel deposit, since some of the bedding is truncated against the lens and the overall shape of the lens was convex downwards with a flatter top. No evidence of layering was found in either of the lenses.

Similar, smaller features were observed elsewhere in the quarry, formed from the stromatiform carbonate, these may be fragments broken from a larger lens or they may be discrete growths.

2.2 PETROGRAPHY.

2.2.1 General Features.

The most striking feature of the succession is the regular, fine laminae (Muir and Walton, 1957). Some horizons are comprised of these laminae and they are mainly carbonate rich or very dark due to compressed organic debris. Many layers consist of a combination of carbonate spherules and organic debris, but some laminae are formed of silica. In hand specimen isolated laminae of dark brown chert can be seen within horizons of the carbonate laminae which vary in their colour, organic and clay content and some contain spherules while others have none. Although the chert is less common than the carbonate, its occurrence throughout the succession suggests that understanding its origin and formation will contribute significantly towards interpretation of the palaeoenvironment. XRD analyses indicate that typical laminated limestone contains major calcite and quartz with minor kaolinite and dolomite (probably ferroan). Tuffaceous layers are mainly calcite with minor kaolinite, quartz and chlorite. Chert layers consist of quartz with minor calcite and trace dolomite.

A suite of thin sections was prepared by the NMS with material from a stratigraphic sequence logged through the quarry succession. By studying the textures of the whole sequence an initial overview of the lithologies was gained before selecting the silica rich horizons to be studied in more detail. Thin sections were then prepared for all these silica laminae and various other types of silica from samples that had been collected *in situ* and loose in the quarry.

2.2.2 Silica Textures.

There are several textural reasons why many chert laminae are considered to be primary. The chert layers (1mm to 3cm thick) are often slumped, like the carbonate and ash horizons around them. This is due to syn-sedimentary deformation (first recognised by Walton and Muir, 1957) where both carbonate and chert horizons have behaved plastically. For the chert a gel-like stage is envisaged for the unlithified layers. This is

confirmed by the pinching of some chert laminae around carbonate spherules. In other horizons there are small silica lenses, flattened and stretched by early compaction (Figure 3a). Similar textures are found in the carbonate, but they are usually of medium grained, granular calcite whereas the silica laminae and lenses are very fine grained.

In Figure 3b, typical carbonate-silica laminae are shown. There is no sharply defined contact between laminae and in many cases the carbonate appears to grade into the silica, with isolated, often euhedral, carbonate crystals growing as though suspended within the chert. These crystals may have formed from carbonate rich fluids trapped in the chert before it was fully hardened, thus allowing the crystals to grow euhedrally. However, they may have grown by replacement of the chert during early diagenesis.

Within the chert laminae a disordered pelloidal texture (Figure 3c) was observed that could only be seen using Ultra-Violet Fluorescence which causes most organic material to fluoresce. Patches of many of the primary chert layers appear to be replaced organic material. From the lack of compaction of the organic pellets it can be concluded that the replacement was an early feature of the primary lacustrine fluids. Similar pellets are found cemented by carbonate.

Many silica laminae have chert-filled and calcite-filled cracks cutting perpendicular to layering. It is thought that these may either be desiccation cracks of the hardening silica gel or represent differential compaction of the layers, since they do not continue into the carbonate laminae (Figure 3d).

Other occurrences of silica include isolated dark chert lenses within carbonated ash horizons and silica cement in stromatiform and pisolithic carbonate, in the lower carbonate lens. The cementing silica is often a bluish white banded chalcedony but can also be amorphous white silica coating the walls of vugs and cavities. The centres of chalcedony coated vugs are often filled with equant megaquartz (Milliken, 1979) but are occasionally filled with a single coarse calcite crystal or even some small droplets of bitumen. In some vugs the chalcedony is zebraic (Figure 3e) and takes an almost spherular form.

2.2.3 Spherulites.

Carbonate spherules are a common feature of the East Kirkton sediments and there may have been a feature of this environment that caused both silica and carbonate phases to take spherular habits. There is a diversity of spherule types, the commonest being of radiating carbonate

with no apparent nucleus. Others, buff-coloured in hand specimen and of more irregular shape, are of carbonate which seems to form a coating around plant fragments.

A few spherules have concentric rings and appear isotropic in thin section. These may consist of microcrystalline silica. Concentric banding of carbonate spherules was only observed when cathodoluminescence (CL) was used. CL is sensitive to changes in the ionic state of Fe and Mn ions inherited from the solutions that formed the spherules. Thus the banding indicates that the Eh and the pH of the fluids changed several times during the formation of each spherule. The more complex shape of some spherules can be explained by banded overgrowths around an original core, also only visible in CL (Figure 3f).

CL shows where neomorphism has occurred within a spherule, usually as a brighter patch of luminescing carbonate that cuts across the growth banding. Where spherules have been bored it is often observed that both the central sphere of carbonate and the later overgrowths have been similarly bored (Figure 3f). These borings may act as the passage-way along which neomorphosing fluids pass, but alteration around them is not often observed. It is not clear why the organisms should choose to bore through these spherules but it can be concluded that they formed a loose aggregate for a period of time long enough for the boring to occur.

In some horizons many spherules are broken and this is another indicator of the transport of the spherulitic sediment. Many of the spherules which appear whole in plane polarised and cross polarised light were observed in CL to have sections of their outermost growth rings broken off.

Some of the primary carbonate is replaced by later carbonate as observed for the neomorphism in the spherules, but the carbonate is also replaced by silica. This is especially common in the stromatiform carbonate where only a skeletal remnant of the carbonate remains. Often the process of replacement appears to highlight the growth banding of the spherule.

2.3 STABLE ISOTOPE ANALYSES.

Oxygen isotope analyses of the silica and hydrogen isotope analyses of the bound water (thought to be present as a silanole group, Si-OH) have obtained for some fifteen samples of variable silica forms, and data will be

reported elsewhere (McGill et al 1993, in press). Here we are concerned with the implications of the data.

Earlier analyses measured $\delta^{18}O$ of only six silica samples (Rolfe et al, 1990). The results that have now been obtained extend the range of oxygen values, while confirming the earlier results, and including hydrogen isotope analyses. Eighteen silica samples give a range of $\delta^{18}O$ = 21.3 to 26.9‰.

Thirteen samples were analysed for hydrogen isotopes. The range of values obtained is δD = -52.2 to -90.7‰. The water contents of the samples were measured during analysis and the range is 0.28 to 0.52 wt% H_2O. There was no correlation between the water contents of the silica samples and δD showing that the isotope results were not influenced by yield.

McGill et al (1993, in press) show that on a $\delta^{18}O / \delta D$ diagram (Figure 4) data plot close to the line defined by chalcedony in agates of different ages from Scotland (Fallick et al, 1985). This argues for a surface derived fluid with a major meteoric water contribution, and rules out formation fluids of magmatic origin. The interpretation is summarised below.

2.4 INTERPRETATION OF ISOTOPE RESULTS.

The East Kirkton isotopic analyses plot relatively close together (Figure 4) suggesting that the different silica samples were formed by similar fluids, or by a fluid with a small variation in isotopic composition, and within a narrow range of temperatures (see line to represent 10°C variation, Figure 4). They plot quite close to the "agate line" indicating similar fractionation and formation processes. The "agate line" is the best fit line through data from Scottish Tertiary and Devonian agates (Fallick et al, 1985). This line has a slope similar to the present day Global Meteoric Water Line (MWL), $\delta D = 7.9\delta^{18}O - 260$ and it was concluded (ibid.) that the East Kirkton silica had formed from slightly heavier meteoric water than Devonian agates. These values are consistent with formation from L. Carboniferous meteoric water which would have approached the zero seawater value as Scotland approached equatorial latitudes.

Assuming a Scottish L. Carboniferous meteoric $\delta^{18}O_{H_2O}$ value of -4‰, the equation of Matsuhisa et al (1979) can be used to obtain temperature estimates:

$$\delta^{18}O\ Qtz - \delta^{18}O\ H_2O = \frac{3.34 \times 10^6}{T^2\ (°K)} - 3.31$$

These calculations yielded a temperature range of 40-90°C corresponding to the equilibrium temperatures of the cooled silica gel and associated fluid. The results are consistent with periodic input of high temperature (near to or above boiling) siliceous solutions into the cool lake water, where mixing of the fluids resulted in the precipitation of silica.

While much of the variation in isotopic composition may be due to temperature differences, it is also probable that the isotopic signature of the meteoric water was modified within the hydrothermal system as the water tended towards re-equilibration with hot basalt. The modified oxygen isotope value would approach +8‰ and this would lead to higher calculated equilibrium temperatures (+80°C approx.) due to the correspondingly smaller fractionation. Organic matter is abundant in the samples and this is known to possibly absorb deuterium giving anomalously light δD measurements. Future analyses will be undertaken on organic-free samples.

2.5 CONCLUSIONS.

1. Regular laminated horizons indicate a quiet, lacustrine environment with minor, fine sediment enriched in organic material and disturbed by influxes of carbonate spherules, often preceded by a chert horizon, and poorly graded basaltic ash.

2. The lake water may have been stratified due to influxes of fluids at different temperatures. Pyrite is also common in some laminated horizons and indicates anoxic conditions, associated with abundant organic material, in deeper parts of the lake.

3. Primary silica originated as a gel because of the syn-sedimentary slumping in some laminae, the possible dehydration cracks, the carbonate rhombs which grow in suspension in the chert horizons, and the occasional grading of carbonate laminae into chert.

4. The prescence of silica spherules suggest similar factors effect the precipitation of silica and carbonate.

5. The silica probably originated from a hydrothermal remobilisation of silica in the mildly alkaline volcanics triggered by the intrusion of the later, high-level, alkali dolerite dykes and sills.

6. Carbonate spherule zones seen with Cathodoluminescence indicate frequent changes in Eh and pH of formation waters.

7. High organic content in silica and carbonate laminae and bituminous shales suggest high biological productivity and preservation potential.

8. A dominantly low temperature environment is suggested by: (i) the temperature range from $\delta^{18}O$ results (ie. 40-90°C), (ii) organic matter eg. spores are well preserved, and (iii) organisms must have lived in the water, since some secreted pellets and others bored into spherules. The above give a picture of mixing fluids, some warmer and some cooler allowing organisms to live close to a hostile hot-spring environment.

9. The isotopic signature is that of the water that was in equilibrium with the silica gel until a certain temperature when it hardened and no further isotopic exchange occurred.

10. Meteoric water is the major component of the silica formation fluids.

2.6 ACKNOWLEDGEMENTS.

This research forms part of a NERC. CASE postgraduate studentship supported by the NMS. For the patient training I received in isotopic techniques and the assistance of the laboratory staff at SURRC, East Kilbride I am very grateful; and for assistance in the use of the CL and UV Fluorescence microscopy I must thank Dr C.J.R. Braithwaite of the Department of Geology and Applied Geology, Glasgow University.

2.7 BIBLIOGRAPHY.

Cadell, H.M. 1925. *The rocks of West Lothian,* Edinburgh: Oliver & Boyd.

Fallick, A.E., Jocelyn, J., Donnelly, T., Guy, M., & Behan, C. 1985. Origin of agates in volcanic rocks from Scotland, NATURE **313**, 672-674.

Francis, E.H. 1983. Carboniferous-Permian igneous rocks, *In* Craig, G.Y., (ed.), *Geology of Scotland.* Edinburgh: Scottish Acad. Press, 297-342.

Gee, H. 1988. Oldest known reptile found in Scotland, NATURE **336**, 427.

Hall, A.J., Banks, D., Fallick, A.E. & Hamilton,P.J. 1989. An hydrothermal origin for Cu-impregnated prehnite and analcime from Boylestone Quarry, Barrhead, Scotland, J. GEOL. SOC. LONDON, **146**, 701-713.

Hibbert, S. 1836. On the fresh-water limestone of Burdiehouse, TRANS. R. SOC EDINBURGH: EARTH SCI. **13**, 169-282.

Matsuhisa,Y. 1979. Oxygen isotopic fractionation in the system qtz-albite-anorthite-water, GEOCHIM COSMOCHIM ACTA **43**, 1131-1140.

McGill, R. A. R., Hall, A. J., Fallick, A. E. & Boyce, A. J. (1993, in press). The East Kirkton palaeoenvironment: stable isotope evidence from silicates and sulphides, TRANS R SOC EDINBURGH: EARTH SCI. **84**, pp 223-238.

Milliken, K.L. 1979. The silicified evaporite syndrome - Two aspects of silicification history of former evaporite nodules from Southern Kentucky and Northern Tennesse, J SED. PETROL **49**, 245-256.

Muir, R.O. & Walton, E.K. 1957. The East Kirkton Limestone, TRANS GEOL. SOC. GLASGOW **22**, 157-167.

Rolfe, W.D.I. 1988. Early life on land; The East Kirkton discoveries, EARTH SCI CONSERVATION **25**, 22-28.

Rolfe, W.D.I., Durant, G.P., Fallick, A.E., Hall, A.J., Large, D.J., Scott, A.C., Smithson, T.R. & Walkden, G.M. 1990. An early terrestrial biota preserved by Visean vulcanicity in Scotland, *In* Lockley, M. G. & Rice, A. (eds.) *Volcanism and fossil biotas,* 13-24. GEOL. SOC. AMERICA, Special Paper **244**.

Scott, A.C. 1990. Preservation, evolution, and extinction of plants in L. Carboniferous volcanic sequences in Scotland. *In* Lockley, M. G. & Rice, A. (eds.) *Volcanism and fossil biotas,* 25-38. GEOL. SOC. AMERICA, Special Paper **244**.

Stephenson, D. & Monro, S.K. 1986. Bathgate Hills. *In* McAdam, A.D. and Clarkson, E.N.K., (eds.) *Lothian Geology: An excursion guide.,* Edinburgh: Scottish Academic Press, 208-216.

Taylor, H. P. & Forester, R. W. 1971. Low-O-18 igneous rocks from the intrusive complexes of Skye, Mull, Ardnamurchan, Western Scotland. JOURNAL OF PETROLOGY **12**, 465-497.

Wood, S.P. , Panchen, A.L. and Smithson, T.R. 1985. A terrestrial fauna from the Scottish Lower Carboniferous, NATURE **314**, 355-356.

2.8 Figure Captions.

Figure 1 Location map and extract from the Lower Carboniferous stratigraphic column indicating the position of the East Kirkton Limestone.

Figure 2 A hypothetical reconstruction of the East Kirkton palaeoenvironment.

Figure 3 (A) Attenuated lenses of chert formed due to compaction of the sediments (PPL). Field of view is 2mm. (B) Typical alternation between carbonate and chert laminae, with rhombs of carbonate growing in the isotropic chert (XPL). Field of view is 2mm. (C) Pelloidal sediment suspended within a laminae of chert (UV Fluorescence). Field of view is 1mm. (D) Laminae of chert and carbonate deposited above a carbonate spherule, which has holes bored through it by some organism. The chert layer shows shrinkage cracks which do not continue into the carbonate horizons (PPL). Field of view is 2mm. (E) Vugs in the sediment of carbonate spherules filled by radiating zebraic chalcedony, which also appears to form spherules (PPL). Field of view is 1mm. (F) A carbonate spherule showing four stages of overgrowth around the original core. In this spherule both the core and the overgrowths have been bored and some of the brighter patches of the spherule appear to have been neomorphosed, due to the irregularity of their boundaries (CL). Field of view is 3mm.

Figure 4 $\delta^{18}O$ and δD plot of East Kirkton chert. Also shown are agate data from Fallick et al (1985), and the best estimates of Devonian and Tertiary (Taylor and Forester, 1971) Scottish meteoric waters. The probable position of L. Carboniferous meteoric water will be heavier than Devonian (-5‰, -20‰) and may be modified by a hydrothermal system (this would result in even heavier $\delta^{18}O$ of closer to 0‰). A 10°C temperature variation about the agate line is indicated (Fallick et al, 1985).

Figure 1

THE LOCATION OF THE EAST KIRKTON LIMESTONE, GEOGRAPHICALLY AND STRATIGRAPHICALLY

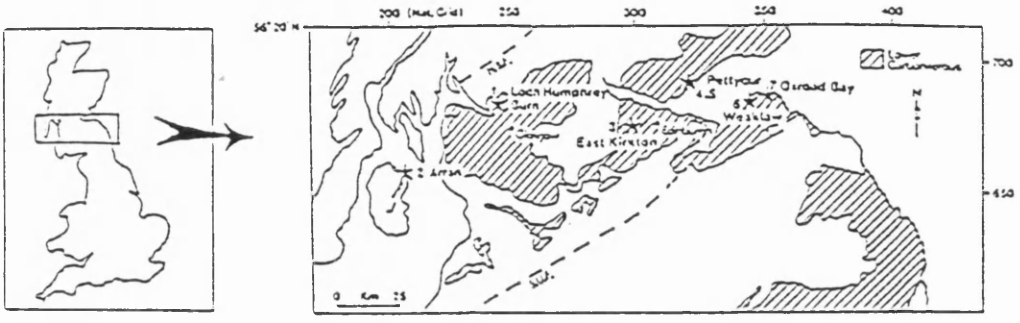

SERIES	STAGE	SPORE ZONE	WEST SCOTLAND	EAST SCOTLAND
VISEAN	BRIGANTIAN	NC	LOWER LIMESTONE GROUP	LOWER LIME-STONE GROUP
		VF	UPPER SEDIMENTARY GROUP	UPPER OIL SHALE GROUP
	ASBIAN	NM		
		TC	CLYDE PLATEAU LAVAS	LOWER OIL SHALE GROUP
	HOLKERIAN	TS		
	ARUNDIAN	Pu		
	CHADIAN			
TOURNAISIAN	COURCEYAN	CM	CEMENTSTONE GROUP	CEMENTSTONE GROUP

(after Scott, 1990).

Figure 2

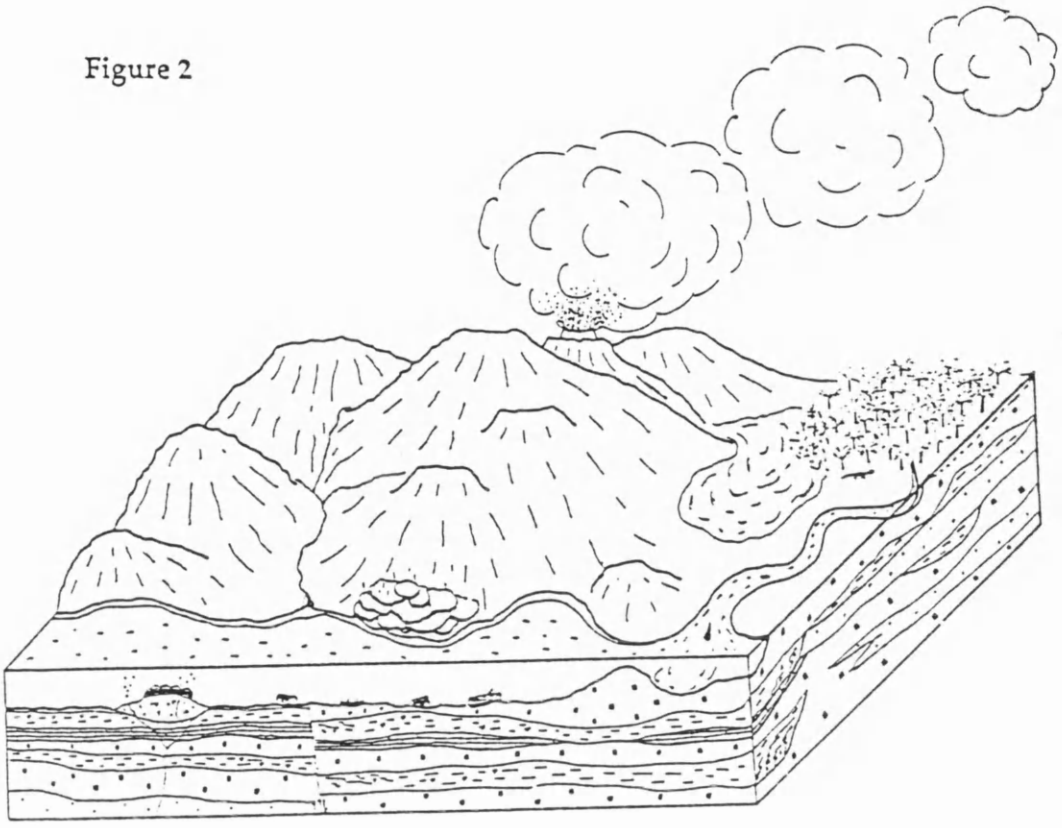

KEY

Carbonate	–	massive carbonate, quite coarsely crystalline and buff in colour except for darker more organic rich patches within it.
	–	carbonate rich patches within other lithologies, usually ash, - both maybe replacive but within the shales, individual laminae are often primary carbonate.
	–	buff coloured carbonate which appears stromatiform, fragments are often found in other horizons especially in the tuff.
Shale	–	well laminated material, with chert and bituminous horizons, often containing carbonate spherules.
Silica / chert	–	forming individual laminae as a primary deposit, but also replacing the organic rich and carbonate rich horizons.
Tuff / ash	–	containing fragments of carbonate, plant material, silica, and lithic volcanic clasts both vesicular and holocrystalline: layers pinch and swell with little lateral continuity.
Basalt	–	generally fine grained with vesicular flow tops.

Figure 3

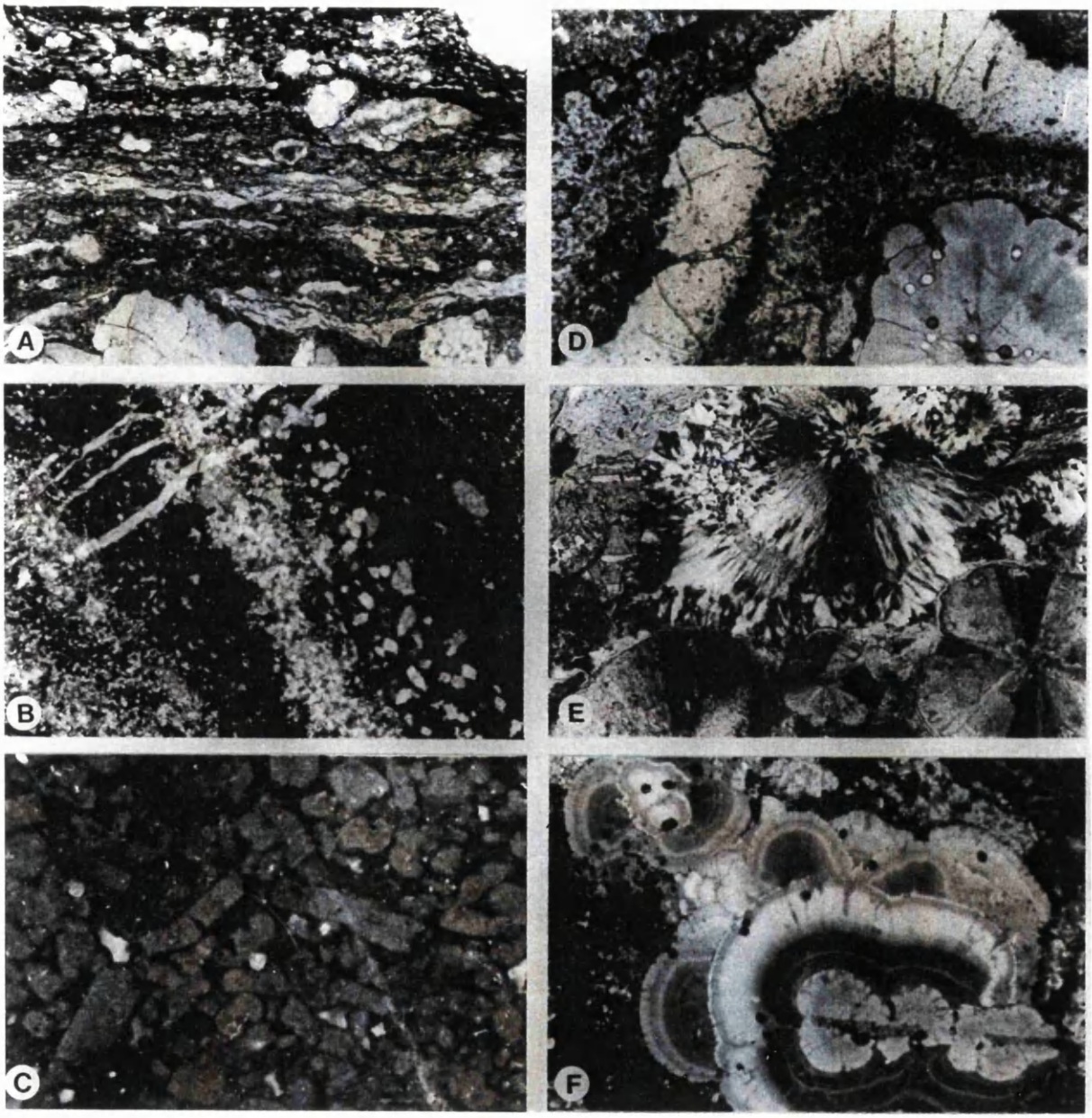

Figure 4

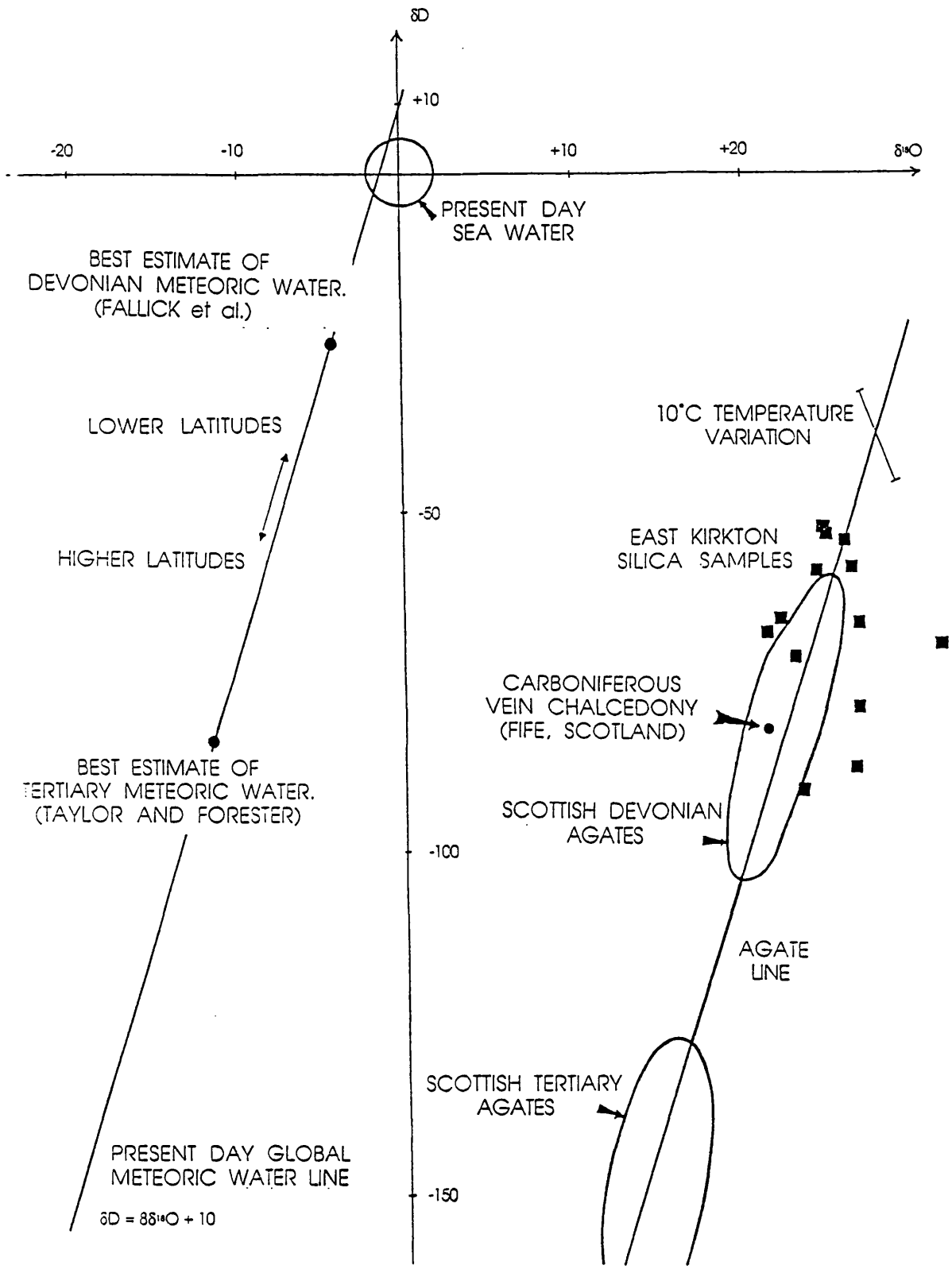
δD
+10
-20
-10
+10
+20
δ¹⁸O
PRESENT DAY
SEA WATER
BEST ESTIMATE OF
DEVONIAN METEORIC WATER.
(FALLICK et al.)
LOWER LATITUDES
HIGHER LATITUDES
10°C TEMPERATURE
VARIATION
-50
EAST KIRKTON
SILICA SAMPLES
CARBONIFEROUS
VEIN CHALCEDONY
(FIFE, SCOTLAND)
BEST ESTIMATE OF
TERTIARY METEORIC WATER.
(TAYLOR AND FORESTER)
SCOTTISH DEVONIAN
AGATES
-100
AGATE
LINE
SCOTTISH TERTIARY
AGATES
PRESENT DAY GLOBAL
METEORIC WATER LINE
δD = 8δ¹⁸O + 10
-150

3. THE EAST KIRKTON PALAEOENVIRONMENT: STABLE ISOTOPE EVIDENCE FROM SILICATES AND SULPHIDES

R.A.R. McGill[1], A.J. Hall[1], A.E. Fallick[2] and A. J. Boyce[2].

[1]Dept. of Geology and Applied Geology, University of Glasgow, Glasgow, G12 8QQ.

[2]Isotope Geosciences Unit, SURRC, East Kilbride, Glasgow, G75 0QU.

3.0 ABSTRACT

Stable isotope data from the East Kirkton succession are used to elucidate the extent of hot-spring influence in the palaeoenvironment by constraining conditions of deposition of the silica and the formation of sulphides.

Petrographically silica occurs as chert laminae thought to be primary, and as patchy chert considered as replacive. No evidence for biogenic silica was observed. For 20 silica samples $\delta^{18}O$ was measured for structural oxygen and δD for bound water. $\delta^{18}O_{(SMOW)}$ varied between +21 and +27‰ with no sample groupings related to petrography. The range in $\delta D_{(SMOW)}$ was from -50 to -90‰ with lower values characterising replacive or altered silica; water contents of both petrographic groups were similar. A plot of $\delta^{18}O$ versus δD for the laminated primary silica defines a grouping about the line defined by Scottish agates (Fallick *et al.*, 1985). This suggests for the unaltered silica a formation temperature of about 60°C and a fluid which contained a strong component of meteoric water. The data imply a Lower Carboniferous meteoric water $\delta^{18}O$ composition of perhaps -3‰, consistent with the known palaeolatitude.

The only sulphide observed was pyrite; 34 samples were selected from a wide variety of lithological and textural occurrences. $\delta^{34}S_{(CDT)}$ ranges widely and continuously between +8 and -34‰ with no strong mode. The sulphur appears to be derived from several sources, and pyrite formation from a variety of conditions as indicated by such wide ranging data, but for the samples with the lowest $\delta^{34}S$ the involvement of bacteria in sulphate reduction is inferred.

3.1 INTRODUCTION.

The East Kirkton Limestone, which outcrops only in the Bathgate Hills, West Lothian, has attracted much geological interest since early in the 19th century. Hibbert (1836) produced the first detailed description of the lithology and compared its textures with Tertiary strata in Auvergne, France, which were also closely associated with volcanic rocks. Hibbert suggested that several of the original features of this lithology - blistered appearance on the surface of the laminae, warping of the strata, and occurrence of mammillated concretionary nodules - indicated a local source of strong heating and "powerful chemical action". He concluded that the calcareous material was deposited "in the form of hot springs, probably at the time in a state of ebullition". Geikie (1861) had observed silica charged hot springs in Iceland and considered that this was the mode of deposition of the bands, nodules and thin laminae of chert. He also described the unit as being isolated to the quarry alone, a "limestone" originating as a small lagoon in a hollow in the lava.

Nearly a century later Muir & Walton (1957) focused on the carbonate spherulites, including a description of the variety of spherulites and their occurrence in the various lithologies. They considered that the hot springs were the source of "salts or ions", e.g. Ca^{2+}, Na^{+}, K^{+}, and with denitrifying bacteria producing ammonia, conditions would be suitable for the formation of spherulites: "spherulitic structures are ascribed to penecontemporaneous development within an aragonite mud. The calcareous material and the salts causing the development of spherulites are thought to have been derived from hot springs" (Muir & Walton, 1957).

The aim of the present study, combining petrographic observations and isotope geochemistry, is to elucidate the extent of hot spring influence on the formation of the East Kirkton "limestone". Isotopic investigation of various silica phases and pyrite, the only sulphide phase observed commonly in the quarry lithologies, was undertaken in order to give a clearer picture of the fluids involved in the precipitation of the deposit.

Details of the stratigraphy and location of the East Kirkton Limestone are given by Rolfe *et al.* (1993); its regional and stratigraphic setting can be found in Smith *et al.* (1993).

3.2 PETROGRAPHY.

3.2.1 Primary Silica

The most striking occurrence of silica at East Kirkton is as dark brown, vitreous chert in the form of thin, continuous laminae conformable with the organic-rich shales and carbonate laminites. The chert layers can be divided into two hand specimen types: individual thick laminae, usually containing carbonate spherules and cross-cut by calcite veins (Figure 1A, NMS G1993.21.1); or multiple, thin layers seldom containing spherules (Figure 1B, NMS G1993.21.2). The laminae (thin and thick) may be observed to continue laterally for the extent of the exposure e.g. in Unit 58 (National Museums of Scotland, stratigraphic log, Rolfe *et al.*, 1993) seven spherulitic laminae (each about 5mm thick, in a bed that is 0.7m thick) continue laterally 14m along the north facing quarry faces and 18m over the east facing faces, disturbed occasionally by local faulting, folding or vegetation. Some laminae are less continuous 0.1-0.5m, and thickness also varies laterally, e.g. 5mm laminae becoming 40mm thick. Clasts of brown chert of similar colour and grain size are often found in carbonate-rich volcanic ash (Figure 1C, NMS G1993.21.3) and may appear to be deformed by compaction. The only example of massive chert (Figure 1D, NMS G1993.21.4) - though not found *in situ* - contains many spherules and some pale, brecciated silica laminae.

The silica laminae and lenses are often observed to show syn-sedimentary deformation (Figure 1E, NMS G1993.21.5). Textures observed in thin section also strongly suggest that this very fine grained, dark brown chert is primary (McGill *et al.*, 1990). Examples of these textures include: layers slumping without fracturing and appearing squashed and stretched by early compaction (Figure 1F, NMS G1993.21.6); intra-layer sedimentary faulting that leaves the overlying layer unaffected (Figure 2A, NMS G1993.21.2); and outlines, of what appear to be borings, cutting into the semi-consolidated silica (Figure 2B, NMS G1993.21.1). The silica laminae have within them many small, euhedral carbonate crystals that give the layers a graded texture (Figure 2C,D, NMS Unit 59); it is possible that these crystals are a late diagenetic feature, with the nuclei for these crystals occurring as a graded sediment within the silica as they were deposited. It is also apparent that organic material is best observed in silica laminae (Figure 2E) because of their fine grain size and the lack of compaction. The clearest examples of this detailed organic preservation are plant stems (Figure 2F), spores, and also fecal pellets which occur in many of the

laminae and in the massive chert sample (Figure 1D, NMS G1993.21.4). Although these fecal pellets, can be seen only as faint shadows in plane polarised light (Figure 2G, NMS G1993.21.4) when observed with an ultraviolet fluorescence microscope structures are seen within individual pellets (Figure 2H). One further, unusual occurrence of silica is as concentrically banded spherules within samples of volcanic ash (Figure 3E, NMS Unit 71).

3.2.2 Altered and Secondary Silica

Besides the primary, dark brown chert, there is another phase of silica that forms laminae. It is a milky brown colour, very similar to the colour of the East Kirkton stromatiform carbonate and though fine grained is not vitreous. This second type of laminae occurs only occasionally within the laminated limestone but is more often found associated with stromatiform carbonate or unstratified carbonate-rich ash (Figure 3A, NMS G1993.21.7). This may be a silica phase which differs from the primary, dark brown chert by a variation of impurities; it may have been primary chert that has recrystallised resulting in this paler colouring; or it could be silica that is totally replacing the similarly-coloured, carbonate phase.

In thin section it is very difficult to differentiate between silica phases. To illustrate the complexities of textural relationships that can occur with silica phases, a hand specimen of a complex breccia, involving at least four silica phases is chosen as an example (Figure 3B, NMS G1993.21.8). It appears that the milky brown silica laminae were brecciated first, then the fragments were cemented by either a darker, grey/brown silica phase (which appears like a disordered sediment) or by a white chalcedonic vug-coating, centrally infilled by quartz or calcite. These latter vug infills were occasionally brecciated and cemented by the grey/brown silica phase. However the white chalcedony may also be observed filling in fine vugs within the grey/brown silica. The fourth silica phase that can be observed in this specimen is darker brown and occurs both as selective replacement in some of the brecciated laminae, and as patchy replacement cutting across textural features. Calcite is observed infilling vugs and as cross-cutting veins. In thin section, without the distinctive colouring of the silica in hand specimen, it is impossible to identify all of these textural details.

The milky brown laminae in one volcanic sample (Figure 1C, NMS G1993.21.3) appear to be composite layers when observed in hand

specimen; centrally, they have medium grained silica, with very fine grained silica rims containing organic matter and small carbonate crystals. The outer rims of these layers are very similar when observed with a microscope, to the primary, dark brown chert laminae, but in hand specimen they are milky brown.

There are several phases of silica which do not form laminae; one occurs as large patches of textureless, grey chert (Figure 3C, NMS G1993.21.9) with remains of concentric carbonate layering or vugs coated with white chalcedony. Vugs with this white chalcedony coating occur most often within the stromatiform carbonate lenses and may even form small agates with bands of blue chalcedony; such vugs are infilled by single crystals of calcite or equant megaquartz. The white silica coating these vugs, when observed in thin section, can be described as radial, zebraic chalcedony (Milliken, 1979) growing out from the carbonate matrix into the vug, often forming half-spherules (Figure 3D, NMS G1993.21.4). With silica spherules occurring in two forms (Figure 3D, NMS G1993.21.4, Figure 3E, NMS Unit 71) and carbonate phases forming such a diversity of spherules, perhaps some special feature of the East Kirkton environment is causing spherules to develop, as suggested by Muir and Walton (1957). Details of appropriate modern analogues were not readily available for comparison.

3.2.3 Pyrite

Pyrite was collected from several of the above silica types: the single, thick, dark brown laminae; dark brown chert lenses in ash; milky brown silica laminae and lenses in carbonate-rich ash and stromatiform carbonate (Figure 4A, NMS G1993.21.10). Wood and plant remains are common sites for pyrite growth (Figure 4B, NMS G1993.21.11) where organic decay produces a localised reducing environment. Pyrite was also found disseminated and as nodules within shale and ash (Figure 4C, NMS G1993.21.12 from Unit 61, figure 4D, NMS G1993.21.13), some of the volcanic clasts containing cubes, amygdales and rare veins of pyrite. Pyrite was also disseminated in carbonate nodules (Figure 4E, NMS G1993.21.14) and in one sample of a carbonate breccia with organic rich matrix (Figure 4F, NMS G1993.21.15), this resembles a ganister, but no rootlet structures were observed.

3.3 ANALYTICAL PROCEDURES.

3.3.1 Silica: Sample Collection and Preparation

When collecting silica samples from within the quarry, the widest variety of silica phases and occurrences were selected to provide as complete a picture as possible of the fluids which deposited the silica. Seven different sample groupings resulted from this selection (Figure 5A,B, & Table 1) with four representing primary chert and three that were considered replacive. For the primary chert samples it was relatively easy to separate manually the hard silica from the softer sediments around them. Unfortunately, white chalcedony infilling vugs and milky brown silica layers had to be separated from dark brown chert, milky grey chert, or blue chalcedony, all phases of similar hardness; they could only be extracted individually by chipping the mixed silica from each sample in small enough pieces to allow selection of chips of different coloured silica. To homogenise the samples, each was ground finely until it passed through a sieve of 180mesh (85μm). To ensure that there was no contamination from carbonate veins, crystals or spherules, each homogeneous powder was treated with 10% HCl acid solution and heated gently (20°C) overnight. After several washes with de-ionised water to remove all of the acid, sample purity was confirmed by XRD analyses.

3.3.2 Pyrite: Sample Collection and Preparation

Pyrite samples were collected from each different lithological type and occurrence that could be found in the quarry, resulting in thirty-four samples from ten lithological categories (Figure 6 & Table 2). Samples were also collected from three other lithologies of similar age, but with no likely hot spring influence: a pyrite nodule from a rootlet horizon exposed on the coast east of St Andrews, Fife; coarse pyrite cubes (3cm across) formed within organic rich strata of Goat Quarry, central Fife; and smaller cubes of pyrite (1cm) found at the Craigs Limestone of the Bathgate Hills, mapped as the stratigraphic equivalent of the East Kirkton Limestone. Where possible the pyrite was drilled from the samples, but often it was disseminated or too fine grained. In these cases the samples were crushed to disaggregate the pyrite from its matrix and the resultant coarse powder was acid treated to remove carbonate impurities (10% HCl, 20°C overnight) and then separated by heavy liquid (tetrabromoethane SG 2.8). The samples that had been mechanically separated were studied petrographically to observe any variation in grain size and crystal habit

that might affect the isotopic signature. In samples where it was possible to hand-pick pyrite crystals of two different habits, these were run as separate analyses but little isotopic difference was observed (see Table 2, and discussion below).

3.3.3 Oxygen extraction for $\delta^{18}O$ analyses

For total oxygen extraction from silica, the procedure followed was that developed by Clayton & Mayeda (1963). The reagent used was BrF_5, with the resultant oxygen converted to CO_2 by reaction with a hot, platinised graphite rod. Twenty samples were run using this method and duplicate analyses give an analytical precision (1σ) of ±0.5‰; standards of NBS28 quartz gave $\delta^{18}O$ within the limits of analytical precision, the same as the standard value of 9.6‰(SMOW). The notation used for isotopic analyses is parts per thousand (per mil, ‰) difference from Standard Mean Ocean Water (SMOW, $\delta^{18}O$ of 0‰).

3.3.4 Hydrogen extraction for δD analyses

Hydrogen was extracted (Friedman,1953), by heating in a previously degassed Pt crucible to >1200°C to release the structurally bound water. This was then cryogenically purified to remove CO_2 and non-condensibles, and converted to hydrogen upon reaction with uranium at 700°C. The same twenty samples were used for hydrogen as for oxygen extraction to allow direct comparison of results. During preliminary analysis of these samples organic matter was considered as a factor that could affect isotopic analysis of the hydrogen gas. To prevent this, several samples were plasma ashed prior to extraction but resultant values of δD and yields of gas were more erratic than for those analysed without pre-treatment. Four standards of DW2 [0‰(SMOW)] were run with the East Kirkton samples and they gave values within the range of analytical precision (1σ) obtained from duplicate analyses, ±5.0‰ and ±0.02wt.% for H_2O^+ yield.

3.3.5 Sulphur extraction for $\delta^{34}S$ analyses

Pyrite samples were converted to SO_2 by reaction with excess Cu_2O following the method developed by Robinson & Kusakabe (1975). Forty-seven samples were analysed, including three duplicates, and fourteen standard analyses completed for three standards (CP1/1 chalcopyrite -4.56‰, NBS123 sphalerite +16.6‰ and Z-40 sphalerite 25.6‰). The analyses gave results that were within ±1.0‰(CDT) analytical precision (1σ)

of the standard values. For $\delta^{34}S$ analyses the reference standard, taken as $\delta^{34}S$=0‰, is troilite from the Canyon Diablo Meteorite (CDT).

3.4 RESULTS

3.4.1 Silica

For twenty silica samples, of phases petrographically described in sections 1.1 and 1.2, $\delta^{18}O$ was measured for structural oxygen and δD for bound water. $\delta^{18}O$ varied between +21 and +27‰ (Figure 5a); when the isotopic results are compared with the petrographic groupings, no correlation is observed. This suggests that the $\delta^{18}O$ for each silica phase originated from (i) a fluid with similar $\delta^{18}O$ and same T, (ii) a fluid with similar $\delta^{18}O$ and slightly variable T, or (iii) a fluid with slightly variable $\delta^{18}O$ with similar T (Figure 5a). From the proposed palaeoenvironment, fluctuations in temperature and $\delta^{18}O$ are expected, but observed variation in $\delta^{18}O$ in silica cannot be ascribed to one of these causes unambiguously. The range in δD was from -50 to -100‰ (Figure 5b) with lower values (-75 to -90‰) characterising replacive or altered silica and higher values (-50 to -75‰) from primary chert samples (Table 1). The water contents of both petrographic groups were similar (0.35±0.02 to 1.10±0.02 wt% H_2O). A plot of $\delta^{18}O$ versus δD (Figure 7), for the primary silica phases, defines a grouping about the line defined by Scottish agates (Fallick *et al*, 1985); samples of the secondary phases fall consistently below this line.

3.4.2 Pyrite

The range of values measured for $\delta^{34}S$ in pyrite varied widely from +12 to -36‰ (Figure 6 & Table 2). From the data set several groupings related to lithological types can be picked out: samples associated with wood/organic matter, range from -26 to -36‰; nodular pyrite and associated shale, mostly span -12 to -24‰; and pyrite from within primary chert laminae, generally varies from +6 to -2‰. However, pyrite from other lithologies cannot be simply grouped, and can show a large spread of $\delta^{34}S$, for example, pyrite in volcanic rocks exhibit a range of $\delta^{34}S$ from +9.4‰ to -34.4‰.

3.5 DISCUSSION.

3.5.1 Oxygen isotopic analyses and their implications for formation temperature.

If silica is precipitated in isotopic equilibrium with its parental fluid, the $\delta^{18}O$ of the silica is a function of the $\delta^{18}O$ of the fluid and the temperature of precipitation. If there is no independent evidence of $\delta^{18}O$ or temperature available for this fluid (eg. fluid inclusion measurements) the interpretation of $\delta^{18}O$ for the silica becomes model dependent.

Studying nodular and bedded cherts, Knauth & Epstein (1976) concluded that (i) samples contained water as hydroxyl groups (-OH), (ii) δD_{water} and $\delta^{18}O_{silicate}$ are preserved with time, (iii) meteoric waters were involved in the crystallisation of many cherts (since the bands obtained from δD and $\delta^{18}O$ data were parallel to the MWL) and (iv) variations were interpreted as reflecting changes in the Earth's surface temperature - the higher the temperature at which isotopic exchange occurs the less the isotopes will be fractionated. Retention of an original δD signature, in cherts, was confirmed by work on deep sea deposits (including chalcedony) by Knauth & Epstein (1975) and Kolodny & Epstein (1976). This basic picture has been refined by Fallick *et al* (1985), in their work on agates, a silica form probably less susceptible to post-precipitation alteration.

Typical $\delta^{18}O$ published for other occurrences of inorganic silica include +9‰ for high temperature igneous quartz (Taylor,1968) forming from granitic magma; quartz from hydrothermal fluids, +14 to +16‰ (Levitan *et al.* 1975) forming at temperatures around 250°C; and siliceous sinter, +23‰ deposited at surface by steam discharge (55-60°C) (Clayton & Steiner, 1974). In each case the control of $\delta^{18}O_{(Qtz)}$ remains $\delta^{18}O_{(fluid)}$ and precipitation temperature (assuming equilibrium). The isotopic composition of crustal fluids is discussed in detail by Sheppard (1986). Primarily magmatic fluids have $\delta^{18}O$ values of about +5.5 to +9.5‰; meteoric fluids have negative $\delta^{18}O$ values which decrease as latitude increases; and geothermal fluids, identified as predominantly meteoric water, have increased $\delta^{18}O$ values due to water/rock interactions.

Using the formula (Matsuhisa *et al*, 1979):-

$$\delta^{18}O_{Qtz} - \delta^{18}O_{H2O} = \frac{3.34 \times 10^6}{T^2(K)} - 3.31$$

temperature can be calculated from measured $\delta^{18}O$, assuming $\delta^{18}O_{(H20)}$. However, what this calculated temperature represents, in the case of chert, is less well understood. Bedded chert is thought to be precipitated on mixing and/or cooling of a siliceous solution with the lake waters. Petrographically the silica in the chert laminae appears to have been deposited in a form allowing soft-sediment deformation. At this stage silica, in contact with lake waters, could continue to cool from the temperature at which it was initially precipitated.

A temperature of about 60°C was calculated for the "agate line", see Fallick *et al*, (1985). The data for East Kirkton primary silica plot around this line implying precipitation at a similar temperature from meteoric water (see Figure 7 and detailed discussion of δD and fluids below). However, this may not reflect the actual precipitation temperature for the silica, as it is not known at which stage in the mixing and/or cooling process the isotopic signature is fixed. It could be that the calculated temperature represents a transition from a mechanically soft state to hardened, brittle silica, a process supported by petrographic observations (McGill *et al*, 1990) e.g. the transition from amorphous silica to microcrystalline quartz. Figure 8, is a plot of temperature versus $\delta^{18}O_{(H2O)}$ for the range in values of $\delta^{18}O_{(Qtz)}$ at East Kirkton, for both primary and secondary silica. The range of values for $\delta^{18}O_{(H2O)}$ in figure 8 as chosen to encompass all likely waters from which the silica could have been precipitated. The temperatures of precipitation that are obtained for the East Kirkton $\delta^{18}O_{(Qtz)}$, for Lower Carboniferous meteoric water with an expected value of -3‰, are between 50°C and 60°C. These values are similar to those calculated for the "agate-line", warmer than is typical for earth surface temperatures.

Figure 9 shows a plot of $\delta^{18}O$ versus δD, showing the "agate line" and the present day Meteoric Water Line. It also provides an estimate of values expected for $\delta^{18}O_{(Qtz)}$ precipitated from meteoric water, of Lower Carboniferous age at a temperature of around 20°C; the temperature at which the carbonate phases precipitated according to Irwin & Walkden, (1991). The silica results for δD and $\delta^{18}O$ correspond more closely to the higher temperature "agate line", indicating that the carbonate and silica phases have precipitated from fluids at different temperatures.

3.5.2 Hydrogen isotopic analyses and their implications for formation fluids.

Petrography clarifies the main reason for the two groupings of δD values. The higher δD values, obtained from primary, dark brown chert samples, range from -50 to -75‰. When these values are plotted against the $\delta^{18}O$ results (Figure 7), they group around a point on the "agate line" (Fallick *et al* 1985). Comparison with the "agate line" gives a minimum temperature estimate for the silica formation, as discussed above, but it can also provide evidence of the nature of fluids involved in silica precipitation at East Kirkton.

The "agate line" is almost parallel to the present day, global, meteoric water line which strongly suggests that the water from which the agates were derived had at least a component of meteoric water. The two fields outlined along this line are for Scottish Tertiary agates and Scottish Devonian agates (ibid); the Devonian agates were formed when Scotland was about 20° south of the equator (Tarling, 1983) and the Tertiary agates when Scotland was approximately at its present day latitude (ibid.).

The oxygen isotope fractionation factor between silica and meteoric water can be used to predict the composition of the original meteoric water from which the agates of the "agate line" formed, as discussed in Fallick *et al* (1985). Using the lowest grouping of values for each set of agate results minimises the chance of including results for fluids with a marine influence (Figure 7, Fallick *et al. op cit* for Devonian meteoric water and Taylor & Forester, 1971 for Tertiary meteoric water). Correspondingly for the East Kirkton data, it is possible to estimate the isotopic signature for the meteoric water from which the primary silica formed. The estimate for Lower Carboniferous meteoric water obtained from the East Kirkton data is $\delta^{18}O$ -3‰ and δD -15‰ this is consistent with temperatures discussed above.

The secondary/altered silica samples plot below the "agate line", due to low δD whilst the $\delta^{18}O$ values fall within the range of results for the primary chert. This appears to indicate that when the silica samples are undergoing alteration, $\delta^{18}O$ for chert is relatively unaffected but δD is changed, most likely by hydrogen isotope exchange with later fluids at low temperature. In one sample of white vug chalcedony, inhomogeneity was suspected when three $\delta^{18}O$ results varied by 4‰. The δD value was, however, readily duplicated and it is suspected that in this silica sample, which was clearly altered and quite porous, δD had already been completely reset and $\delta^{18}O$ alteration was incipient.

The hydrogen that is extracted for analyses from these silica phases is thought to occur as an hydroxyl group bound within the silica lattice possibly as silanole (Si-OH) (discussed in Fallick *et al*, 1985 and Fallick *et al*, 1987). It has recently been established for kaolinite, that H of -OH groups can be isotopically exchanged with no apparent shift in $\delta^{18}O$ (Longstaffe & Ayalon, 1990). The lower δD values for the East Kirkton altered/replaced chert are consistent with hydrogen isotope exchange occurring more readily than $\delta^{18}O$ in cherts, similar to the results observed for kaolinite. The scatter of these results is more comparable with data for cherts (Knauth & Epstein, 1976) than agates (Fallick *et al*, 1985, 1987).

3.5.3 Sulphur isotope analyses

The histogram of $\delta^{34}S$ (Figure 6) shows a broad spread for the East Kirkton pyrite samples. Many of the individual lithological occurrences give widely variable values but for "wood", "nodules in shale", and "primary chert laminae", results define relatively narrow ranges.

The most likely source of isotopically light sulphur (-10‰ to -40‰) in *all* lithologies is from open system bacteriogenic reduction of sulphate (Figure 10, after Nielsen, 1979), which has a fractionation of between 30‰ and 60‰ from the parent sulphate. The extent of fractionation is controlled by (i) availability and type of organic matter; (ii) the type of bacteria, and, most dramatically, (iii) the availability of sulphate.

Differences in $\delta^{34}S$ ranges, for example, between "wood" samples ($\delta^{34}S$ -26 to -36‰) and "nodules and their background shale" (generally from -12 to -24‰) probably relate to variations in the availability and type of organic matter (Briggs *et al*, 1991), although differences in bacteria type cannot be discounted, given the very distinct environments of precipitation (Kaplan and Rittenberg, 1964). In any case, bacteriogenic reduction would imply that the $\delta^{34}S$ value of the original sulphate was positive, i.e. ≥0‰. What was the source of this sulphate? The East Kirkton lithology is non-marine, but two potential sources of marine sulphate were available: (a) the overlying West Kirkton and Petershill Limestone are fully marine, and it can be envisaged that sulphate could percolate downwards through the sediments; and (b) sulphate could be remobilized from underlying evaporite beds in the Lower Carboniferous Cementstone Group (especially in the Midland Valley, Anderton, 1985; Scott, 1986). Thus, by remobilisation, evaporitic SO_4^{2-} can be utilised (as the dominant source of SO_4^{2-} in a meteoric system) even though the sequence

is non-marine. In either case, the $\delta^{34}S$ of the sulphate would have been around +20‰ (Claypool *et al.* 1980 and Pattrick *et al.* 1983).

To explain the ^{34}S-enriched values, two potential processes can be envisaged. Firstly, when a bacteriogenic system is closed with respect to sulphate, then $\delta^{34}S$ of product sulphide can approach or exceed the $\delta^{34}S$ of the starting sulphate. It is possible that some of the higher pyrite $\delta^{34}S$ resulted from this process because of the potential for sulphate depletion in this non-marine sequence (e.g. within the volcanic sequences), but the distribution of $\delta^{34}S$, and the absence of pyrite $\delta^{34}S$ approaching or exceeding a parent sulphate value of +20‰ suggests that closed system reduction of such marine sulphate was not a significant process (Ohmoto & Rye, 1979). However, for such a variable and sporadic occurrence of pyrite as found at East Kirkton, isotopic fractionation corresponding to closed system sulphate reduction might be expected, and an appropriate $\delta^{34}S$ value for original sulphate would have to be near the heavy range of the measured values for the pyrite, i.e. about 0‰. Such sulphate could have been produced by the oxidation during weathering of magmatic sulphide in the local volcanics.

The second group of ^{34}S-enriched values particularly relates to the range of $\delta^{34}S$ for "primary chert laminae" from +6 to -2‰, clustering around 0‰ (Figure 6). Chert laminae-hosted pyrite is found in an environment where the occurrence of pyrite precipitated from hydrothermal sulphide would not be surprising - and it is notable that the sulphide here is isotopically distinct from the general background bacteriogenic signature. It is possible that the source of this sulphur could have been magmatic (0±3‰, Ohmoto, 1986) and leached from local volcanic lithologies by the hydrothermal system.

It is not possible to conclusively identify the sulphur source or conditions of pyrite formation from these results. However bacteriogenic reduction of sulphate to sulphide, may be inferred for the lightest $\delta^{34}S$ results in samples associated with organic material but the distribution in $\delta^{34}S$ values makes it unlikely that the sulphur is solely from a Lower Carboniferous seawater source.

3.6 CONCLUSIONS

1. In accordance with the findings of Geikie (1861) it is considered that the silica laminae are a primary feature and a result of hot spring influence in the lagoon.

2. Formation of the silica was from meteoric water, $\delta^{18}O$ around -3‰, δD around -15‰, at a temperature of about 60°C, this represents a minimum temperature for the siliceous fluids.

3. Observed petrographic divisions between primary silica and altered/replacive silica phases are confirmed by results of the δD analyses forming two groups, the higher group correlating with the primary chert laminae and the lower group corresponding to samples that appeared petrographically to be replacive or altered.

4. Pyrite, especially associated with plant material, is isotopically light indicating its formation involved bacterial sulphate reduction.

5. Isotopic groupings for pyrite in nodules and chert rule out closed system marine sulphate reduction. Pyrite in primary chert varies mostly from +6 to -2‰ possibly indicating a direct, magmatic/hydrothermal source for the sulphur.

3.7 ACKNOWLEDGEMENTS

This research forms part of a NERC. CASE postgraduate studentship supported by the National Museums of Scotland and co-supervised by Dr W. D. I. Rolfe. Isotopic analysis was completed at the SURRC, East Kilbride with much assistance from the very patient laboratory staff. Samples from Goat Quarry were obtained by Gordon Todd, and J. Jocelyn was also most helpful with comments, references and practical assistance in the mechanical separation of sulphide samples for $\delta^{34}S$ analysis. The Isotope Geology Unit at SURRC is supported by NERC and the Scottish Universities. A. J. Boyce was supported by NSS and seconded to SURRC from NIGL.

3.8 BIBLIOGRAPHY

Anderton, R. 1985. Sedimentology of the Dinantian of Foulden, Berwickshire, Scotland. TRANS. R. SOC. EDINBURGH: EARTH SCI. **76**, 7-12.

Briggs, D. E. G., Bottrell, S. H. & Raiswell, R. 1991. Pyritisation of soft-bodied fossils: Beecher's trilobite bed, Upper Ordovician, New York State. GEOLOGY **19**, 1221-1224.

Claypool, G. E. , Holster, W. T., Kaplan, I. P., Sakai, H. & Zak, I. 1980. The age curves of sulphur and oxygen isotopes in marine sulphate and their mutual interpretation. CHEMICAL GEOLOGY **28**, 199-260.

Clayton, R. N. & Mayeda, T. K. 1963. The use of bromine pentafluoride in the extraction of oxygen from oxides and silicates for isotopic analysis. GEOCHIM COSMOCHIM ACTA **27**, 43-52.

Clayton, R. N. & Steiner, A. 1974. Oxygen isotope studies of the geothermal system at Wairakei, New Zealand. GEOCHIM COSMOCHIM ACTA **39**, 1187-1192.

Fallick, A. E., Jocelyn, J., Donnelly, T., Guy, M. & Behan, C. 1985. Origin of agates in volcanic rocks from Scotland. NATURE **313**, 672-674.

Fallick, A. E., Jocelyn, J., & Hamilton, P. J. 1987. Oxygen and hydrogen stable isotope systematics in Brazilian agates. *In* Rodriguez-Clemente, R. & Tardy, Y., (ed.) *Geochemistry and mineral formation in the earth surface*, 99-117. Madrid: CNRS, Paris: CSIC.

Friedman, I. 1953. Deuterium content of natural waters and other substances. GEOCHIM COSMOCHIM ACTA **4**, 89-103.

Geikie, A. 1861. *In* Howell, H. H. & Geikie, A. *The geology of the neighbourhood of Edinburgh: Memoirs of the Geological Survey of the United Kingdom* 1-151.

Grinenko, V. A. 1962. Preparation of sulfur dioxide for isotopic analyses. Z. NEORGAN. KHIMII. **7**, 2478-2483.

Hibbert, S. 1836. On the fresh-water limestone of Burdiehouse. TRANS R SOC EDINBURGH: EARTH SCI **13**, 167-282.

Irwin, R & Walkden, G. M. 1991. Pouring cold water on the East Kirkton hot spring. *Abstracts 30th Annual Meeting BSRG.*

Kaplan, I. R. & Rittenberg, S. C. 1964. Microbiological fractionation of sulphur isotopes. J. OF GENERAL MICROBIOLOGY **34**, 195-212.

Knauth, L. P. & Epstein, S. 1975. Hydrogen and oxygen isotope ratios in silica from the JOIDES deep sea drilling project. EARTH AND PLANETARY SCIENCE LETTERS **25**, 1-10.

Knauth, L. P. & Epstein, S. 1976. Hydrogen and oxygen isotope ratios in nodular and bedded cherts. GEOCHIMICA ET COSMOCHIMICA ACTA 40, 1095-1108.

Kolodny, Y. & Epstein, S. 1976. Stable isotope geochemistry of deep sea cherts. GEOCHIM COSMOCHIM ACTA **40**, 1195-1209.

Levitan, M. A., Dontsova, E. I., Lisitsyn, A. P. and Bogdanov, Yu. A. 1975. The origin of chert in the sediments of the Pacific Ocean from data of oxygen isotopic analysis and a study of the distribution of chert. GEOCHEMISTRY INTERNATIONAL. **12**, 95-104.

Longstaffe, F. J. & Ayalon, A. 1990. Hydrogen isotope geochemistry of diagenetic clay minerals from Cretaceous sandstones, Alberta, Canada: evidence for exchange. APP GEOCHEM 5, 657-668.

Matsuhisa, Y., Goldsmith, J.R., and Clayton, R.N. 1979. Oxygen isotope fractionation in the system qtz-albite-anorthite-water. GEOCHIM COSMOCHIM ACTA **43**, 1131-1140.

McGill, R.A.R., Hall, A.J., Braithwaite, C.J.R., Fallick, A.E. & Rolfe, W.D.I. 1990. Petrography & geochemistry of a L. Carboniferous, lacustrine, hot-spring deposit, East Kirkton, Bathgate, Scotland. PROC 12TH NEW ZEALAND GEOTHERMAL WORKSHOP 203-208.

Milliken, K. L. 1979. The silicified evaporite syndrome - Two aspects of silicification history of former evaporite nodules from Southern Kentucky and Northern Tennesse. J SED. PETROL **49**, 245-256.

Muir, R. O. & Walton, E. K. 1957. The East Kirkton Limestone. TRANS GEOL SOC GLASGOW **12**, 157-168.

Nielsen, H. 1979. Sulphur isotopes. *In* Jager, E & Hunziker, J. C. *Isotope geology*. 283-312. Springer-Verlag, Berlin, Heidelberg, New York.

Ohmoto, H. 1986. Stable isotope geochemistry of ore deposits. *In* Valley, J. W., Taylor, H. P. Jr. & O'Neil, J. R. (eds.) *Stable isotopes in high temperature geological processes*. vol. **16**, 491-560. Min. soc. of America, Book Crafters Inc. Chelsea, Michigan.

Ohmoto, H. & Rye, R. O. 1979. Isotopes of sulfur and carbon. *In* Barnes, H.L. *Geochemistry of hydrothermal ore deposits*, 2nd. Edition, 509-567. New York: J. Wiley & Sons.

Pattrick, R. A. D., Coleman, M. L. & Russell, M. J. 1983. Sulphur isotopic investigation of vein lead-zinc mineralisation at Tyndrum, Scotland. MINERAL. DEPOSITA **18**, 477-485.

Robinson, B. W. & Kusakabe, M.1975. Quantitative preparation of SO2 for 34S/32S analysis from sulphides by combustion with cuprous oxide. ANALYTICAL CHEMISTRY **47**, 1147-1181.

Rolfe, W.D.I., Durant, G.P., Fallick, A.E., Hall, A.J., Large, D.J., Scott, A.C., Smithson, T.R. & Walkden, G.M. 1990. An early terrestrail biota preserved by Visean volcanicity in Scotland. *In* Lockley, M. G. & Rice, A. (eds.) *Volcanism and fossil biotas.* Geol. Soc. America, Special Paper **244**, 13-24.

Rolfe, W.D.I., Durant, G.P., Baird, W.J., Chaplin, C., Paton, R.L. & Reekie, R.J. 1993. The East Kirkton Limestone, Lower Carboniferous, West Lothian, Scotland: introduction and stratigraphy. TRANS R SOC EDINBURGH: EARTH SCI [this volume].

Savin, S.M. & Epstein, S. 1970a. The oxygen and hydrogen isotope geochemistry of clay minerals. GEOCHIM ET COSMOCHIM ACTA **34**, 25-42.

Scott, W. B. 1986. Nodular Carbonates in the Lower Carboniferous, Cementstone Group of the Tweed Embayment, Berwickshire; evidence for a former sulphate evaporite facies. SCOTTISH JOURNAL OF GEOLOGY **22**, 325-345.

Sheppard, S. M. F. 1986. Igneous Rocks: III, Isotopic case studies of magmatism in Africa, Eurasia and oceanic islands. *In* Valley, J. W., Taylor, H. P. Jr. & O'Neil, J. R. (eds.) *Stable isotopes in high temperature geological processes.* vol. **16**, 319-371. Min. soc. of America, Book Crafters Inc. Chelsea, Michigan.

Smith, R.A., Stephenson, D. & Monro, S.K. 1993. The geological setting of the southern Bathgate Hills. TRANS R SOC EDINBURGH: EARTH SCI [this volume].

Tarling, D. H. 1983. *Palaeomagnetism, Principles and Applications in Geology, Geophysics and Archaeology,* Ch 9. Geological Applicatons, Fig 9.23, 292-293. London, New York: Chapman & Hall.

Taylor, H. P. Jr. 1968. The oxygen isotope geochemistry of igneous rocks. CONTRIB MINERAL PETROL **19**, 1-71.

Taylor, H. P. Jr. & Forester, R. W. 1971. Low-O-18 igneous rocks from the intrusive complexes of Skye, Mull, Ardnamurchan, Western Scotland. JOURNAL OF PETROLOGY **12**, 465-497.

3.9 Figure Captions.

Figure 1 Hand specimens of dark brown chert from East Kirkton; (A) thick silica lamina with carbonate spherules, (B) multiple silica laminae (C) isolated silica clast within volcanic material, (D) massive silica breccia with carbonate spherules in silica cement, (E) multiple silica laminae showing syn-sedimentary slumping, (F) photomicrograph (Plane Polarized Light (PPL), x3) showing syn-sedimentary slumping.

Figure 2 Photomicrographs exhibiting the textures that make the silica appear primary; (A) syn-sedimentary faulting, affecting individual layers (PPL, x4) ,(B) light coloured silica horizon cut by burrows, or algal filaments/bacteria, similar in texture to those cutting the carbonate spherules (PPL, x5), (C & D) laminae of silica and carbonate, with the crystals of carbonate suspended within the silica laminae as though forming a graded sediment (PPL and XPL, x4), (E) one single lamina in which the paler half (left) is fine grained silica and displays many delicate textures that cannot be observed in the other half (right) which is coarse grained carbonate (PPL, x4), (F) section through a plant stem showing original structure well preserved in silica (reflected light PPL, x10), (G) dark regular shaped organic remains of either fecal pellets or algae/bacteria preserved in detail in the silica laminae (PPL, x5), (H) same pellets showing how much more clearly the details, e.g. of banding, can be observed with Ultra Violet fluorescence (U.V. fluorescence, x10).

Figure 3 Hand specimen examples of replacive/altered silica from East Kirkton with two photomicrographs of silica spherules; (A) pale brown laminae breaking off laterally, into an ash horizon, (B) breccia of several silica phases, predominantly pale brown silica, with some of the darker brown chert also in the laminated material and early fractures infilled by white or blue banded chalcedony, later vein fillings are calcite, (C) stromatiform carbonate that has had vugs infilled by white chalcedony and has subsequently been replaced by grey textureless chert, (D) clear edged carbonate spherules surround a vug that has been infilled by radial zebraic chalcedony which encrusts the edges of the vug and forms a spherule centrally (XPL, x10), (E) in this sediment of predominantly volcanic ash several silica spherules were observed with a texture of concentric banding, similar to tree growth rings, these spherules were isotropic since

the silica is so fine grained these spherules often appear to have an eroded outer surface as occurs in the carbonate spherules (PPL, x4).

Figure 4 Hand specimen samples of lithologies from which pyrite was sampled, (A) stromatiform carbonate with occasional paler laminae of silica which contain small lenses of pyrite, (B) remains of plant material, often branches and trunks of trees, are the most common sites of pyrite formation, (C,D) nodules of pyrite occurring in shale and ash layers, (E) stromatiform carbonate nodules that contain disseminated pyrite, (F) carbonate breccia with an organic matrix that contains disseminated and framboidal pyrite.

Figure 5 $\delta^{18}O$ and δD composition of East Kirkton silica samples, frequency of occurrence of sample results within 0.5‰ intervals and 5.0‰ intervals, respectively. The key indicates to which petrographic type each symbol refers. For the δD histogram the results form two distinct groups, Group I are mostly samples thought to be primary and GroupII are mostly samples thought to be altered or replacive silica.

Figure 6 $\delta^{34}S$ composition of East Kirkton pyrite samples, frequency of occurrence of sample results within 2.0‰ intervals. A wide variety of lithologies contain pyrite, results were only observed to form groups for "fossil wood", "nodules in shale" and "primary chert laminae".

Figure 7 $\delta^{18}O$ versus δD plot of the East Kirkton silica data -with error bars- with a filled, black diamond motif for Group I primary silica samples and an open diamond motif for GroupII replacive or altered silica. Fields are also shown for agate data (Fallick *et al*, 1985) and data for Carboniferous vein chalcedony, Fife, unpublished SURRC data. The "Kaolinite line" (Savin & Epstein, 1970a) is shown for comparison to the "Agate line" (Fallick *et al*, 1985) around which lies the East Kirkton data; with calculated Devonian Meteoric Water (ibid.), Tertiary Meteoric Water (Taylor & Forester, 1971), and Carboniferous Meteoric water -as calculated from East Kirkton data- indicated on the meteoric water line.

Figure 8 Temperature versus $\delta^{18}O_{H_2O}$ calculated from the formula of Matsuhisa (1979) using a range of values for $\delta^{18}O_{H_2O}$ from +10 to -10‰, within which range the value of Carboniferous meteoric water was thought to lie, and a range of temperatures obtained for the $\delta^{18}O_{Silica}$

values of 24.85‰, the average of all the East Kirkton $\delta^{18}O$ data, 21‰ and 27‰ being the highest and lowest values obtained for the East Kirkton samples, thereby giving a range of temperatures and $\delta^{18}O_{H_2O}$ values within which the East Kirkton results must lie.

Figure 9 $\delta^{18}O$ versus δD plot showing the field for the East Kirkton primary silica data, Kaolinite line, Agate line, Meteoric water line, and the field for Standard mean ocean water (SMOW) and a fourth line which indicates the approximate position where the agate line and East Kirkton would plot if they had formed at about 20°C and thereby undergone greater fractionation.

Figure 10 Adapted from a figure in Neilsen (1979), showing ranges of $\delta^{34}S$ values for a variety of lithologies, providing a framework for comparison with the East Kirkton data.

Table 1 Petrographic description, $\delta^{18}O$, δD and wt% H_2O for East Kirkton silica samples.

Table 2 Paragenesis, pyrite crystal habit, extraction method and $\delta^{34}S$ for East Kirkton pyrite samples. The table also includes pyrite samples of Lower Carboniferous age from (i) a marine influenced environment (STA 10, from St. Andrews in Fife), (ii) a lacustrine environment (GQ1 & 2, from Goat Quarry, central Fife) and (iii) a lacustrine/marine? environment from Craigs Limestone in the Bathgate Hills often mapped as a lateral equivalent of East Kirkton.

Figure 1

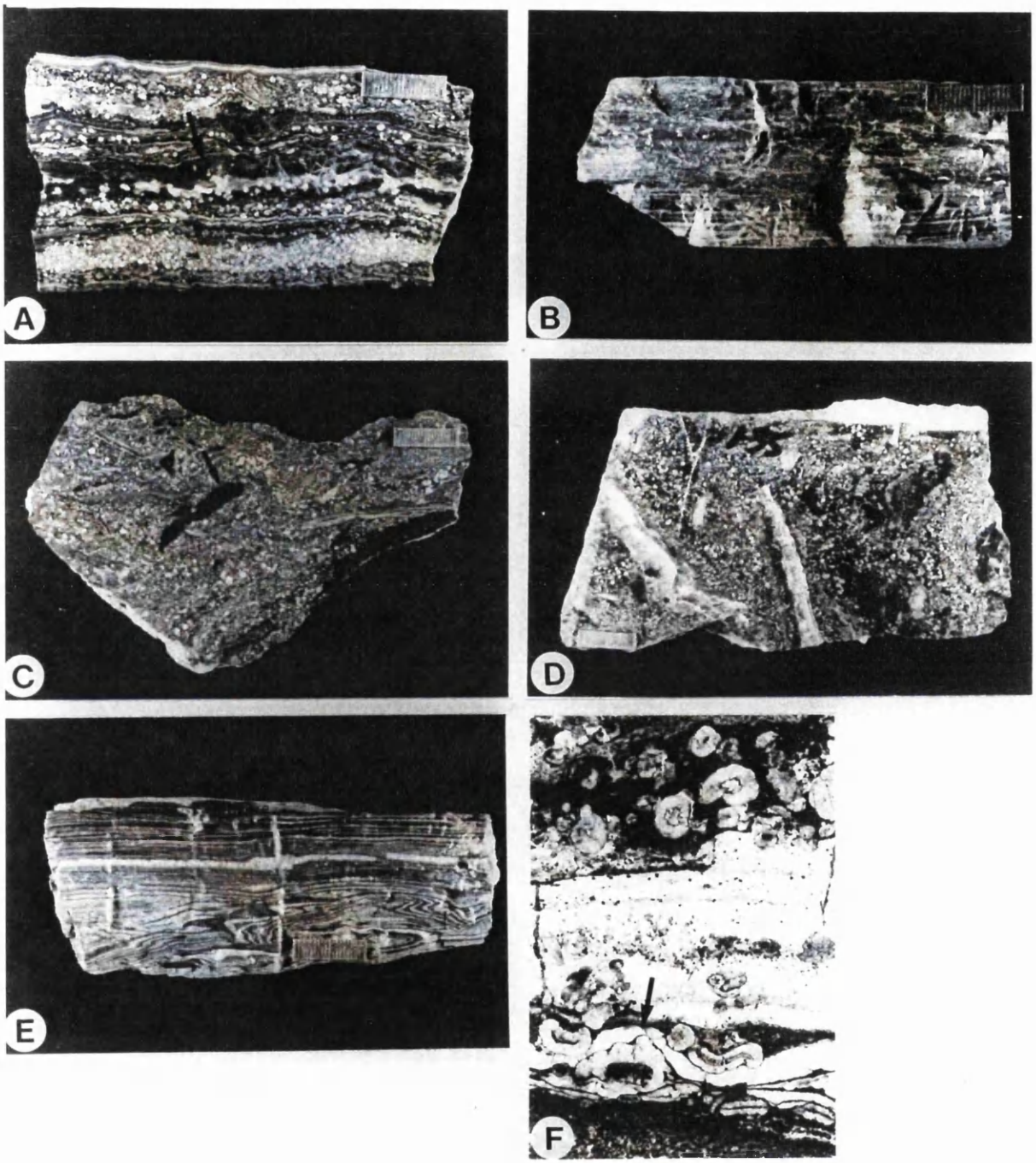

Figure 2

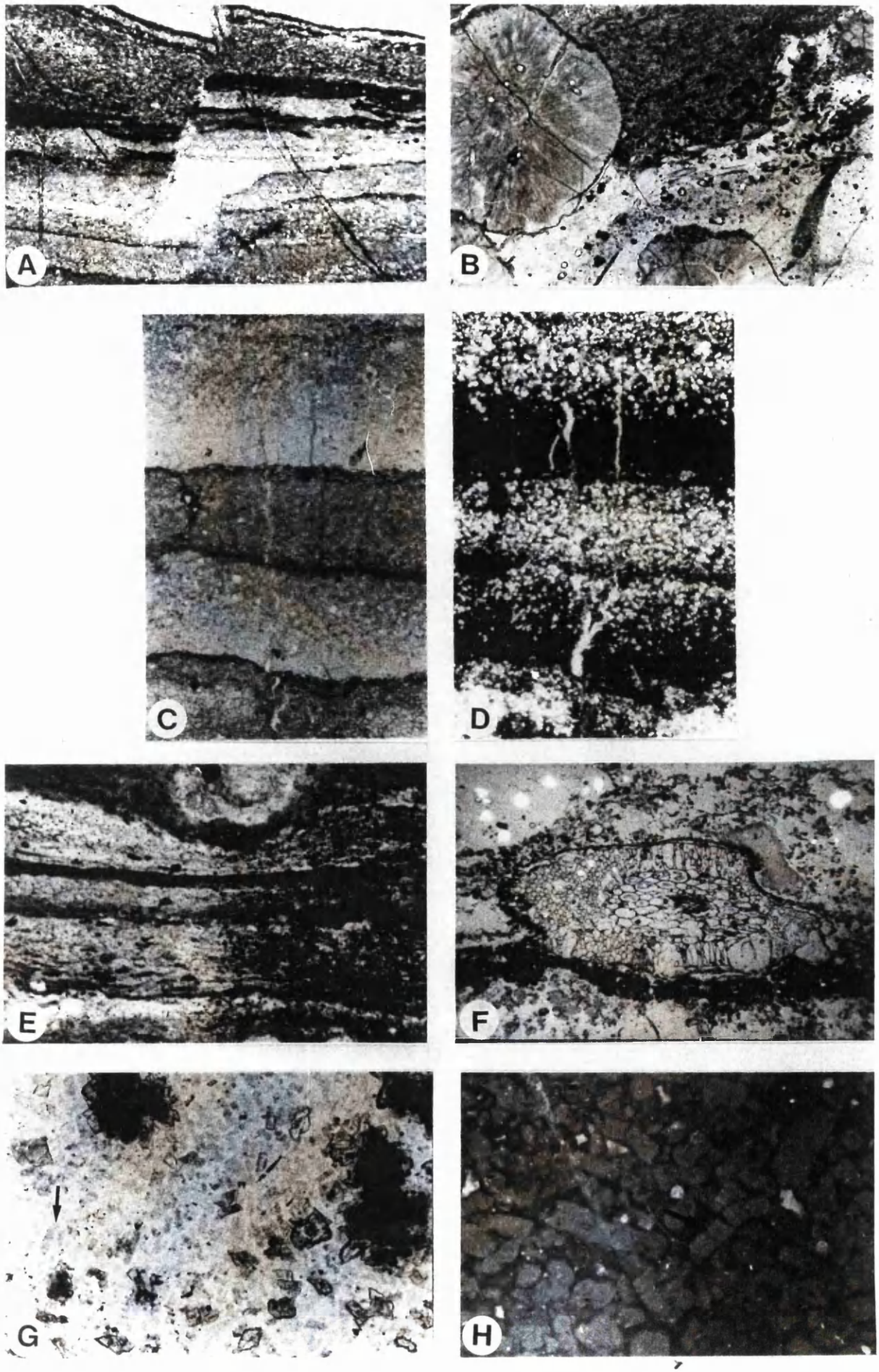

Figure 3

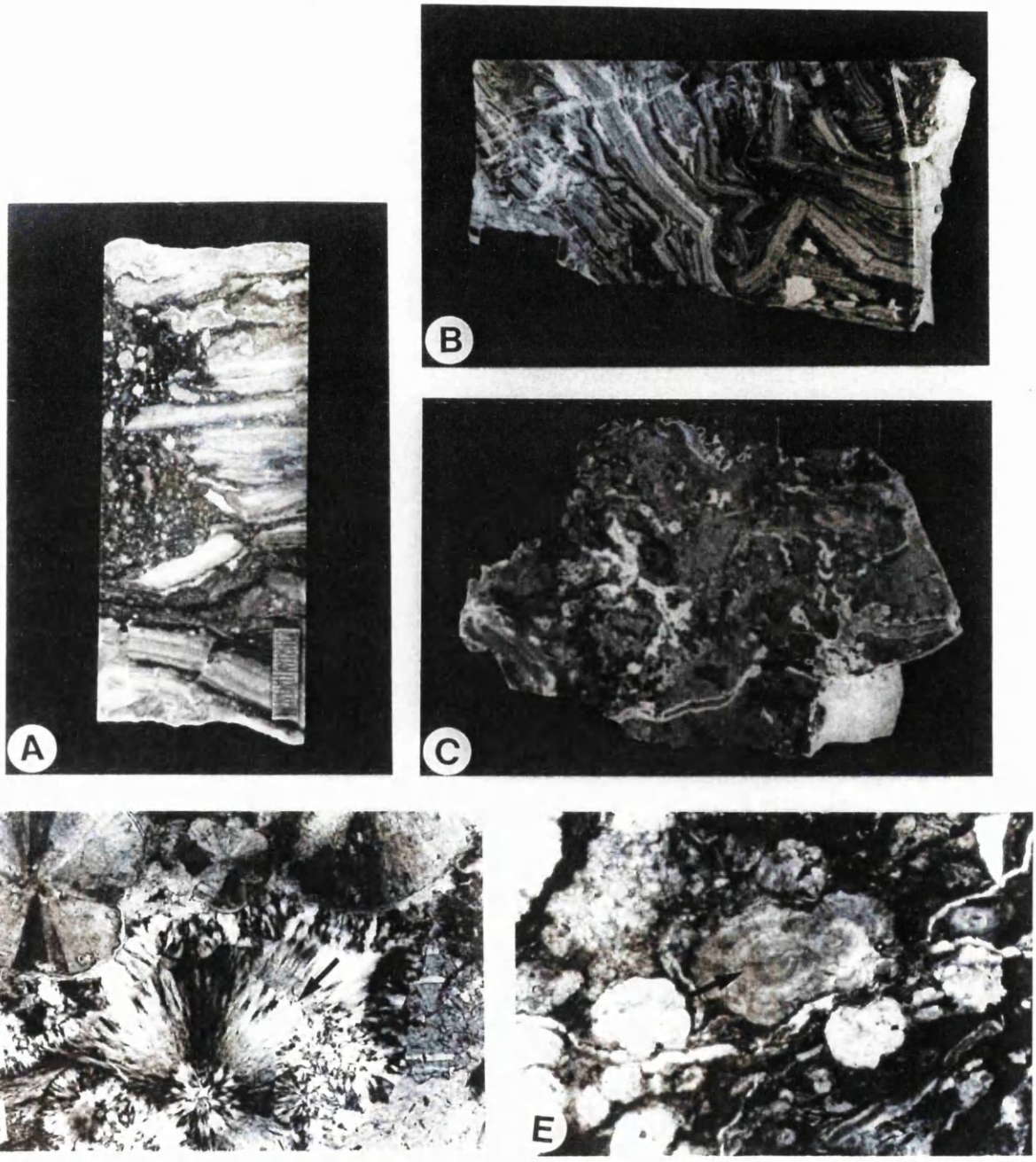

Figure 4

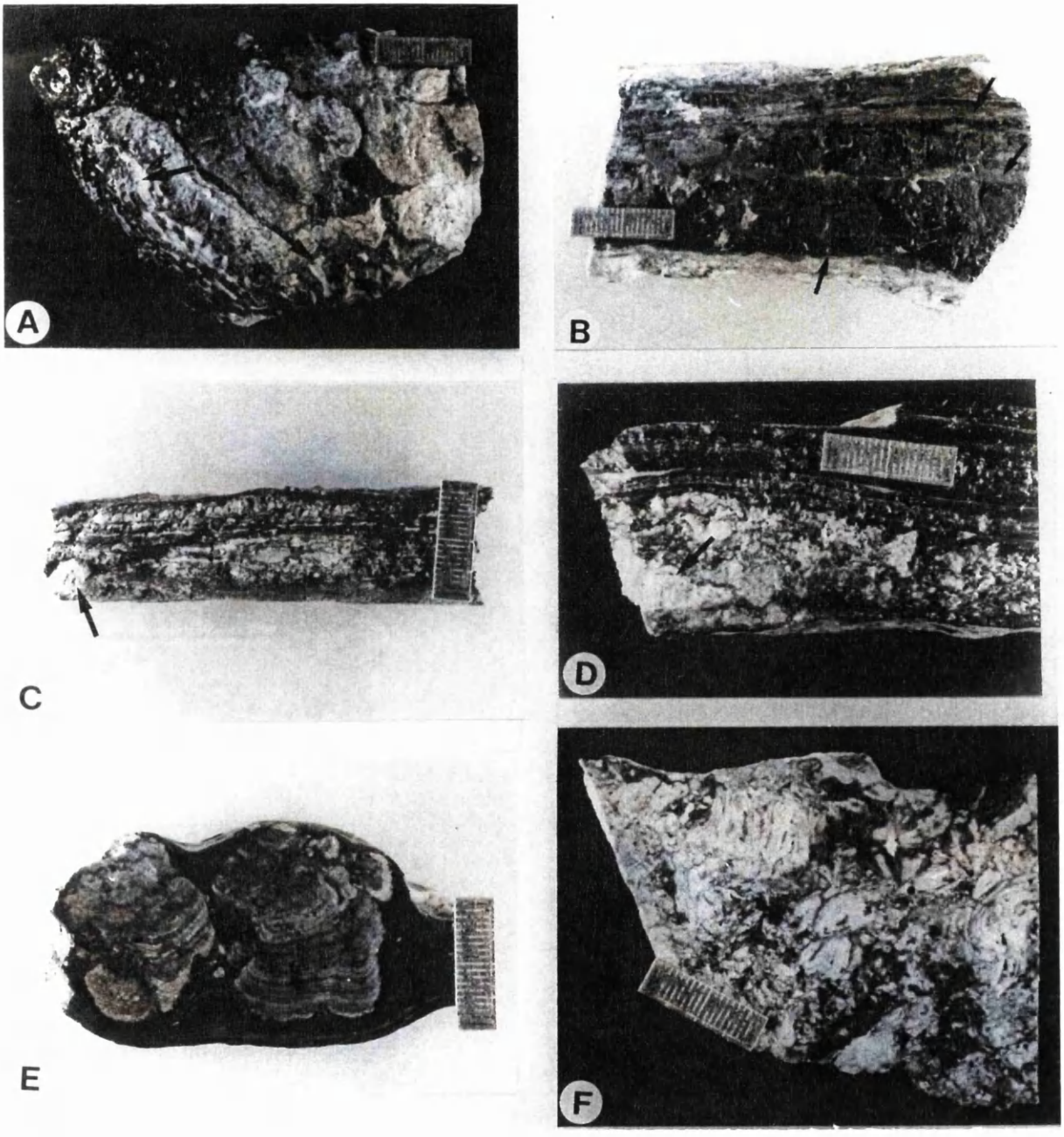

Figure 5

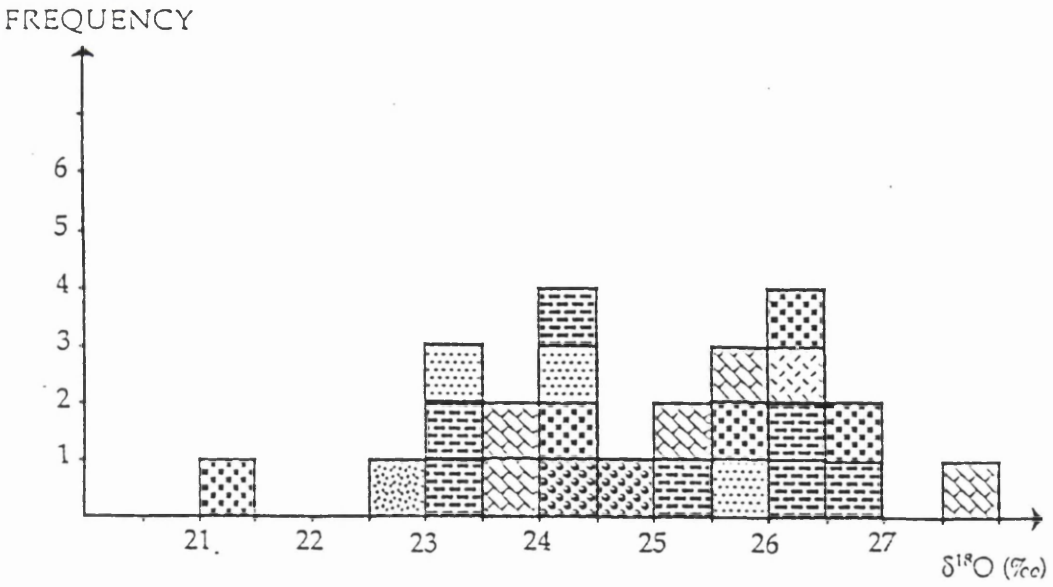

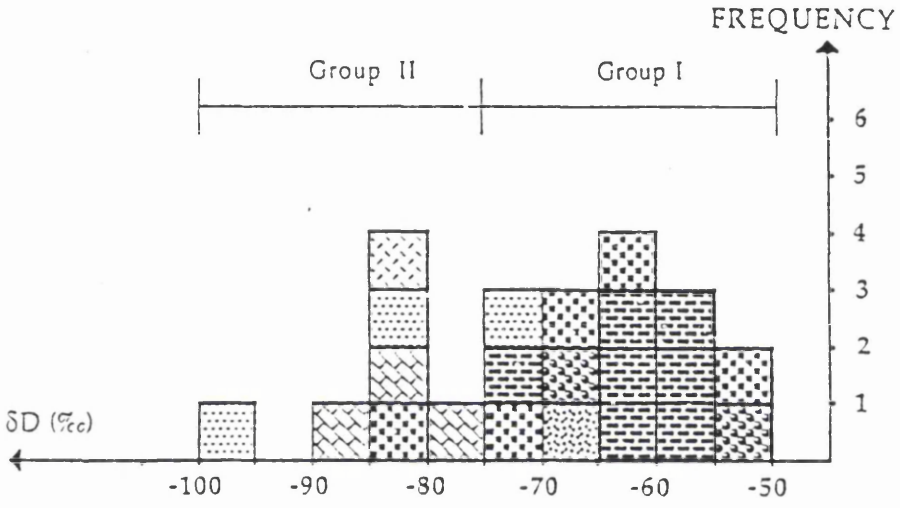

Key for $\delta^{18}O$ & δD frequency histograms.

CHERT CLASTS IN ASH

BANDED CHALCEDONY INFILLING VUGS

MULTIPLE, THIN CHERT LAMINAE

MILKY BROWN CHERT LAMINA

SINGLE, THICK CHERT LAMINA

MILKY GREY, PATCHY CHERT

MASSIVE AND BRECCIATED CHERT

Group I

Group II

Figure 6

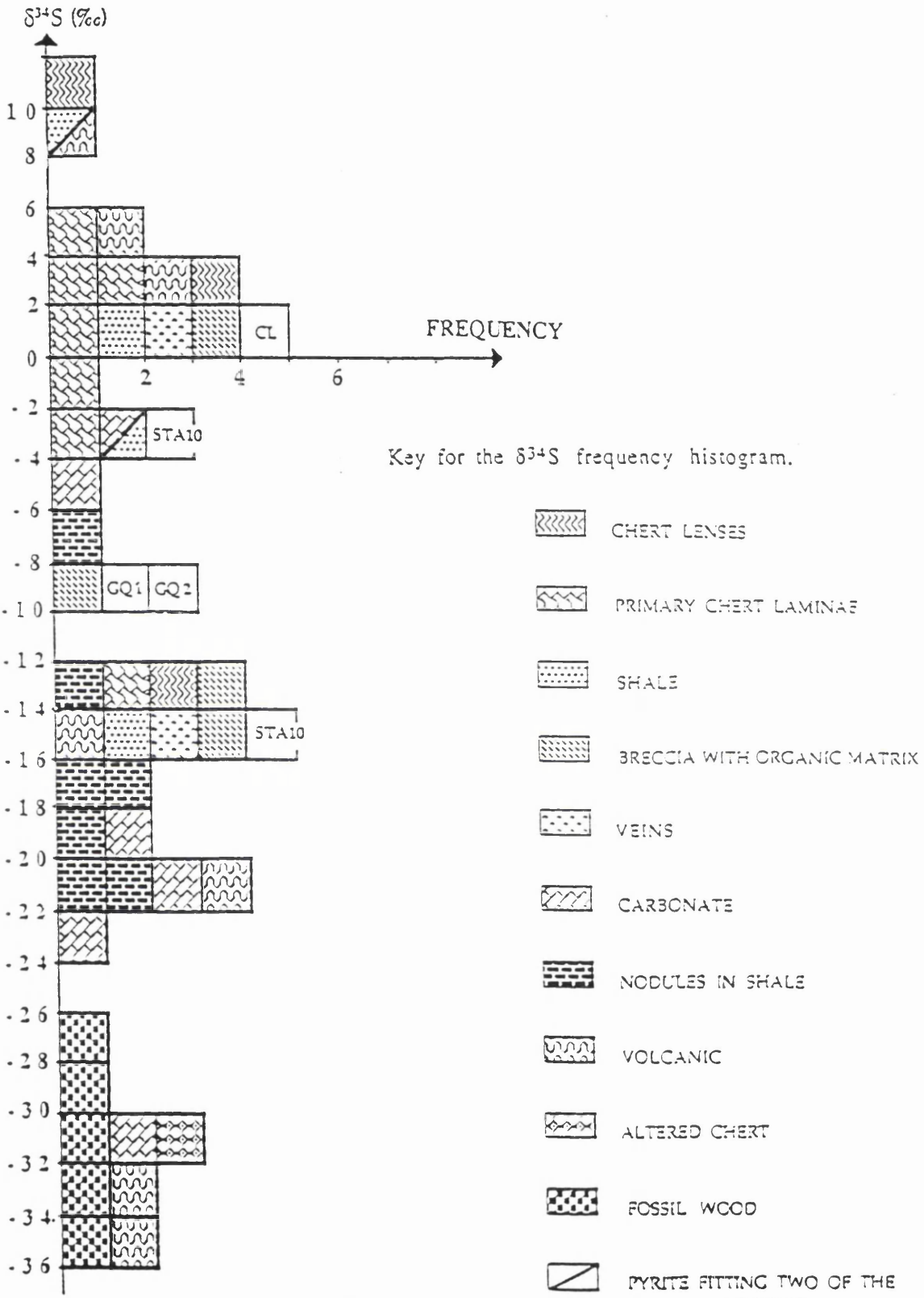
δ34S (‰)
10
8
6
4
2
0
-2
-4
-6
-8
-10
-12
-14
-16
-18
-20
-22
-24
-26
-28
-30
-32
-34
-36
2
4
6
FREQUENCY
CL
STA10
GQ1
GQ2
STA10
Key for the δ34S frequency histogram.
CHERT LENSES
PRIMARY CHERT LAMINAE
SHALE
BRECCIA WITH ORGANIC MATRIX
VEINS
CARBONATE
NODULES IN SHALE
VOLCANIC
ALTERED CHERT
FOSSIL WOOD
PYRITE FITTING TWO OF THE ABOVE CATEGORIES

Figure 7

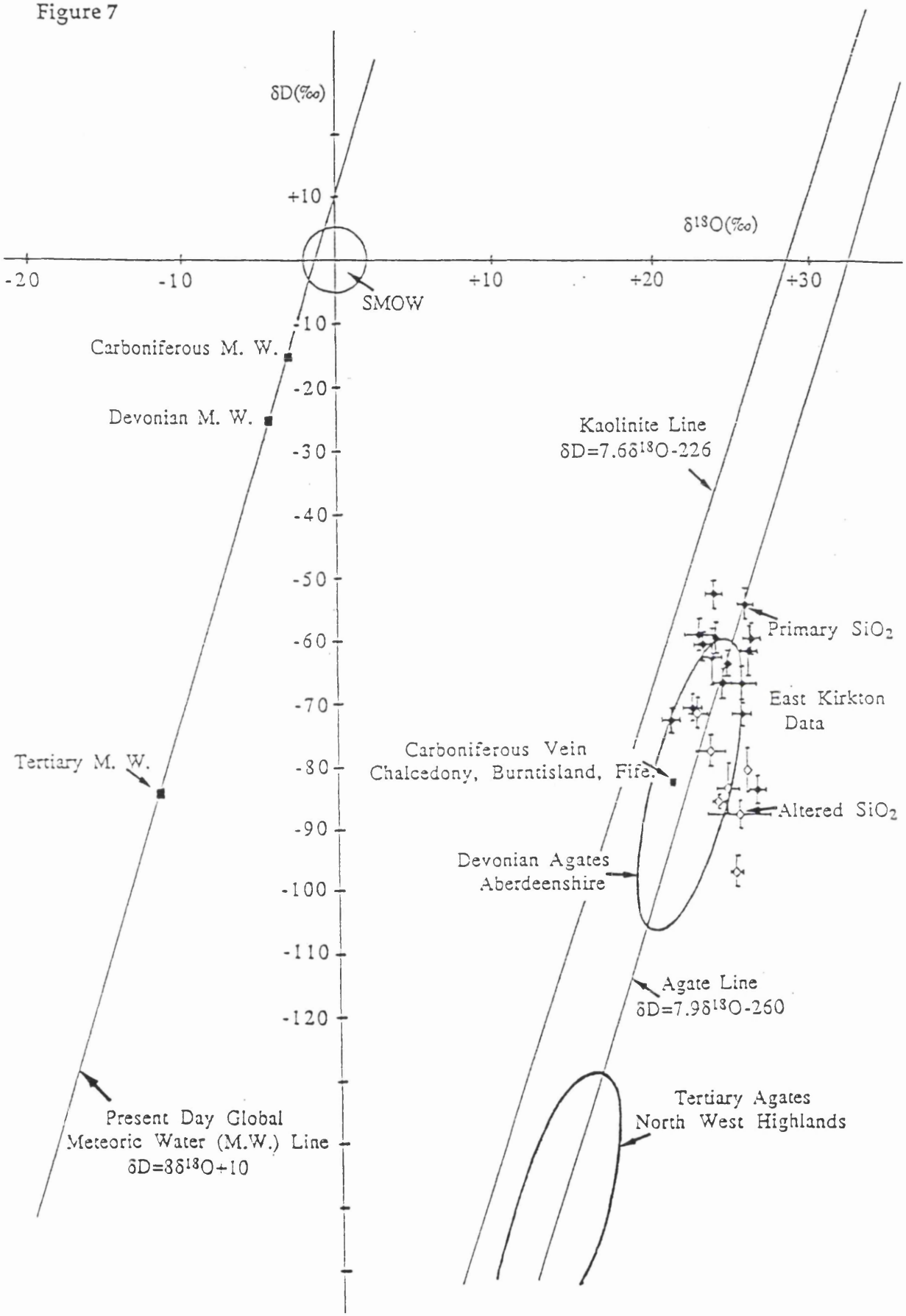
δD(‰)
+10
δ18O(‰)
-20
-10
+10
+20
+30
SMOW
-10
Carboniferous M. W.
-20
Devonian M. W.
-30
Kaolinite Line
δD=7.6δ18O-226
-40
-50
Primary SiO2
-60
East Kirkton
Data
-70
Tertiary M. W.
-80
Carboniferous Vein
Chalcedony, Burntisland, Fife.
Altered SiO2
-90
Devonian Agates
Aberdeenshire
-100
-110
Agate Line
δD=7.9δ18O-260
-120
Tertiary Agates
North West Highlands
Present Day Global
Meteoric Water (M.W.) Line
δD=8δ18O+10

Figure 8

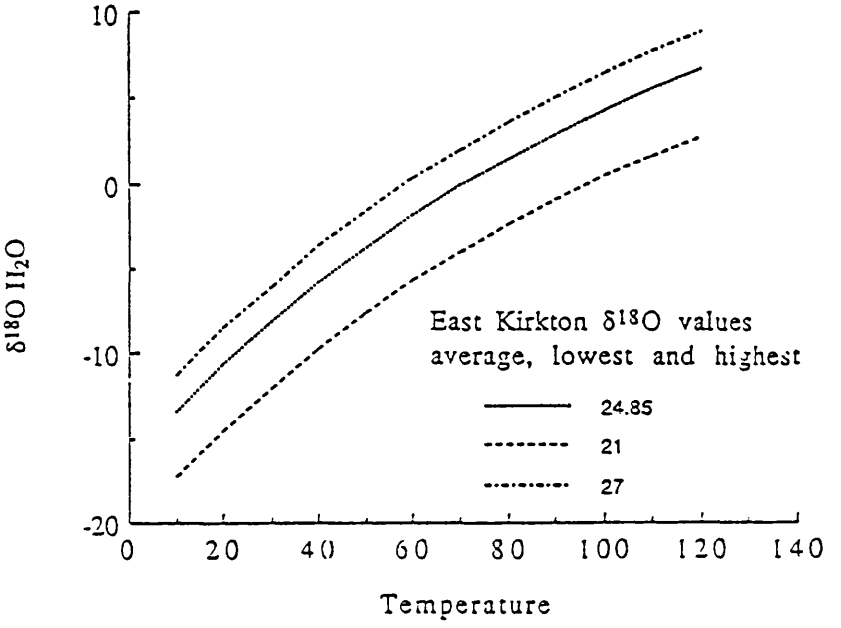
10
0
-10
-20
0
20
40
60
80
100
120
140
δ18O H2O
Temperature
East Kirkton δ18O values
average, lowest and highest
24.85
21
27

Figure 9

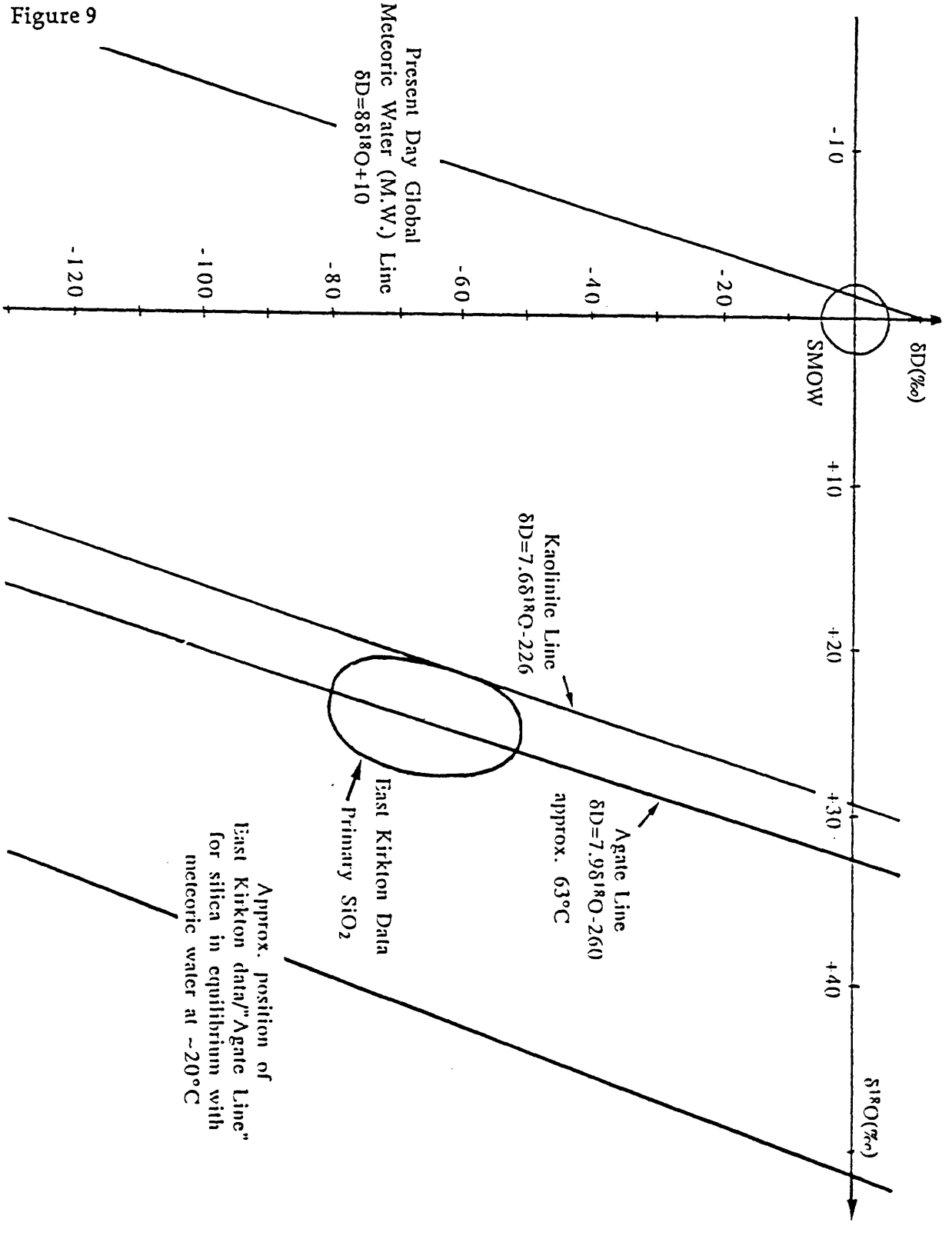
δD(‰)
-10
SMOW
-20
-40
-60
-80
-100
-120
Present Day Global
Meteoric Water (M.W.) Line
δD=8δ18O+10
+10
+20
+30
+40
δ18O(‰)
Kaolinite Line
δD=7.6δ18O-226
Agate Line
δD=7.9δ18O-260
approx. 63°C
East Kirkton Data
Primary SiO2
Approx. position of
East Kirkton data/"Agate Line"
for silica in equilibrium with
meteoric water at ~20°C

Figure 10

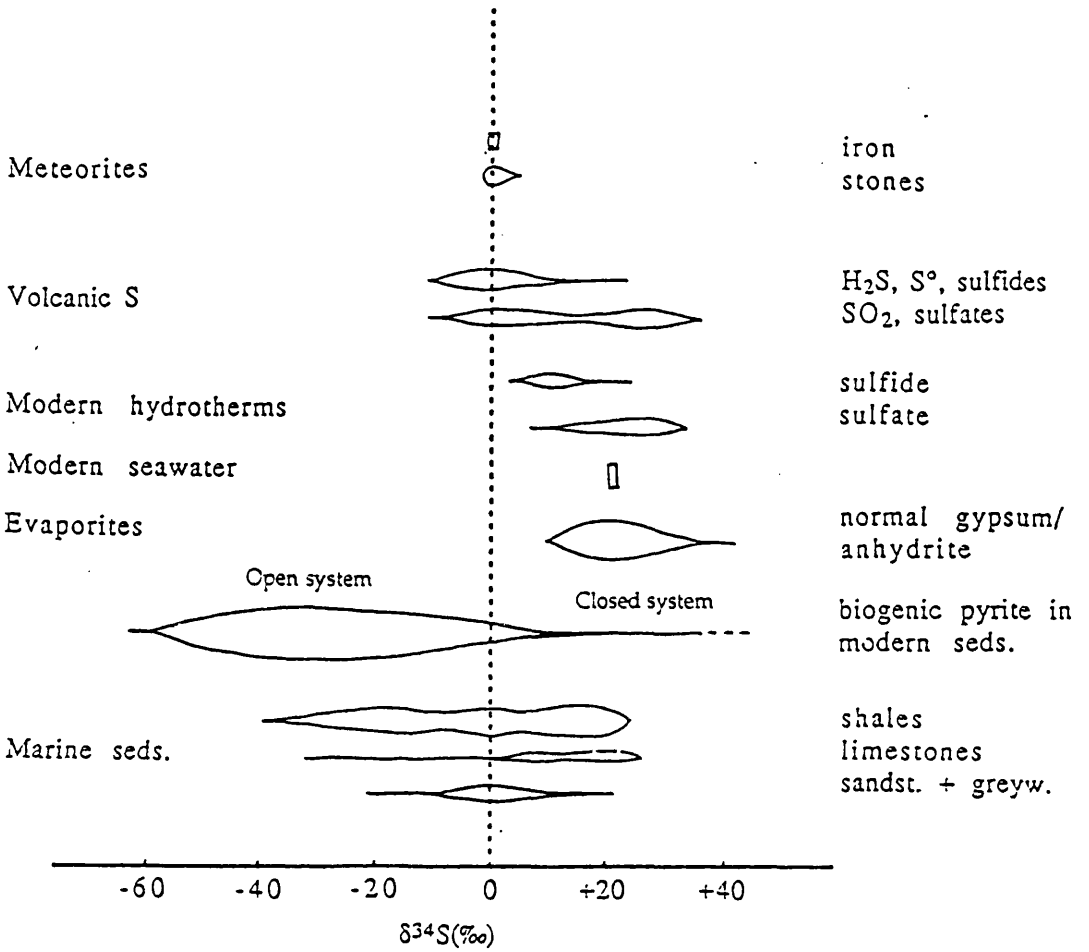
Meteorites
iron
stones
Volcanic S
H_2S, S°, sulfides
SO_2, sulfates
Modern hydrotherms
sulfide
sulfate
Modern seawater
Evaporites
normal gypsum/
anhydrite
Open system
Closed system
biogenic pyrite in
modern seds.
Marine seds.
shales
limestones
sandst. + greyw.
-60
-40
-20
0
+20
+40
$\delta^{34}S$(‰)

Table 1.

RESULTS OF $\delta^{18}O$ AND δD ANALYSES FOR EAST KIRKTON SILICA SAMPLES

Sample#	Description	$\delta^{18}O$(‰)	δD(‰)	wt% H_2O*
Primary silica samples				
EK11	thick layers and carbonate spherules	23.2±1.1	-59±5.0	0.35±0.02
1.39	thick layers and carbonate spherules	26.5±0.5	-58±5.0	0.34±0.02
2.30	thick layers and carbonate spherules	23.3±0.5	-60±4.0	0.80±0.02
2.60	thick layers and carbonate spherules	26.1±0.5	-71±2.8	0.76±0.01
2.79	thick layers and carbonate spherules	24.3±0.1	-59±4.8	0.84±0.01
2.14	thick layers with no spherules	26.4±0.5	-61±8.8	0.68±0.01
2.15	thick layers with no spherules	25.1±1.4	-63±4.6	0.66±0.01
86-29	multiple thin layers and carbonate spherules	26.0±0.5	-54±5.0	1.13±0.02
1.94	multiple thin layers with few spherules	26.9±0.5	-83±4.5	0.75±0.02
2.07	multiple thin layers, no spherules	21.3±0.5	-72±4.5	0.52±0.02
2.67	multiple thin layers, no spherules	25.9±1.1	-66±5.0	0.41±0.02
2.68	multiple thin layers, no spherules	24.0±0.6	-62±8.8	0.89±0.05
1.35	carbonate spherules in massive chert, laminated and brecciated	22.8±0.5	-70±3.9	0.44±0.02
2.59	chert clasts in ash	24.9±0.5	-66±13.4	0.47±0.02
2.61	chert clasts in ash	24.1±0.5	-52±5.0	0.44±0.02
Silica that appears late or replacive				
2.36	vug infillings	23.9±0.9	-77±5.0	0.83±0.03
2.66	vug infillings	25.1±0.7	-83±0.8	0.42±0.04
2.69(w)	vug infillings	23.88 25.69 27.74	-87±4.4	0.46±0.01
86-25	grey replacive chert	23.0±0.5	-71±5.0	0.49±0.02
2.36(m)	brown replacive chert	25.5±0.4	-96±5.3	1.02±0.02
2.69(b)	brown replacive chert	24.4±0.3	-85±2.0	0.56±0.02
2.83	milky brown chert	26.3±0.1	-80±6.9	0.54±0.02

*The analytical procedure is capable of precision of 0.02 wt% H_2O 1σ, variation greater than this on replicates are thought to reflect real sample inhomogeneity.

Table 2.
PYRITE SAMPLES FOR $\delta^{34}S$ ISOTOPE ANALYSES

Sample #	$\delta^{34}S$	Paragenesis	Pyrite crystal habit	Extraction method
Fossil Wood				
X1	-33.4	buff carb. with wood	fine grained lens	drilled
X51(i)	-35.4	fossil wood	v. fine grained lenses	drilled
X51(ii)	-26.9	" "	" " "	"
X51(iii)	-30.1	" "	" " "	"
88/1c	-29.7	fossil wood	fine grained lens	drilled
Nodules in Shale Matrix				
55/1	-13.6	shaley laminae, small, regular nodules (1cm)	v.fine grained	drilled
61a	-21.2	diffuse nodule in shale	shiny grains with framboids	heavy liquid /acid treated
61b(i)	-18.1	shale surrounding 61a	shiny grains with framboids	heavy liquid /acid treated
61b(ii) -	17.6	" " "	framboids, cubes and irregular grains	heavy liquid /acid treated
62(i)a	-17.6	nodule in shale + ash	shiny grains with smooth irregular surface	heavy liquid /acid treated
62(i)b	20.6	shale around 62(i)a	fine aggregate + cubes smooth irregular surface	heavy liquid /acid treated
62(ii)	-6.7	small nodule + shale	v. fine grained	heavy liquid /acid treated
2.09	-21.7	nodule + ash + shale	shiny grains with smooth irregular surface	heavy liquid /acid treated
Shale				
X25	1.8	dark shale	v. fine grained	heavy liquid
81	-14.9	organic shale	v. fine grained pyrite	heavy liquid
Carbonate				
X42(i)	-22.2	buff carb. nodule	cubes and shiny, sharp fragments	heavy liquid /acid treated
X42(i) [D]	-19.2			
X42(ii)	-31.1	" " "	skeletal cubes (2-3mm)	heavy liquid /acid treated
2.22	-4.6	buff carbonate	shiny bladed forms and cubes	heavy liquid /acid treated
2.28	-21.3	buff carbonate	shiny bladed forms	heavy liquid /acid treated
2.65(i)	-3.6	carbonate rich shale laminae	shiny aggregates with some crystal faces	heavy liquid /acid treated

Sample #	$\delta^{34}S$	Paragenesis	Pyrite crystal habit	Extraction method
Veins				
EK 59	-15.2	chert laminae (vein)	v. fine grained	drilled
2.12(clast)	1.6	volcanic clast (vein)	fine grained	drilled
Primary Chert Laminae				
X50	-0.9	chert laminae	v. fine grained	drilled
X52(ii)	0.6	chert laminae	v. fine grained lens	drilled
80(i)	-13.4	chert laminae	v. fine grained	drilled
2.30	3.7	chert laminae	octahedra + cubes	heavy liquid
2.30 [D]	4.2			
2.88	3.7	chert + shale laminae	v. fine grained	drilled
Poster 1	-2.0	chert laminae	octahedra + cubes	heavy liquid /acid treated
Chert lenses				
X40	2.6	chert lenses in buff	cubes,octahedra	heavy liquid
X40 [D]	10.9	carbonate.	(0.5mm) and fine aggregates	
X41	-13.7	chert lenses in buff carbonate	cubes,sharp fragments and fine aggregates	heavy liquid
Altered Chert				
X43	-30.3	milky brown, broken silica layers in ash	v. fine grained	drilled
Volcanic				
63 (cube)	-34.4	volcanic clast	single cube (1cm)	drilled
80(ii)	-21.9	carbonated ash	radial pyrite spherule	drilled
88	-32.0	volcanic clast	cubes, shiny-platy crystals elongate	heavy liquid /acid treated
1.38	5.8	ash with shales	cubes + fine aggregate	heavy liquid /acid treated
2.12(i)a	3.2	ash with pyrite visible	cubes	heavy liquid /acid treated
2.12(i)b	9.4	in dark shaley patch	cubes + fine aggregate	heavy liquid /acid treated
2.40	-15.9	carbonated ash	v. fine aggregate	drilled

Sample #	$\delta^{34}S$	Paragenesis	Pyrite crystal habit	Extraction method
Carbonate Breccia				
2.89(i)	-13.4	breccia with organic	framboids	drilled
2.89(ii)	-14.4	matrix (gannister?)	v. fine grained lens	drilled
2.89a	0.2	breccia with organic matrix (gannister ?)	cubes + bladed forms	heavy liquid /acid treated
2.89b	-8.6	breccia with organic matrix (gannister ?)	cubes + fine aggregates	heavy liquid /acid treated
Samples selected for comparison with East Kirkton.				
Craigs lst [CL]	0.1	pure, massive limestone + ash	skeletal cubes	heavy liquid acid treated
St. Andrews, Fife [STA10]	-3.0	nodule in rootlet horizon		drilled
St. Andrews, Fife [STA10]	-14.4	nodule in rootlet horizon		heavy liquid /acid treated
Goat Quarry1 [GQ 1]	-8.1	shales	cubes	drilled
Goat Quarry2 [GQ 2]	-8.0	shales	cubes	drilled

4. THE INFLUENCE OF VOLCANIC MATERIAL ON THE EAST KIRKTON GEOCHEMICAL SIGNATURE.

R. A. R. McGill[1], A. J. Hall[1], and W. D. I. Rolfe[2].

1. Department of Geology and Applied Geology, University of Glasgow, Glasgow, G12 8QQ.
2. National Museums of Scotland, Chambers Street, Edinburgh.

4.0 ABSTRACT

Thirty-one whole rock samples were collected from a range of lithologies and from a variety of stratigraphic levels within the East Kirkton Limestone (EKL). The samples were divided into five groups based on field observation of their lithology, i.e. Groups I to V, stromatiform carbonate, ash & shale, carbonate-rich ash, shaley laminites, and carbonate-rich laminites.

From analyses of these samples, by XRD and XRF, the five lithological groups were characterised geochemically. All the East Kirkton samples had high calcite and/or high silica, comprising 85-100% of the samples' composition. The trace element Sr also had ubiquitously high concentrations (1000-5000ppm). Samples which consisted primarily of carbonate phases (i.e. mostly calcite, but sometimes a mixture of dolomite and ankerite) were generally found to have low trace element concentrations, except for Sr, whereas samples with a higher content of shale or tuff, tended to have a more enriched trace element geochemistry, higher total Fe and higher Al_2O_3.

The main source of sediment for the East Kirkton lake, was from the ash and basalt of the local, contemporary, Bathgate Volcano. The basalts originated from magmas of a primitive composition, and they are relatively Sr enriched (Smedley, 1986). It is felt that volcanic material is the source for all major, minor and trace elements, except SiO_2 and CaO, which are anomalously enriched. This enrichment in SiO_2 and $CaCO_3$, shown by the East Kirkton samples, could have come from hydrothermal fluids that had circulated through sediments of the Tyninghame or Gullane Formations, which occur directly below the Lower Limestone Group. No evidence of precious, or base metal mineralisation was found (several samples were assayed by Navan Resources plc.) and it is likely that hydrothermal fluids associated with the EKL would have been stripped of metallic elements by the West Lothian Oil Shale Formation lithologies, found below the East Kirkton sequence (Bottrell *et al*, 1988).

4.1 INTRODUCTION.

Thirty-one samples were collected from a variety of stratigraphic units, within the East Kirkton Quarry. These were sampled to reflect chemical variations that were controlled by (i) stratigraphy, (ii) rock type and (iii) large scale lateral variations within single units. The aim of this was to detect whether there was an anomalous horizon or lithology, or if there was an area of the quarry that was enriched in more unusual elements. It is intended primarily as a reconnaissance survey to pinpoint general geochemical variations; the sample population is not large enough statistically for significant conclusions tc be drawn about small scale lateral variations, within lithological groups, but they can be characterised geochemically from this data.

4.2 SAMPLE COLLECTION AND PETROGRAPHIC GROUPINGS.

The sample distribution was as follows: samples 1-11 were collected from our logged section 1 (see Appendix C) also figure 1, quarry photograph; samples 13-16 from "the mound" a limestone lens at the north end of the quarry; sample 17 to the south of this, from the horizon in which the "mound" occurs, and sample 12 from a small mound to the east of this; samples 18-20 from "the channel", another limestone lens, but within the main face of the quarry, slightly of the north of logged section 1; samples 21, 22, 24-28, were collected as lateral equivalents of lithologies sampled from stratigraphic. log 1; and samples 29-31 were collected from two exposed faces along the quarry track, south of the other samples and probably higher up the sequence.

Field terms for the hand specimens were used to place the 31 samples into five main lithological groups: Group I, stromatiform carbonate (1,13,14,15,16,18,19,20); Group II black shale, often including friable volcanic tuff (2,3,10,11,12,25); Group III, carbonate-rich volcanic tuff (4,9,23,24); Group IV, shaley laminites (5,7,8,17,21,22,26); Group V, carbonate-rich laminites (27,28,29,30,31); and one sample that is a chert lamina (6) but which is generally included with Group IV samples.

Results of XRD analyses are presented in Table 1 (I-V, for each lithological group), and XRF analyses for major and trace elements are presented in Table 2 (I-V). Sample by sample analyses descriptions are given in Appendix A.

4.3 ANALYTICAL PROCEDURES.

4.3.1 X-Ray Diffraction.

The East Kirkton Limestone has a mineralogy dominated by carbonate and silicate minerals. The XRD results (see Appendix D for technique) reflect this, i.e. the major peaks for minerals in each of the sampled rocks are calcite, quartz or, less commonly, dolomite/ankerite. Other minerals that feature on the XRD trace are chlorite/kaolinite, a mixed-layer clay of illite-smectite type (with a peak at 11Å), potassium feldspar and a little plagioclase. The feldspars only occur in small concentrations, and a small feldspar peak will be masked in many samples by the wide base of an intense quartz peak. Pyrite also occurs in most lithologies here, as was observed from pyrite separations for $\delta^{34}S$ isotopic analyses, but the position of the main XRD peak for pyrite is overlapped by one of the stronger ankerite/dolomite peaks and is consequently masked by this in most East Kirkton samples. No figures are given for pyrite from the XRD analyses and it is possible that feldspar may occur in some samples where a distinct peak was not observed.

4.3.2 X-Ray Fluorescence.

4.3.2.1 Major Element Analyses.

Samples were prepared for analyses using the standard Glasgow Departmental technique (see Appendix D for details). The results are dominated by SiO_2 and CaO, the only other elements that occur in concentrations greater than 10%, are Al_2O_3 for 3 samples (2,11&25 all of which are black shales) and FeO for two samples (2&25, black shales).

The results of FeO determinations for East Kirkton samples are predominantly high FeO and lower Fe_2O_3 (only sample 1, has higher Fe_2O_3 than FeO). Most of the mineral phases occurring in these samples (from XRD and petrographic study) tend to contain FeO rather than Fe_2O_3 so the relative proportions of iron, in these two oxidation states, was not

unexpected.

The determination of H_2O and CO_2, by gravimetric analyses, gave results which were inconsistent and relatively inaccurate. This was due to (i) very high values for CO_2 (30-40%), and (ii) soot, that accumulated in the H_2O collecting tube, probably produced from oxidation of organic carbon, occurring in shaley samples in particular. Results are given where reasonable accuracy was obtained, but some analyses required to be repeated up to 10 times before concordant results were achieved.

East Kirkton samples give values between 10% and 45% for Loss on Ignition (LOI), which are high, but not unusually so for limestones. LOI in these samples, is an expression of the carbonate content of each sample, including calcite and dolomite/ferroan dolomite. Only the clay-rich samples will contain significant amounts of water (from the mineral lattices), and from the results of H_2O determinations this could amount to some 7-8% of the samples, but these results may be exaggerated. It is thought that the LOI value may also include the oxidation of some organic carbon, nitrates and possibly sulphates, but these volatile phases are insignificant compared to the carbonate contribution. The LOI determinations were considered to be more reliable than the data obtained from the CO_2 and H_2O determinations.

4.3.2.2 Minor Element Analyses.

The most enriched minor element in the East Kirkton lithology was Sr, particularly in the shaley laminites, Group IV (up to 6300ppm). The black shales, Group II, are the samples which are generally most enriched, ie. most elements, except for Sr/Th/Zr. It also appears that the base of the sequence is generally more enriched than the top, but this trend is less well defined than the variation from one rock type to another.

Minor element analyses of Zr gave a strong correlation with Sr. This was felt to be due to the overlap of the Sr Kβ peak with Zr Kα. Appropriate corrections have been made, see Appendix E.

4.4 SUMMARY OF THE GEOCHEMICAL CHARACTERISTICS OF THE FIVE LITHOLOGICAL GROUPS.

4.4.1 Group I: Stromatiform Carbonate Samples (samples 1,13,14,15,16,18,19,20).

This group consists of almost pure carbonate, generally precipitated through biogenic mediation, with very little clastic sediment input. This group has therefore a different chemistry to those groups in which samples contain clastic material. The XRD analyses of these samples indicate that all have high calcite with minor quartz and ankerite/dolomite in varied amounts. Samples 1, 13 & 16, all have high quartz, whereas samples 14, 18 & 19 have high ankerite/dolomite peaks. In samples 1 & 18 there is a very small peak indicating the presence of some chlorite/kaolinite.

The XRF analyses for major elements shows the sum of CaO and LOI to be generally high, up to 90% in samples 15 & 20 which consist of almost pure calcite. Measurements of CO_2 and H_2O for these samples, shows LOI to be mostly CO_2, derived from the carbonate phases. The samples which had highest quartz peaks, 1, 13 & 16, also have highest SiO_2 content (41.87, 30.06 and 44.89 wt %, respectively). Samples 14, 18 & 19, have the highest MgO (7.32, 5.40 and 2.78 wt %) and FeO compositions (3.81, 2.86 and 1.82 wt %). They also have high LOI which corresponds clearly to the high ankerite/dolomite XRD peaks for these samples. The MnO content for samples 14 (0.40 wt. %) and 19 (0.30 wt. %) are the highest for this group. In general, samples with high MnO are also carbonate-rich.

Samples 1, 15 & 18 all have high Al_2O_3, for Group I, (0.70, 0.77 and 0.88 wt %). The XRD trace for samples 1 & 18 both indicate the presence of a little chlorite or kaolinite, whereas sample 15 has an almost insignificant plagioclase feldspar peak. Sample 1 was collected from the algal coating to a fossil tree trunk and has the highest minor element concentrations for this group. The Ba (272ppm) and Sr (5131ppm) concentrations are particularly high. Other elements are generally above group average, though none are over 30ppm. Of the samples from the "mound" (13, 14, 15 & 16), sample 15 has the highest Ba (77ppm) and Sr (2030ppm), with Ce, Cu, La, Ni, Rb and Zr also highest for the sub-group of four, ranging from 10-17ppm. The samples from the "channel" (18, 19 & 20) have slightly higher Sr (all have values just over 2000ppm) and sample 18 has the highest Ni (20ppm), Rb (15ppm), Zn (31ppm) and Zr (44ppm).

There is a strong correspondence between those samples which have the highest trace element contents and those which contain minor amounts of clay/feldspar. The presence of clay/feldspar, seems to imply a small volume of clastic input, probably of volcanic origin. FeO and MgO contents of each sample can be correlated with the intensity of the XRD peaks for ankerite/dolomite. This is the only mineral phase which can accommodate FeO and MgO in this carbonate-rich group. Samples which appear to contain an anomalous amount of quartz are generally those which have vug and vein infillings of silica, most common in samples 13 and 16 which were from the outer edges of the "mound".

4.4.2 Group II: Black Shales and Tuff Samples (samples 2, 3, 10, 11, 12, 25).

The shale and tuff samples are grouped together for three main reasons: the similarity in chemistry of all six samples (they are most enriched in all elements, except CaO and Sr); the samples were physically difficult to separate, occurring in units where tuffs and shale interfingered or were interbedded; and because the shales are generally composed of the same material as the tuffs, but with a finer grain size. These samples consist of material that has mostly been transported into the lake, or is reworked from sediments that had already been deposited.

The XRD analyses of these samples shows the presence of chlorite and/or kaolinite in each sample. Samples 2 and 25 have the highest peaks. Each sample has also a broad bulge in areas of the XRD trace which indicate that other clay phases are present. From sedimentation and glycolation of these samples the main clay found to be present was an 11Å mixed layer illite-smectite clay. Small peaks are also observed for potassium feldspar in samples 10, 11, 12 & 25.

Most samples have high quartz with samples 2, 3 & 12 having the highest quartz. All samples are rich in calcite, but samples 3, 10 and 11 are richest. Sample 2 is the only sample which does not show a distinct peak for the ankerite/dolomite phase.

From the XRF major element analyses, all samples have a higher SiO_2 than CaO content (this is the only group in which this occurs), and the two samples with highest SiO_2 are 3 (50.86 wt.%) and 12 (60.25 wt. %), the two which have the highest quartz XRD peaks. The highest CaO (27.12 wt.%) and LOI (24.26%) occur in sample 10 which has the highest calcite XRD peak. The CaO contents of the other samples are in proportion with their calcite peak heights.

Samples 2 and 25 have the highest chlorite/kaolinite XRD peaks and the highest Al_2O_3 (14.13 and 14.66 wt. %). The Al_2O_3 content for other samples is not dominated by the chlorite or kaolinite, but a combination of clay phases. High chlorite/kaolinite in samples 2 and 25 also corresponds with high MgO (6.81 and 5.05 wt.%), FeO (15.33 and 10.64 wt.%) and Fe_2O_3 (2.94 and 2.45 wt.%). TiO_2 (1-1.5 wt.%) and K_2O (1.5-3 wt.%) are highest in samples 10, 11 and 25; trace elements are also most enriched in these three samples with Ba (397-465ppm), Ce (69, 45 & 86ppm), Cr (131, 100 & 94ppm), Cu (33, 43 & 38ppm), La (30, 36 & 41ppm), Rb (65, 123 & 122ppm), Zn (71, 79 & 76ppm), and Zr (113, 145 & 191ppm). Samples 10, 11 & 25 are all from the same horizon (Unit 42). Sample 2 has the highest Ni value (131ppm), with fairly high Cr (79ppm) and Zn (56ppm). These three metallic elements can occur in chlorite. Sample 25 also has a high Ni value (119ppm) and also contains chlorite. Sr is highest in samples 3 (3081ppm) and 10 (3591ppm); these samples also have the highest values for CaO.

In this group are samples with the lowest CaO values and calcite XRD peaks; with some very high SiO_2 and quite high quartz peaks. They are characterised by chlorite/kaolinite, an 11Å mixed-layer illite-smectite clay phase and high Al_2O_3. They have the highest values for most trace elements but not Sr. This enrichment seems to correspond to the occurrence of clay/aluminous phases. MgO and FeO in these samples can be accommodated in chlorite, since the ankerite/dolomite content of the samples is very low; trace elements Ni, Cr and Zn are also thought to occur in the chlorite phase. There appears to be a difference in trace element (plus TiO_2 and K_2O) composition between two sub-groups of samples. Values are generally lower in samples 2, 3 and 12, collected from the base of the East Kirkton quarry sequence (NMS Unit 76/77 & 80), and higher in samples 10, 11 and 25, from NMS Unit 42. This may reflect changes in the source material from which the samples were derived.

NB. In these shale/tuff samples LOI is mainly CO_2, but the shales have the highest measured H_2O. This may be due to high water content in clay rich phases, but the H_2O results were not really considered reliable for these samples due to soot collecting in the tube that was weighed to calculate H_2O content. This soot occurred only when running samples which appeared to be rich in organic carbon, i.e. shale samples in particular.

4.4.3 Group III: Carbonate-rich Tuff Samples (samples 4,9,23,24).

The four samples in this group are all comprised of volcanic material, with coarse clasts (1cm size common, or finer) and with a fine grained matrix. Clasts are often comprised of pyroclastic material, but bedded limestones, calcareous mudstone, fragments of pre-existing volcanic tuff and shale, and carbonate spherules are also common. In each sample, the shaley matrix has been cemented by carbonate. The samples still retain a patchy chloritic colouration, but generally volcanic clasts are altered and appear white and often powdery. It is thought that the East Kirkton tuffs are either "waterlain epiclastic or secondary pyroclastic deposits, produced by the transport and subsequent aqueous deposition of volcanogenic material" (Durant, 1993, in press). These samples are expected to show similar chemical characteristics to the carbonate-rich lithologies and the shale/tuff samples.

XRD analyses shows that each sample has a very high calcite content, but only sample 24 is also quartz rich. Ankerite/dolomite is quite low in samples 4, 9 and 24, but high in sample 23. Each sample has a small kaolinite/chlorite peak (except 23), and sample 4 has also a small plagioclase feldspar peak.

The chemistry of these tuffaceous samples is dominated by the calcite that cements them and indurates them. CaO content for these samples is generally about 40%, with relatively low SiO_2 (9-12%). The exception to this being sample 24, with higher SiO_2 (25.87%) and lower CaO (32.50%); this sample has the highest quartz content. The LOI measurements correspond closely to the CaO values, except for sample 23, which has especially high LOI (37.50%) due to the occurrence of ankerite/dolomite in this sample as well as calcite. Sample 23 has highest MgO (4.31 wt.%) and MnO (0.46 wt.%) values, but not the highest FeO, suggesting that dolomite is the second carbonate phase in this sample.

Samples 4 & 24, collected from the same horizon, have high concentrations of Al_2O_3 and FeO (about 4%), with Fe_2O_3 (~1%), and moderate MgO (~2.5%); both these samples have high chlorite XRD peaks. These samples also have highest TiO_2 compositions (0.78 and 0.44 wt.%); most trace element enrichment, with high values for elements which are generally immobile e.g. Ce (30 and 27ppm), Cr (56 and 44ppm), La (30 and 20ppm), Ni (52 and 50ppm), Zr (23 and 30ppm); and high values for Ba (194 and 250ppm), Sr (3887 and 3941ppm) and Zn (37 and 29ppm) which tend to be mobile. Usually Ba and Sr are associated with calcite-rich samples, but in this group, samples 9 and 23 have the highest CaO and LOI contents.

Sample 23 has the most intense XRD peaks for the carbonate phases calcite and dolomite, but has lowest Ba, Sr, Al_2O_3, TiO_2, (and other trace element values) and it has no clay peak.

Apart from ubiquitous calcite, samples generally have low contents of quartz, ankerite/dolomite and chlorite/kaolinite. Sample 24, has higher quartz than the group norm, and sampie 23 has high dolomite, moderate quartz and no chlorite/kaolinite. MgO in this group can occur in dolomite or chlorite. In samples 4 and 24 which have highest chlorite/kaolinite, MgO is associated with high FeO, Al_2O_3 and high trace element concentrations, but in sample 23 it is associated with high MnO and low trace element values. It is assumed that the source of most trace elements, at East Kirkton, is the volcanic material transported into the lake as they are generally concentrated in samples containing high Al_2O_3, and clay phases.

4.4.4 Group IV: Shaley Laminite Samples (samples 5,7,8,17,21,22,26).

This group of laminites is characterised by shaley horizons which are often spherulitic, fine grained layers of carbonate mud, occasionally chert laminae and some tuff. Quite often these laminite units show syn-sedimentary slumping and they are commonly cut by calcite veining. Sample 6, a single, thick, chert lamina is also included in this group; it was sampled from the same locality as sample 5 and has similar trace element values to the samples of this group, though it has a different major element chemistry, as it is dominated by SiO_2.

This group has ubiquitous, high calcite XRD peaks, high quartz in samples 7, 17, 21 and 22 (and sample 6) and slightly lower quartz in samples 5, 8 and 26. The group also contains ankerite/dolomite with most in samples 7, 21 and 22. Sample 17 has the highest chlorite/kaolinite peak, and also contains a small, broad clay peak, indicating the presence of an 11Å mixed-layer illite-smectite clay. Samples 5, 7, 21 and 26 contain small chlorite/kaolinite peaks.

From the XRF analyses, CaO (39-44 wt.%) and LOI (32-37 wt.%) are highest in samples 5, 8 and 26 , but they have the lowest values for SiO_2 (16-20 wt.%). Samples 6, 7, 21 and 22 have higher SiO_2 values and lower CaO and LOI, but the sum of these three components for most Group IV samples is about 90% of the analyses total. The only sample with a lower total for SiO_2, CaO and LOI is sample 17, which contains the highest Al_2O_3

(4.08 wt.%), high TiO_2 (0.36 wt.%), K_2O (0.36 wt.%) and showing general trace element enrichment (not Sr). Samples 6, 8 and 22 have lowest values for TiO_2, Al_2O_3, Fe_2O_3 (FeO and MgO, also for samples 6 and 8), and trace elements this is probably because there is no chlorite and only a little ankerite/dolomite on their XRD trace. Sample 5 has the highest Sr (6300ppm) and Ba (272ppm); it has high CaO, but not the highest.

This group, generally, have a similar chemistry to Group III, carbonate-rich tuffs. Samples also show that where chlorite/kaolinite, clays and aluminous phases occur, there is also the greatest trace element enrichment, particularly of immobile elements. Sample 17 has tuffaceous lenses within its laminae and it is probably for this reason that it has a high clay content, and consequently high trace element concentration. The other unusual feature of the group is the extremely high Sr in sample 5. Sr is also high in the other six shaley laminite samples (and chert sample 6); most Sr values for this group exceed 3000ppm (except sample 6 - 2991ppm, and sample 26 - 2582ppm). These samples are commonly spherulitic, and the spherules are often Sr-enriched (Walkden, 1993 in press), therefore they seem to be a concentrated source of Sr. Ostracods with radial fibrous carbonate infills are also commonly Sr-enriched, and may provide a second source of enrichment, but infilled ostracods are less common in these samples than the ubiquitous spherulites.

4.4.5 Group V: Carbonate-rich laminite Samples.

The Group V laminites are geochemically similar to Group I samples, almost pure carbonate. They are quite coarsely crystalline, and it is unlikely that this is an original feature of the laminite, but indicates that alteration or recrystallisation has occurred. This process gives the laminae a more homogeneous appearance. The XRD analyses show high calcite for each sample; high quartz for samples 29 and 30, lowest for sample 31; and high ankerite/dolomite in samples 31 and 30. All samples contain only calcite, quartz and ankerite/dolomite.

This is echoed by the XRF major element analyses. The CaO content for all five samples is very high (35-47 wt.%), combining with high LOI (33-42%), to account for 84% of samples 27 and 28 (67-80% of the other samples), and points to the dominance of the carbonate phases, particularly calcite, in these samples.

Sample 31 has the highest LOI, but low CaO; this corresponds to its

high FeO (5.77 wt.%) and MgO (8.86 wt.%) and the high ankerite/dolomite peak observed from the XRD trace. Sample 30 also has slightly elevated FeO and MgO; this sample has the second highest ankerite/dolomite XRD peak. The high proportion of MgO to FeO in sample 31 suggests that the second carbonate phase in this sample is dolomite.

The highest percentages of SiO_2 (23.72 and 26.07 wt.%) occur in samples 29 and 30, they are the two samples in which the quartz peak is highest. Sample 31 has least SiO_2 (5.05 wt.%) and has the lowest quartz XRD peak. MnO (0.11-0.34 wt.%) is relatively high in these samples, similar values to those observed for Group I. All five samples have very low Al_2O_3 (0.09-0.48 wt.%), TiO_2 (0.05-0.09 wt.%), Na_2O (0.22-0.33 wt.%), K_2O (0.03-0.07 wt.%) and very low trace element concentrations (generally below 10ppm), even Ba (35-92ppm) and Sr (796-2271ppm).

These samples most closely resemble the other most carbonate-rich group, Group I, in geochemical signature. That is, high calcite, significant quartz, and ankerite/dolomite which is high in samples 30 & 31, but much lower in the other samples. Sample 31 is one of only two samples which has higher LOI than CaO (sample 14, Group I was the other), due to the occurrence of a second carbonate phase (dolomite). CaO content and Sr concentration are in proportion for this group; samples 27 & 28 have the highest values for both Sr and CaO, samples 30 & 31 have the lowest. All other trace element values are too low to be significant (10ppm or less). This appears to correspond to the absence of clay minerals, spherulitic, tuffaceous or shaley material in these samples. These laminites are quite coarsely crystalline; this is possibly a result of the passage of cool, carbonate-rich hydrothermal fluids, or maybe produced by diagenetic processes.

4.5 INTERPRETATION.

This section begins with a description of elements which correlate with aluminium. This is because: (i) aluminous samples tend to be more enriched in most trace, and many major, elements than carbonate-rich samples; (ii) aluminous samples reflect, most closely, the chemistry of the detrital material that has been transported into the East Kirkton lake; and (iii) these samples give the best indication of alteration, replacement and diagenetic processes that occurred, associated with the East Kirkton palaeoenvironment, changing them from a basaltic geochemistry to the unique East Kirkton geochemical signature.

The minerals chlorite and kaolinite are the most common aluminous phases in these samples, therefore it follows that the Al_2O_3 contents of samples will generally correspond to the presence or lack of a chlorite/kaolinite XRD peak. Where other clay or feldspar peaks are present the Al_2O_3 is higher than expected for the chlorite/kaolinite peak height alone, but where there is no peak present Al_2O_3 values generally lie around 0.5 wt.% of the sample, or less.

Higher Al_2O_3 was also expected and noted for samples comprised of terrigenous clastic material, which has been mainly derived from the volcanic hinterland. The shales are generally very fine grained and organic-rich, which makes it difficult to identify individual clasts. It is assumed that the shales (and shaley laminae) are comprised of similar material to the tuffs, including more organic debris (possibly derived from leaf litter or palaeosol, from the land surface).

The data is not ideal, from a statistical outlook, for proving correlations between elements, but in each case knowledge of the mineralogy, from petrographic observations and XRD analyses, complements these geochemical conclusions.

The calculation of correlation coefficients (r), quoted in the text, are used to identify elements which have a greater tendency to correlate with one another, although the absolute values are of limited use for this data set ('r' values greater than 0.7 or less than -0.7 are generally good correlations), Table 3 a + b. The spread of data for each element does not generally show a normal distribution. This is one of the assumptions made of data used in the calculation of Pearson Product - Moment correlation matrices, Table 3 a + b (which are comprised of the correlation coefficient data), arithmetic means and standard deviations, Table 1 (I-V). The range of data from East Kirkton samples is probably too heterogeneous

for a normal distribution, and for individual lithologies, our sample population is often too small to show clearly any trends or correlations.

The XRF data may provide artificial correlations because analytical values are given as a percentage, and are therefore a "closed array" of "compositional data" (Rollinson, 1993). There is a particular danger of forced correlation where analyses are dominated by one or two elements in particular, such as CaO and SiO_2 for the East Kirkton samples. As was stated in the introduction, the following interpretation is intended as a reconnaissance survey, to give a clearer perspective of the overall geochemistry of East Kirkton, and it is hoped that this can be a guide for future work in this area.

4.5.1 Correlations between Al_2O_3 and other major elements.

4.5.1.1 Al_2O_3 plotted against TiO_2 (and P_2O_5).

High Al_2O_3 is often associated with high TiO_2. This is illustrated in figure 2, which shows a good correlation between the two elements (correlation coefficient, r = 0.914). It is not always a proportional association, ie. sample 2, the main outlier from this linear trend, which appears to be depleted in TiO_2 or enriched in Al_2O_3. The black diamond symbols on the graph represent Group II samples, which comprise six of the seven highest values for Al_2O_3 and TiO_2. Samples 4, 9 and 24, carbonate-rich tuffs from Group III, and sample 17 (a shaley laminite), also have relatively high values for both elements. In general, samples which contain aluminous minerals, and those that appear volcanically derived, have the highest TiO_2.

Titanium concentrations probably reflect the values which existed in the original tuffaceous sediment. Variations in TiO_2 for tuff samples possibly reflect the percentage of volcanic material in the sediment, or compositional variations in the erupted volcanic ash/tuff. From SEM observation the TiO_2 was observed to occur as discrete TiO_2-rich grains eg. rutile (Figure 3). These grains could occur as part of larger volcanic clasts, or as individual grains, but they are most likely to be derived from terrigenous sediment, possibly epiclastic (Durant, 1993). TiO2 can also occur in colloidal form, in amorphous aluminous phases, on the breakdown of volcanic material (Mohamad, 1980).

High P_2O_5 also seems to occur in the shaley laminites/shales and tuffs. It is unlikely that much phosphate originates from a volcanic source, but it is likely that bone fragments - very rich in phosphate - would be terrestrially derived and transported, by water, along with the tuffaceous material. P_2O_5 does not correlate very well with Al_2O_3 (r = 0.691), but has a good correlation with TiO_2 (r = 0.869). This may indicate that both elements are terrestrially derived - TiO_2 representing epigenetic volcanic material, P_2O_5 representing dead amphibians - and transported via flooding, or river into the lake (different source, same transport). The preservation of many skeletal fragments by silica does, however, suggest that the porous bones are commonly permineralised, though fragments would still result in local P_2O_5 enrichment.

4.5.1.2 Al_2O_3 plotted against K_2O (and Na_2O).

The correlation coefficient for Al_2O_3 and K_2O is quite high (r = 0.861) and the relationship between the two elements is shown in Figure 4a. Generally, the data clusters below 4 wt.% Al_2O_3 and 0.5 wt.% K_2O, except for Group II samples. Na_2O has a poor correlation with Al_2O_3 (r = 0.024), the data on Figure 4b, can be seen to have a wider spread than on Figure 4a. K_2O occurs in clay phases eg. illite and smectite, and also in potassium feldspar. It is therefore related to samples with high Al_2O_3, especially those samples of the shale/tuff group which include potassium feldspar. In Figure 4a, Group II samples are illustrated by the black diamond symbols (sample 2 is the outlier from this trend, with low K_2O, or enriched Al_2O_3).

Na_2O has a poor correlation with Al_2O_3 (r = 0.024) which indicates that much of the plagioclase feldspar, which would be volcanically derived, has been broken down to clay (possibly kaolinite), and Na_2O released into solution. It is also possible that the results of Na_2O analyses are dubious in some cases, as Na contamination can easily occur in preparation (e.g. salt from hands, although handling was avoided as far as possible) and XRF detection of this element has a relatively low precision. Small amounts of plagioclase and potassic feldspar may also occur in other shaley or tuffaceous samples (Groups III and IV), but, small feldspar peaks can be masked by quartz, and not be observed from the XRD trace.

In Groups I, III, IV and V the values for Na_2O exceed K_2O, and this represents either (i) the relative proportions of the two elements in

solution, derived from volcanic material, and incorporated as impurities within the carbonate phases, (ii) the tendency of meteoric fluids to "dissolve more albite than potassium feldspar" (Bjorlykke and Aagard, 1992), hence K_2O would remain in shaley samples and Na_2O would remain in solution and be relatively enriched, as in the carbonates precipitating from this solution, or (iii) the amount of each element that can be accommodated by the carbonate phases. Na_2O and K_2O can occur within other mineral phases, e.g. illite or smectite clays, and the relative stability of these phases in various lithologies may also affect the relative concentrations of the two elements.

It is unusual for potassium feldspar, derived from basaltic volcanic material, to exceed plagioclase feldspar from the same source. In most samples (except Group II shales 3, 10, 11 & 25), the small quantities of K_2O found, are consistent with a basic, volcanic source; in Group II shales, K_2O values exceed Na_2O content. Only in these Group II samples does the K_2O content also exceed 1.12 wt.%, the value observed for Bathgate basalt samples (Smedley, 1986). Samples 10, 11, 12 and 25 have small potassium feldspar XRD peaks, but apparently no plagioclase feldspar. K_2O content may be further increased by the occurrence of mixed layer illite-smectite clay phases, in which, uptake of K^+ is preferred to Na^+. It is possible that potassium feldspar may have formed diagenetically: this would require high K^+ activity in the diagenetic fluids, as may occur in some brines (Wedepohl, 1972). Fluids of this type may have been present during the marine incursion which followed the deposition of the East Kirkton limestone. This was, however, not a mechanism which appeared to affect the $\delta^{34}S$ isotopic signature (see Chapter 3), and no other evidence is found to support its occurrence.

4.5.1.3 Al_2O_3 plotted against SiO_2.

Al_2O_3 correlates poorly with SiO_2 ($r = 0.354$) as shown in Figure 5. For reference, a line derived from the analyses of Al_2O_3 and SiO_2 for samples of Bathgate basalt (Smedley, 1986) has been added. Only a few samples occur on or near this line (Group II, shale/tuff samples 2,10,11&25, and Group III, carbonate-rich tuff samples 4 & 9). The majority of the East Kirkton data lies to the silica-enriched (Al_2O_3 depleted) side of this line. Petrographic observations confirm that in many cases the samples will be silica-rich. In this case it is not the elemental correlation which is important (they do not correlate), but what the lack of correlation suggests

about the origin of the samples.

Al_2O_3 correlates poorly with SiO_2, even for samples dominated by detrital material, which may suggest that the two are not from the same source. In Figure 5, when the data is compared to the Bathgate basalt analyses (Smedley, 1986), some of the Group II samples can be seen to lie close to this line, suggesting that, for these two elements, shales have a close geochemical relation to the basalts. Another indication that most of the detrital material appears to be derived from the volcanic hinterland.

Samples from the other groups are all siliceous, compared to the basalt. They have not the same input of terrigenous material, but have petrographic features which include; silica laminae, chert patches, and vugs filled by chalcedony and euhedral mega-quartz. These features all suggest an input of silica that is not detrital, and the imbalance between Al_2O_3 and SiO_2 indicates that a source, other than the local volcanics, is required to provide the silica. It is thought that the most likely local source of silica is the underlying Calciferous Sandstone Series sediments, and that remobilisation of the silica from here may have occurred via hydrothermal fluids, which precipitated silica on mixing with the cooler lake water, and through diagenetic fluids.

4.5.1.4 Al_2O_3 plotted against CaO & LOI (and MnO).

There is a weak, negative correlation between CaO and Al_2O_3 (r = -0.716) Figure 6a, and between Al_2O_3 and LOI (r = -0.642), Figure 6b. Outliers from the main linear trends on these two plots include those samples which have moderate/high SiO_2, (samples 1,3,6,12,16 &21), and, for the Al_2O_3 v's CaO plot, those samples with high dolomite/ankerite contents (samples 14, 30 &31). These outliers fall below the line, so they are depleted in both CaO and Al_2O_3.

MnO has a poor negative correlation with Al_2O_3 (r = -0.581). MnO only appears to correlate with CaO and LOI. This also may be a feature of results from a closed data set, ie. MnO correlates positively with CaO and LOI, LOI and CaO correlate negatively with Al_2O_3, therefore, MnO shows a similar, negative correlation.

The trend observed in Figures 6a & 6b was expected because of the lack of detrital material, and therefore, lack of the associated aluminous phases in the most carbonate-rich samples, eg. those from Groups I and V.

The carbonate phases are precipitated directly from fluid solutions, not derived from fluid/sediment suspensions.

The outliers from the general linear trend of the Al_2O_3 versus CaO plot (Figure 6a), include all those samples with significant XRD peaks for silica or dolomite/ankerite. In the Al_2O_3 versus LOI plot (Figure 6b) only samples with intense silica peaks, were expected to be outliers. SiO_2-rich samples were the furthest from the line of correlation in both plots and the positions of these outliers hardly vary from Figure 6a to 6b, there appears to have been little change in the relative positions of many of the other samples too.

It is, however, noted that the correlation coefficient for Figure 6b is lower than for 6a. For both figures, the line of correlation appears to lie through Group I samples 15, 18 and 20 (with lowest SiO_2), shale group samples (2, 10, 11 and 25), Group III carbonate-rich tuffs, and Group V samples 27 and 28. Group IV samples have an almost random distribution in these figures, probably because there is no strict relationship between the amount of calcite, dolomite or ankerite in a sample, and the quantity of detrital material that it incorporates.

It is probable that the negative correlation for Al_2O_3 with CaO and for some samples on the LOI plot, is statistically forced, by the closed data set. Where element oxides associated with the carbonate phases e.g. CaO, LOI, MgO and FeO, have high values (~50% of the sample, or above), the percentage of other element oxides present becomes an increasingly small proportion of the sample, statistically, i.e. their upper values are limited by what is left over from 100% - dominant element oxides.

4.5.1.5 Al_2O_3 plotted against MgO & Fe_{total}

MgO gives a poor correlation with Al_2O_3 ($r = 0.322$) as illustrated in Figure 7. Some aluminous samples have also high MgO (eg. samples 2, 25, 10 &11), but most of the carbonate-rich samples have very little Al_2O_3. The plot shows these two trends. The calculation for a correlation coefficient does not take into account the possibility of two correlations, and consequently the Al_2O_3 versus MgO has a low correlation coefficient.

Fe_{total} has a good correlation with Al_2O_3 ($r = 0.887$), Figure 8. The data mainly clusters in the area of low Fe_{total} (below 5%) and Al_2O_3 (below 2%), with only shale/tuff samples outside this region (samples 2, 3, 4, 10, 11, 12, 17, 24 & 25). Samples 3, 10, 11 & 25, fall below the general line of the trend, and are, therefore, relatively enriched in Al_2O_3 or depleted in FeO.

Samples from Groups I and V, in which little detrital material is found, are depleted in Al_2O_3 (with very low Fe_{total} values too). Any Fe_{total} in the Group I and V samples will occur in a carbonate phase (dolomite or ankerite).

Magnesium is an element which can be volcanically derived (Bathgate basalts are MgO-rich, ~ 9%, Smedley, 1986). It can occur in clays and chlorite, especially when these minerals are formed from the breakdown of volcanic material. East Kirkton shales/tuffs would be expected to contain volcanically derived MgO (probably occurring in samples 2, 10, 11 &25), but for carbonate-rich samples, which lack the input of detrital material, MgO occurs in dolomite/ankerite.

In the carbonate phases Fe_{total} is a minor component, compared to MgO and CaO. Fe_{total} (FeO and Fe_2O_3) will be a major component in chlorite and clay phases; it therefore correlates better with Al_2O_3, than does MgO. The plot of MgO and Al_2O_3 has two trends along which the samples correlate; the set of carbonate-rich samples with high MgO and low Al_2O_3, and the shale samples with moderate/low MgO and high Al_2O_3.

It is likely that oxidised iron as Fe_2O_3 has an "epiclastic" origin. Many of the tuff clasts in the East Kirkton sequence, are fragments of volcanically derived lithologies, that have been broken up, and transported into the E.K. lake to be re-sedimented (Durant, 1993). The Fe_2O_3 may be a result of terrestrial Carboniferous weathering, since the depositional environment in the lake was more anoxic than oxidising and Fe_2O_3 is unlikely to occur as a result of lake processes.

It follows that Fe_2O_3 derived in this manner would be most common in the shaley and tuffaceous sediments (these samples also contain the chlorite and clay phases which can accommodate Fe_2O_3). Fe_2O_3 also correlates with TiO_2 ($r = 0.790$) which is thought to be similarly derived ie. epiclastic.

4.5.2 Other major element correlations (not including Al_2O_3).

4.5.2.1 MgO plotted against Fe (total).

The relationship observed between MgO and Fe_{total} (as Fe_2O_3), Figure 9, is unusual because the data correlates along two separate trends; this seems to be a feature of the East Kirkton MgO plots (see also section

4.5.1.5, Figure 7). This results in a relatively low correlation coefficient (r = 0.648); r, can only reflect only one linear correlation for each plot.

As described in the previous section (4.5.1.5), MgO, FeO and Fe_2O_3, can occur in detrital material, from the volcanic source, or they can be incorporated in carbonate phases. This is the reason for the two trends which occur when data from these two elements are plotted together. The trend of data with the steeper gradient is comprised of samples from the shale and tuff groups (Groups II and III), whereas the line with the more gentle gradient is made up mostly from carbonate samples (Groups I and V).

The basalt line, on Figure 9 (from MgO and Fe_{total} values of Bathgate basalt, Smedley, 1986) is compared with the two East Kirkton trends. The shale/tuff samples are enriched in iron but depleted in MgO relative to the basalt line. Conversely, the carbonate samples are enriched in MgO and depleted in Fe_{total}, particularly samples that contain dolomite or ankerite (samples 14, 19, 23, 30 & 31).

It is felt that the carbonate trend represents (i) the proportion of MgO and Fe_{total} that could be taken up by these carbonate phases, as determined by the precipitation mechanism, or (ii) the relative proportions of the two elements present in the fluids, ie. availability. In either case, the carbonate phases are more enriched in MgO than Fe_{total}. In ankerite (or ferroan dolomite) iron will predominantly occur as Fe^{2+}, FeO, therefore, the carbonate samples have very low Fe_2O_3, even where they have high FeO, unlike the samples which contain detrital material.

The shales, falling to the other side of the basalt line are relatively enriched in Fe_{total}, but depleted in MgO. The volcanic material is the only apparent source of iron in this area, although MgO could be derived from other carbonates (as considered for CaO, see section 4.5.3.4). In the shale and tuff samples, FeO and Fe_2O_3 occur in chlorite and clays (eg. smectite), which contain only a little MgO (compared to the Fe content). These samples contain less MgO than the basalt source material. The process by which tuff and basalt were broken down to clays/chlorite, may have concentrated iron in these mineral phases and taken MgO into solution. If this is the case, it seems quite possible that the MgO is also derived from the volcanic source.

4.5.2.2 MnO plotted against CaO (&LOI).

There is a weak correlation between MnO and CaO (r = 0.606), Figure 10a, but a stronger correlation between MnO and LOI (r = 0.727), Figure 10b, the LOI in these samples representing mainly, their CO_2 content (and small amounts of water). The trend observed for these correlations, is that the MnO v's CaO plot has a steeper gradient, but the data, for each plot, is spread around a central line rather than focussed along it. The spread of data in Figure 10a, encompasses ±0.067 wt.% MnO, and ±18.75 wt.% CaO; while the spread of data in Figure 10b is ±0.067 wt.% MnO and ±11.25 wt.% LOI.

There are four outliers from the main trend in both figures, samples 14, 19, 23 & 31; they have the highest MnO values. These four samples are all carbonate rich, and contain dolomite/ankerite in addition to calcite (the four highest XRD peaks for ankerite/dolomite occur in these samples). This indicates that the highest MnO is associated with carbonate phases other than calcite.

MnO appears very depleted in East Kirkton samples compared to the Bathgate basalt value of 0.185 wt.% MnO, for 10.26 wt.% CaO and 5.46 % LOI (Smedley, 1986). This trend can also be attributed to enrichment of the samples in CaO and LOI. The latter is the more likely explanation, as the value quoted for basalt MnO is quite low (0.185 wt.%).

Occurrence of the manganese may be affected by precipitation on to organic substrates; (i) subaerially outside the lacustrine environment, and subsequently transported into the lake, or (ii) associated with algae/bacteria, or organic debris within the lake. Manganese apparently is more abundant in carbonate (particularly calcite and dolomite, not ankerite) than in the detrital fraction of carbonate rocks, contrary to the behaviour of most other trace/minor elements (Wedepohl, 1972). If this is true for the East Kirkton samples it may explain why MnO is the only element oxide, which has a positive correlation coefficient, with CaO. Diagenetic processes can mobilise the manganese under reducing conditions, and cause it to become more concentrated in carbonate rocks (Wedepohl, 1972). The managanese is most probably derived from the volcanic source, but concentrated by all of the above processes.

4.5.2.3 SiO_2 plotted against CaO (&LOI).

SiO_2 has a slightly stronger negative correlation with LOI (r = -0.925), Figure 11b, than CaO (r = -0.860), Figure 11a. The data seems to have a relatively diffuse distribution in Figure 11a, but focuses along a linear trend in Figure 11b.

Outliers in Figure 11a include shale samples 2, 10, 11 & 25; tuff sample 4; Group I samples 14 & 19; and Group V sample 31, which all occur in the area of the plot with less CaO and SiO_2 than is normal in these samples, i.e. below the marked CaO/SiO_2 mixing line. Samples 2, 4, 10, 11 & 25 are also outliers in Figure 11b, with SiO_2 and LOI depletion, relative to the general East Kirkton trend. These samples have the highest XRD peaks for chlorite/kaolinite and clays. Samples 14, 19 & 31, have the highest ankerite/dolomite XRD peaks. These samples, containing significant amount of clays or the second carbonate phase, bear least geochemical resemblance to the $CaCO_3/SiO_2$ phase system illustrated by the mixing line (Figure 11a).

When dealing with the main elements which comprise the East Kirkton samples (SiO_2, CaO and LOI) correlations should be distrusted. The statistical imperfections of a closed data set (with a fixed total of 100%), are most likely to produce forced correlations for these, the dominant components of the system.

It is possible that the geochemical system is responsible for this negative correlation. Fluctuations in temperature or Eh, pH conditions can determine whether SiO_2 or $CaCO_3$ is more likely to precipitate. It has also been suggested that perhaps wet and dry season conditions could affect which of the two phases was preferentially precipitated (pers. comm. R. Renaut).

The periodic introduction of hot-spring, siliceous fluids would tend to raise the lake temperature a little, and increase the rate of carbonate precipitation (by CO_2 degassing and the resulting increase in pH). The mixing of the warmer siliceous fluids and cooler lake waters would also tend to precipitate the silica from the cooling fluid. At the end of this brief episode the lake would resume more normal levels of carbonate precipitation, via bacterial mediation.

It should be noted that the solution and precipitation mechanisms within the lake environment are not the only factors affecting the quantity of $CaCO_3$ and SiO_2 in these samples. These two phases have been remobilised, forming replacive features and extensive veining in most

East Kirkton lithologies (see Chapters 2 and 3).

4.5.3 Correlations between major elements and trace elements.

4.5.3.1 Al_2O_3 plotted against trace elements (Ce, Co, Cr, Ga, Ni, Zn & Zr).

There is a strong correspondence between the Al_2O_3-rich samples and enriched trace element concentrations, especially Ce, Co, Cr, Ga, Ni, Zn and Zr (all have $r > 0.820$), and to a lesser extent Ba, Cu, La and Y ($r > 0.700$). For all of these trace elements and Al_2O_3 the highest values are observed in the shale/tuff group. Five of these elements have $r > 0.9$. They are Cr, Ga, Ni, Zn, and Zr. The elements Cr, Ni, and Zn can be associated with chlorite and smectites, and are shown plotted against Al_2O_3 in Figures 12a, b & c.

The sample which is most often observed as an outlier when trace elements are plotted against Al_2O_3 is sample 2. It is either (i) depleted in trace elements, or (ii) enriched in Al_2O_3 (the same pattern occurs in the Al_2O_3 plots against TiO_2, Figure 2, and K_2O, Figure 4a). This may be due to its close association with organic material (lies just above a tree trunk encrusted by stromatiform carbonate, sample 1), or it may be related to the sample's low stratigraphic level (only samples 3 and 12 are comparable in stratigraphic level, and lithology, but both tend to contain more tuff, and have lower Al_2O_3).

The correlation coefficient for Al_2O_3 and Rb is 0.876, but the data mainly forms a cluster close to the origin, except for Group II samples, four of which compose the line that is the main trend (sample 2 is again the main outlier). There is not really a sufficient scatter of data in this plot to justify a true correlation. There is no relationship between Al_2O_3 and Sr ($r = -0.085$) or Th ($r = 0.007$). Fe_{total} has a similar correlation pattern with trace elements, but the correlation coefficients are lower (see table 3b).

The trace elements with which the Al_2O_3 correlates best, Ce, Co, Cr, Ga, Ni, Zn and Zr, can all be associated with clay phases (Wedepohl, 1972), particularly chlorite, montmorillonite/smectites, iron and manganese oxides and kaolinite. In many carbonate rocks these elements are observed to occur in proportion to the detrital clay/silt fraction of the sample (Wedepohl, 1972). This appears to correspond with what is observed for East Kirkton samples; where Al_2O_3 wt.%, is taken as a close reflection of

the clay content of these samples.

Cr, Ni and Zn are plotted against Al_2O_3 (Figures 12a, b & c). They are elements which can occur in chlorite and smectite phases. They do not always occur in the same proportions, from one sample to the next, but there is a strong correlation between their occurrence and that of Al_2O_3 and chlorite/clays (though not so closely related to kaolinite). Variation amongst these three elements may depend on relative availability within the volcanic, source material, or the relative mobility of each element, and the fluids which have interacted with their host sediments. The Ni content of these samples seems particularly enriched.

Hand specimens containing chlorite were occasionally collected and analysed (XRD), as their intense green colour was suggestive of Cu mineral phases. They did not contain copper minerals, but it is now considered that the bright green colour could have been related to higher chrome content.

4.5.3.2 K_2O plotted against Rb.

There is a close association between K_2O and Rb ($r = 0.985$), as shown in Figure 13. Although many of the samples have low values, the cluster of data in this area of the graph is distributed along a similar linear trend to the Group II samples, which have higher values.

This correlation, Figure 13, is a very common geochemical correlation, as K and Rb have a similar ionic radius and may easily substitute for one another. Rb, does not actually form any Rb-rich minerals, but is almost always incorporated in K-minerals (Wedepohl, 1972). Often Sr shows a similar distribution, but not in East Kirkton samples, where Sr distribution is affected by carbonate phases.

The size of the sample population for shales is considered too small to conclude whether or not the K/Rb ratios indicates marine or freshwater conditions of deposition (though marine conditions are felt to be an unlikely occurrence). K/Rb ratios for East Kirkton, Group II samples range from 163-250, with tuff and shaley laminae samples tending to have lower values, 107-190. Havard (1967), found high K_2O and K/Rb ratios in black shales, and suggested that this was a result of authigenic growth of K-minerals (see also section 4.5.1.2).

4.5.3.3 TiO_2 and trace elements (Cr, La, Rb, Zn & Zr).

TiO_2, like Al_2O_3, correlates with many of the trace elements (see table 3b); $r > 0.9$, for Cr, La, Rb, Zn and Zr. All the other trace elements have values of $r > 0.8$, except for Pb, Sr, and Th. Plots of TiO_2 versus trace elements have generally higher correlation coefficients than for Al_2O_3 versus traces.

Group II samples usually comprise the majority of the 6 highest values for each trace element (except Pb, Sr and Th). These correlations maybe due to statistical closure of the data set (ie. TiO_2 correlates well with Al_2O_3, and both major elements show a similar correlation pattern when plotted against trace elements), but less concentrated elements, such as Al_2O_3 and TiO_2, are perhaps less likely to be affected by closure than dominant elements like SiO_2 and CaO. It is also noted that, though similar, the correlation patterns from the trace element plots are not exactly the same for Al_2O_3 and TiO_2, many elements correlate better with TiO_2 than Al_2O_3, but a few have lower values (differences are not consistent with a forced trend, but it is possible that these small variations occur because the data set does not always show a normal distribution).

Zirconium could be derived from volcanic material in a similar way to TiO_2 Figure 14 (both are generally immobile elements - particularly TiO_2 - and often occur as accessory minerals in igneous rocks). Titanium often occurs as rutile, ilmenite, or anatase (besides occurring in pyroxenes), and from SEM studies of the East Kirkton samples (Figure 3), the mineral does occur in discrete TiO_2-rich grains. The inclusion of one grain of TiO_2 in a sample prepared for analyses can radically change the concentration of Ti for that sample. If this were the case for any of the East Kirkton samples, it is felt that the correlation between TiO_2, Al_2O_3 and many of the trace elements would be much poorer.

Titanium can also occur with clay minerals eg. kaolinite (Wedepohl, 1972). In section 4.5.3.1, it was observed that this is a common association of many trace elements, including Cr, Zn, Zr, and Rb (section 4.5.3.3). The coexistance of all these elements in similar groups of phases - all related to the breakdown of volcanic material - would seem to suggest that their correlation is quite strongly related to the clay fraction of each sample.

4.5.3.4 CaO/SiO_2 and trace elements (especially CaO v's Sr).

CaO and SiO_2 have poor trace element correlation patterns. In the case of CaO in particular, the weak correlations with Ba, Cr, Cu, Zn and Zr are all negative correlations (r = -0.600 to -0.700), and probably reflect the negative relationship between CaO and Al_2O_3 (positive relationship between Al_2O_3 and traces). Ni has the strongest negative correlation with CaO (r = -0.795), see table 3b.

These elements appear to be concentrated where there is least CaO (and probably carbonate generally), therefore it is likely that they will occur predominantly in the shales/tuffaceous groups (as observed from other correlations, sections 4.5.3.1 and 4.5.3.3). It is possible that this is a forced statistical correlation and not a "real" one, but the carbonate-rich samples which have depleted trace element concentrations, and lack phases which could accommodate these element (eg. clays).

The only positive values on the CaO: trace element correlation matrix are Sr (r = 0.034), Figure 15, and Th (r = 0.151), but both are very low values, indicating random distribution. Sr and Th do not correlate with each other either (r = 0.010).

A CaO versus Sr graph is plotted, Figure 15, and the relative ratios for these two elements are added from the Bathgate basalt data (Smedley, 1986). The shale/tuff samples appear to show a correlation for these two elements, along a line which has higher Sr than CaO, when compared to the basalt line. This shift is due either to CaO depletion or Sr enrichment; one possible explanation for this may be that Sr is mobilised less during weathering than Ca, and that Sr is therefore held more tightly in clays, Wedepohl (1972).

In East Kirkton samples the highest Sr occurs in spherules (7584 - 16160ppm), rhombohedral calcite in laminae (6843 - 13799ppm) and radial fibrous calcite infills in ostracods (9490 - 10659ppm), but the Sr in the vein calcite has lower values (1870 - 8303ppm) (Walkden *et al* , 1993). The concentration of the Sr in the samples analysed by Walkden *et al.* does not appear to correlate with Mg, Fe or Mn values also quoted for these samples. It is possible that shales or shaley laminites may contain one/ or more of the above carbonate groups, eg. spherules, and be anomalously enriched in Sr. It also appears from the data that the veining, a later feature than spherules etc., was not so enriched in Sr, therefore the earlier source of Sr (possibly the lake waters) may no longer exist, or these later fluids may not encounter it.

Many of the East Kirkton samples, however, are enriched in CaO relative to Sr, when compared to the basalt line; especially samples from Groups I and V. These samples are pure carbonates, containing very little detrital material, and this enrichment in CaO seems to require additional CaO for the geochemical system, than that which is introduced from the volcanic material. As the East Kirkton lithologies are not of marine derivation, and the CaO is not from the volcanic source, it is proposed that the second CaO source could from hydrothermal fluids circulating through the Tyninghame or Gullane Formations, which lies below the East Kirkton Limestone, and has also been suggested (above) as the source for some of the hydrothermal silica.

It is proposed that the carbonate fluids were hydrothermal, warm (not hot) fluids which circulated/convected through the underlying calciferous sandstones (a sequence which includes cornstones), and became enriched in carbonate. These fluids mixed at surface with the cooler lake water, producing a lake that was enriched in carbonates, but, which mainly precipitated carbonate through biological mediation.

4.7 CONCLUSIONS.

1. From the results of our analyses it is concluded that most major elements and trace elements were derived from the volcanic material (represented by analyses of local Bathgate basalt samples, Smedley 1986), either directly or from epigenetic material, reworked by water.

2. Only SiO_2 and CaO require a source other than volcanic material, to supply the concentrations in which they occur in the East Kirkton samples. This second source is thought to be the cornstones and/or limestone horizons of the Tyninghame or Gullane Formations, which occur stratigraphically below the East Kirkton limestone. It is also proposed that the silica and calcite were remobilised from this source via hydrothermal fluids, and reprecipitated upon mixing with lake fluids, and/or via biogenic mediation.

3. Strontium occurs in greatest concentrations in the carbonates that are considered to have been precipitated via biogenic mediation (eg. spherules, ostracod infillings, and rhombs). High Sr values do not appear

to occur in the veins, and from major/trace element correlation patterns, it too appears to be from the volcanic source. It is suggested that future investigation of the sources of East Kirkton fluids would perhaps gain some useful information from the Sr/CaO ratios of carbonate-rich members of the Tyninghame or Gullane Formations.

4. Shales seem enriched in mobile and immobile elements alike. This may reflect the impermeable nature of the shale horizons, which can limit fluid circulation. It is also a feature of the concentration/retention /adsorption of many trace elements by clay minerals. Slow deposition of these shale horizons could also concentrate trace elements. Trace elements, in East Kirkton samples, typically correlate with Al_2O_3, Fe_{total} and TiO_2, and are therefore likely to be derived from the volcanic source.

4.8 ACKNOWLEDGEMENTS.

The authors would like to thank staff of the geochemistry lab. in the Department of Geology and Applied Geology, University of Glasgow; Jim Gallagher, Murdo McLeod and Dugald Turner for help with the preparation and analyses of XRD and XRF samples. Also Dr Bell, Dr Farrow and Dr Durant for advice about geochemical techniques and their interpretation; Douglas MacLean for the photographs; Dr G. Bowes for help with the statistics; and David Hastie for help with the figured diagrams.

4.9 BIBLIOGRAPHY.

Bjorlykke, K. and Aagaard, P. 1992. Clay minerals in North Sea Sandstones. In "Origin, diagenesis, and petrophysics of clay minerals in sandstones." SEPM Special Publication No. 47.

Bottrell, S. H., Shepherd, T. J., Yardley, B. W. D. and Dubessey, J. 1988. Journal of the Geological Society of London, vol. 145 pp139-145.

Deere, W. A., Howie R. A. and Zussman, J. 1992. *The Rock Forming Minerals*. 2nd. Ed. Longman Scientific and Technical, UK.

Durant, G.P. 1993. Volcanogenic sediments of the East Kirkton Limestone (visean) of West Lothian, Scotland. *Transactions of the Royal Society of Edinburgh: Earth Sciences* 84. pp 203-208.

Mohamad, H. B. 1980. (Government of Malaysia) Geochemistry and petrology of the Southern Highlands (Upper Dalradian pelitic-psammitic schists of Glen Esk,) Angus, Scotland. Unpublished PhD thesis, Strathclyde University.

Harvey, P.K., Taylor, D.M., Hendry, R.D. and Bancroft, F. 1973. An accurate fusion method for the analyses of rocks and chemically related materials by X-ray fluorescence spectrometry. *X-ray Spectrometry* **2**. pp 33-44.

Havard, K.R. 1967. Mineralogy and Geochemistry: Epshaw Formation, Southern Alberta, Unpublished M.S. thesis, University of Calgary.

Rollinson, H. R. 1993. *Using Geochemical Data: Evaluation, Presentation, Interpretation*. Longman Scientific and Technical, U.K.

Smedley, P.L. 1986. The relationship between calc-alkaline volcanism and within-plate continental rift volcanism: evidence from Scottish Palaeozoic lavas. *Earth and Planetary Science Letters* **76**. pp 113-128.

Walkden, G.M., Irwin, J.R. and Fallick, A.E. 1993. Carbonate spherules and botryoids as lake floor cements in the East Kirkton Limestone of West Lothian, Scotland. *Transactions of the Royal Society of Edinburgh: Earth Sciences* **84**. pp 213-223.

Wedepohl, K. H. (Ed.) 1978. *Handbook of Geochemistry*. Springer-Verlag, Berlin-Heidelberg.

4.10 Figure Captions

Figure 1 The East Kirkton Quarry, main section (photograph taken facing WSW). The scale figure is about 6 feet tall. Coloured, numbered dots on this figure indicate where the samples for whole rock analyses were taken. Orange dots represent stromatiform carbonate samples (Group I); red dots represent shale samples (Group II); yellow dots represent carbonate-rich tuff samples (Group III); green dots represent the shaley laminites (Group IV); and the blue dots are where carbonate-rich laminite samples were collected (Group V).

Figure 2 A plot of Al_2O_3 versus TiO_2.

Figure 3 Four images of one, rectangular grain of Titanium-oxide photographed using the SEM. The grey and white image is the backscattered electron image from the SEM, and the other three indicate the concentrations of a variety of elements within the image. In the top/left image red represents Si, and blue S; in the top/right image green represents Ti, and Ca is red; with the bottom/left image showing Fe in blue and Al in red. It shows that the grain is predominantly Ti-rich.

Figure 4a A plot of Al_2O_3 versus K_2O.

Figure 4b A plot of Al_2O_3 versus Na_2O.

Figure 5 A plot of Al_2O_3 versus SiO_2; the "Basalt Line" indicated on this plot is derived from a ratio of Al_2O_3 to SiO_2 from the values obtained for local Bathgate basalts, by Smedley (1986).

Figure 6a A plot of Al_2O_3 versus CaO.

Figure 6b A plot of Al_2O_3 versus LOI.

Figure 7 A plot of Al_2O_3 versus MgO; the "Basalt Line" indicated on this plot is derived from a ratio of Al_2O_3 to MgO from the values obtained for local Bathgate basalts, by Smedley (1986).

Figure 8 A plot of Al_2O_3 versus Fe_{total}.

Figure 9 A plot of MgO versus Fe_{total}; the "Basalt Line" indicated on this plot is derived from a ratio of MgO to Fe_{total} from the values obtained for local Bathgate basalts, by Smedley (1986).

Figure 10a A plot of MnO versus CaO.

Figure 10b A plot of MnO versus LOI.

Figure 11a A plot of SiO_2 versus CaO; the "Mixing Line" indicated on this plot is derived from the relative amount of SiO_2 in silica (100 wt.%) and the amount of CaO in calcite (56 wt.%), and a rough estimate of where concentrations of a mixture of the two phases would lie, between these two extreme values.

Figure 11b A plot of SiO_2 versus LOI.

Figure 12 A plot of Al_2O_3 versus Ni, Zn and Cr.

Figure 13 A plot of K_2O versus Rb.

Figure 14 A plot of Zr versus TiO_2.

Figure 15 A plot of Sr versus CaO; the "Basalt Line" indicated on this plot is derived from a ratio of Sr to CaO from the values obtained for local Bathgate basalts, by Smedley (1986).

Table 1 (Group I - V)	Five tables with the XRD results for each of the five lithological groups.
Table 2 (Group I - V)	Five tables with the XRF results for each of the five lithological groups.
Table 3 (a & b)	Pearson Product - Moment Correlations for (a) major element XRF analyses. (b) mixed major and minor element XRF results

Figure 1


29
30
31
28
27
25
26
19
18
11
10
20
9
8
22
7
13
21
6
5
15
17
16
14
24
1
2
3
4
12

Figure 2

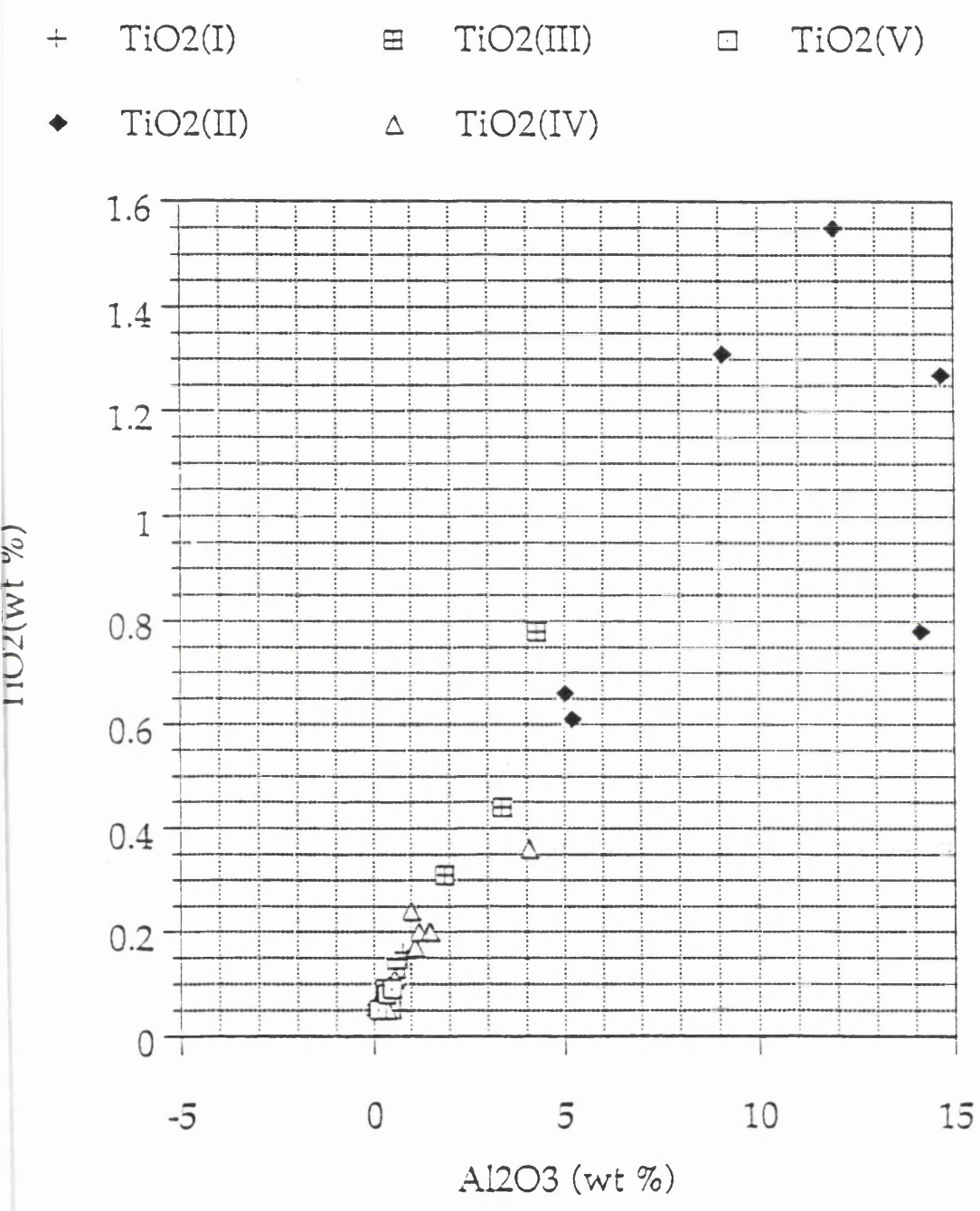
+ TiO2(I)
⊞ TiO2(III)
□ TiO2(V)
◆ TiO2(II)
△ TiO2(IV)
1.6
1.4
1.2
1
0.8
0.6
0.4
0.2
0
-5
0
5
10
15
Al2O3 (wt %)

Figure 3

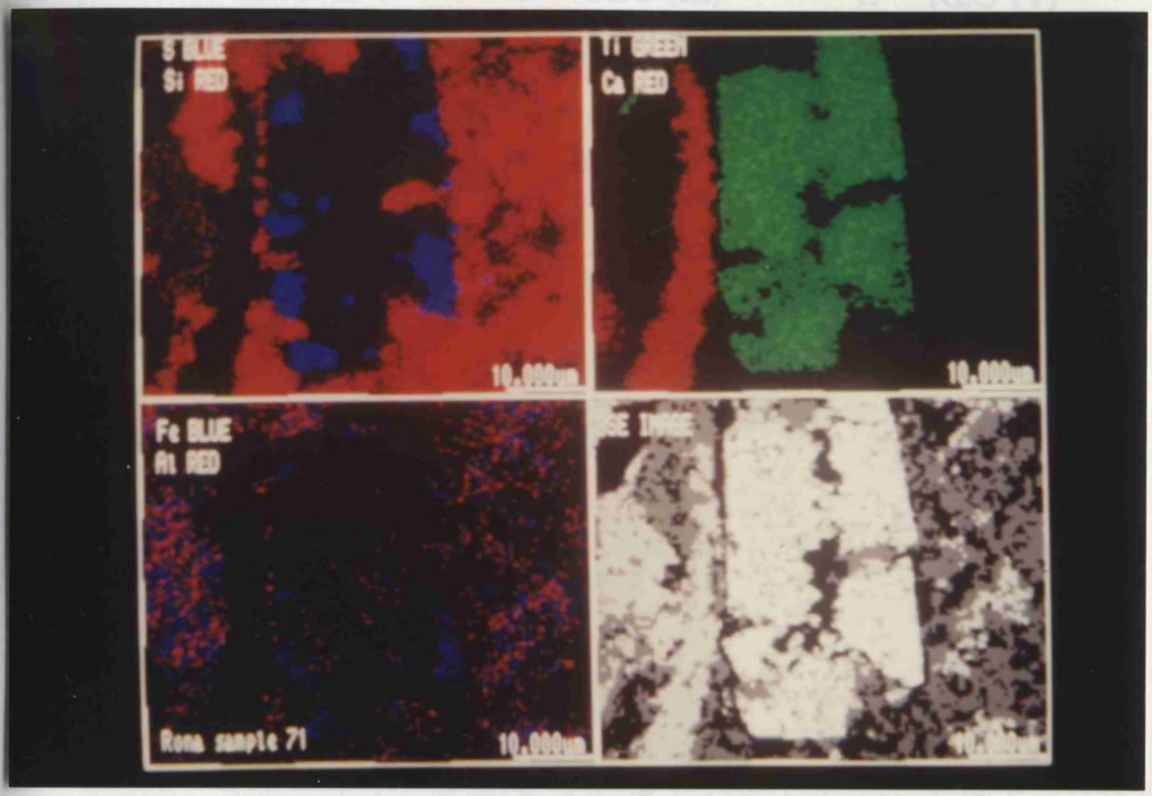

Figure 4a

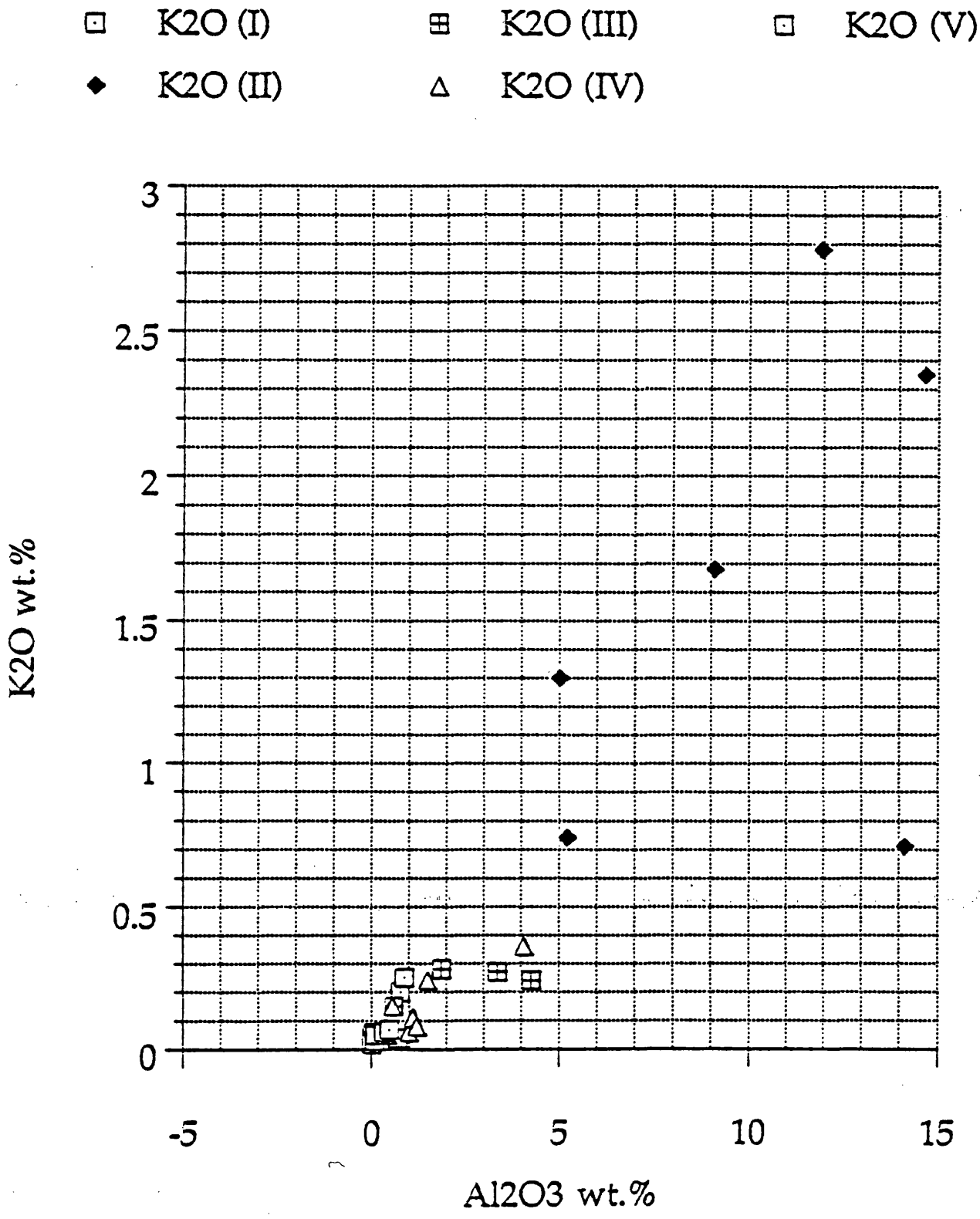
K2O (I)
K2O (II)
K2O (III)
K2O (IV)
K2O (V)
3
2.5
2
1.5
1
0.5
0
-5
0
5
10
15
K2O wt.%
Al2O3 wt.%

Figure 4b

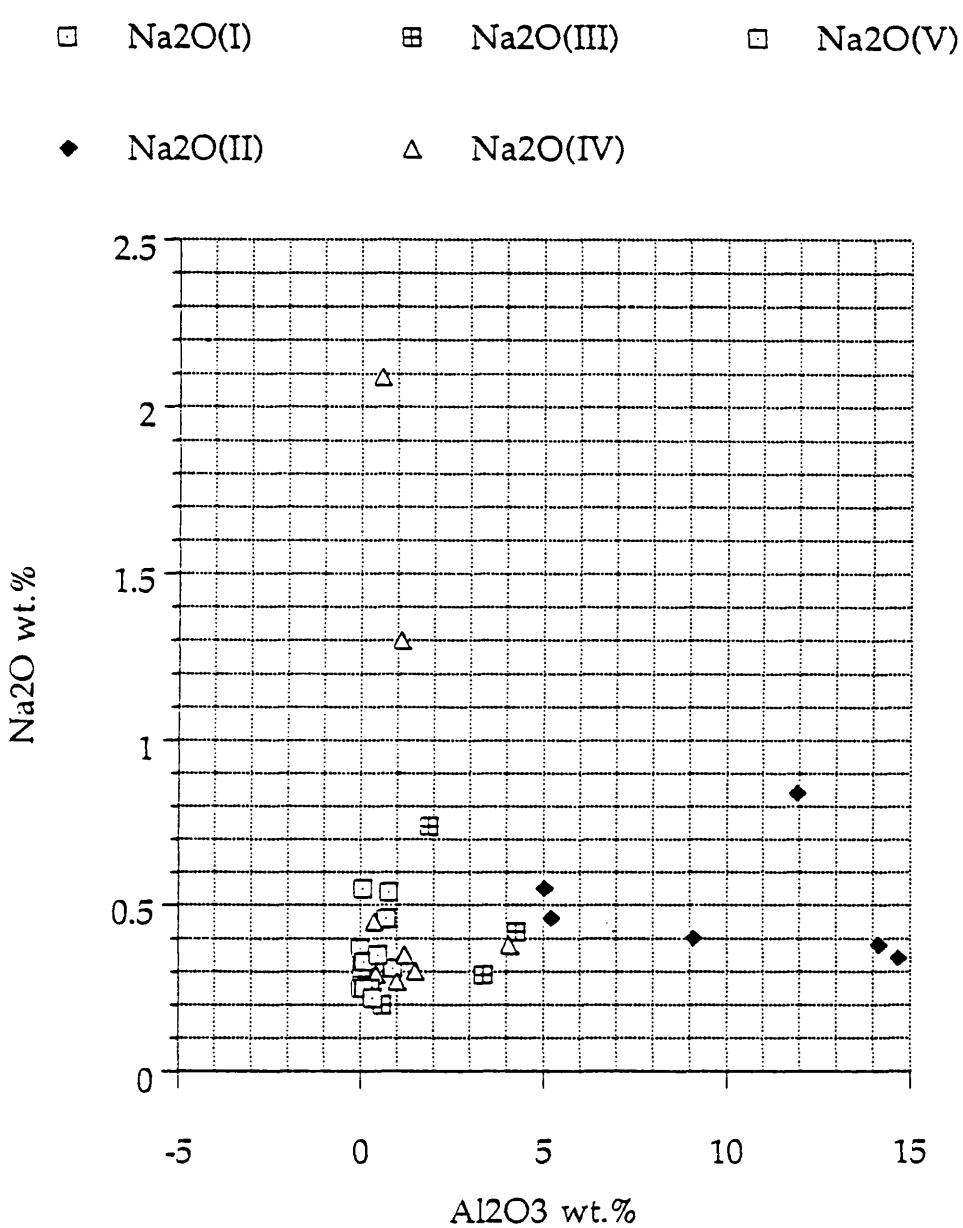
Na2O(I)
Na2O(III)
Na2O(V)
Na2O(II)
Na2O(IV)
2.5
2
1.5
1
0.5
0
Na2O wt.%
-5
0
5
10
15
Al2O3 wt.%

Figure 5

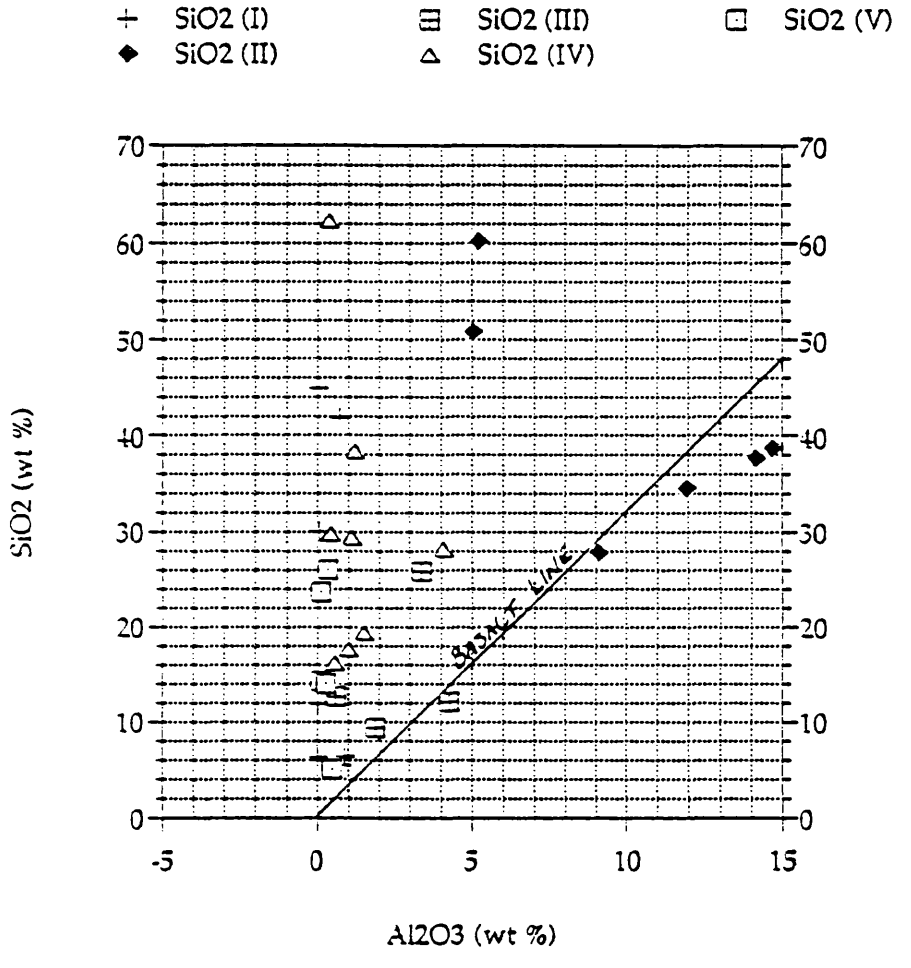
SiO2 (I)
SiO2 (II)
SiO2 (III)
SiO2 (IV)
SiO2 (V)
70
60
50
40
30
20
10
0
-5
0
5
10
15
SiO2 (wt %)
Al2O3 (wt %)

Figure 6a

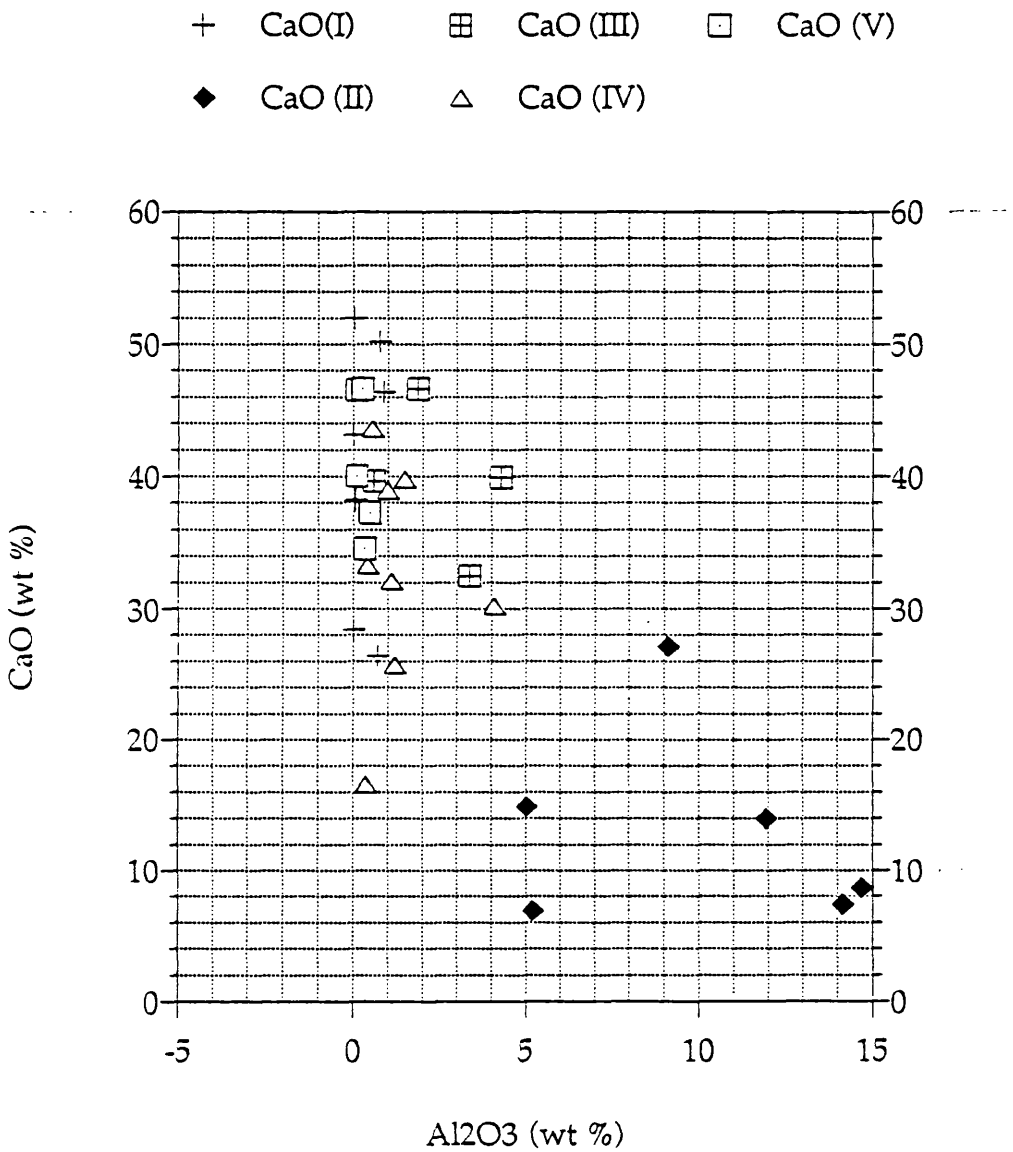
CaO(I)
CaO (III)
CaO (V)
CaO (II)
CaO (IV)
60
50
40
30
20
10
0
-5
0
5
10
15
CaO (wt %)
Al2O3 (wt %)

Figure 6b

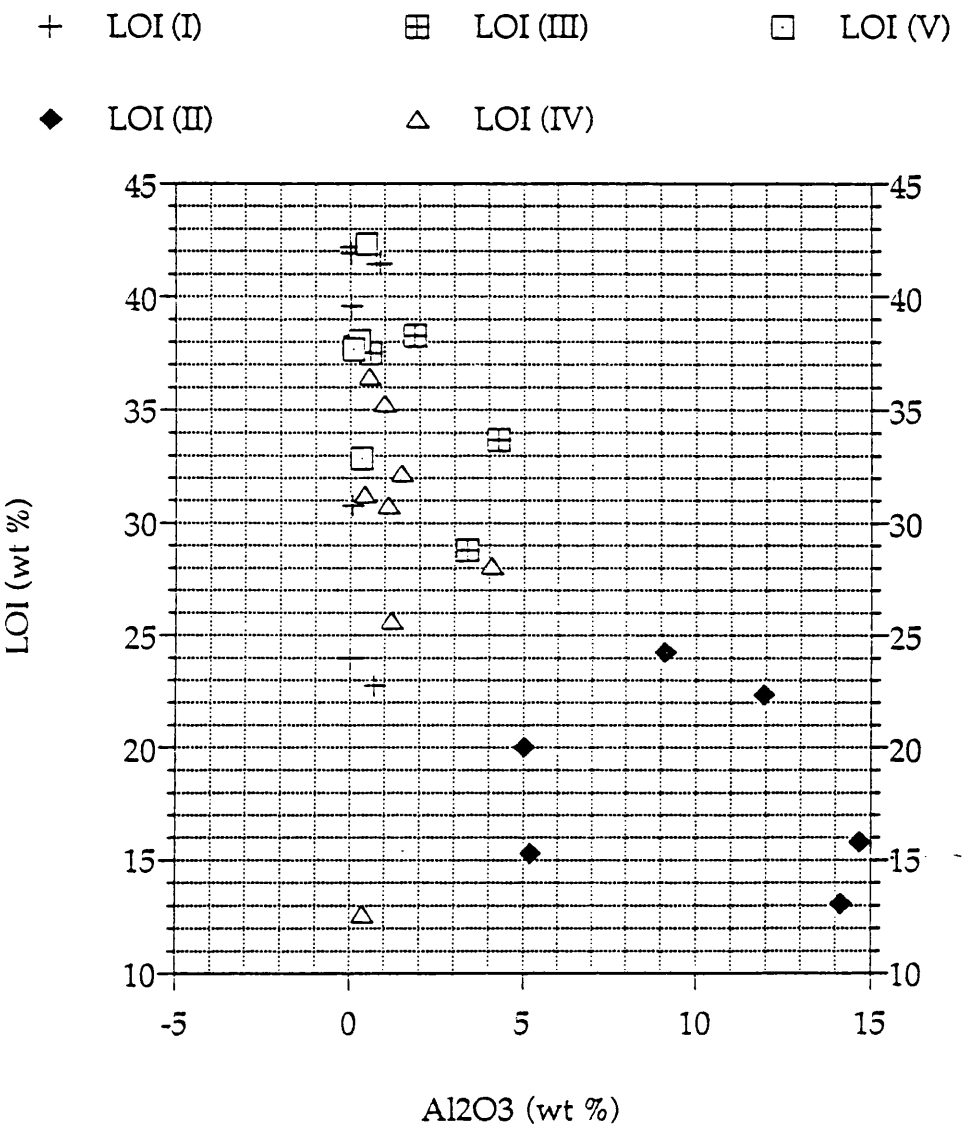
+ LOI (I)
⊞ LOI (III)
□ LOI (V)
◆ LOI (II)
△ LOI (IV)
45
40
35
30
25
20
15
10
-5
0
5
10
15
LOI (wt %)
Al2O3 (wt %)

Figure 7

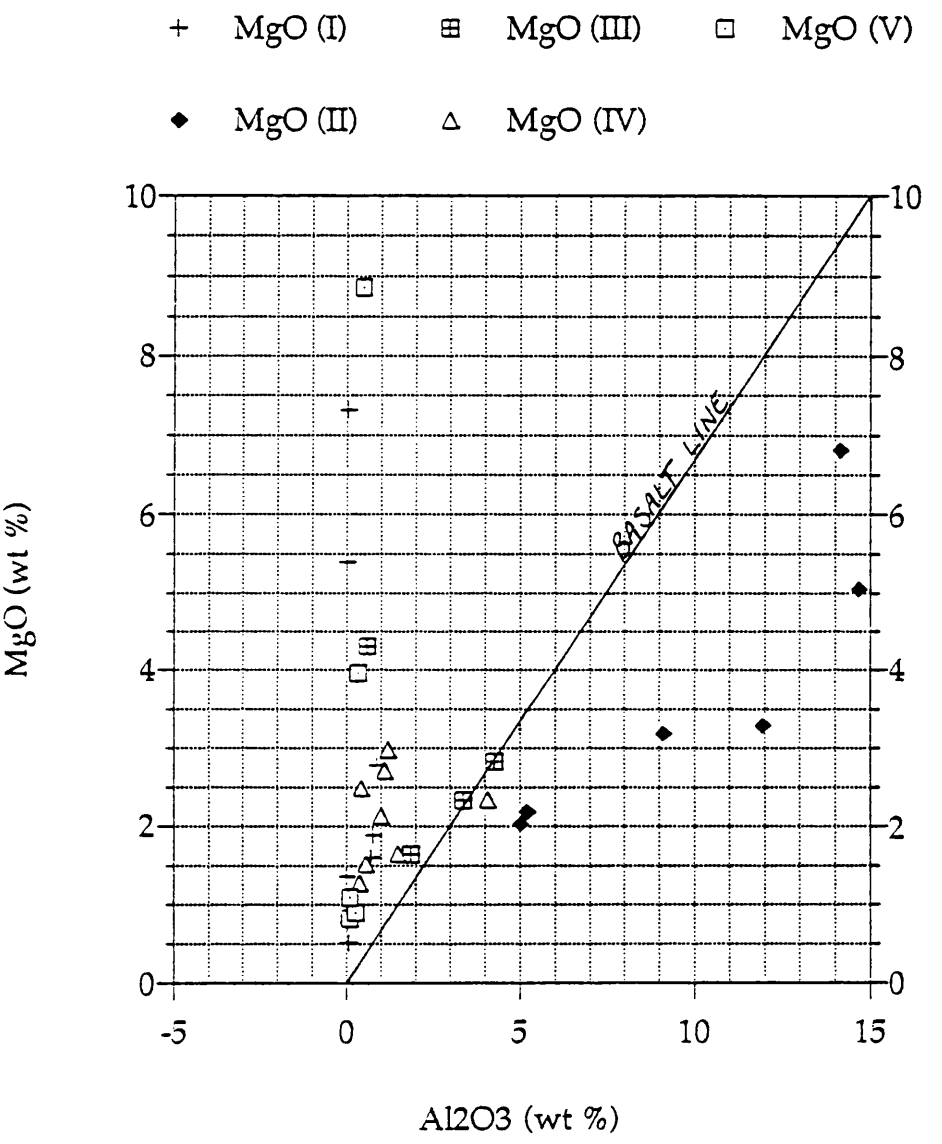
+ MgO (I)
⊞ MgO (III)
□ MgO (V)
◆ MgO (II)
△ MgO (IV)
BASALT LINE
MgO (wt %)
Al2O3 (wt %)
10
8
6
4
2
0
-5
0
5
10
15

Figure 8

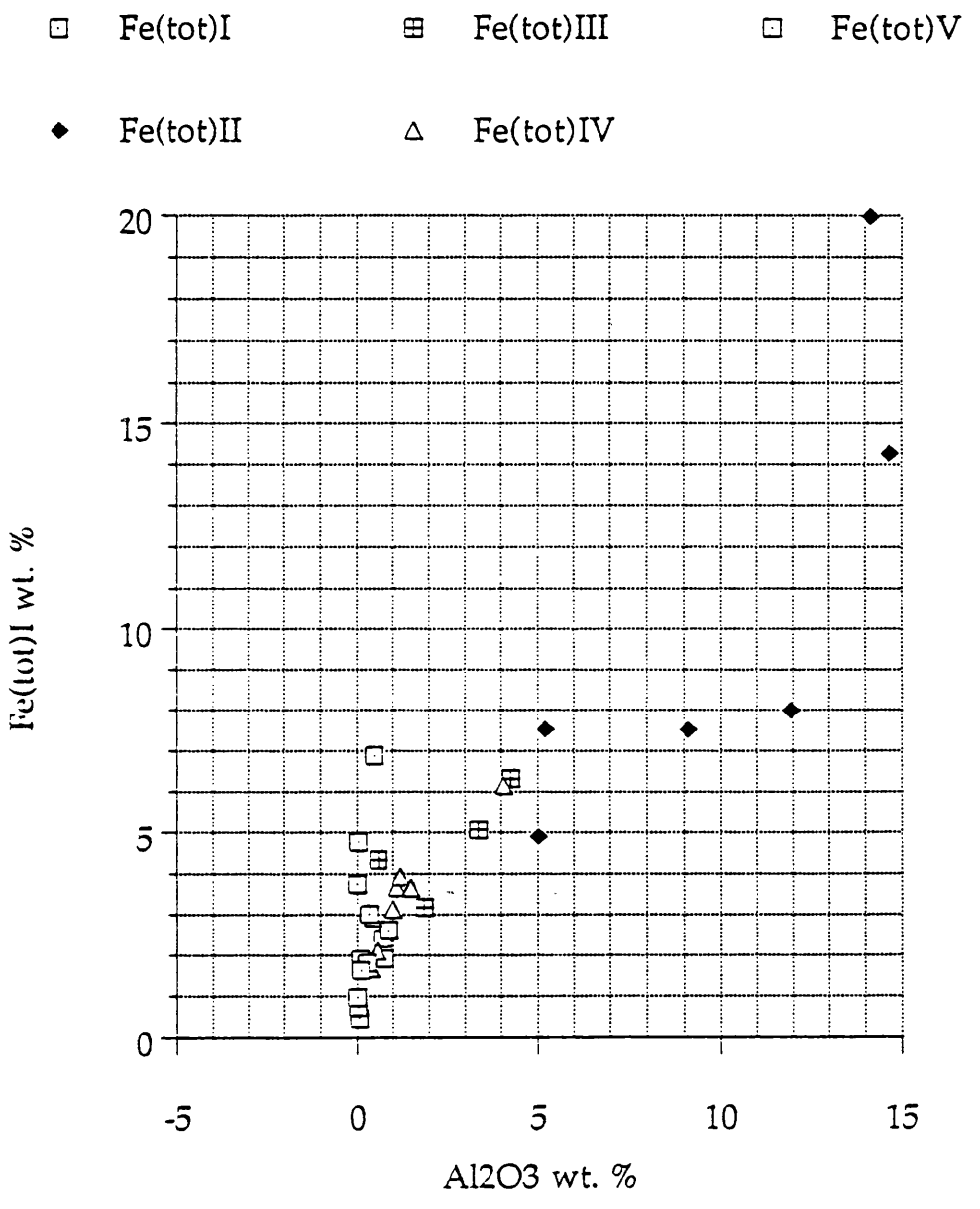
Fe(tot)I
Fe(tot)III
Fe(tot)V
Fe(tot)II
Fe(tot)IV
20
15
10
5
0
-5
0
5
10
15
Fe(tot)I wt. %
Al2O3 wt. %

Figure 9

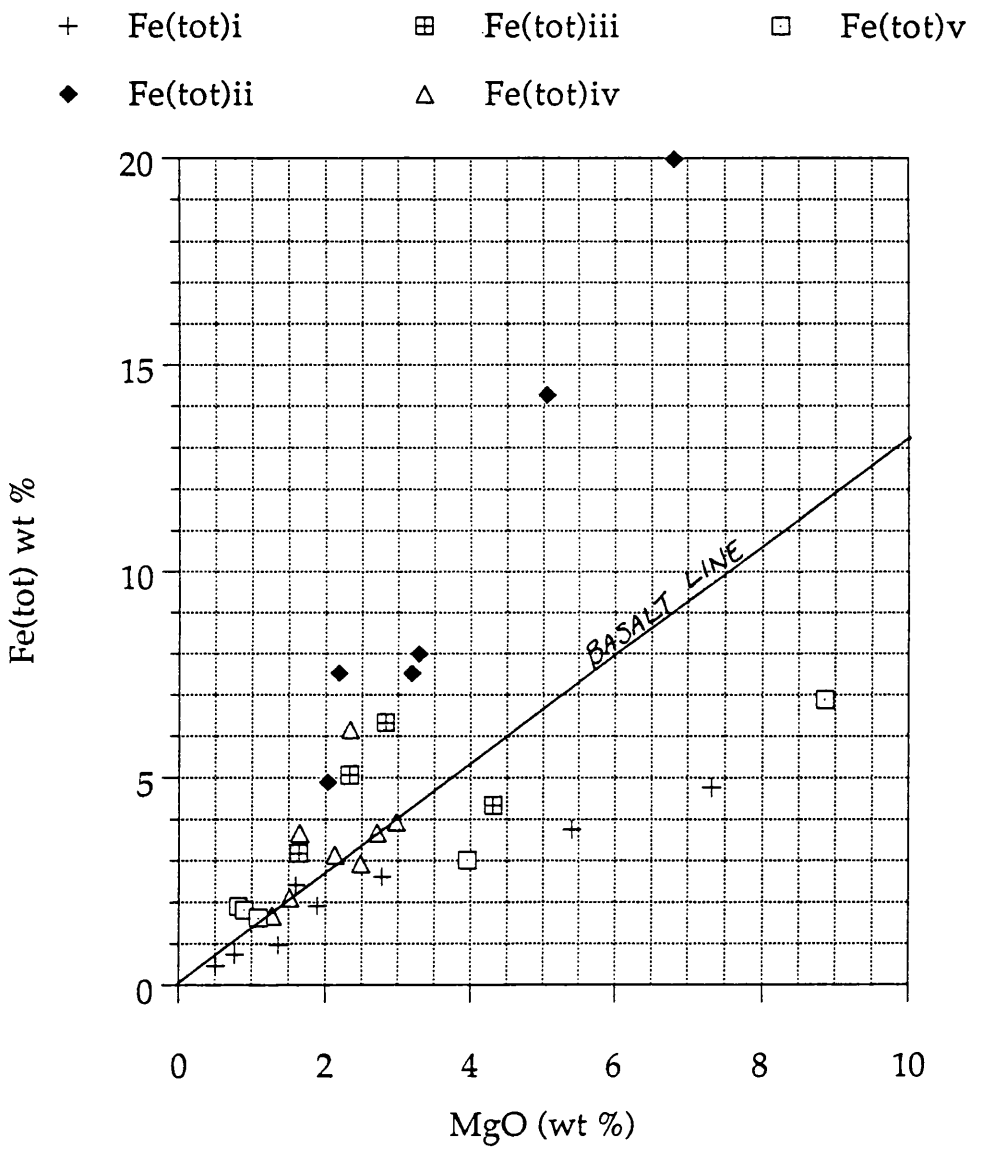
+ Fe(tot)i
⊞ Fe(tot)iii
⊡ Fe(tot)v
◆ Fe(tot)ii
△ Fe(tot)iv
20
15
10
5
0
Fe(tot) wt %
BASALT LINE
0
2
4
6
8
10
MgO (wt %)

Figure 10a

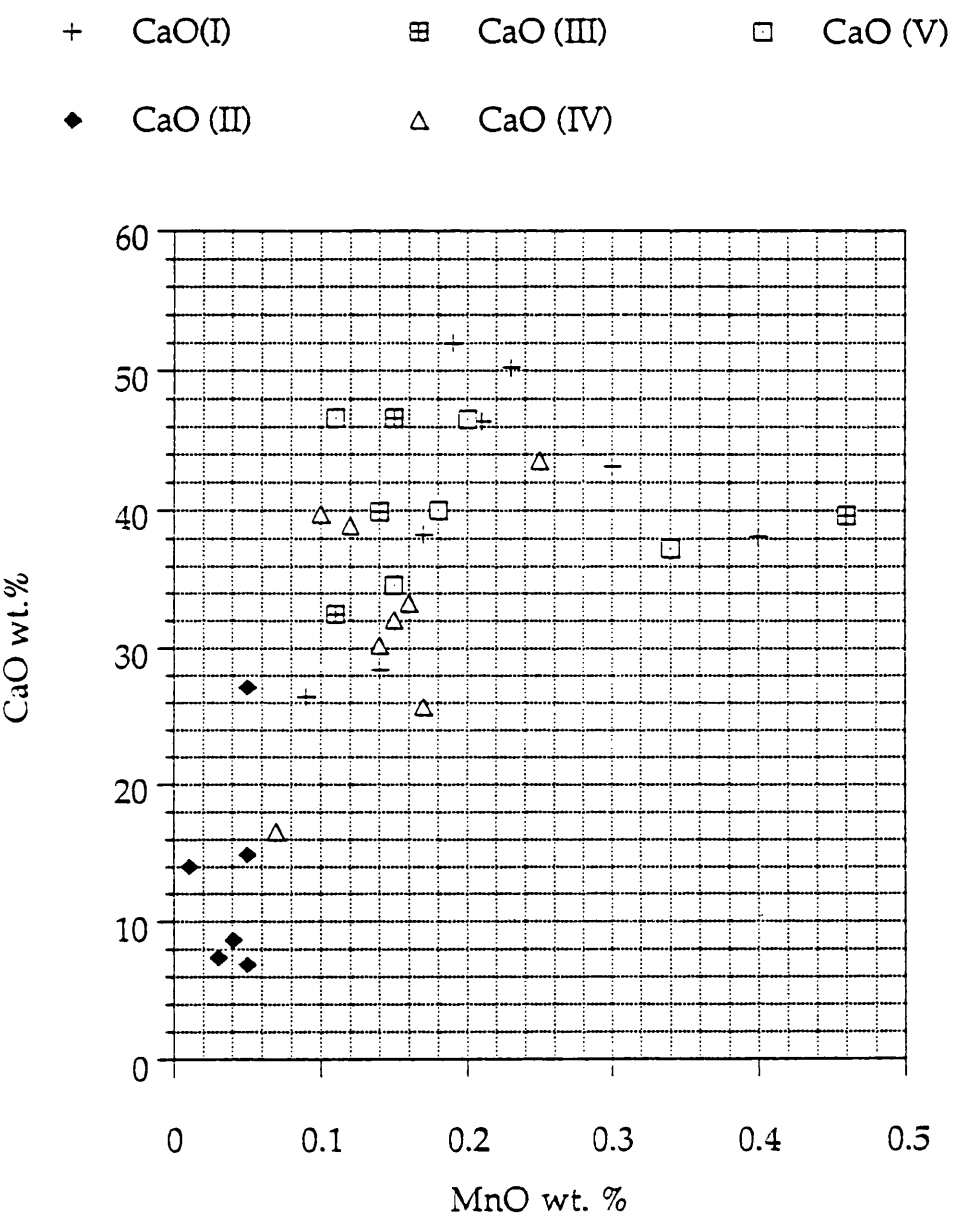
+ CaO(I)
⊞ CaO (III)
□ CaO (V)
◆ CaO (II)
△ CaO (IV)
60
50
40
30
20
10
0
CaO wt.%
0
0.1
0.2
0.3
0.4
0.5
MnO wt. %

Figure 10b

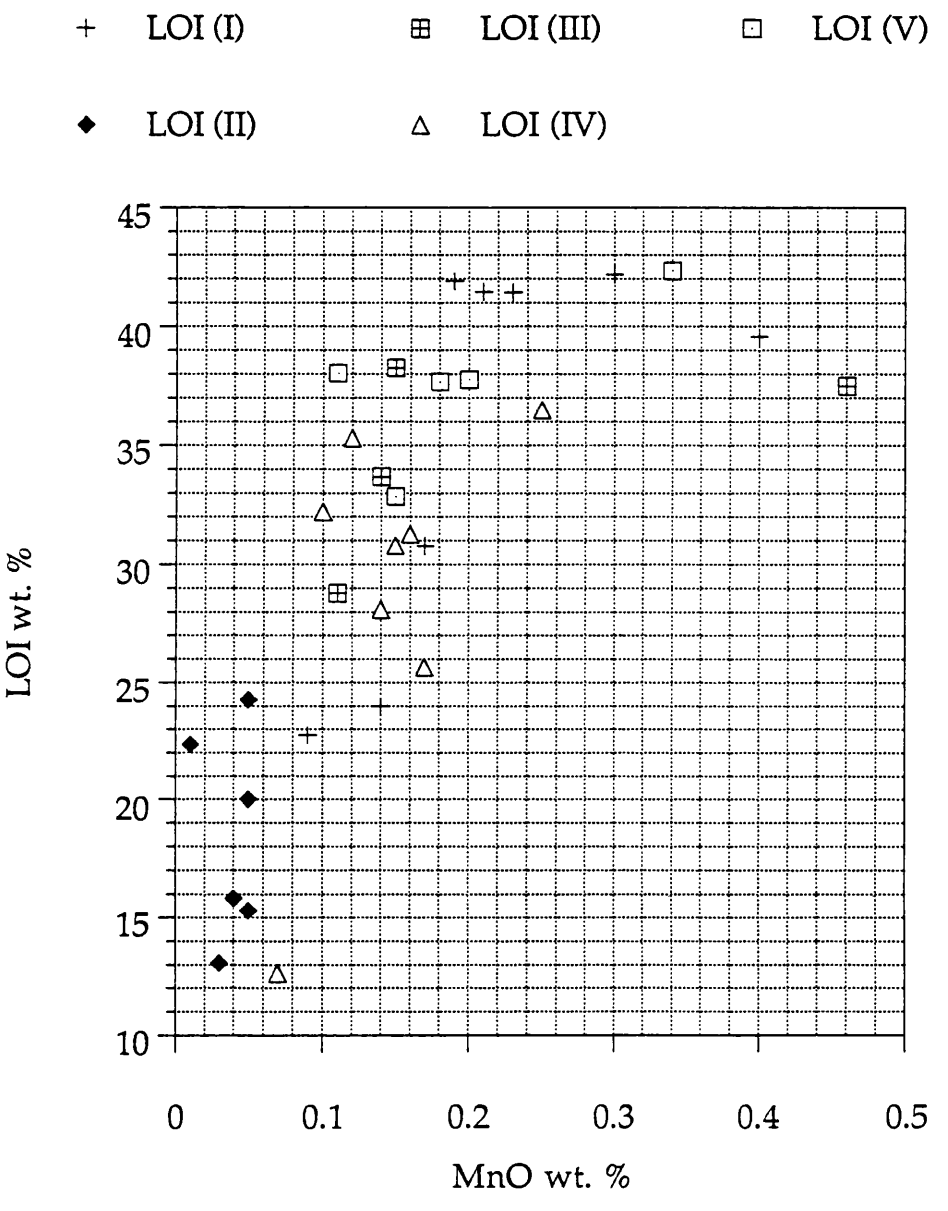
+ LOI (I)
⊞ LOI (III)
⊡ LOI (V)
◆ LOI (II)
△ LOI (IV)
45
40
35
30
25
20
15
10
LOI wt. %
0
0.1
0.2
0.3
0.4
0.5
MnO wt. %

Figure 11a

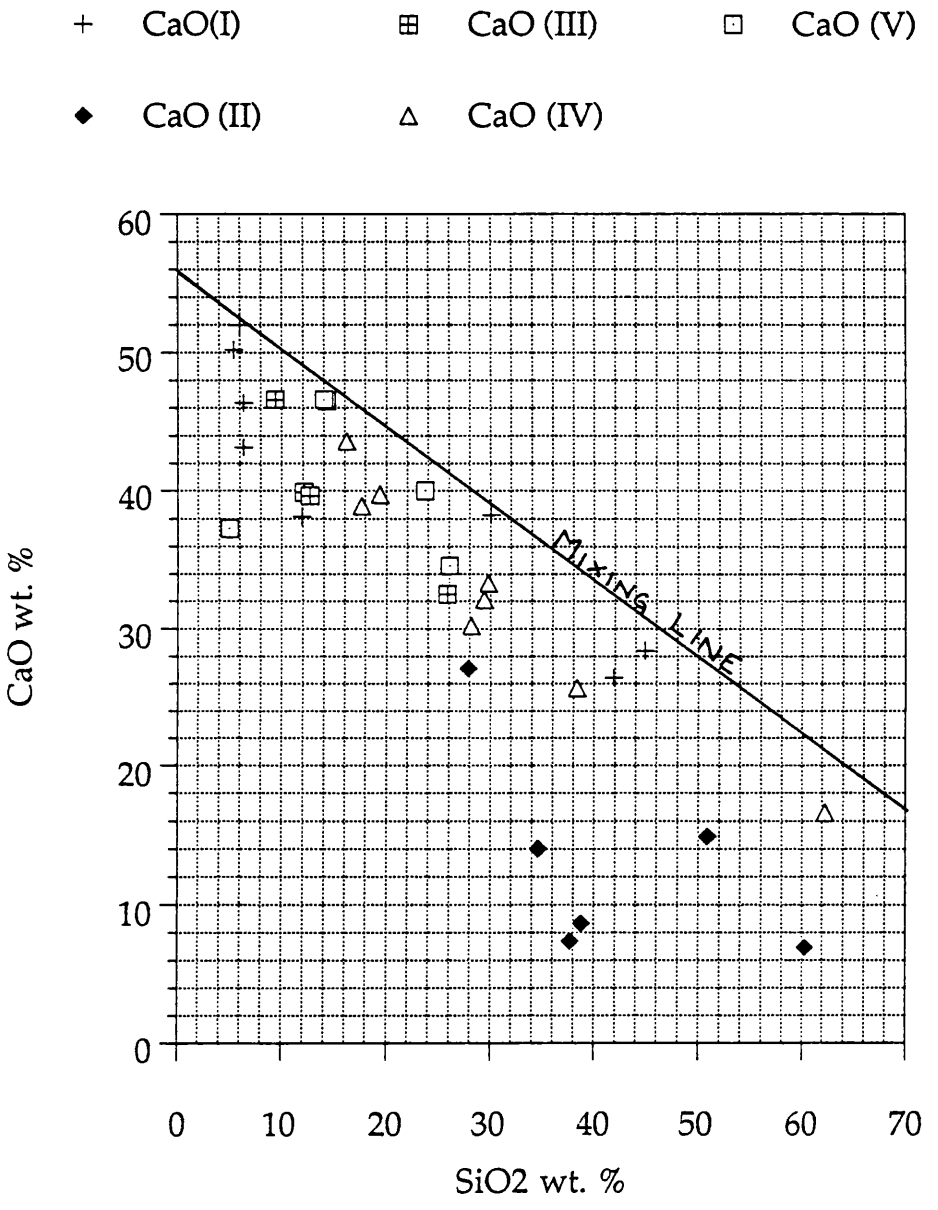
+ CaO(I)
⊞ CaO (III)
□ CaO (V)
◆ CaO (II)
△ CaO (IV)
MIXING LINE
CaO wt. %
SiO2 wt. %
0
10
20
30
40
50
60
70

Figure 11b

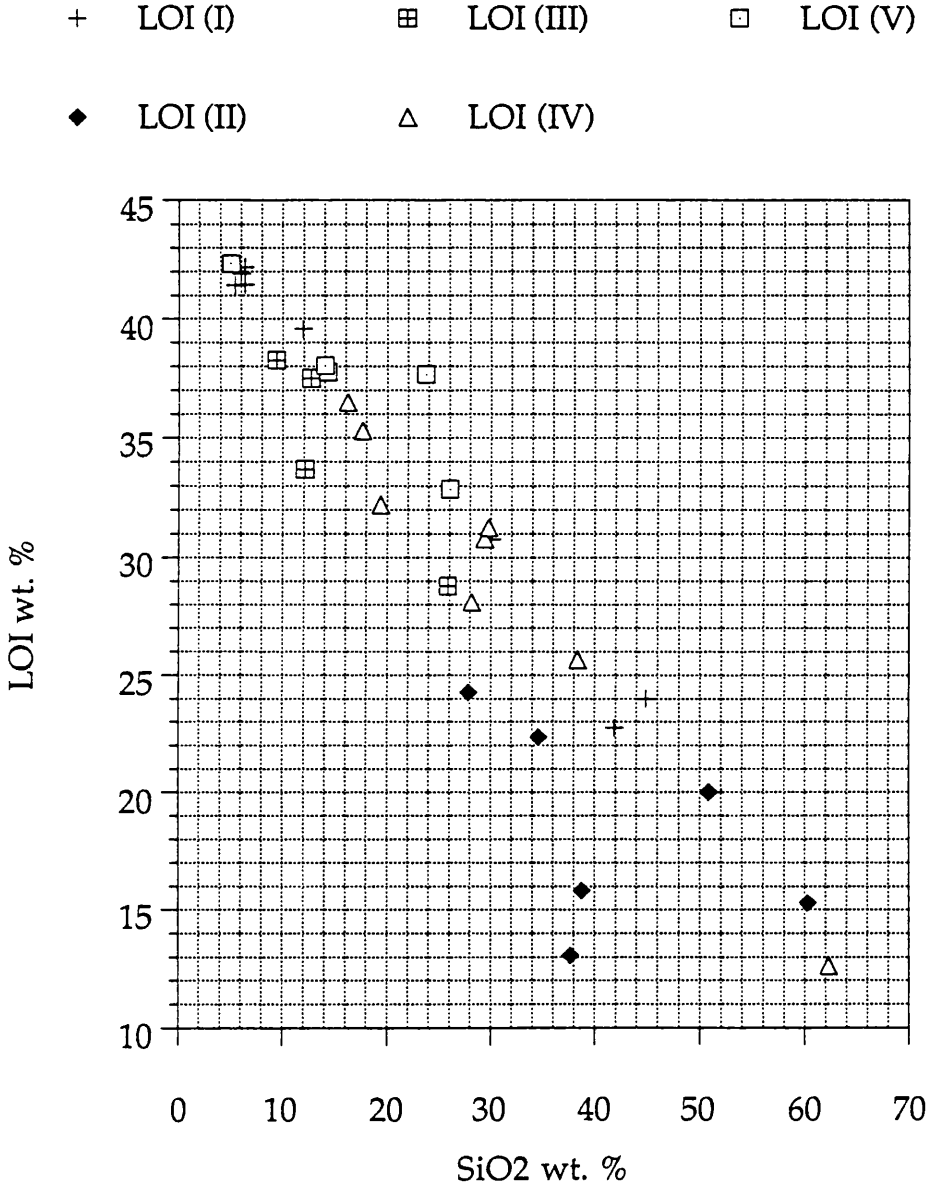
+ LOI (I)
⊞ LOI (III)
⊡ LOI (V)
◆ LOI (II)
△ LOI (IV)
LOI wt. %
45
40
35
30
25
20
15
10
0
10
20
30
40
50
60
70
SiO2 wt. %

Figure 12a

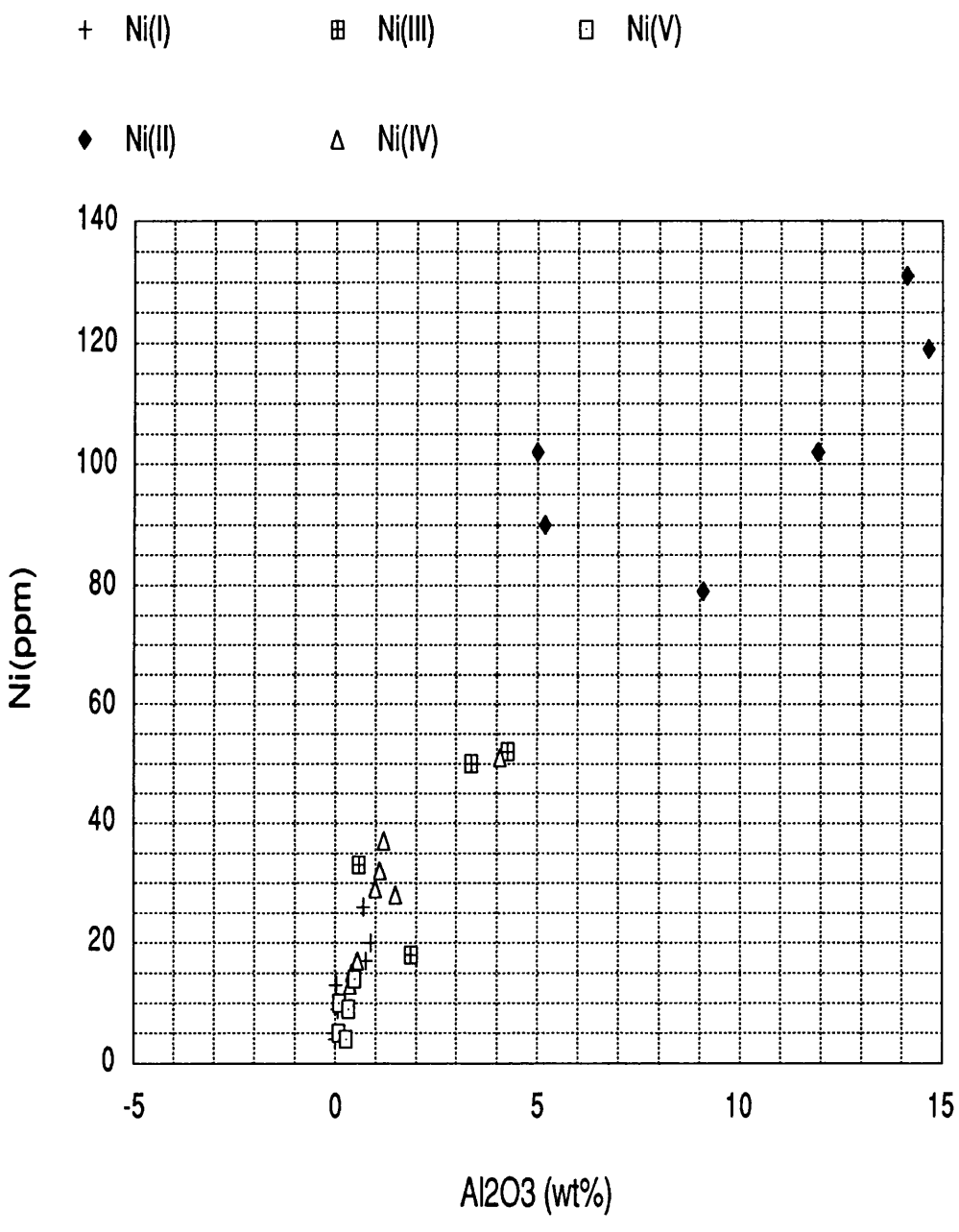
+ Ni(I)
⊞ Ni(III)
⊡ Ni(V)
♦ Ni(II)
Δ Ni(IV)
140
120
100
80
60
40
20
0
Ni(ppm)
-5
0
5
10
15
Al2O3 (wt%)

Figure 12b

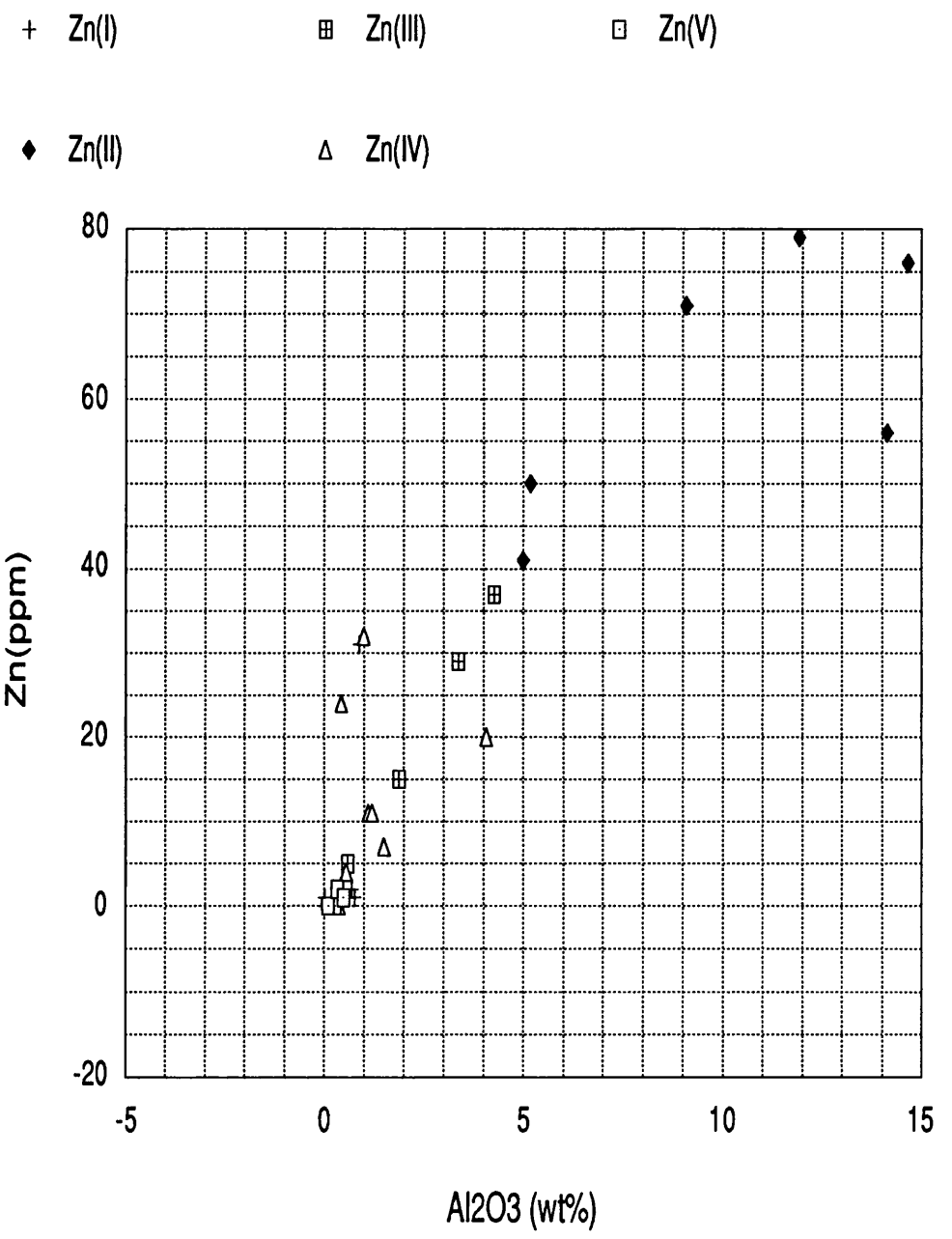
+ Zn(I)
⊞ Zn(III)
⊡ Zn(V)
♦ Zn(II)
Δ Zn(IV)
80
60
40
20
0
-20
Zn(ppm)
-5
0
5
10
15
Al2O3 (wt%)

Figure 12c

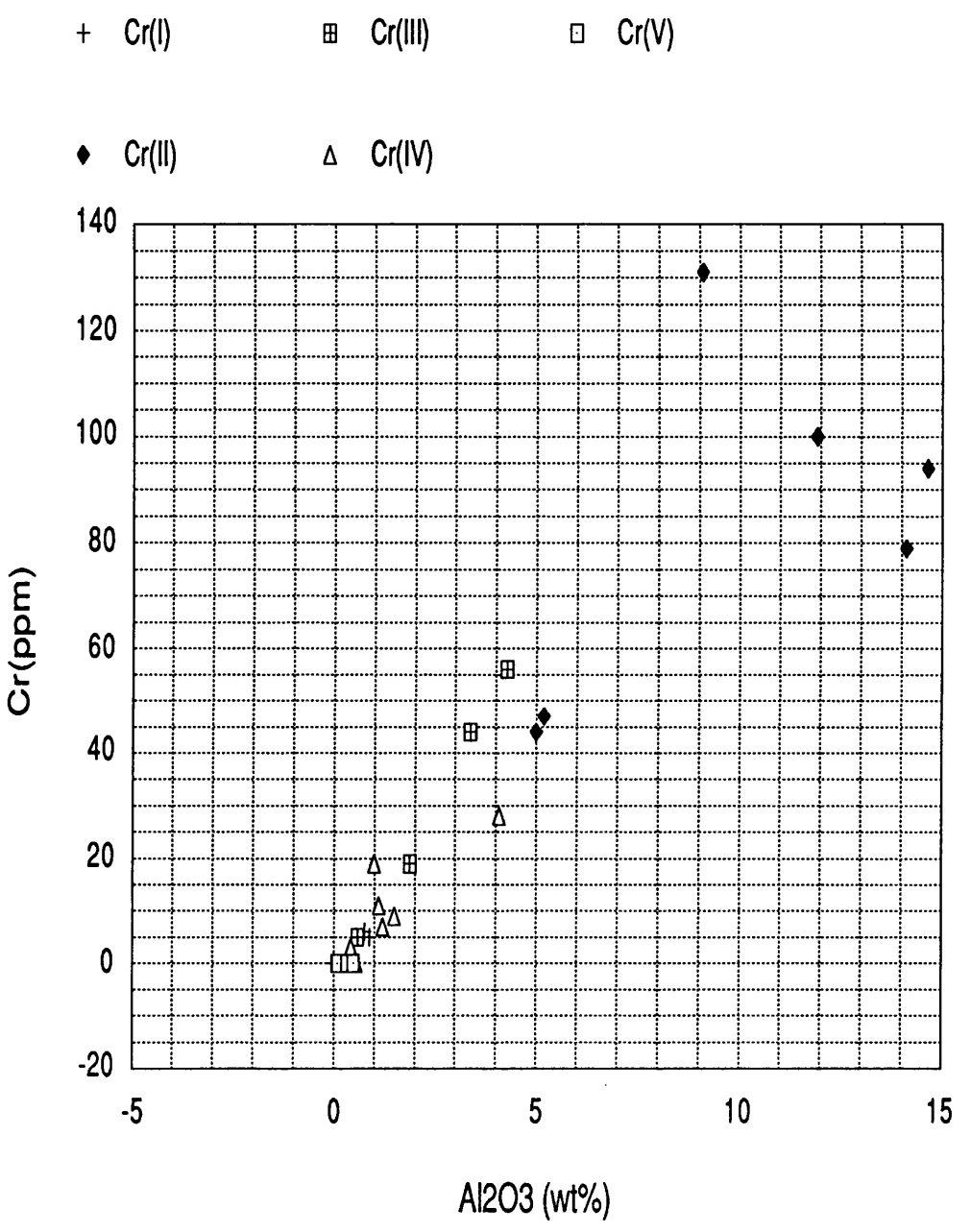
+ Cr(I)
⊞ Cr(III)
⊡ Cr(V)
♦ Cr(II)
Δ Cr(IV)
140
120
100
80
60
40
20
0
-20
Cr(ppm)
-5
0
5
10
15
Al2O3 (wt%)

Figure 13

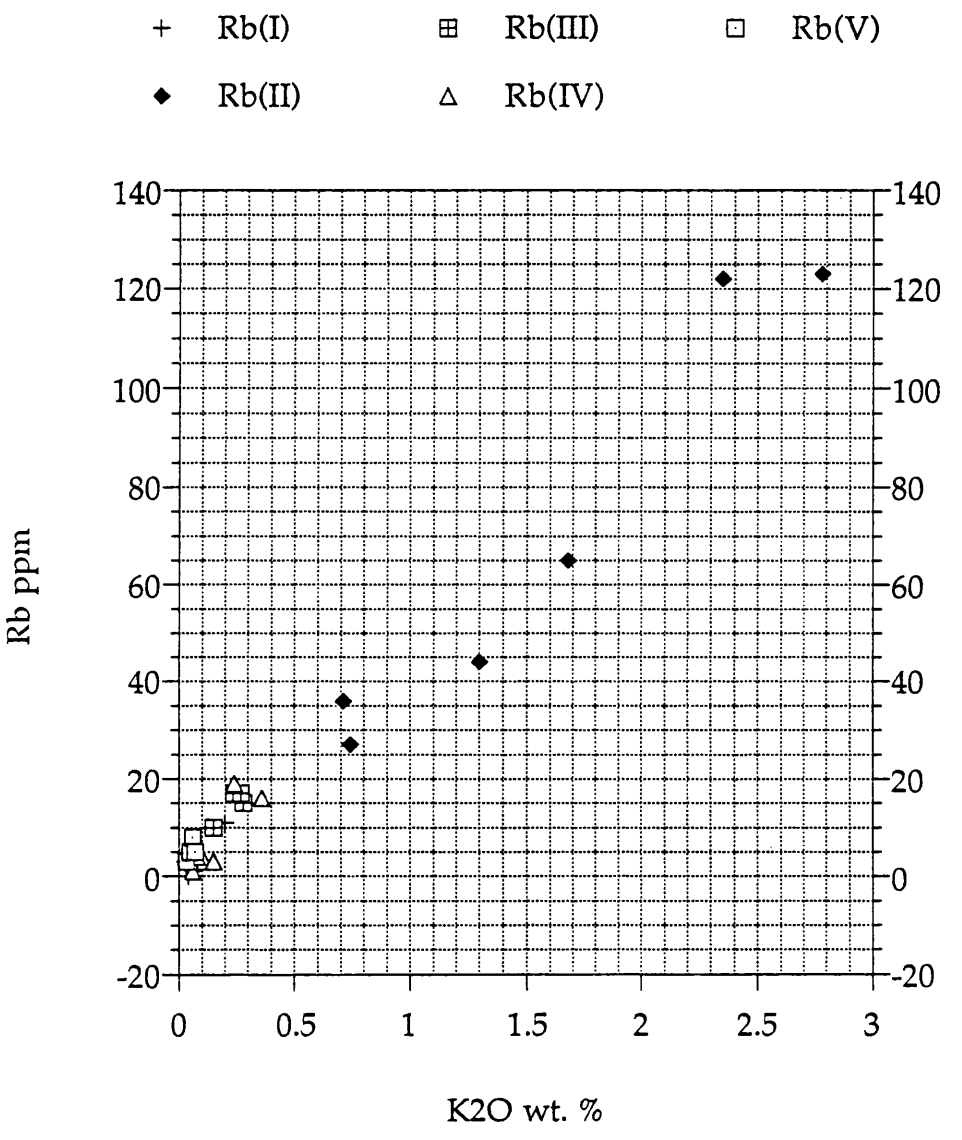
+ Rb(I)
⊞ Rb(III)
⊡ Rb(V)
◆ Rb(II)
△ Rb(IV)
140
120
100
80
60
40
20
0
-20
0
0.5
1
1.5
2
2.5
3
Rb ppm
K2O wt. %

Figure 14

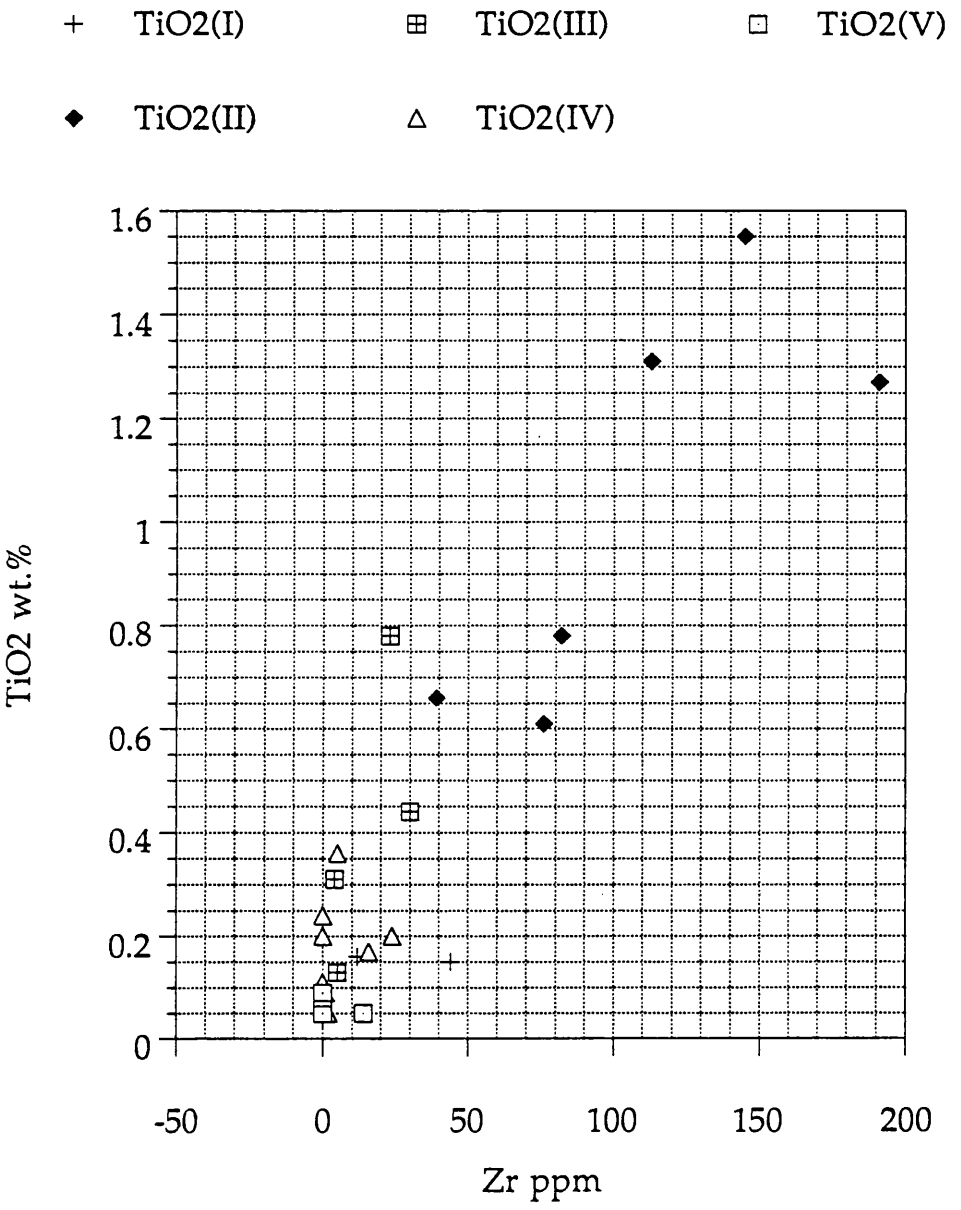
+ TiO2(I)
⊞ TiO2(III)
⊡ TiO2(V)
◆ TiO2(II)
△ TiO2(IV)
TiO2 wt.%
1.6
1.4
1.2
1
0.8
0.6
0.4
0.2
0
-50
0
50
100
150
200
Zr ppm

Figure 15

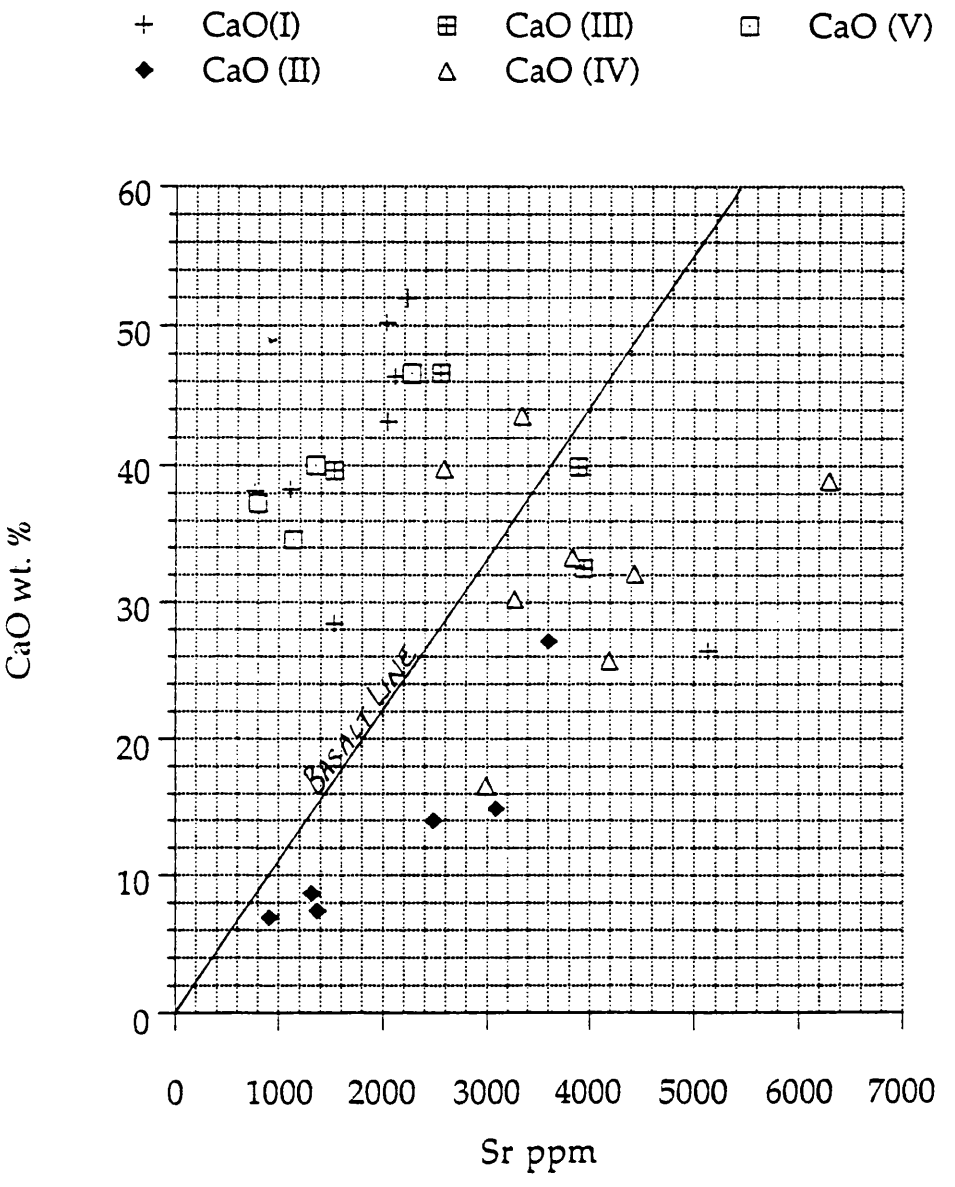
+ CaO(I)
⊞ CaO (III)
□ CaO (V)
◆ CaO (II)
△ CaO (IV)
CaO wt. %
60
50
40
30
20
10
0
BASALT LINE
0
1000
2000
3000
4000
5000
6000
7000
Sr ppm

Table 1

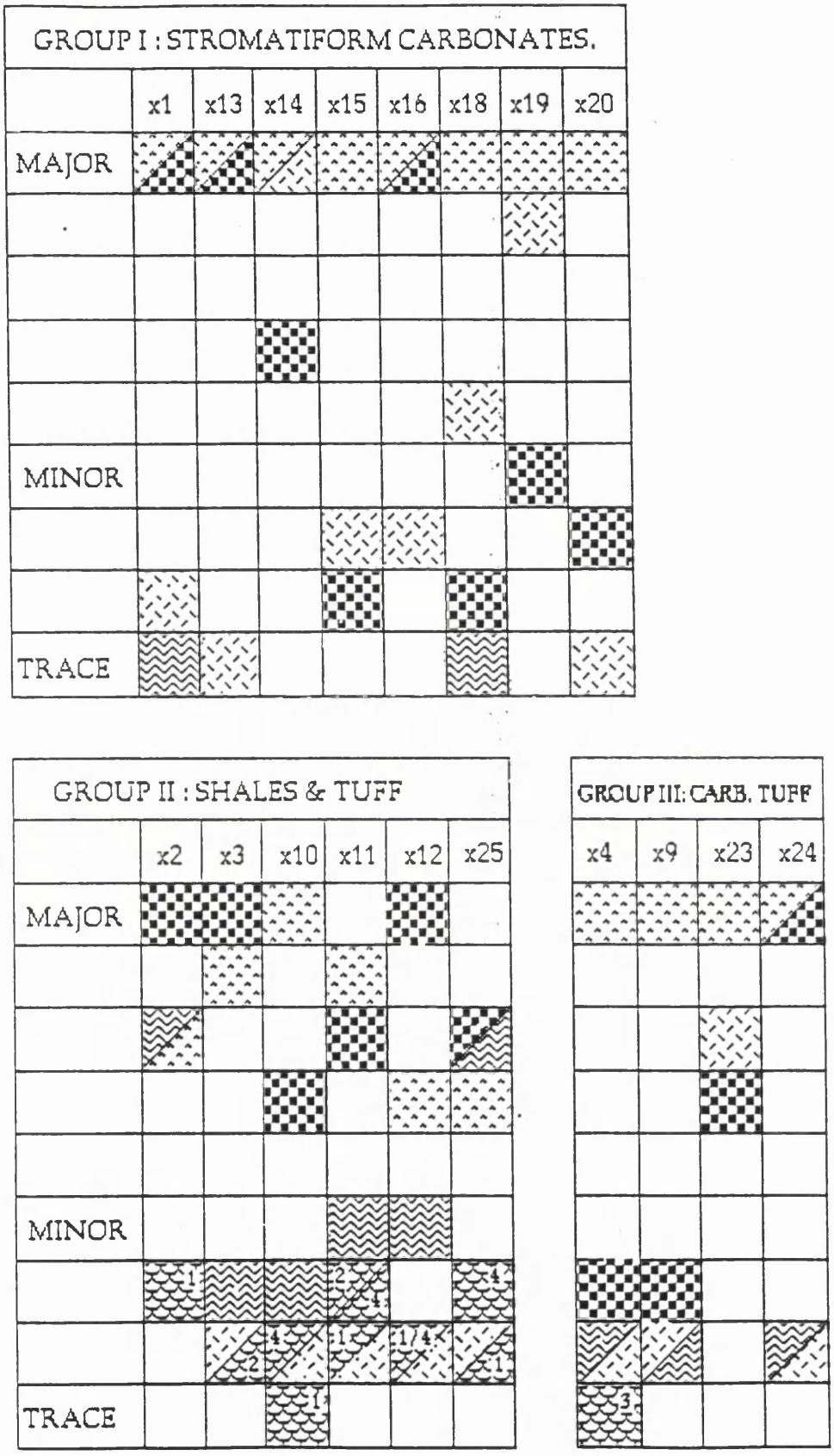
GROUP I : STROMATIFORM CARBONATES.
x1
x13
x14
x15
x16
x18
x19
x20
MAJOR
MINOR
TRACE
GROUP II : SHALES & TUFF
x2
x3
x10
x11
x12
x25
MAJOR
MINOR
TRACE
GROUP III: CARB. TUFF
x4
x9
x23
x24

Table 1

GROUP IV : SHALEY LAMINITES.								
	x5	x6	x7	x8	x17	x21	x22	x26
MAJOR								
MINOR								
TRACE					1			

GROUP V : CARB. LAMINITES.					
	x27	x28	x29	x30	x31
MAJOR					
MINOR					
TRACE					

KEY

CALCITE

QUARTZ

ANKERITE/DOLOMITE

CHLORITE/KAOLINITE

CLAY/FELDSPARS

1 CLAY MOUND

2 CLAY PEAK

3 PLAGIOCLASE FELDSPAR

4 POTASSIUM FELDSPAR

Sample No.	SiO2	TiO2	Al2O3	Fe2O3	FeO	MnO	MgO	CaO	Na2O	K2O	P2O5	Total	L.O.I.	H2O & CO2	H2O	CO2
1	41.87	0.05	0.70	1.21	1.08	0.09	1.60	26.42	0.46	0.04	0.03	73.55	22.75	20.52	1.30	19.22
13	30.06	0.05	0.06	0.13	0.30	0.17	0.51	38.27	0.55	0.06	0.02	70.18	30.78	30.01	1.09	28.92
14	11.94	0.05	0.03	0.54	3.81	0.40	7.32	38.15	0.26	0.03	0.04	62.57	39.57	38.17	0.63	37.54
15	5.45	0.16	0.77	0.31	1.44	0.23	1.89	50.21	0.54	0.20	0.06	61.26	41.43	38.04	1.22	36.82
16	44.89	0.04	0.00	0.03	0.84	0.14	1.36	28.42	0.25	0.02	0.01	76.00	24.00	22.13	0.77	21.36
18	6.38	0.15	0.88	0.59	1.82	0.21	2.78	46.36	0.31	0.25	0.04	59.77	41.45	41.30	1.34	39.96
19	6.36	0.06	0.00	0.57	2.86	0.30	5.40	43.13	0.37	0.04	0.02	59.11	42.19	"40.02"	"1.22"	"38.80"
20	6.00	0.05	0.02	0.22	0.46	0.19	0.77	51.97	0.31	0.05	0.03	60.07	41.90	"40.83"	"1.26"	"39.57"
Range: Low	5.45	0.04	0.00	0.03	0.30	0.09	0.51	26.42	0.25	0.02	0.01	59.11	22.75	20.52	0.63	19.22
High	44.89	0.16	0.88	1.21	3.81	0.40	7.32	51.97	0.55	0.25	0.06	76.00	42.19	41.30	1.34	39.96
Average	19.12	0.08	0.31	0.45	1.58	0.22	2.7	40.37	0.38	0.09	0.03	65.31	35.51	33.88	1.10	32.77
Std Dev. σ	15.96	0.05	0.37	0.35	1.14	0.09	2.26	8.82	0.11	0.08	0.01	6.39	7.83	7.97	0.25	7.93

Sample No.	Ba	Ce	Co	Cr	Cu	Ga	La	Ni	Pb	Rb	Sr	Th	Y	Zn	Zr
1	272	15	8	5	19	7	6	26	3	0	5131	6	4	2	0
13	67	0	0	0	4	3	6	9	4	1	1108	2	7	0	0
14	26	0	2	0	6	2	6	13	2	2	763	5	7	0	0
15	77	10	2	6	12	4	11	17	3	11	2030	4	8	1	12
16	49	0	0	0	5	1	3	4	0	3	1525	7	6	0	0
18	49	4	4	5	3	5	6	20	1	15	2110	5	9	31	44
19	41	0	0	0	9	5	6	5	4	2	2041	11	6	0	0
20	65	3	4	0	10	2	0	13	3	2	2228	4	8	1	0
Range: Low	26	0	0	0	3	1	0	4	0	0	763	2	4	0	0
High	272	15	8	6	19	7	11	26	4	15	5131	11	9	31	44
Average	81	4	2.5	2	8.5	3.5	5.5	13.5	2.5	4.5	2117	5.5	6.9	4.5	7
Std Dev. σ	73.8	5.27	2.60	2.60	4.92	1.87	2.92	7.02	1.32	5.07	1240	2.5	1.45	10.1	14.5

Table 2 (Group I)

Sample No.	SiO2	TiO2	Al2O3	Fe2O3	FeO	MnO	MgO	CaO	Na2O	K2O	P2O5	Total	L.O.I.	H2O & CO2	H2O	CO2
2	37.68	0.78	14.13	2.94	15.33	0.03	6.81	7.38	0.38	0.71	0.09	86.26	13.06	15.47	5.72	9.75
3	50.86	0.66	5.00	1.27	3.26	0.05	2.03	14.87	0.55	1.30	0.19	80.04	20.00	"33.31"	5.81	"27.50"
10	27.86	1.31	9.09	1.48	5.42	0.05	3.19	27.12	0.40	1.68	0.35	77.95	24.26	27.44	4.30	23.14
11	34.62	1.55	11.92	2.12	5.28	0.01	3.29	13.98	0.84	2.78	0.35	76.74	22.35	35.89	7.63	28.26
12	60.25	0.61	5.19	1.66	5.27	0.05	2.18	6.88	0.46	0.74	0.17	83.46	15.29	29.58	6.80	22.78
25	38.74	1.27	14.66	2.45	10.64	0.04	5.05	8.64	0.34	2.35	0.25	82.32	15.80	———	———	———
Range: Low	27.86	0.61	5.00	1.27	3.26	0.01	2.03	6.88	0.34	0.71	0.09	76.74	13.06	15.47	4.30	9.75
High	60.25	1.55	14.66	2.94	15.33	0.05	6.81	27.12	0.84	2.78	0.35	86.26	24.26	35.89	7.63	28.26
Average	41.57	1.03	10.00	1.99	7.53	0.04	3.76	13.14	0.50	1.59	0.23	81.13	18.46	28.34	6.05	22.29
Std Dev. σ	10.7	0.36	3.90	0.58	4.15	0.02	1.68	6.97	0.17	0.77	0.09	3.26	4.03	7.07	1.12	6.65

Table 2 (Group II)

Sample No.	Ba	Ce	Co	Cr	Cu	Ga	La	Ni	Pb	Rb	Sr	Th	Y	Zn	Zr
2	202	24	24	79	25	19	17	131	9	36	1365	7	13	56	82
3	347	38	34	44	26	10	20	102	5	44	3081	3	14	41	39
10	397	69	22	131	33	14	30	79	3	65	3591	8	21	71	113
11	460	45	26	100	43	18	36	102	3	123	2477	6	19	79	145
12	198	36	18	47	22	7	22	90	6	27	906	4	14	50	76
25	465	86	44	94	38	22	41	119	12	122	1313	6	14	76	191
Range: Low	198	24	18	44	22	7	17	79	3	27	906	3	13	41	39
High	465	86	44	131	43	22	41	131	12	123	3591	8	21	79	191
Average	345	49.5	28	82.5	31	15	27.5	104	6.5	69.5	2122	5.5	16	62	108
Std Dev. σ	110	20.9	8.60	30.4	7.50	5.20	8.70	17.2	3.20	39.2	992	1.70	3.00	14.1	49.5

Sample No.	SiO2	TiO2	Al2O3	Fe2O3	FeO	MnO	MgO	CaO	Na2O	K2O	P2O5	Total	L.O.I.	H2O & CO2	H2O	CO2
4	12.13	0.78	4.27	1.45	4.38	0.14	2.83	39.91	0.42	0.24	0.18	66.73	33.69	32.97	2.95	30.02
9	9.39	0.31	1.87	0.49	2.42	0.15	1.64	46.61	0.74	0.28	0.17	64.07	38.26	34.92	1.54	33.38
23	12.70	0.13	0.59	1.03	2.97	0.46	4.31	39.64	0.20	0.15	0.02	62.20	37.50	____	____	____
24	25.87	0.44	3.37	0.96	3.70	0.11	2.33	32.50	0.29	0.27	0.11	69.95	28.79	____	____	____
Range: Low	9.39	0.13	0.59	0.49	2.42	0.11	1.64	32.50	0.20	0.15	0.02	62.20	28.79	____	____	____
High	25.87	0.78	4.27	1.45	4.38	0.46	4.31	46.61	0.74	0.28	0.18	69.95	38.26			
Average	15.02	0.42	2.52	0.98	3.37	0.22	2.78	39.66	0.41	0.24	0.12	65.74	34.56	____	____	____
Std Dev. σ	6.39	0.24	1.41	0.34	0.74	0.14	0.98	5.0	0.2	0.05	0.06	2.92	3.75	____	____	____

Table 2 (Group III)

Sample No.	Ba	Ce	Co	Cr	Cu	Ga	La	Ni	Pb	Rb	Sr	Th	Y	Zn	Zr
4	194	30	9	56	18	11	30	52	4	17	3887	5	13	37	23
9	127	19	2	19	8	6	19	18	3	15	2548	7	14	15	4
23	100	6	6	5	10	4	16	33	4	10	1527	8	11	5	5
24	250	27	12	44	24	11	20	50	5	17	3941	6	12	29	30
Range: Low	100	6	2	5	8	4	16	18	3	10	1527	5	11	5	4
High	250	30	12	56	24	11	30	52	5	17	3941	8	14	37	30
Average	168	20.5	7	31	15	8	21	38	4	15	2976	6.5	12.5	21.5	15.5
Std Dev. σ	58.5	9.29	3.70	20.1	6.40	3.10	5.26	13.8	0.70	2.86	1006	1.12	1.12	12.4	11.3

Sample No.	SiO2	TiO2	Al2O3	Fe2O3	FeO	MnO	MgO	CaO	Na2O	K2O	P2O5	Total	L.O.I.	H2O & CO2	H2O	CO2
5	17.65	0.24	1.00	0.80	2.10	0.12	2.13	38.92	0.27	0.06	0.13	63.42	35.29	"31.75"	"2.25"	"29.50"
6	62.28	0.05	0.38	0.76	0.82	0.07	1.28	16.58	0.45	0.05	0.02	82.74	12.63	"13.25"	"0.75"	"12.50"
7	29.42	0.17	1.11	0.64	2.74	0.15	2.71	32.09	1.30	0.11	0.16	70.60	30.80	32.64	2.41	30.23
8	16.19	0.11	0.56	0.28	1.64	0.25	1.52	43.57	2.09	0.15	0.14	66.50	36.49	33.84	1.49	32.35
17	28.21	0.36	4.08	1.02	4.62	0.14	2.34	30.22	0.38	0.36	0.08	71.81	28.10	28.34	3.31	25.03
21	38.36	0.20	1.21	0.68	2.92	0.17	2.98	25.70	0.35	0.08	0.11	72.76	25.66	____	____	____
22	29.83	0.09	0.43	0.25	2.40	0.16	2.49	33.30	0.29	0.05	0.07	69.36	31.27	____	____	____
26	19.39	0.20	1.50	1.58	1.87	0.10	1.65	39.75	0.30	0.24	0.10	66.68	32.21	____	____	____
Range: Low	16.19	0.09	0.43	0.25	1.64	0.10	1.52	25.70	0.27	0.05	0.07	63.42	25.66	____	____	____
High	38.38	0.36	4.08	1.58	4.62	0.25	2.98	43.57	2.09	0.36	0.16	72.76	36.49			
Average	25.58	0.20	1.41	0.75	2.61	0.16	2.26	34.79	0.71	0.15	0.11	68.73	31.40	____	____	____
Std Dev. σ	7.49	0.08	1.14	0.42	0.92	0.04	0.50	5.75	0.66	0.10	0.03	3.09	3.50	____	____	____

Sample No.	Ba	Ce	Co	Cr	Cu	Ga	La	Ni	Pb	Rb	Sr	Th	Y	Zn	Zr
5	272	35	11	19	21	7	18	29	3	1	6300	9	9	32	0
6	148	0	4	0	12	5	5	13	2	3	2991	4	3	0	2
7	200	15	14	11	26	6	6	32	3	3	4432	4	10	11	16
8	137	3	6	0	14	4	6	17	3	3	3339	6	8	4	0
17	190	17	16	28	13	12	19	51	5	16	3270	6	12	20	5
21	215	15	14	7	19	9	1	37	3	4	4190	5	8	11	0
22	198	3	4	3	11	6	0	15	2	3	3834	6	5	24	1
26	128	13	8	9	15	5	11	28	5	19	2582	8	8	7	24
Range: Low	128	3	4	0	11	4	0	15	2	1	2582	4	5	4	0
High	272	35	16	28	26	12	19	51	5	19	6300	9	12	32	24
Average	192	14.5	10.5	11	17	7	8.5	30	3.5	7	4000	6.5	8.5	15.5	6.5
Std Dev. σ	45.0	10.0	4.2	8.9	4.9	2.5	7.0	11.3	1.1	6.7	1102	1.6	2.0	9.3	8.9

Table 2 (Group IV)

Sample 6 is not included in the average calculations on this table, though it was from a laminite, the sample consists purely of one chert horizon, and is therefore not typical of this lithology.

Table 2 (Group V)

Sample No.	SiO2	TiO2	Al2O3	Fe2O3	FeO	MnO	MgO	CaO	Na2O	K2O	P2O5	Total	L.O.I.	H2O & CO2	H2O	CO2
27	14.31	0.05	0.09	0.27	1.46	0.20	0.82	46.52	0.33	0.03	0.08	64.15	37.77	____	____	____
28	14.04	0.09	0.27	0.25	1.40	0.11	0.90	46.61	0.25	0.06	0.08	64.06	38.03	____	____	____
29	23.72	0.05	0.10	0.38	1.11	0.18	1.09	40.03	0.25	0.05	0.10	67.06	37.67	____	____	____
30	26.07	0.08	0.33	0.60	2.17	0.15	3.96	34.60	0.22	0.06	0.14	68.38	32.87	____	____	____
31	5.05	0.09	0.48	0.47	5.77	0.34	8.86	37.28	0.35	0.07	0.02	58.78	42.33	____	____	____
Range: Low	5.05	0.05	0.09	0.25	1.11	0.11	0.82	34.60	0.22	0.03	0.02	58.78	32.87	____	____	____
High	26.07	0.09	0.48	0.60	5.77	0.34	8.86	46.61	0.35	0.07	0.14	68.38	42.33			
Average	6.64	0.07	0.25	0.39	2.38	0.20	3.13	41.01	0.28	0.05	0.08	64.49	37.73	____	____	____
Std Dev. σ	7.56	0.02	0.15	0.13	1.73	0.08	3.10	4.85	0.05	0.01	0.04	3.31	3.00	____	____	____

Sample No.	Ba	Ce	Co	Cr	Cu	Ga	La	Ni	Pb	Rb	Sr	Th	Y	Zn	Zr
27	92	0	0	0	11	3	6	5	2	3	2267	6	5	0	14
28	64	0	0	0	6	5	6	4	3	6	2271	6	6	0	0
29	35	0	0	0	6	3	1	10	1	5	1350	6	7	0	0
30	40	0	0	0	3	1	10	9	3	8	1138	9	8	2	0
31	40	5	0	0	11	2	3	14	3	5	796	9	7	1	0
Range: Low	35	0	0	0	3	1	1	4	1	3	796	6	5	0	0
High	92	5			11	5	10	14	3	8	2271	9	8	2	14
Average	54	1	0	0	7.5	3	5	8.5	2.5	5.5	1564	7	6.5	0.5	3
Std Dev. σ	21.4	2.0	0	0	3.1	1.3	3.1	3.6	0.8	1.6	602	1.5	1.0	0.8	5.6

Table 3a

	SiO2	TiO2	Al2O3	Fe2O3	FeO	MnO	MgO	CaO	Na2O	K2O	P2O5	LOI
SiO2	1.00											
TiO2	0.29	1.00										
Al2O3	0.35	0.91	1.00									
Fe2O3	0.39	0.79	0.90	1.00								
FeO	0.20	0.65	0.86	0.82	1.00							
MnO	-0.64	-0.57	-0.58	-0.53	-0.28	1.00						
MgO	-0.18	0.20	0.32	0.36	0.65	0.37	1.00					
CaO	-0.86	-0.61	-0.72	-0.74	-0.63	0.61	-0.24	1.00				
Na2O	0.01	0.06	0.02	-0.06	-0.07	-0.02	-0.16	0.02	1.00			
K2O	0.33	0.93	0.86	0.71	0.54	-0.52	0.17	-0.62	0.10	1.00		
P2O5	0.22	0.87	0.69	0.55	0.37	-0.56	-0.01	-0.42	0.28	0.82	1.00	
LOI	-0.92	-0.54	-0.64	-0.67	-0.49	0.73	0.03	0.94	-0.01	-0.52	-0.37	1.00

Pearson Product - Moment Correlation.
Table 3a.

	Ba	Ce	Co	Cr	Cu	Ga	La	Ni	Pb	Rb	Sr	Th	Y	Zn	Zr	Fe(tot)
Ba	1.00															
Ce	0.89	1.00														
Co	0.88	0.88	1.00													
Cr	0.82	0.89	0.80	1.00												
Cu	0.94	0.86	0.87	0.84	1.00											
Ga	0.84	0.83	0.87	0.88	0.84	1.00										
La	0.77	0.88	0.76	0.87	0.75	0.80	1.00									
Ni	0.79	0.81	0.93	0.86	0.83	0.89	0.78	1.00								
Pb	0.51	0.64	0.73	0.55	0.55	0.72	0.62	0.75	1.00							
Rb	0.79	0.83	0.81	0.84	0.80	0.82	0.83	0.79	0.56	1.00						
Sr	0.44	0.20	0.14	0.07	0.32	0.18	0.06	-0.01	-0.15	-0.13	1.00					
Th	-0.08	-0.01	-0.16	0.03	-0.05	-0.01	0.06	-0.12	0.01	-0.01	0.01	1.00				
Y	0.68	0.78	0.70	0.88	0.71	0.71	0.85	0.77	0.43	0.74	0.02	0.01	1.00			
Zn	0.84	0.88	0.85	0.94	0.83	0.88	0.85	0.89	0.56	0.86	0.10	-0.02	0.84	1.00		
Zr	0.76	0.86	0.82	0.88	0.80	0.83	0.80	0.83	0.64	0.95	-0.15	-0.03	0.73	0.90	1.00	
SiO2	0.48			0.30	0.41			0.48	0.25	0.28	0.09	-0.35	0.13	0.34		
MgO	0.01	0.14	0.18	0.22	0.15	0.23	0.16	0.28	0.33	0.21	-0.36	0.44	0.16	0.21	0.24	
CaO	-0.67			-0.61	-0.67			-0.79	-0.55	-0.59	0.03	0.15	-0.42	-0.66	-0.64	0.61
TiO2	0.84	0.89	0.82	0.97	0.86	0.88	0.90	0.86	0.54	0.92	0.01	0.02	0.88	0.94	0.91	0.69
Al2O3	0.76	0.82	0.86	0.91	0.81	0.94	0.81	0.93	0.74	0.88	-0.09	0.01	0.76	0.90	0.91	0.89
Fe(tot)	0.52	0.63	0.71	0.73	0.62	0.81	0.62	0.85	0.79	0.63	-0.19	0.16	0.57	0.73	0.72	1.00

Pearson Product - Moment Correlation.
Table 3b.

5. CONCLUSIONS.

5.1 SUMMARY OF RESULTS.

5.1.1 Palaeoenvironment.

The units which comprise regular laminae, are typical of a lake deposit, reflecting a low energy environment. The preservation of organic material, i.e. as fossils, and its occurrence in bituminous shales, both associated with pyrite, suggests that anoxic conditions have occurred within this lake. This indicates that fluid circulation was restricted and the lake may have been stratified.

These periods of calm were interrupted by influxes of coarse volcanic tuff which formed thick units of material which is sometimes graded. Much of this material is now believed to be epigenetic; i.e. lithified and reworked before its deposition in the East Kirkton lake (Durant, 1993). Most of these units have been permineralised by carbonate-rich fluids, and are consequently well cemented and indurated. It is thought that the intervals of volcanic activity may be responsible for triggering the syn-sedimentary slumping and faulting observed in the laminated units.

Within the lake, lenses of massive carbonate have formed. These lenses have a distinctive stromatiform texture. The lower of the two lenses (referred to as the "mound", Chapter 4, Units 61-64) had originally an open texture; i.e it was quite vuggy. These vugs are now infilled, and the stromatiform carbonate is permineralised by multiple phases of silica and carbonate, with inclusions of bitumen in some vugs. This feature is considered to represent stromatolitic growth around a hydrothermal seepage. The upper lens, or the "channel" has a less vuggy texture and was not affected by such pervasive alteration. The quarry was cleared of rubble and soil (in the summer of 1992) and another lens very similar to the "mound" was revealed. It is found beneath the "channel", within the same units as the "mound", and it may be a lateral continuation of this.

The other main feature of the lithology is the occurrence of chert within the laminites. Primary chert laminae may imply a hot-spring influence in this lacustrine environment. A biogenic source for the silica is ruled out; the silica does not appear to have come from the local volcanics and a Magadiite precursor is considered unlikely (Chapter 1). Within this setting of volcanic activity, a hot-spring hypothesis for the formation of chert laminae is quite possible. The reasons why the chert

laminae are considered to be primary are given below.

5.1.2 Textures in Primary Silica Laminae.

The main features of the silica laminae which makes them appear primary are (pp. 21-22): the syn-sedimentary slumping and faulting; pinch and swell textures; and borings within the silica. All these features appear to occcur in a phase which was able to deform plastically without fracturing. This was originally interpreted as a "gel"-like phase, but may equally have occurred within an unlithified, viscous, siliceous mud.

In some chert laminae there are euhedral carbonate rhombs, which appear to be suspended within the silica, and can even resemble a graded carbonate sediment which has settled through the silica. Chert laminae also preserve pellets, which have been interpreted as fecal pellets possibly from some small aquatic organism (they may also be filaments of bacterial/algal origin). These pellets are preserved uncompacted. The original organic material has been replaced very early by the silica and this has prevented compaction destroying the organic detail. Organic material is generally better preserved within the chert horizons than in the carbonate.

Dark brown chert, similar to that of the laminae, can also be found as isolated lenses within the tuff horizons. These small lenses often show plastic deformation, similar to that observed in the laminae. It is thought that these may be rip-up clasts incorporated within the tuff due to the increased energy of the environment, associated with deposition of the tuffs.

5.1.3 Secondary Silica.

There are many phases of secondary silica and details are given in Chapter 3. Most of these are associated with the stromatiform "mound". In these samples, silica phases cut across carbonate textures, and often do not preserve any fine detail of the original texture. These phases are generally followed by the phases which infill the vugs, i.e. banded chalcedony, equant mega-quartz, bitumen and coarse calcite.

The zebraic chalcedony within the vugs can form spherulitic features. The laminites contain numerous carbonate spherules, one of the unique features of the East Kirkton lithology. Spherulitic habits often occur in mineral phases associated with hot-spring environments. The formation of the carbonate spherules is considered to be biogenically mediated (Walkden *et al* , 1993) but it is possible that some feature of the

East Kirkton lake fluids influences the formation of spherules in carbonate and chalcedony phases (Muir and Walton, 1957).

5.1.4 $\delta^{18}O$ and δD Stable Isotope Analyses.

$\delta^{18}O$ was measured for structural oxygen, Si-O, and δD was measured for bound water, within the silicate structure. A range of values from +21 to +27‰ was obtained for $\delta^{18}O$ and these values were not related to different petrographic types of silica. δD values gave a range from -50 to -90‰, and it was observed that the lower δD values corresponded with those silica phases which were considered to be secondary (i.e. altered or replacive). The variation between the two groups of δD values was not related to the sample yield obtained during extraction.

When $\delta^{18}O$ and δD results are plotted they are observed to form a tight isotopic, grouping which lies on the "Agate-line" (Fallick *et al* , 1985). This indicates a similar origin for all the East Kirkton samples. That is, formation from fluids with a strong meteoric water signature and at a temperature of around 60°C, as deduced for the Scottish agates, from the results of which the "Agate-line" was derived.

From the fractionation factors of Fallick *et al* (1985), for isotopic fractionation of $\delta^{18}O$ and δD between silica and water, the isotopic signature of the formation water is estimated. The lower Carboniferous meteoric water, from which the East Kirkton silica formed, had $\delta^{18}O$ of around -3‰, and δD of around -15‰. This is consistent with the palaeolatitude which is known to be close to the equator.

The lower δD values for the altered or replacive silica samples cause the results for these samples to plot below the "Agate-line". This appears to indicate that the δD from the structurally bound water in these samples has been reset by later fluids which interacted with these rocks (particularly, the most porous sample, EK 1.69 (w), for which duplicate $\delta^{18}O$ results, could not be obtained).

5.1.5 Lithological Occurrences of Pyrite.

Pyrite was found in almost every type of lithological occurrence within the East Kirkton succession. It was commonly found within silica and carbonate phases; associated with fossilised plant remains; and as disseminated nodules in shales and tuffs.

5.1.6 $\delta^{34}S$ Stable Isotope Analyses.

$\delta^{34}S$ was measured for a variety of the pyrite samples and a wide range of values was obtained. $\delta^{34}S$ varied between +8 and -34‰. Those samples which were associated with fossilised plant material gave the lowest values (-26 to -36‰), and it is likely that the formation of this pyrite involved bacterial sulphate reduction.

There was an isotopic grouping for pyrite that had been extracted from nodules, centred around -18‰, and for chert laminae around 0‰. These results rule out closed system, marine sulphate reduction, but the pyrite from the chert samples may indicate a direct magmatic or hydrothermal source for the sulphur. The pyrite obtained from tuffaceous samples and carbonates had no apparent grouping.

5.1.7 Description of Whole Rock Samples Used in XRD and XRF Analyses.

Thirty-one whole rock samples were collected from a variety of different stratigraphic levels within the East Kirkton Limestone. The lithologies from which they were taken have been divided into five main categories.

Group I, were samples comprised of beige-coloured, stromatiform carbonate, probably formed by biogenic mediation. Group II samples were of organic-rich black shales, with lenses of friable volcanic tuff. Samples in Group III were volcanic tuffs which had been permineralised by carbonate-rich fluids; these carbonate fluids have also created a hard, crystalline cement in these horizons. The Group IV samples are from horizons which contain mainly shaley laminites; they also contain occasional chert laminae and numerous carbonate spherules. Group V samples are also laminites, but these are mostly comprised of carbonate. The carbonate probably represents a late alteration of muddy sediments by carbonate-rich fluids.

These samples were collected to reflect the range of types of deposition which had occurred in this environment. The variety of sedimentary material which was transported into the lake, or precipitated out of solution on mixing with lake waters is also encompassed by these samples.

5.1.8 XRD and XRF Analyses.

The analyses obtained for the samples described above were compared with results obtained for the local Bathgate Basalts (Smedley, 1986). With so much of the East Kirkton succession comprised of volcanic material, it was thought that this would be the main source for most of the elements in the EKL samples. Any element which was enriched in the EKL samples would either be a product of fluids from a different source, or would require some process of enrichment, by which it could become concentrated in the East Kirkton lake.

The analyses show that most elements, as suspected, had concentrations which were consistent with a local volcanic source. The only two major elements which showed significant enrichment, with respect to the basalt concentrations, were SiO_2 and CaO. One local source for these elements could be the Tyninghame or Gullane Formations's sediments which lie below the limestones and volcanic material in the Bathgate Hills. It is suggested that hydrothermal fluids, heated by the proximal volcanic activity, remobilised these elements from the sediments below. The effect of mixing the hydrothermal fluids with the cooler lake waters, causes silica to precipitate and form the chert laminae, but the carbonate is precipitated via biogenic mediation.

Analyses of trace elements indicate that the East Kirkton samples have high strontium values (760 - 6300ppm). The highest values were obtained from samples which contained spherules, and other forms of carbonate that are thought to be biogenic precipitates (Walkden *et al*, 1993). The Bathgate Basalts have relatively high values for Sr in basalts, but the values are considerably lower than those of the EKL samples. It is considered possible that biogenic processes may be sufficient to concentrate the Sr to these levels, but it is not possible from these data alone, to rule out some additional source of Sr, possibly from the underlying sediments.

The group of samples which were most generally enriched in trace elements, was Group II, the shale samples. This may be due to preferential adsorption of many trace elements by clay minerals, or the retentive properties of the clay minerals in the shales where the trace elements occur. Most trace elements correlate with Al_2O_3, Fe_{total} and TiO_2, and this appears to suggest that they are derived from the local volcanic source.

5.2 COMPARISON OF CONCLUSIONS WITH ORIGINAL OBJECTIVES.

It is felt that this research has produced some very important results which help to define conditions of the East Kirkton palaeoenvironment. In particular, characterisation of the nature of the fluid involved in the precipitation of the silica phases, and the range of sources from which the sulphur in pyrite was derived. The preliminary XRD and XRF whole rock analyses characterise the five lithological groups that were sampled, and indicate that the main source of the elements found in the EKL, was the local volcanic material. These analyses indicate also the need to identify an additional source for calcareous and siliceous fluids.

The results are consistent with the hypotheses that hot-spring fluids influenced the lacustrine environment, and that the main fluids involved with this lake were meteoric rather than marine. Research has not produced any evidence for precious, or base, metal mineralisation, and no contemporary lacustrine deposits were found that were formed under similar conditions to those found at East Kirkton, or that had a definite hot-spring influence.

5.3 SUGGESTIONS FOR FUTURE WORK.

From the geochemical analyses that have been completed, for suites of East Kirkton samples, several areas have been identified in which the research could be further developed.

It is suggested that a $^{87}Sr/^{86}Sr$ fingerprint could be obtained from lithologies that are potential local sources of Sr. This could possibly test conclusively whether the Sr is derived from the local volcanic material; from Lower Carboniferous sea water; or from the sediments of the Tyninghame or Gullane Formations, which lie below the EKL. This would be potentially useful for determing the source of the calcium in the carbonates as Sr behaves geochemically in a similar way to Ca.

There is also potential for gathering more isotopic data from carbonate samples. Values obtained from previous analyses gave wide ranges, and it is felt that closer petrographic control, e.g. for spherules, could identify areas which had been neomorphosed by different carbonate fluids. It is possible to analyse carbonates on a micro-scale, and this may be required for these samples. There are several potential sources for carbonate fluids in these samples and their individual influences might

become clearer through further analyses of this type.

The nature and signature of the fluids influencing the East Kirkton environment, particularly those that were in equilibrium with the silica phases, may be confirmed by $\delta^{18}O$ and δD analyses of kaolinite. The main difficulty that this will present is the extraction of the kaolinite from the shales and volcanic tuffs. It is also possible that the isotopic signature may have been reset by later diagenetic fluids.

Finally, it may be possible to analyse the $\delta^{34}S$ from the sulphate in gypsum samples, or from whole rock samples in which gypsum pseudomorphs are observed. If enough samples can be obtained for analyses, the results may determine whether the sulphate has undergone bacteriogenic fractionation, or has been precipitated in evaporitic conditions.

5.4 BIBLIOGRAPHY.

Durant, G. P. 1993. Volcanogenic sediments of the East Kirkton Limestone (visean) of West Lothian, Scotland. TRANS. R. SOC. EDINBURGH: EARTH SCIENCE **84**, pp 203-208.

Fallick, A. E., Jocelyn, J., Donnelly, T., Guy, M. & Behan, C. 1985. Origin of agates in volcanic rocks from Scotland. NATURE **313**, 672-674.

Muir, R. O. & Walton, E. K. 1957. The East Kirkton Limestone. TRANS GEOL SOC GLASGOW **12**, 157-168.

Smedley, P. L. 1986. The relationship between calc-alkaline volcanism and within-plate continental rift volcanism: evidence from Scottish Palaeozoic lavas. EARTH & PLANETARY SCIENCE LETTERS, **76**, pp 113-128.

Walkden, G. M., Irwin, R. and Fallick, A.E. 1993. Carbonate spherules and botryoids as lake floor sediments. TRANS. R. SOC. EDINBURGH: EARTH SCIENCE, **84**, pp 213-222.

APPENDICES.

APPENDIX A: DATA DESCRIPTION FROM XRD CHAPTER, 4.

Bold typeface for section titles, or parts of text that are interpretation.

GROUP I

Stromatiform/Buff Carbonate (samples 1,13,14,15,16,18,19,20.) 8 samples, see Table 1(Group I) and Table 2 (Group I).

Sample 1 was collected from the stromatiform, carbonate coating around a fossil tree trunk, near the base of the quarry sequence, the base of Log 1 (top of NMS unit 77, see Appendix C). It is comprised of buff carbonate, some of which is quite coarse grained, and has a stromatiform habit, with a small radius. It has minor chert and possibly a little pyrite associated with preserved wood. From its XRD trace it contains mostly calcite and quartz, with a small peak indicating a mixture of ankerite and dolomite, and a very small peak for pyrite.

Sample 1, has high SiO_2 (41.87%) and has CaO (26.42%), which is the lowest concentration of this group. CO_2 appears to be around 20%; LOI was measured to be 22.75%; and expected CO_2 is 20.76% - calculated from CaO which, it is assumed, occurs mainly as carbonate. This indicates that there is a fairly high proportion of calcite in this rock with little CO_2 that is not involved in this phase, confirmed by the ratio of the XRD peaks for calcite and ankerite/dolomite. It has also 0.7% Al_2O_3, 1.21% Fe_2O_3, 1.08% FeO and 1.6% MgO, all of which are moderate concentrations for this grouping, and which are probably components of the ankerite/dolomite and pyrite that are indicated to be present from minor XRD peaks; there is also the suggestion of a chlorite phase present, but the XRD peak is very small. The sample has the lowest CaO for this group, but with calcium carbonate at about 45%, it shows that this group is carbonate-rich. Samples 13 and 16 have similarly high SiO_2 and low CaO, both samples were collected from the extremities of the "mound".

This sample has the most enriched minor element chemistry of the group, especially for the elements Sr (5131ppm or 0.51%) and Ba (272ppm), and also high Zr (102ppm). Sample 1 has also highest group values for Ce (15ppm), Co (8ppm), Cu (19ppm), Ga (7ppm) and Ni (26ppm), all of these, though highest for the group, only amount to trace concentrations and are of little significance.

Sr is expected to correlate with calcite yet this Sr-rich sample has lowest CaO for Group I, this seems to suggest that there is another factor influencing

Sr concentration. *(According to analyses by G. Walkden, spherule calcite ~1.6% Sr, rhombohedral calcite ~1.3% Sr, pore filling radial fibrous calcite ~1.0% Sr, and botryoidal cements ~1.0% Sr)* Ba is highest in the black shales/ash group, so perhaps the Ba enrichment in this sample is related to a minor ash component in the sample.

Sample 13 is one four samples collected from the "mound" (within NMS units 61-64), and comes from its north eastern end. It is typical, petrographically, of this upper end of the mound, with buff coloured carbonate and a network of vugs infilled by porcellanous white silica, coarse crystalline carbonate, microcrystalline quartz and minor bitumen. The sample shows little of the distinctive stromatiform texture. There are only two elements in its composition that comprise over 1%, i.e. SiO_2 30.06% and CaO 38.27%. Measured CO_2 was 28.92%, and LOI 30.78%, which correlate with CO_2 calculated from CaO content (30.07%), it can therefore be seen that this specimen is mainly comprised of calcite and quartz. The XRD trace confirms this and shows a very small peak suggesting a mixture of ankerite and dolomite is present, in trace quantities; this sample has the lowest FeO and MgO contents of all 31 samples. The minor element concentrations in this sample are very low, i.e. all below 10ppm, except for Sr (1108ppm), Ba (67ppm) and Zr (29ppm).

Considering the petrographic texture of the stromatiform carbonate in this "mound" the high SiO_2 in this sample and sample 16 are probably due to either veining or a high vuggy porosity, infilled by silica phases. These elements (Sr, Ba, Zr) may be ubiquitous to all East Kirkton rock types, as are calcite and quartz suggesting some correlation between them, most probably with the carbonate phase. The carbonate in this sample (13) appears relatively compatible with these elements, though less so than other samples of the same group.

Sample 14 is from the central portion of the "mound" (within NMS units 61-64), close to an area that was strongly veined, by quartz, bitumen and calcite. It has a powdery appearance, is very pale coloured and has more of a spherulitic texture than stromatiform, with many vugs of silica, carbonate and a little bitumen. Its chemistry is mostly dominated by carbonate phases, CaO (38.15%), CO_2 (37.54%) and LOI (39.57%). This sample has calcite and ankerite according to the XRD trace, which corresponds with the variation between calculated CO_2 (29.98%) and

measured CO_2/LOI of about 9.5%, because the calculated CO_2 only accounts for calcium carbonate and there is excess CO_2 in this sample, more than is required to form calcite. The presence of other carbonate phases is also reflected by high concentrations of the following elements MgO (7.32%), FeO(3.81%), Fe_2O_3(0.54%), MnO (0.4%). The MnO (0.4%) for sample 14 is the highest for any East Kirkton sample, and appears to occur in carbonate-rich samples.

The elements Sr (763ppm), Ba (26ppm) and Zr (20ppm) are more depleted in this sample than any other East Kirkton sample (except for sample 31, a laminite, which has lower Zr, 16ppm). Other elements occur in concentrations of less than 7ppm, except Ni at 13ppm.

Samples 14 & 15 both have low SiO_2 (11.94% SiO2 for sample 14) and high CaO. Sample 14 has slightly lower CaO content than sample 15, though equally high CO_2 and LOI - they both have a roughly equal amount of carbonate, but in sample 14 there is ankerite as well as calcite, with sample 15 it is purer calcite - the difference between calculated CO_2 and measured CO_2/LOI for each sample, 9.59% for sample 14 and 1.98% for sample 15, also gives an indication of which sample has more calcite. The MnO (0.4%) for sample 14 is the highest for any East Kirkton sample, and would appear to occur in carbonate samples rather than with chlorite, it may contribute to the unique buff colouring of so much of the carbonate. Sample 14 is unusual because it has carbonate with more of an ankerite composition, than other samples which have dolomite or a mixture of the two. It was also collected close to pervasive carbonate veining. These factors suggest that (i) the ankerite is less attractive to these elements than other carbonate phases, (ii) perhaps these later carbonate fluids in the veins had a source that was not influenced by the local Sr enriched volcanics, or even (iii) that the later veining could have leached/depleted Sr, Ba and Zr from the stromatiform carbonate.

Sample 15, from the centre, of the top of the "mound" (within NMS units 61-64), is a more heterogeneous sample including; chloritic, ashy material; organic-rich patches; buff coloured stromatiform carbonate; and a matrix of coarse crystalline carbonate, quite dark brown in colour. It is predominantly comprised of calcite, CaO(50.21%), measured CO_2(36.82%) and LOI(41.43%) with a calculated CO_2 of 39.45%. It appears to contain more dolomite (possibly ferroan) than it does quartz. Of the "mound samples", sample 15 has the highest concentrations of TiO_2(0.16%) and Al_2O_3(0.77%); high Fe_2O_3(0.31%), FeO(1.44%), MgO(1.89%),

Na_2O(0.54%), and K_2O(0.2%). It is most similar to sample 14 for CaO, SiO_2, Fe total, and MgO; but is also comparable to the Al_2O_3 for samples 1 and 18. Sr (2030ppm), Ba (77ppm) and Zr (80ppm) are most concentrated in this "mound" sample, compared to samples 13, 14 & 16. Other minor elements occur in trace quantities, but are also more enriched for sample 15 than the other three.

Although the carbonate is quite pure calcite, the sample (15) has small inclusions of minerals more commonly found in the shale and ash groups. This is likely because sample 15 was taken from the top of the mound, just below the ash layer which covers it, and may also be due to the heterogeneity of the sample. It is also likely that the small amount of volcanic material incorporated in this sample is responsible for its slight enrichment in trace elements.

Sample 16 is the fourth "mound" sample, and came from the thin, southern end which consists of buff, stromatiform carbonate with banded chalcedony and very coarse carbonate in the ubiquitous vugs, and patches of blue/grey chert. The mound (within NMS units 61-64) appears to be faulted here and the area is quite highly veined. The sample has the highest SiO_2 concentration for this group (44.89%) and low CaO (28.42%), mostly as calcite since CO_2 (21.36%), LOI (24.00%) are similar to calculated CO_2 (22.33%). Most of the other elements in this sample occur in very small amounts (less than 0.1%) except MnO(0.14%), Na_2O(0.24%), FeO(0.84%) and MgO(1.36%). The MgO and FeO may both exist in the dolomite phase (probably ferroan) that can be observed from the XRD trace. The SiO_2 and CaO content occurs in similar proportions to sample 1 and the less extreme sample 3. This sample has relatively low Sr (1525ppm), Ba (49ppm) and Zr (46ppm) and has no other minor element concentration greater than 10ppm.

The high percentage of quartz in this "carbonate" sample is again suggestive of a very vuggy texture or some silicification by fluids that could be associated with the local faulting. It is similar to samples 1 & 13 for its high SiO_2, and sample 13 for its general lack of enrichment in any other elements. Since it is quartz rich and contains no suggestion of chlorite or clay minerals, the theory that - the trace elements are preferentially partitioned into the weathered ferro-magnesian minerals and, to a lesser extent, carbonate phases - is confirmed.

Sample 18, like samples 19 & 20, was taken from a second massive, stromatiform carbonate lens, located higher up the quarry sequence (probably from NMS units 38/39, partially overgrown in places). This second lens is cut by fewer veins and has less vuggy porosity; sample 18 was taken from its centre and is comprised of fine grained, pale-beige coloured carbonate, with some shaley patches, some areas of coarse carbonate and a texture that is sometimes like a breccia.

This sample is mainly calcite, CaO(46.36%); but CO_2(39.96%) and LOI(41.45%) are higher than calculated CO_2 of 36.43%, which indicates that another carbonate phase is present. From the XRD trace the second carbonate phase appears to be closer to the dolomite peak position than ankerite, and it has produced a higher peak than quartz for this sample, which has very low SiO_2(6.38%). It is probably a ferroan dolomite, since FeO(1.82%), Fe_2O_3(0.59%) and MgO(2.78%) are high, for a Group I sample. The sample includes small quantities of Al_2O_3(0.88%), MnO(0.21%), Na_2O(0.31%) and K_2O(0.25%). Most of these are relatively high for a sample that is so carbonate-rich, and suggests that some volcanic material is incorporated in the sample, possibly from shaley partings in this sample. Its high Al_2O_3 compares only with samples 1 &15, but its SiO_2 and calcite/dolomite content, compare well with other samples from the same carbonate lens.

Sample 18 has moderate Sr (2110ppm), low Ba (49ppm) and the highest Zr (114ppm) and high Cr (5ppm), Ni (20ppm) and Zn (31ppm), for this group. This sample may include small amounts of volcanic material, and though this has not affected the concentration of Sr or Ba, it may be partially responsible for the small enrichment in Zn, Ni and Cr, elements that may be incorporated in a chlorite phase. These three elements are not enriched in the other two samples from the same lens.

Sample 19 is from the southern end of this lens (from NMS units 38/39), where it thins out and becomes less than 1m thick. It exhibits a good stromatiform texture which is exaggerated by preferential weathering of interlayer material, leaving a thin pale carbonate parting, which highlights the sub-spherical, concentric texture. In unweathered areas of the sample a mid-brown, coarse-grained carbonate phase is observed between paler partings. This may be the original interlayer material, partially removed by weathering or an infilling/replacement. The sample is comprised mostly of calcite (CaO 43.13%) and a mixture of ankerite and dolomite (MgO 5.40%, FeO 2.86%), which produced an XRD peak that was

almost off the trace, (larger than for the other two samples from the same lens); **like samples 14 & 18 there is a significant difference between measured CO_2(38.80%), or LOI(42.19%), and calculated CO_2(33.89%), caused by the presence of a second carbonate phase.** Na_2O (0.37%) is also fairly high in this sample, but unlike sample 18, few of the other elements show any enrichment above 0.1% except Fe_2O_3(0.57%) and MnO (0.30%). The low SiO_2 (6.36%) in this sample is typical of the three, second-lens, samples.

There is little variation between the minor element concentrations for samples 18,19 & 20, though sample 19 appears to have marginally lower values for most elements than the other two. It has lowest Sr (2041ppm), Ba (41ppm) and Zr (39ppm), with only Th (11ppm), of the remaining minor elements, above 10ppm.

Sample 20 was collected to the northern end of the lens (from NMS units 38/39), where the rock was more strongly fractured (recent feature). Formed from buff-coloured, coarse-crystalline carbonate, it has an indistinct stromatiform texture and occasional organic-rich patches which appear to be associated with fractures. It has the highest CaO for this group (51.97%) forming fairly **pure calcite** - since CO_2(39.57%) and LOI (41.90%) have values similar to calculated CO_2(40.83%) - SiO_2(6.00%) is very low, and none of the other elements have greater concentration than 1%.

The XRD trace shows a very small peak for dolomite, and, correspondingly, the chemistry shows MgO(0.77%) and FeO(0.46%) to be the only elements with greater than 0.2%; also indicating how little dolomite is actually present. When compared to samples 18 & 19, sample 20 has higher Sr (2228ppm) and Ba (65ppm), with moderate Zr (52ppm). **It is possible that the higher Sr coincides with the higher calcite content, Sr is commonly incorporated into a calcite phase; but this sample has half the quantity of Sr that occurred in sample 1, which contained less calcite, but probably more volcanic material.**

GROUP II

Black Shale/Ash (samples 2,3,10,11,12,25). 6 samples, see Table 1(Group II) and Table 2 (Group II).

Sample 2 was collected from above the carbonate-coated, fossilised tree trunk (sample 1), from a finely laminated, organic-rich shale horizon (NMS units 76/77), which contained lenses of coarse volcanic ash; the material selected for crushing was the black shale, avoiding the coarse ash. It is expected to be geochemically similar to sample 3, which was collected from the same unit but contains slightly more ash.

The dominant element oxide in this sample is SiO_2 (37.68%), occurring as quartz which has the strongest XRD trace. The other main phases observed from the XRD analysis are calcite, chlorite and kaolinite, and a clay peak at about 11Å which shows characteristics, on glycolation and heating, of an illite-smectite mixed layer clay. Al_2O_3 (14.13%), FeO (15.33%), MgO (6.81%) and Fe_2O_3 (2.94%) are the main elements in this sample, including low CaO (7.38%). High Al_2O_3 will relate to chlorite and the clay phases. Chlorite will also account for much of the FeO and MgO, but it does not appear to contain MnO, as this sample has only 0.03% MnO (one of the lowest values for MnO in all 31 samples). This sample has no dolomite on its XRD trace (although others in the group have) but it has the highest MgO, so the percentage of chlorite and clay phases occurring in this sample will control the concentration of MgO, and probably FeO too. Chlorite and smectite group clays, enriched in FeO and MgO, are typical weathering products of basic volcanic material. The XRD shows calcite with the second highest peak on the trace, but it has only 7.39% CaO; CO_2 (9.75%) and LOI (13%), vary by a few percent from calculated CO_2 (5.80%) suggesting that there is (i) another carbonate phase present, besides calcite, or (ii) that there may be other volatile phases contributing to the LOI total e.g. organic carbon and water. The lack of calcite or other carbonate phases in this horizon may indicate that there has been no replacement or alteration by later carbonate fluids, and apparently there was only a little carbonate present when this horizon was being formed. When comparing major element analyses, sample 2 is actually most similar to sample 25, but samples 2, 3 & 12, from the same horizon, have similar moderate concentrations of trace elements.

The minor elements are moderately depleted in this sample relative to the other shales (except sample 12); Sr (1365ppm), Ba (202ppm) and Zr (127ppm), but

enriched when compared to carbonate-rich samples. The most enriched element is Ni (131ppm - highest for the group), with Cr (79ppm) quite high and moderate Zn (56ppm). These elements will probably be included in the chlorite phase. **These three elements are not proportionately enriched or depleted in Group II; they are similar in samples 2 & 3 (i.e. Ni highest), but for samples 10 & 11, Ni is lower but Cr and Zn are more enriched. This may reflect a variation in the composition of the chlorite phase.**

Sample 3 is a very black shale with interbedded, fine-grained ash layers, that were a greenish, chloritic colour, and also contains small, buff-coloured spherules. It was collected from the horizon above the friable shale of sample 2 (NMS unit 76); sample 3 is well cemented by a carbonate phase and is quite indurated. It is comprised of 50.86% SiO_2, mostly as quartz, and the other main phase is calcite; the sample has 14.87% CaO from which CO_2 (as calcite) was calculated as 11.68%, this is lower than measured LOI (20%). The difference in LOI and calculated CO_2, was similar for this sample and samples 2, 12, and 25 (measured CO_2 of 27.50%, was considered to be an inaccurate result and difficult to duplicate, LOI was more reliable). Small XRD peaks occur for chlorite and kaolin, with very small peaks for clay (again an 11 Å clay, showing characteristics of a mixed layer illite-smectite clay) dolomite and potassium feldspar. These phases will account for the 5% Al_2O_3, 3.26% FeO, 2.03% MgO and 1.27% Fe_2O_3. **The element concentrations (Al_2O_3, Fe_{total} and MgO) are the lowest for this group and appear to be more comparable with the concentrations for these elements in the Carbonate-rich ash group (although dissimilar in other respects).**

The small peak on the XRD trace for potassium-feldspar corresponds to the 1.3% K_2O in this sample, though the potassium could also be associated with clay phases (e.g. illite). **Potassium feldspar is an unusual component for basaltic ashes, and illite is unusual as a weathering product of basaltic ash, but if the feldspar has been present it could be the source of the illite (in the illite-smectite mixed layer clay phase). Sample 3, collected close to sample 2 has considerably less chlorite, the ashy material is much paler in colour, and does not have such a strong greenish colour. Most of the geochemical variation between samples 2 & 3, is due to the amount of volcanic material that they contain.**

The correlation between CaO and Sr (3081ppm) is observed for Group II's chemistry; i.e. sample 3 has the second highest concentration of CaO and the second highest Sr component. This sample and sample 10 have the largest percentages of volcanic ash, in hand specimen, and both have high values for CaO and Sr. Ba (347ppm) is also quite high, Zr (142ppm) and Ni (102ppm) moderate with Cr (44ppm) and Zn (41ppm) quite low. This sample has low Al_2O_3 and contains little chlorite, this is thought to influence Cr, Ni and Zn concentrations. The small quantity of chlorite that is present in this sample appears to be relatively Ni-rich, compared with the more Cr/Zn-rich chlorites of the shaley horizon further up the sequence. Samples 2, 3 and 12 have high Ni relative to Cr and Zn; but samples 10, 11 and 25 have high Cr, quite high Ni and a Zn concentration that is lower than Cr or Ni, but is higher than the Zn concentration for samples 2, 3 and 12 (and for any other sample).

Sample 10, was collected together with sample 11, from a friable horizon (NMS unit 42) that passed from chloritic, ashy shale (sample 10) into black shale (sample 11). Sample 10 has clasts of 2-3mm size and some larger clasts of 1cm size, it is poorly sorted, weakly bedded with no apparent gradation, and it is very poorly cemented. Clasts occur in a matrix of dark shale, and generally appear to be of altered volcanic material; rusty by iron staining, green and chloritic or, commonly, white and powdery, probably including kaolinite.

This sample has 27.86% SiO_2 and 27.12% CaO, which represents the lowest SiO_2 for this group, but the highest CaO and probably highest calcite since the LOI for this sample is 24.26%, quite close to calculated CO_2 (21.31%). It has quite high TiO_2 (1.31%) which is probably of local volcanic derivation (highest for group); moderate Al_2O_3 (9.09%), FeO (5.42%), MgO (3.19%) and Fe_2O_3 (1.48%) will occur in the chlorite/kaolinite and clay phases observed from the XRD trace (clay peak is at 11Å, and is probably a mixed-layer illite-smectite clay), and possibly in a mixed ankerite/dolomite phase, which had a very small peak. The clay composition also contains K_2O (1.68%) and to a lesser extent Na_2O (0.40%). K_2O is especially enriched in samples 10 & 11 and may correlate with a small peak at potassium feldspar on the XRD trace, shown by both samples. The P_2O_5 content of the sample, 0.35% (same in sample 11), is the highest for any analysed East Kirkton sample, and suggests that there is either apatite in this

horizon, or fossil bone (though not coarse enough to be observed in hand specimen).

Sr (3591ppm), Ba (397ppm) and Zr (233ppm), are relatively enriched in this sample, which has a correspondingly high CaO content. The chlorite phase appears to be dominated by Cr (131ppm) rather than Ni (79ppm) or Zn (71ppm), and this may relate to local variations in the composition of the chlorite phase. Ce (69ppm), Cu (33ppm), La (30ppm) and Y (21ppm) are also enriched compared with concentrations in other East Kirkton samples, only samples 11 and 25 have equal or higher concentrations for these elements.

Sample 11, was collected close to sample 10 and from the same horizon as sample 25 (NMS unit 42), and is a black shale with fine-grained ashy lenses, in which the ash fragments are often chloritic. Sample 11 has higher SiO_2(34.62%) and lower CaO (13.98%) than 10, but with very similar, high values for TiO_2(1.55%), P_2O_5(0.35%), moderate Fe_2O_3(2.12%), FeO(5.28%), MgO(3.29%); 3% higher Al_2O_3 (11.92%), and higher Na_2O(0.84%) and K_2O(2.78%). The XRD trace for sample 11 shows predominantly calcite and quartz, and more of the potassium-feldspar and clay phases (kaolin, a 10.9Å mixed layer clay component, probably illite-smectite, and a little chlorite) than in sample 10. This accounts for its higher Al_2O_3 and K_2O, and is partially accountable for the large discrepancy between the calculated CO_2 (10.98%) and LOI (22.35%) values for this sample, through the water content of the clays (oxidation of organic matter will contribute to the LOI total and minor CO_2 will also be associated with the small quantity of ankerite that is present in the sample). Both samples have low MnO, sample 11 especially with only 0.01%.

Samples 10, 11 & 25 have high minor element concentrations: Sr (2477ppm), Ba (460ppm) and Zr (228ppm). Sample 11 has the third highest percentage of CaO for the shale group and the third highest Sr content. Cr (100ppm), Ni (102ppm) and Zn (79ppm) are all enriched in sample 11 and will probably be incorporated in the chlorite, or smectite phase. Cr and Zn appear to be more enriched than Ni, relative to the concentrations of these elements in most other shale samples, but in similar proportion to sample 10. Sample 11 has also relatively high Rb (123ppm) which may correlate with its high K_2O (2.8%) content, though sample 25 has Rb 122ppm and K_2O of only 0.24%.

Sample 12 was a well-laminated, fine-grained, organic-rich, black shale, that coated a small stromatiform, carbonate lens (NMS unit 80, now buried), close to the main "mound" (NMS units 61-64). This sample has the highest SiO_2 for Group II (60.25%) - highest of all the East Kirkton samples except for the chert, sample 6 - and is obviously dominated by quartz. As might be expected of a sample with high SiO_2, sample 12 has correspondingly low CaO and LOI, it contains only 6.88% CaO; this gives a calculated CO_2 of 5.41%, which accounts for only a third of the LOI total of 15% (measured CO_2 is 22.78% and appears to be inaccurate). The presence, on the XRD trace, of kaolinite and a little chlorite, clay (probably an 11Å mixed layer illite-smectite phase) and ankerite/dolomite, may account for some of the LOI total, as will oxidation of organic carbon. It has very little TiO_2(0.61%), and low Al_2O_3(5.19%), FeO(5.27%), and MgO(2.18%), elements that are likely to be found in the chlorite, clay and ankerite/dolomite phases. It may be that these phases were not so well developed in this horizon, or possibly, that they were replaced or altered by later fluids. In this sample, because of the high silica content, it would appear that any later fluids were SiO_2 enriched. Its high SiO_2, low TiO_2, Al_2O_3, FeO and MgO, are comparable with sample 3 (50%)

This sample is least enriched in trace elements for the shale/ash group, though relative to the other, four, lithological groups it is enriched in minor elements. This may correspond to a lower percentage of chlorite and clay for this sample than was observed for the other shales (possibly due to silicification as indicated by its high silica content). It may be that without chlorite and clay there is less opportunity for the lattice substitutions which accommodate the minor elements. The elements Cr, Zn, and Ni, that are most likely to be associated with the chlorite phase are also in very low concentration in this sample, like the chlorite.

Sample 25 is a lateral equivalent of samples 10 & 11 (NMS unit 42). It is a well-laminated, fairly-fissile black shale, containing none of the coarser ashy material, often observe in other shale group samples (e.g. sample 3 & 10). Samples 10, 11 & 25 were taken from a horizon that was relatively continuous compared with the common, but often extreme pinching and swelling of these friable ash-shale lithologies.

Sample 25 has higher SiO_2(38.74%) than the other two samples (10 & 11), and lower CaO(8.64%), but considerably more chlorite - Al_2O_3(14.66%), FeO(10.64%), MgO(5.05%), Fe_2O_3(2.45%). Its XRD trace shows quartz as the dominant phase, then chlorite, clay (a 10.9Å mixed layer illite-smectite phase) and then calcite. **This sample also shows a large discrepancy between calculated CO_2 (6.79%) and LOI (15.8%), and like the other shale samples, contains H_2O-rich phases e.g. clay and chlorite, and a small quantity of a second carbonate phase, probably a mixture of dolomite and ankerite. In common with samples 10 & 11, it has high TiO_2(1.27%) and relatively high P_2O_5(0.25%), this may be a geochemical signature, common to samples in this horizon, i.e. elevated titanium and phosphate.**

Samples 10, 11 & 25 are all very enriched in minor elements, sample 25 has the highest Ba (465ppm) and Zr (235ppm) for the group, though its Sr is rather lower (1313ppm), which may correspond to its lower CaO content. It also has highest Ce (86ppm), Co (44ppm), Ga (22ppm), La (41ppm), Pb (12ppm) and Rb (122ppm), and relatively high Cu (38ppm), Cr (94ppm), Ni (119ppm) and Zn (76ppm) too. **Elements Ni, Zn and Cr are probably from the chlorite phase, other elements may also occur in chlorite or within clay or possibly carbonate phases.**

GROUP III

Carbonate-rich Volcanic Ash (samples 4,9,23,24). 4 samples, see Table 1 (Group III) and Table 2 (Group III).

Major Element Analyses.

Sample 4 was collected from the horizon above Group II-samples 2 & 3 (NMS unit 75), and consists of chloritic ash, that has been permineralised by a carbonate phase, and has predominantly pale-green, chloritic, volcanic clasts and small (buff), carbonate spherules (5mm). It is geochemically dominated by calcite with high CaO (40%), **this gives a calculated CO_2 content of 31.16%, and measured CO_2 was around 30%, LOI 33.7%, indicating that calcite is the dominant carbonate phase, and that there is little organic carbon or water present in this sample.** There was a corespondingly pronounced calcite peak in the XRD trace, with only small XRD peaks for quartz, chlorite, a mixture of dolomite and ankerite, and possibly some kaolinite and plagioclase feldspar. **The sample has low SiO_2 (12.13%), which reflects the small XRD peak for quartz, but there will**

also be some silica in the chlorite, kaolinite and plagioclase feldspar. These latter phases will also contain the 4.27% Al_2O_3, which is the highest value for Group III. Chlorite, and to a lesser extent the dolomite/ankerite phase, will account for the 4.4% FeO and 2.8% MgO; this is not an especially high value for MgO, and may indicate that both mineral phases are relatively iron-rich. The MnO concentration of 0.14% is quite low for a carbonated ash sample, but relatively high compared with the MnO in the black shales - possibly suggesting that the manganese is found within the carbonate phases rather than in chlorite.

The 0.78% TiO_2 is highest in sample 4 (for Group III) and it is assumed that this component will have been derived from ferro-magnesian minerals in the local volcanics, and, that its concentration in the East Kirkton samples will be determined by its relative concentration in the contemporary basalts/ashes from which the sediments were derived. The sample has also the highest P_2O_5 composition, suggesting the existence of fossil bone remains in this horizon, in small quantities. It should also be noted that sample 4 and sample 24 are geochemically similar; for TiO_2, Al_2O_3, Fe_2O_3, FeO, MnO and MgO major element proportions (not for CaO and SiO_2, for which sample 4 is best compared to 23) and enrichment in trace elements. Samples 4 and 24 were collected from the same horizon in order that lateral variations could be observed, see description of sample 24.

This sample is has some of the largest concentrations of trace elements within this lithological group (as for sample 24). In sample 4, elements Ce(30ppm), Ga (11ppm), La (30ppm) and Rb (17ppm) have the group's highest values; Cr (56ppm), Ni (52ppm) and Zn (37ppm) also in very high quantities are probably related to the high chlorite content of the sample. There is also high Sr (3887ppm), Ba(194ppm) and Zr(153ppm), which may relate to the high CaO and calcite enrichment, but other samples in this group have higher CaO/calcite content and have lower values for Sr, Ba, & Zr (e.g. sample 9 & 23). Minor amounts of plagioclase were noted from the XRD trace and this phase, too may contain Ba (±Ce, La, Rb).

Sample 9; this sample was collected from the upper part of Log 1 (NMS unit 51, from the same unit as sample 27), below the horizon where shale/ash samples 10 &11 were found. It is a sample of indurated, ash with a coarse-crystalline, carbonate-rich matrix, which is quite shaley in some areas. Clasts are comprised

of thin, white, discontinuous laminae (either silica or kaolinite), pale-green, powdery volcanic clasts and organic material. It was sampled close to a carbonate vein, and may thus be particularly carbonate enriched. Sample 9 has the lowest SiO_2 content for its group (9.39%) but has the highest CaO (46.61%) (in Group III, especially, there seems to be a balance between SiO_2 and CaO, i.e. where one element is enriched the other is proportionately depleted). A strong calcium carbonate presence is indicated by the group's highest LOI. (38.26%), which compares closely with the calculated CO_2 value (36.62%).

The XRD confirms the dominance of the calcite mineralogy (the major peaks on the trace all relate to calcite), with minor quantities of quartz, a mixture of ankerite and dolomite, and chlorite (± kaolinite). These secondary peaks are of relatively little importance in the geochemical balance of this sample since, for its group, it has lowest concentrations of Fe_2O_3 (0.49%), FeO (2.42%) and MgO (1.64%). It also has only minor amounts of TiO_2 (0.31%), Al_2O_3 (1.87%) and MnO (0.15%), but has highest percentages of Na_2O (0.74%) and K_2O (0.28%), which would suggest some minor feldspar component, though none was apparent on the XRD trace. Samples 10 &11 from the horizon above also have high Na_2O and K_2O contents, so this slight enrichment in sample 9 may be a localised feature, perhaps related to the volcanic source.

Sample 9 is a relatively unenriched sample, bearing little resemblance to shales 10 & 11. Sr (2548ppm), Ba(127ppm) and Zr (89ppm) have only moderate concentration in this, the sample with the most calcite (in Group III), which suggests strongly that calcite composition is not the limiting factor for Sr content in these carbonate-rich ashes (see also samples 4 &24). The sample has very low values for Cr (19ppm), Ni (18ppm) and Zn (15ppm), corresponding to a lack of chlorite development.

Sample 23 is a sample collected from the base of the quarry sequence, but on the eastern side of the quarry next to a small stromatiform carbonate mound (now backfilled by debris from new quarry excavations). The sample is indurated ash of pale coloured, sometimes chloritic, volcanic clasts, small, (buff), carbonate spherules, occasional organic material, chert patches and a matrix which is mostly carbonate enriched, but can be shaley. It has relatively low SiO_2 (12.70%) and quite high CaO (39.64%), similar proportions to those for sample 4, which was also collected from the lower part of the sequence, and quite close to the main carbonate "mound". Sample 23, however does not show any XRD trace of

chlorite (which is present in sample 4), but shows a significant XRD peak for ankerite, a low quartz peak, and a little pyrite (this peak is possibly exaggerated by a nearby ankerite peak). Measured LOI (37.59%) is high relative to calculated CO_2 (31.15%) because of the presence of ankerite. This is confirmed when CaO and LOI are compared for samples 23 and 4; CaO values are very similar, but LOI is 4% higher for sample 23 which contains the ankerite phase, lower in sample 4, which has purer calcite. The relatively high concentrations of FeO (2.97%), Fe_2O_3 (1.03%) and MgO (4.31%) (highest concentration for this group) will mostly be associated with the ankerite phase, though they might seem to suggest a potential for formation of chlorite. A low value for Al_2O_3 (0.59%) is also consistent with the absence of chlorite. The sample has highest MnO (0.46%) for the group, suggesting that this element is found in carbonates rather than chlorite.

Sample 23 is the least enriched sample for most of the minor elements; this may possibly correlate with its low Al_2O_3 value, indicating the phases with which these trace elements are associated (chlorite and clays, see Group II). It has the lowest values for Sr (1527ppm), Ba(100ppm), Zr(56ppm) which can be associated with carbonate phases, although this sample contains mostly carbonate; lowest Cr (5ppm) and Zn (5ppm) that occur with chlorite; and lowest Ce (6ppm), Ga (4ppm), La (16ppm), Rb (10ppm) and Y (11ppm). This sample has quite a high ankerite content, and this may account partially for the lack of Sr in the carbonate phases (Sr being less likely to substitute into the ankerite lattice than a calcite lattice).

Sample 24 is the lateral equivalent of sample 4, both were collected from the base of the sequence (NMS unit 75), though there is more friable shaley material around the site where sample 4 was collected than for sample 24. It is an indurated chloritic ash with small (buff) carbonate spherules (2mm), larger stromatiform spherules (3-4cm across) and a carbonate-rich matrix, which is sometimes shaley and can be weakly laminated.

The main difference between samples 4 and 24, is the balance between SiO_2 CaO content. Sample 24 has the highest SiO_2 (25.87%) for this group and the lowest CaO (32.50%), if this is considered along with LOI (28.79%) - quite similar to calculated CO_2 (25.54%) - it indicates that the dominant phase is calcite, although it occurs in smaller quantities here than in the other three samples of Group III. According to the XRD trace it also contains small

quantities of chlorite (±kaolinite) and an ankerite/dolomite mixture. The presence of these phases is reflected in the concentrations of Al_2O_3 (3.37%), FeO (3.70%), Fe_2O_3 (0.96%), and MgO (2.33%), and it would appear from the relative proportion of MgO to FeO/Fe_2O_3, that chlorite is iron rich. The high SiO_2 in sample 24 may be due to veining, or inclusion of chert patches/layers in the analysed sample, but it is more likely to be a local effect than a marked lateral change (this will be confirmed or refuted by comparison with other samples that are laterally equivalent to Log 1).

Sr (3941ppm), Ba (250ppm) and Zr (161ppm), are highest in sample 24 (within Group III) though the sample has the lowest value for CaO. Co (12ppm), Cu (24ppm), Ga (11ppm), and Rb (17ppm) are highest for the group and Ce (27ppm), Cr (44ppm), La (20ppm), Ni (50ppm) and Zn (29ppm) are also concentrated in this sample. Sample 24 is also comparable, for its enriched trace chemistry, to sample 4, this may be related to the fact that they both have high chlorite peaks (relative to other samples in the group).

GROUPS IV AND V.

Laminites (samples 5,7,8,17,21,22,26,27,28,29,30,31). 12 samples, see Tables 1(Group IV and V) & 2(Group IV and Group V). This group of samples is divided into two for discussion, because a large difference was observed between the analysis results for samples from the area of Log 1, and those from nearer the museum section (NMS log), most of which were from higher up the stratigraphic column. Differences were also apparent between the samples' general lithological composition.

Group IV Laminites (5,7,8,17,21,22,26), Table 1(Group IV) and Table 2 (Group IV), are those samples which were more shaley/spherulitic, containing also chert laminae and ash fragments, and were generally from low in the stratigraphic sequence (below the equivalent of the 5m mark in log 1). Group V Laminites (27,28,29,30,31), Table 1 (Group V) and Table 2 (Group V), are those that contained finer grained, laminated, crystalline carbonate and very little shaley material (with no spherules) and which probably occur higher in the sequence (unit 50 or higher, difficult to correlate unit numbers to samples that occur to the southern end of the quarry e.g. samples 29,30 & 31).

GROUP IV

Laminites.

Major Element Analyses

Sample 5 is a spherulitic, laminated shale with pale, fine-grained carbonate laminae, patches of chloritic and ashy material, and was collected from the same part of the horizon as the chert of sample 6 (NMS units 61-62); from the same unit as sample 17 & 21. The base of the unit is a well cemented tuff, but it grades up into the spherululitic, weakly laminated shale, where samples 5 & 6 were obtained.

SiO_2 of 17.65% is low for Group IV; CaO (38.92%) and LOI (35.29%) are amongst the highest values corresponding to a high calcite peak, on the XRD trace, and lower quartz, but LOI is almost 5% greater than calculated CO_2 (30.58%), therefore the CO_2 from calcite does not account for all of the LOI. The XRD trace also indicates minor quantities of a dolomite/ankerite mixture and a little chlorite, which will contribute CO_2 and H_2O respectively to the LOI measured, and these two phases will account for the MgO (2.13%), FeO (2.10%), Fe_2O_3(0.80%) and Al_2O_3(1.00%) contents. The concentration of TiO_2 (0.24%) is quite high for this group, and coincides with the TiO_2 enrichment of the carbonated ash (sample 4) which was from the unit below.

This is the sample with the highest Sr (6300ppm) six times more concentrated than occurred in the basalts that are assumed to be the local Sr source (P.L Smedley, 1986). Calcite spherules are also known to be rich in Sr (G. Walkden, 1993), and the high value for this sample may be due to presence of highly Sr-rich spherules, formed perhaps when fluids were being derived from an especially Sr-rich basalt (the ash in sample 4, from a unit below, had 3887ppm Sr, - sample 24, same horizon 3941ppm - quite high values).

Sample 5, has high trace element values, especially Sr, Ba (272ppm), Ce (35ppm), Cr (19ppm), Cu (21ppm), La (18ppm), Th (9ppm), Zn (32ppm) and Zr (143pm) compared with other samples of the laminite group (IV). It has a similar pattern of trace element concentration to carbonate-rich ash samples 4 & 24 from unit 75, but contains more Sr and Ba (often associated with carbonate phases) and less Cr, Ni, Rb and Zr, the former two are probably linked to chlorite content (sample 5 has only a small amount of chlorite). Therefore it is likely that the enrichment of element concentration in sample 5 is due to the geochemistry of contmporary, volcanic source-material rather than a result of the sample's formation as a laminite.

Sample 7 is an indurated, finely-laminated, spherulitic shale, containing deformed chert layers, carbonate cemented laminae and fine-grained white laminae. The horizon (NMS unit 58) from which the sample was taken weathers a rusty orange colour. It has 29.42% SiO_2 and 32.09% CaO, the relative proportions of SiO_2 and CaO in this sample are similar to those observed in samples 17 & 22 (the latter being the lateral equivalent of sample 7). LOI was measured to be 30.80%, which is high when compared to calculated CO_2 (25.68%), this difference suggests that other phases besides calcite have contributed to the LOI for this sample. The XRD trace shows the presence of a dolomite/ankerite mixed carbonate phase and small quantities of chlorite (±kaolinite); these phases will contribute to the measured LOI, and they will include the 2.71% MgO (which for Group IV is high), 2.74% FeO and 1.11% Al_2O_3 (Fe_2O_3, 0.64%, low in proportion to FeO) that analyses indicates to be present in this sample.

Na_2O (1.30%) is very high in this sample though the phase in which it occurs is not apparent, it would normally be associated with feldspars or in clay but neither phase is observed from the XRD trace, only carbonate or chlorite (NB. it is easy to obtain exaggerated Na_2O values by experimental contamination, through handling XRF fused discs, but this is not generally a significant error).

This sample has a high Sr concentration (4432ppm) (which may again be associated with the chemistry of the local basalts, see sample 5) and also contains high Ba (200ppm), Zr (164ppm), two elements often associated with high Sr in the East Kirkton samples. It contains also relatively high Cu (26ppm) and Y (10ppm). The elements associated with chlorite, Cr (11ppm), Ni (32ppm) and Zn (11ppm), occur in small quantities in this sample; as would be expected, this appears to correlate with low Al_2O_3 and chlorite.

Sample 8 is comprised of fine grained shale and carbonate-rich laminae with some bands of chert. Only a few of the thicker, shaley laminae are spherulitic but syn-sedimentary slumping is often observed in this unit (NMS units 55-56). The sample has the lowest SiO_2 (16.19%) and highest CaO (43.57%) in Group IV, comparing more closely with the CaO/SiO_2 content of the samples in Group V; it has a measured LOI (36.49%) and calculated CO_2 (34.23%) comparing quite closely (1 or 2% difference in these values is equivalent to the standard range

of H_2O values for these samples, without requiring to invoke the presence of additional volatile-rich mineral phases). Calcite is the dominant mineral phase on the XRD trace, with some quartz and a very small peak representing an ankerite/dolomite mixture.

The other major elements have relatively low values for this sample (for Group IV); TiO_2 (0.11%), Al_2O_3 (0.53%), Fe_2O_3 (0.28%), FeO (1.64%) and MgO (1.52%). Samples 8 and 22 have the lowest concentrations of these elements in Group IV, and neither has chlorite on its XRD trace, but both have some ankerite/dolomite in which the Fe and Mg will occur. The MnO (0.25%), Na_2O (2.09%) and P_2O_5 (0.14%), in sample 8, are high for laminites. Na_2O and P_2O_5 are similarly high in sample 7, and neither sample (7 or 8) appears to contain a unique mineral phase which could explain the extra high Na_2O.

Sample 8 is depleted in most trace elements, which coincides with the lack of chlorite observed from the XRD trace, and a high proportion of pure calcite which does not appear to accommodate many trace elements in East Kirkton samples. The Sr (3339ppm) content is higher than samples 17 & 26 but low relative to the other Group IV laminites (Group IV have all high Sr values relative to the other groups); Ba (137ppm) and Zr (103ppm) are also low for Group IV, but high compared to Groups I, III and V. Cr (0ppm), Ni (17ppm) & Zn (4ppm) are very poorly represented in this sample where no chlorite is present, this observation would tend to confirm their association with the chlorite phase.

Sample 17 was taken from the same horizon as the "mound" (NMS unit 61-62), immediately to the south of its faulted margin (any displacement associated with this small fault has not affected the lateral continuity of the beds/units), and is also a lateral equivalent of samples 5, 6 & 21. It is a shaley, laminated, spherulitic sample with carbonate-rich ash lenses, and was collected near thick carbonate veins.

According to the XRD trace the specimen consists of calcite and quartz, with chlorite (± kaolinite) as the most dominant of the minor phases) and some ankerite/dolomite. Disaggregation and sedimentation of this sample, followed by repeated XRD analyses, revealed a small amount of a 10.9Å clay which behaves like a mixed layer illite-smectite phase on glycolation and subsequent heating to 300°C. This sample has almost equal proportions of SiO_2 (28.21%) and CaO (30.22%), and has high values for Al_2O_3 (4.08%), FeO (4.62%), Fe_2O_3 (1.02%),

TiO_2 (0.36%) and K_2O (0.36%), with moderate MgO (2.34%). Since there is only a small amount of ankerite/dolomite and clay in this sample, the chlorite phase must account for the high FeO and Al_2O_3, and possibly also for the TiO_2 and K_2O, which must also be related to material from a volcanic source. The sample does not show carbonate enrichment as might have been expected from its proximity to calcite veins, but the percentage of chlorite (and Al_2O_3) in the sample suggests that the ashy lenses in the laminite have strongly influenced its chemical signature.

Elements Ce (17ppm), Co (16ppm), Cr (28ppm), Ga (12ppm), La (19ppm), Ni (51ppm), Pb (5ppm), Rb (16ppm) and Y (12ppm) are all high in this sample, with Ba (190ppm), Zn (20ppm) and Zr (114ppm) only moderately enriched (relative to other Group IV samples), and low Sr (3270ppm) and Cu (13ppm).

The sample has widespread chlorite which appears to be related to the increase in trace element concentration, but with relatively low CaO in proportion to low Sr. Zn and Cr are not especially enriched for this sample even though it has high chlorite (compared to sample 4, e.g. Cr (56ppm), Ni (52ppm), Zn (37ppm)), perhaps the Fe^{2+}, Fe^{3+} or Al^{3+} atoms are not being substituted by the trace elements in this chlorite phase. A relative enrichment in Rb (16ppm) reflects a high K_2O value; Rb is likely to substitute into K sites in whichever phase they occur, normally it would be expected to occur in potassium feldspar, but this phase does not appear on the XRD trace, so the K_2O and Rb may occur in the clay phases.

The trace element characteristics of sample 17, have nothing in common with the "mound" samples, which are from the same horizon, this can easily be explained by the totally different ways in which the two lithologies were formed and by the chemical influence of the volcanic ash in the laminite. Samples 5 & 21 which are also lateral equivalents, do not have significant chlorite or clay, and have lower Al_2O_3, FeO and Cr, Ni, but have higher Ba, Sr, Zr and Zn.

Sample 21 is the lateral equivalent of sample 5 (NMS unit 61-62) and is comprised of pale carbonate laminae, with spherules, and dark shaley laminae. Compared with sample 5, sample 21 has more SiO_2 (38.36%) and less CaO (25.70%). It was from this horizon that the chert, sample 6, was obtained, and it is probable that concentrations of chert (laminae, lenses or patches) vary locally throughout this unit. The XRD trace shows high intensity peaks for quartz and

calcite, indicating also the less distinctive presence of ankerite and a little chlorite (±kaolinite). These latter two phases contribute to the measured LOI(25.66%), causing it to be higher than the calculated CO_2(20.19%), by more than would be expected simply from the standard sample water content (usually 1-2%).

The MgO (2.98%) content is the highest for the group and combined with high FeO (2.92%) corresponds to ankerite being the most dominant of the minor phases. Al_2O_3 (1.21%) is relatively low and will relate to the proportion of chlorite present; but, the Fe_2O_3 (0.68%) and FeO that give the sample quite a high iron content can be accommodated in ankerite and chlorite.

The lowest CaO in the group coincides with the third highest Sr (4190ppm), and, as for Group III, this shows that very high concentrations of Sr do not relate directly to CaO content. The high Sr does correlate with high Ba (215ppm) and Zr (136ppm). Samples 5 & 21 have both high Sr, Ba and Zr which is probably related to the geochemistry of the contemporary volcanic source material; sample 21 is less enriched in some of the other trace elements and this maybe related to the marked variation in CaO and SiO_2 between the two samples. Sample 21 has a little chlorite and high FeO and Ni (37ppm), but Cr (7ppm) and Zn (11ppm) are low (this is similar to the concentrations of these elements observed for sample 17).

Sample 22 is comprised of 30-40% spherulitic, crystalline carbonate laminae, 10% pale, fine-grained carbonate laminae, 5-10% chert laminae and the remaining 40-55% of organic-rich shaley material. It is the lateral equivalent of sample 7 (NMS unit 58). Calcite and quartz are the dominant phases shown by the XRD trace, with SiO_2 at 29.83% and CaO 33.30%. The measured LOI 31.27% is higher than calculated CO_2 (26.16%) due to the presence of a second carbonate phase, a mixture of dolomite and ankerite, that can also be observed from the XRD trace. In common with sample 8, the lack of a chlorite phase results in low Al_2O_3 (0.43%), Fe_2O_3 (0.25%), K_2O (0.05%) and TiO_2 (0.09%), but in contrast sample 22 has high MgO (2.49%) and FeO (2.40%) since it contains ankerite/dolomite, and sample 8 does not.

Sample 7, from the same horizon also has ankerite/dolomite, but has chlorite too, therefore, having higher values for Al_2O_3, Fe_2O_3, FeO and MgO. The SiO_2 and CaO occur in very similar quantities for samples 7 & 22, indicating the possibility that this horizon has a more uniform distribution of calcite and quartz phases than was apparent from comparison of samples 5 &

21 (though this may be an artifact of the sampling process). There is a contrast between the contents of Na_2O and P_2O_5 for samples 7 & 22; sample 22 is depleted in both elements relative to sample 7. This is not very significant for the P_2O_5, but for Na_2O it is the difference between a sample with one of the lowest (0.29%) concentrations in the group, and one of the highest (1.30%), and may indicate Na_2O contamination during preparation for the analysis.

Sample 22 is not enriched in any elements other than Sr (3834ppm), Ba (198ppm), and Zr (129ppm). These elements are also less concentrated than in sample 7 (except Ba which is almost the same). Sample 22 has the lowest values for Ce, Co, Cr, Cu, La, Ni, Pb, and Y, but shows a relatively high content of Zn. This lack in trace elements is probably related to the absence of chlorite from the sample.

Sample 26 is comprised of medium grained carbonate laminae with fine-grained, organic-rich, shaley partings. It was sampled from a horizon (NMS unit 42) just below shale sample 25, which was extremely enriched in most elements.

The chemistry of the sample is dominated by calcite, with very high CaO (39.75%). LOI (32.21%) is very close in value to calculated CO_2 (31.23%) which suggests that this sample has very little trapped H_2O. The MgO (1.65%) and FeO (1.87%) are relatively low compared to other samples from Group IV, but the Fe_2O_3 (1.58%), Al_2O_3 (1.50%) and K_2O (0.24%) are relatively high. The XRD trace also shows very small peaks for chlorite (±kaolinite) and ankerite/dolomite. SiO_2 only amounts to 19.39% which may be due to fewer chert laminae in the horizon/sample.

In this sample, CaO has the second highest value and Sr, the lowest (2582ppm), for Group IV. There is therefore no correlation between these two elements in this sample. Relative to the other Group IV samples, Ba (128ppm) and Zr (110ppm) are also low in low concentration. Cr, Ni and Zn have quite low values when compared to other samples containing chlorite, but sample 26 has only small chlorite peaks. Ni appears to be higher than Cr or Zn, which seems to be typical for this group and the sample is enriched in Rb (19ppm) which correlates with relatively high K_2O, probably some relict volcanic signature.

GROUP V

Laminites.

Sample 27 was collected from a horizon, just below samples 25 & 26 (NMS unit 51), and is comprised of grey and white, alternating, crystalline carbonate laminae which often show deformation, this may be syn-sedimentary or tectonic. The XRD trace indicates the predominance of calcite, and shows a little quartz and small peaks for a mixture of ankerite and dolomite. The sample has very high CaO (46.52%), with LOI (37.77%) correlating closely to calculated CO_2 (36.55%) indicating that calcite is the main carbonate phase (as observed form XRD); and low SiO_2 (14.31%), Al_2O_3 (0.09%), MgO (0.82%), Fe_2O_3 (0.27%), but moderate FeO (1.46%) for Group V. The low Al_2O_3 indicates that there is hardly any volcanic material or shale in this sample, and that the sample consists of fairly pure calcite, with occasional chert laminae. The second carbonate phase, which is represented on the XRD trace by a very small peak, will probably be a ferroan dolomite since the sample has high FeO relative to MgO.

The only trace elements in this sample which significantly exceed concentrations of 10ppm, are Sr (2267ppm), Ba (92ppm) and Zr (90ppm), the elements that are enriched in all the East Kirkton samples analysed. This sample has the highest values for these three elements (like sample 28), and the highest proportion of CaO, as calcite, and it may be that the elements Sr, Ba & Zr are partitioning into the calcite phase.

Sample 28 is from the core of an 's'-shaped fold, quite close to the NMS logged section (NMS unit 48-49), collected as a lateral equivalent of sample 27. Individual lamina are either pale, fine-grained carbonate; coarse crystalline carbonate; or darker shaley material (not spherulitic). The XRD trace indicates that calcite is the main mineral phase present, with some quartz, small quantities of ankerite and dolomite, and a possible chlorite peak (too small to be distinctive).

Sample 28 has CaO (46.61%) and SiO_2 (14.04%), in similar quantities to sample 27. The measured LOI(38.03%) corresponds well with the calculated CO_2 (36.62%) for sample 28, confirming that the calcite is the main supplier of the CO_2 evolved on ignition. It has low Al_2O_3 (0.27%), and values for FeO (1.40%), Fe_2O_3 (0.25%) and MgO (0.90%) that are similar to those of sample 27. In both samples FeO is high relative to MgO, and tends to indicate the presence of a ferroan dolomite/ankerite carbonate phase. Where no chlorite

phase is present only the carbonate will accommodate both elements. Dark shale laminae, observed in the hand specimen, have had no apparent effect upon this sample's chemistry.

Sr (2271ppm), Ba (64ppm) and Zr (51ppm) are relatively similar to sample 27; Sr is slightly higher (4ppm) and Ba and Zr are both a little lower. Sample 28 has marginally higher CaO (+0.09%) than 27, which may explain the variation in Sr concentration between the two, but it is unlikely that the analytical apparatus is sensitive enough to draw any conclusions from these small variations.

Sample 29 was taken from a outcrop to the south of the NMS section, away from the main quarry face. It is considered possible that there is some fault displacement between the NMS section and the cutting from which this sample was taken (J.J. Doody et al, 1993) fluids channelled through such a feature might have some effect on the chemistry of the rocks on either side. The predominant mineral phase in this sample is calcite, though some quartz and a little ankerite/dolomite are also present.

It has high CaO (40.03%) as was expected from the calcite peak intensity on the XRD trace. The calculated CO_2 (31.45%) is considerably lower than the measured LOI (37.67%), this sample does not appear to contain significant quantities of a second carbonate, chlorite/clays, or any other phase which is associated with this discrepancy in other samples. The sample has high SiO_2 (23.72%), like sample 30, suggesting that there is more quartz/chert in these two samples than others in Group V. MgO (1.09%) is slightly higher here than in samples 27 & 28, FeO (1.11%) is a little lower and both will occur in the minor carbonate phase, which is shown to be mixed ankerite/dolomite from the XRD trace (when compared to the quantities of FeO and MgO observed for sample 30 & 31, which contain significant ankerite/dolomite, it can be seen that this phase does not occur significantly in sample 29, but all three samples show a large difference between calculated CO_2 and LOI).

The values for Sr (1350ppm), Ba (35ppm) and Zr (30ppm) are low in sample 29 (like samples 30 & 31 - some of the lowest values for all the samples). In sample 29, Sr is higher than for 30 & 31, as is CaO, but there is little difference between their Ba and Zr concentrations.

Sample 30 is from a cutting that overhangs the quarry track, and appears stratigraphically to have come from high up the sequence, just below the Little Cliff Shale (see Rolfe *et al.*, 1993) that caps the East Kirkton limestone. The laminae in this sample show small scale syn-sedimentary deformation, and are either, darker in colour, appearing more shaley, more organic-rich, or as crystalline carbonate, a grey/brown colour. Calcite and quartz are the most common phases, but this sample also has a high XRD peak for a carbonate phase that is a mixture of ankerite and dolomite.

Compared with samples 27 - 29, sample 30 is richer in SiO_2 (26.07%), Al_2O_3 (0.33%), Fe_2O_3 (0.60%), FeO (2.17%) and MgO(3.96%); this will in part be related to the higher ankerite/dolomite content of the sample (i.e. for the FeO and MgO). The Al_2O_3.is still in too small a quantity to suggest a significant input of ash/shale material. The balance of SiO_2 (26.07%) and CaO (34.60%) in this sample, shows CaO reduced where SiO2 is increased, but when CaO and SiO_2 are added together the total is very similar to that obtained from samples 27 & 28 (most samples from East Kirkton - except Group II - are 85-100% comprised of CaO, SiO_2 and CO_2/LOI).

This sample has lower CaO, than any other Group V sample; Sr (1138ppm) decreases too, and low values are also observed for Ba (40ppm) and Zr (35ppm). There is a slight enrichment (not significant) in elements Rb (8ppm), Th (9ppm) and La (10ppm), when compared with other unenriched samples .

Sample 31 was collected from the same exposure as sample 30. Most of the horizons next to the track are slumped and in the vicinity of samples 30 & 31 were many carbonate veins, especially close to sample 31. This sample appeared to be mostly crystalline carbonate, occasionally appearing brecciated. The XRD trace indicates that an ankerite/dolomite mixture was the dominant phase along with the ubiquitous calcite; minor quartz was also present.

In common with sample 30, 31 has two dominant carbonate phases (calcite and the ankerite/dolomite mixture) and this second carbonate accounts for the high values for FeO (5.77%) and MgO (8.86%). This is the only sample, outside Group II, that falls below 85% for the sum of its CaO (37.28%), SiO_2 (5.05%) and LOI (42.33%) (Total=84.66%), due to the presence of a third dominant phase (not calcite or quartz). LOI (42.33%) and calculated CO_2 (29.29%) are very different, as would be expected for a sample with two

carbonate phases. Sample 31 has the lowest value for SiO_2 (5%) compared to any other East Kirkton analysis (close to samples 15, 18, 19 & 20, Group I). It also shows a relatively high concentration of MnO (0.34%), and it is possible that this can be correlated to the vein carbonate, which appears slightly pink in colour, perhaps also affecting the background carbonate which was observed to be buff coloured, unlike other samples from this group.

As was observed for sample 30, low CaO and low Sr (796ppm) correlate relative to other Group V samples; as with Ba (40ppm) and Zr (16ppm). Other elements show small increases, Ce (5ppm), Cu (11ppm), Ni (14ppm) and Th (9ppm), but they are not large enough to be significant.

Chert (sample 6). 1 sample, see Table 1 (Group IV) and Table 2 (Group IV).
Major Element Analyses.

Sample 6 is a chert layer (from NMS unit 61-62) that was about 3cm thick, containing spherules and pyrite, and appeared to show some syn-sedimentary slumping. This individual lamina pinched out laterally, but all along this horizon there was some chert at the same level as this sample. Not surprisingly the main constituent of this sample is SiO_2 (62.26%) as quartz, but it also contains calcite, CaO (16.58%), with a minor XRD peak for dolomite and ankerite, MgO (1.28%) and Fe total (1.58%). LOI (12.63%) is lower than calculated CO_2 (13.03%), suggesting that there is very little bound water in this sample and that some of the CaO must exist in a phase other than calcite (this is the only sample in which this occurs; other samples with low CaO, e.g. Group II, have organic carbon and H_2O-rich phases like chlorite, to contribute to LOI).

The Al_2O_3 (0.38%) is high relative to Group V, but the sample was collected from the same locality as sample 5, a Group IV sample which has more Al_2O_3. Its geochemistry is similar to samples from the stromatiform carbonate group that have a suspected small input of volcanic material, but less enriched than most other samples which have stronger volcanic components. It is therefore possible that this chert has a very weak volcanic signature. It also has 0.45% Na_2O, which is relatively high compared with carbonate-rich samples but more typical of samples with a moderate ash or shale content.

The concentration of the elements in this chert, not including CaO and SiO_2, seems most similar to those in Groups I & V. These two groups have only the smallest amounts of chlorite or clay, but are dominated by a carbonate phase. Sample 6 is mostly quartz, also lacking chlorite and clay, and it is

probably the absence of these phases that gives it a similar chemistry to the carbonate-rich samples.

Sample 6, in common with Groups I & V, has very little enrichment in any trace elements except for Sr (2991ppm), Ba (148ppm) and Zr (102ppm). Only Cu (12ppm) and Ni (14ppm) exceed 10ppm in concentration. Group V samples all have equivalent or lower trace element concentrations than sample 6 (except Th and Y where all samples have a few ppm more); but in Group I, samples 1 and 15 (most enriched for this group) have generally higher values for each trace element (sample 1, all higher except for equal values of Zr, and lower Rb; sample 15 has slightly more Cr, La, Ni, Rb & Y but less Sr, Ba & Zr). It is apparent that the trace elements are concentrated in neither quartz or calcite phases.

Full citations of the references are given in Chapter 4.
Tables of results are also in Chapter 4.

APPENDIX B: PROSPECTING FOR A SECOND EAST KIRKTON- TYPE DEPOSIT.

From the geochemical evaluation of the East Kirkton Limestone it appears likely that hot-spring activity occurred locally. The geological setting in which the lake deposit was formed, i.e. its close association with volcanic activity, is the kind of setting in which hot-springs can occur e.g. modern examples in Iceland; Yellowstone, USA; the Kenyan Rift; and in North Island, New Zealand.

In the eastern part of the Midland Valley of Scotland, in southern Fife, the Bathgate Hills and East Lothian, are sequences of volcanic material of lower Carboniferous age (Visean series), associated with the margins of Lake Cadell (see Chapter 1). It is possible that hot-spring activity might also have occurred in these areas and formed a similar deposit to the East Kirkton Limestone.

Part of the remit of this project was to consider how to identify any potential equivalents of East Kirkton, around the margins of the Oil Shale basin, of similar age and in a similar setting; and to attempt to find them. For this purpose three weeks of reconnaissance fieldwork was carried out (Summer 1991) investigating sedimentary lithologies, associated with volcanic activity, particularly looking for outcrops of silica-rich laminated limestone, with spherules and stromatiform features. Target areas to be studied were chosen from the geological maps of the region, where volcanic activity of this age was associated with sediments. Details of the area were also obtained from The Midland Valley of Scotland, BGS British Regional Geology Series (1985 edition) and Lothian Geology: An excursion Guide, by McAdam and Clarkson (Eds.) (1986 edition)

The Limestones of Scotland, and The Limestones of Scotland: chemical analyses and petrography, by the Geological Survey of Great Britain (1956), were also very useful for a rapid reference to limestones of the Calciferous Sandstone Series and Carboniferous Limestone Series. These publications offer chemical analyses of these limestones, from which those with high SiO_2 contents could be identified; descriptions of the limestones, by which lithologies with detrital quartz grains, or chert laminae could be differentiated; and a clear description of where outcrops could be found. They do not, however, give a record of every limestone in Scotland. No analyses of limestones from the Bathgate Hills are included, so it is therefore possible that some small limestone outcrop, similar to the East Kirkton Limestone, may have been overlooked by the reconnaissance

survey of this project.

The following sections give details of the findings of the Lower Carboniferous limestone survey. Particularly, the ways in which limestones and laminated sediments, with strong volcanic associations, differed from the East Kirkton Limestone (EKL). It is felt that the limestone which was most similar to the EKL, was that which was found in East Lothian, south of East Linton, around Traprain Law, a phonolitic laccolith forming a prominent local landmark. Although this limestone is similar to the EKL there are still too many differences between the two lithologies (see below) to conclude that they have a common hot-spring origin.

Southern Fife.

Laminated limestones are uncommon in the sedimentary sequences of the lower Carboniferous, in Fife. Target areas were the volcanic sequences in the Cleish and Saline Hills of western Fife; Largo Law, the Lomond Hills (associated with the Midland Valley Sill complex) and the southern coast of Fife, particularly around Burntisland.

There were no apparent examples of lacustrine deposition to be found in western or central Fife, or at Largo Law. Sediments which were observed, associated with volcanic material showed no evidence of silicification.

At Pettycur and Kingswood, near Burntisland, are sites known for calcareous permineralisations of plant material (Scott, 1990). The detailed preservation of the plant material, and proximity to volcanic material are similar to that found at East Kirkton, but there was no associated silicification.

Bathgate Hills.

The areas around the East Kirkton Limestone, particularly along strike to the north, were examined closely, including observation of some field float specimens. Nothing was found which had textures similar to the EKL.

At Craigs, approximately 1km north of East Kirkton, beneath the outcrop of a quartz dolerite sill, is a limestone which is correlated with the EKL on the Geological Survey maps, but not in Lothian Geology: an excursion Guide, (Stephenson and Monro, 1986). The limestone in this quarry is coarsely bedded, and horizons are generally of a pure carbonate. It has none of the unique features that characterise the EKL. If this

limestone is indeed a lateral equivalent of the EKL then the conditions under which this limestone was forming are almost completely different from those at East Kirkton; a dramatic lateral facies change has occurred. It contains some pyrite (see Chapter 3, Table 2).

South Queensferry to Granton.

This area was mainly investigated to find outcrops of the Burdiehouse Limestone (Loftus and Greensmith, 1988). It is also a freshwater limestone, and contains some stromatolites. From shore samples, at South Queensferry, collected close to where the outcrops were located (none were found) the typical laminated mature of the sediments seemed very familiar, but samples lacked the cherty laminae of East Kirkton.

Outcrops of laminated limestones and shales also occur to the east at Granton, where the Granton Shrimp Bed preserves fossil crustaceans in fluorapatite. Shales in this sequence show slump feature but no other similarities with East Kirkton.

Coastal East Lothian.

To the east of Edinburgh, coastal exposures of lower Carboniferous sediments were visited, but few argillaceous, and even fewer finely, laminated sediments occur in this sequence (especially around North Berwick and Dunbar). The coast between Gullane and Dirleton (Yellow Craigs) provides sediments in which calcareous, permineralised plants (around Weaklaw Vent) and shrimps (Cheese Bay) are preserved in sediments deposited in low energy environments, and associated with volcanic material.

To the south (and west) of the locality where the shrimps were found are sediments which have been baked by the intrusion of a basaltic sill. This has caused the formation of a white trap, by remobilisation of carbonate phases from the sediments. Pervasive veining and alteration is found locally associated with this intrusion, and phases in these veins include carbonates and silica. The silica forms agates and small geodes within vugs in the sediments.

These vug infillings occur in a different context from those at East Kirkton, but the proximity of volcanic activity in both cases could provide the source of heat required to mobilise and remobilise carbonate and silica phases.

East Linton, East Lothian.

A thin limestone unit, was followed to the south of East Linton. Localities of the small farm quarries, where it outcrops, were obtained from The Limestones of Scotland. These quarries were generally overgrown, and infilled, and none of the samples collected were *in situ*, though it appeared from the text book descriptions that the samples were derived locally.

Best examples of the variation in this lithology were found in a wall, encompassing fields, and a small pine plantation, to the south of the first quarry (just south of East Linton). Some samples were laminated while others were more massive. Samples which contained the "occasional bands of chalcedony" were very rare, and these "bands" often crossed laminae boundaries and were apparently a later feature, probably associated with the quartz veinlets and stringers, also observed in the samples. There were no samples found where the whole rock was silicified; in patches or laminae. The silica was mainly limited to late veins and to planes of weakness which were exploited parallel to the laminae. The most striking feature of this lithology is its red colouring, derived from iron oxides.

Samples of this lithology were also collected along the Whittinghame Water (1/4 of a mile WNW of Ruchlaw Mains), some *in situ*, and others from the river bed, which appeared to be similar to the lithological descriptions and samples already found. Samples from this locality included many well laminated sediments, some with spherulitic structures associated with nodular, stromatiform features. The stromatiform features were not found occurring as massive lenses, as at East Kirkton.

Although this lithology is described as containing "occasional bands of chalcedony" and "in places crowded with stringers and vesicles of chalcedony" it does not contain significant quantities of silica, in particular, no chert laminae; or any equivalent of the stromatiform limestone lens, with its multiple generations of silica and carbonate phases. Petrographically the spherulitic structures are not comparable with the textures of East Kirkton's carbonate spherules, they have a diameter of 3-10mm, with concentric banding like pisolites, when weathered. They are generally larger than those found at East Kirkton, and on a fresh surface, they seem to be formed of recrystallised carbonate as they are less powdery than the carbonate-rich matrix which surrounds them.

Bibliography.

Cameron, I. B. and Stephenson, D. 1985. *The Midland Valley of Scotland* (Third Edition). British Regional Geology, British Geological Survey. London: HMSO

Loftus, G. W. F. and Greensmith, J. T. 1988. The lacustrine Burdiehouse Limestone Formation - a key to the deposition of the Dinantian Oil Shales of Scotland. *In* Fleet, A. J., Kelts, K and Talbot, M. R. (Eds.) *Lacustrine Petroleum Source Rocks*, pp 219-34. London: Geol. Soc. Special Publication **40**.

McAdam, A. D. and Clarkson, E. N. K. (Eds.) 1986. *Lothian Geology: an excursion guide* (New Edition). Edinburgh: Scottish Academic Press.

Scott, A. C. 1990. Preservation, evolution, and extinction of plants in Lower Carboniferous volcanic sequences in Scotland. *In* Lockley, M. G. and Rice, A. (Eds.) *Volcanism and Fossil Biotas*', pp 25-38. Boulder: Colorado. Geol. Soc. of America, Special Paper **244**.

Stephenson, D. and Monro, S. K. 1986. Bathgate Hills. *In* McAdam, A. D. and Clarkson, E. N. K. (Eds.). *Lothian Geology: an excursion guide* (New Edition). Edinburgh: Scott. Acad. Press.

APPENDIX C: STRATIGRAPHIC LOG OF EAST KIRKTON QUARRY SECTION.

This stratigraphic log was measured from a section, 10m north of the National Museums' of Scotland, stratigraphic log. It was considered that further logged sequences should be measured within the quarry, due to the lateral variations which are commom in some lithologies e.g. the tuff horizons and massive, limestone lenses in particular.

The petrographic details of the lithological sequence are given below.

0.1m	SHALE	Shale with fine, but weak lamination (only occasional well defined partings). The horizon has been weathered and is friable and brown.
0.05m	SHALE	Finely laminated carbonate and black shale. (carb.)
0.8m	CARB. LENS	Massive, indurated, carbonate-rich lens (2m max. thickness, and pinches out along strike). It appears to have a stromatiform texture, and is a buff (beige) colour. It also appears to contain buff spherules. It contains a few plant fragments, and vugs formed between the stromatiform features are most commonly infilled by calcite.
0.02m	SHALE	A soft, black shale parting.
0.25m	CARB.	Massive, indurated, carbonate-rich horizon with (tuff?)siltsized grains (it maybe carbonate-rich tuff). The horizon is spherulitic and contains irregular chert patches.
0.03m	SHALE	Shale with carbonate lenses.
0.09m	CARB. (tuff?)	Indurated carbonate-rich layer (maybe tuff?) contains irregular siliceous patches. Layer pinches out laterally.
0.04m	SHALE	Soft, black shale with carbonate lenses.
0.37m	SHALE	Indurated, finely alminated chales - showing soft sediment deformation in places. Patches of chert occur within some layers, and also fine, white siliceous laminae. Botryoidal nodules are also found in this horizon, commonly coated by the white, siliceous material.
0.14m	TUFF (carb. ?)	Indurated tuff layer - very few larger ash clasts, mostly mostly fine grained and carbonaceous. Contains some buff coloured carbonate spherules.
0.1m	TUFF	Indurated, well cemented ash, with thin parting of black

		shale (few mm thick) at the top of the bed.
0.07m	SHALE	Soft, black shale grades upwards into a mixture of black shale and tuffaceous material.
0.24m	SHALE	Indurated, finely laminated, organic-rich shales and carbonaceous shales. Alternating with fine white siliceous laminae. Slumping occurs towards the south east side of the rock face. Ash lenses (2 cm) within layers.
	[Also see botryoidal nodules coated in white material.- Algal?]	
0.66m	VOLC SEDS	Close to the 5m MARKER occurred some fine white laminae - distinct against orange of weathered rock surface - continue to feature upwards in succession. Sequence of clastic and volcaniclastic sediments in one one distinct, coherent unit with gradational contacts between varying lithologies. Sequence of friable finely bedded ashes (2 - 3 cm thick). Thin organic rich, black shale partings (1 cm thick). Well cemented, indurated tuffaceous layers (approx. 25 cm). Some laminated siltstone layers, indurated and lighter in colour than the shale partings.
0.15m	ASH	Hard carbonated ash - only a few fragments appear chloritised. Buff carbonated spherules and some layered organic matter.
0.02m	SHALE	Soft black, organic rich shale.
0.04m	ASH	Well cemented ash, clasts 1 cm maximum, layer of variable width.
0.13m	SHALE	Finely laminated, dark shale.
0.1m	SHALE	Organic rich shale, showing soft sediment slumping at the thin end of the ash lens below. Only a little chert in these layers. Alternation of light and dark layers.
0.2m	TUFF	Chloritised tuff which is quite well cemented - clasts approx. 1 cm size. Thickness of the unit is quite variable - forms a lens of this tuff material.
0.16m	SHALE	Finely laminated shale with alternating light and dark layers
0.15m	TUFF	Friable tuff with lateral pinch and swell. Highly altered and poorly sorted.
0.48m	SHALE	Indurated black shale - possibly silicified - contains some spherules. Chert layers are between 5 - 10 mm thick and have been plastically deformed [THEORY - perhaps partially lithified chert was deposited on unlithified ash and

		slumping of the chert occurred, triggered by local tectonics]. Chert layers contain fewer spherules than surrounding shale. The horizon weathers a rusty orange colour and is cut by many calcite veins.
0.36m	TUFF	Friable, chloritised tuff - fragments commonly upto 3 cm size (larger fragments also found). Contains some buff coloured carbonate spherules (5 - 10 mm). Layer thins out laterally and to the north is cut by an internal low angle thrust - slumping occurs near this thrust.
0.22m	TUFF	Indurated, tuffaceous layer with irregular darker partings, particularly at the top of the layer. The layer seems to give fining upwards sequence. Also spherulitic.
0.03m	SHALE	Dark, organic rich shale parting, appears slickensided.
0.11m	TUFF	Indurated tuff in a layer which pinches and swells (15 cm maximum). Bed thins and becomes slickensided near a fracture to the north.
0.38m	SHALE	Weakly laminated shale with abundantspherules. Layer tends to pinch and swell (50 cm maximum). Interbedded chert occurs in the layered material, layers pinch out laterally and can slump internally. Some spherules in chert, thickest layer 3 cm. Hard tuffaceous material grading into tuffaceous shale. [Chert layers have been stretched, yeilding tension gashes].
0.05m	TUFF	Soft greenish tuff.
0.14m	SHALE	Hard shale with tuffaceous material, organic fragments and abundant spherulites. Patchy carbonate cement.
0.01m	SHALE	Thin tuffaceous shale.
0.1m	TUFF	Very hard carbonated tuff - also chloritised.
0.01m	SHALE	Dark shale parting - possibly organic rich.
0.04m	TUFF	Indurated tuffaceous material.
0.05m	SHALE	Shale with some tuffaceous material, thins to 1 cm laterally.
0.06m	TUFF	Coarse, green tuff with scattered spherules.
0.05m	SHALE	Tuffaceous shale with scattering of spherules.
0.1m	TUFF	Coarse, chloritised tuff with scattering of 5 - 15 mm sized, buff, carbonated spherules [bed pinches and swells laterally].
0.1m	SHALE	Tuffaceous shaley material with small carbonated spherules.

0.27m	MARKER HORIZON - FIRST SILICIFIED LAYER.	Laterally persistant, indurated layer, never of constant width, often interbedded with ash bands, often with wood fragments surrounded by algal material. Chert occurs as discontinuous bands and patches.
0.3m	ASH	Chloritised ash with many discontinuous shale partings. Shale forms approx. 1 cm (maximum) thick bands, possibly organic because of very dark colour. Where shale bands are broken slickensides can be seen on the broken surfaces.
0.09m	TREE	FUSAINISED tree trunk forms lens, coated by a few centimetres of calcareous algal material.
0.44m	ASH	Greenish grey coloured, poorly sorted volcanic ash with disrupted shale partings. Ash fragments, maximum size 1 cm and are sub-rounded.

APPENDIX D: ANALYTICAL PROCEDURES.

1. X-Ray Diffraction.

To prepare each sample for analyses, approximately 0.02-0.05g of the sample is taken and crushed finely, with a mortar and pestle, in a small volume of acetone. The sample slurry is poured onto a glass slide, coating it evenly, and once dried it can be placed in the XRD sample holder. The Phillips X-ray Diffractometer in the Geology Department at Glasgow is Co Kα.

The East Kirkton Limestone has a chemistry dominated by carbonate and silicate minerals. The XRD results reflect this i.e. the major peaks for minerals in each of the sampled rocks are calcite, quartz or, less commonly, dolomite/ankerite. Other minerals that feature on the XRD trace are chlorite/kaolinite, a mixed-layer clay of illite-smectite type (with a peak at 11Å), potassium feldspar and a little plagioclase. The feldspars only occur in small concentrations, and a small feldspar peak will be masked in many samples by the wide base of an intense quartz peak. Pyrite also occurs in most lithologies here, as was observed from pyrite separations for $\delta^{34}S$ isotopic analyses, but the position of the main XRD peak for pyrite is overlapped by one of the stronger ankerite/dolomite peaks and is consequently masked by this in most East Kirkton samples. No figures are given for pyrite from the XRD analyses and it is possible that feldspar may occur in some samples where a distinct peak was not observed.

2. X-Ray Fluorescence.

2.1 Major Element Analyses.

Samples were made into fused discs, according to the method of Harvey *et al.*, 1973; taking 0.3750g of dried sample, at 100mesh to be weighed and mixed with 2g of spectroflux 105, Q (containing lithium tetraborate, lithium carbonate and lanthanum oxide). This was heated in a furnace at 1000°C, in a lidded platinum crucible, for 25 minutes, re-mixed and re-heated on a bunsen burner to keep the sample fluid and ensure that sample and flux are thoroughly mixed. The mixture is then decanted onto a hot pewter platten (on a hotplate at 225°C) and pressed flat into the mould by a metal plunger. The plattens and resultant glass discs were

cooled slowly to prevent the samples from cracking, via a second hotplate (200°C) on which they were set between two, warmed, asbestos blocks for 10 minutes. The asbestos blocks, platten and sample were then removed from the second hotplate and left to cool at room temperature. The glass discs were placed in the sample holder of the Phillips PW1450/20 automatic X-ray fluorescence spectrometer for analysis.

The results are dominated by SiO_2 and CaO, the only elements that occur in concentrations greater than 10%, are Al_2O_3 for 3 samples (2,11&25 all of which are black shales) and FeO for two samples (2&25, black shales).

2.2 Ferrous Iron Determinations.

To determine the FeO contents of the samples 0.5g of rock powder (100/250mesh) from each sample was heated with a solution of 10ml of 50% sulphuric acid and 5ml of 40% hydrofluoric acid and added to 10ml of 50% sulphuric acid, 10ml of conc. orthophosphoric acid, 10g boric acid powder, 300ml deionised water and 10 drops of a 0.2% solution of sodium diphenlyamine sulphonate (as indicator). This was titrated with standard potassium dichromate solution, to a purple end point, the volume of KCr_2O_4 required to reach the end point, determines the relative quantities of FeO for each sample.

$$\%FeO = \frac{0.2 \times \text{vol. dichromate}}{\text{weight of sample}}$$

The percentage of Fe_2O_3 in the sample can then be calculated from the following ratio:-

$$Fe_2O_3 = \text{Fe total} - (FeO \times 1.1113)$$

The results for East Kirkton samples are predominantly high FeO and lower Fe_2O_3 (only sample 1, has higher Fe_2O_3 than FeO). Most of the mineral phases observed to be present, by XRD and petrographic study, tend to contain FeO rather than Fe_2O_3 so the relative proportions of iron, in these two oxidation states, was not unexpected.

2.3 Carbon Dioxide and Water Determinations.

The simultaneous determination of CO_2 and H_2O content of a powdered rock sample (100/250mesh) is carried out by gravimetric analyses. 0.5g of dried sample is weighed into a rectangular alumina boat, pre-heated to remove any moisture, then sample and boat are inserted into the combustion tube of a furnace at 1100-1200°C. Nitrogen is passed

through the combustion tube, to eliminate atmospheric H_2O and CO_2 from the system, and gas that is evolved from heating the rock sample is collected by two absorption tubes. The absorption tubes contain (1) anhydrous magnesium perchlorate, which absorbs water from the sample, the gas is then passed through saturated chromium trioxide in phosphoric acid to remove any sulphur dioxide that was present, and (2) CO_2 is absorbed by a tube of carbosorb (80% NaOH). Absorption tubes (1) & (2) are weighed before and after the sample is ignited, the increase in weight is proportional to the samples CO_2 and H_2O contents.

The analyses of H_2O and CO_2 gave results which were inconsistent and relatively inaccurate. This was due to (i) very high values for CO_2 (30-40%), and (ii) soot, that accumulated in the H_2O collecting tube, probably produced from oxidation of organic carbon, occurring in shaley samples in particular. Results are given where reasonable accuracy was obtained, but some analyses required to be repeated up to 10 times before concordant results were achieved.

2.4 Weight Loss from Sample Ignition.

The major element analyses can usefully be combined with results for loss on ignition (L.O.I.) analyses, indicating that significant quantities of vapour/gas is evolved during heating in sample preparation and will be lost to the total percentage analyses. This is quite important in samples such as these with high carbonate, relatively high organic carbon and water contents. About 1-1.5g of dried sample was weighed into a platinum crucible. Samples were left in a desiccator to cool, then each crucible and its contents were placed in a furnace at 1000°C for 1hour and 30 minutes. When the crucibles were removed from the furnace they were replaced in the desiccator and then reweighed when cool (several hours later). The resultant weight loss, or Loss On Ignition, is given as a percentage of the sample:-

$$\text{LOI \%} = \frac{\text{loss in weight} \times 100}{\text{sample weight.}}$$

East Kirkton samples give values between 10% and 45% for LOI, which are high, but not unusually so for limestones. LOI in these samples, is an expression of the carbonate content of each sample, including calcite and dolomite/ferroan dolomite. Only the clay-rich samples will contain significant amounts of water (from the mineral lattices), and from the results of H_2O determinations this could amount to some 7-8% of the samples, but these results may be exaggerated (soot

contamination in the collection tube). It is thought that the LOI value may also include the oxidation of some organic carbon, nitrates and possibly sulphates, but these volatile phases are insignificant compared to the carbonate contribution.

2.5 Minor Element Analyses.

Samples were powdered to 250mesh, dried, then 1g of each was weighed out and mixed with 6g of phenol formaldehyde resin (R. 0214/1), the resulting powder was pressed into a disc (pressure 25kbars) and baked in an oven at 60-70°C for 25 minutes. The discs of each sample were then placed, for analyses, in the sample holder of the Phillips PW1450/20 automatic X-Ray fluorescence spectrometer.

The most enriched minor element in the East Kirkton lithology was Sr, particularly in the shaley laminites, Group IV (up to 6300ppm). The black shales, Group II, are the samples which are generally most enriched, ie. most elements, except for Sr/Th/Zr. It also appears that the base of the sequence is generally more enriched than the top, but this trend is less well defined than the variation from one rock type to another.

Harvey, P. K., Taylor, D. M., Hendry, R. D. and Bancroft, F. 1973. An accurate fusion method for the analyses of rocks and chemically related materials by X-ray fluorescence spectrometry. *X-ray Spectrometry* **2**, pp33-44.

APPENDIX E: CORRECTION REQUIRED FOR Zr TRACE ELEMENT ANALYSES.

During the interpretation of data in Chapter 4, it was observed that the highest analyses' results for trace elements were obtained for Sr, Ba and Zr. When the East Kirkton trace element results were compared with the results from Bathgate basalts (Smedley, 1986), it was observed that Sr and Ba were high in both sets of results, but Zr was only high for the East Kirkton samples. There was a particularly good correlation between Sr and Zr for the East Kirkton samples; for which there seemed to be no apparent logical or mineralogical reason.

It is noted, for XRF analyses, that the Sr Kβ peak can overlap the position of the Zr Kα peak when very high results are obtained for Sr. It is considered that the Sr results for the East Kirkton samples fall into the category of very high Sr results (ranging from 763 - 6300 ppm), and therefore the Zr results will be strongly influenced by the Sr Kβ peak. The automatic corrections made for XRF results do not generally include a carbonate standard (in the Glasgow Department of Geology and Applied Geology), and do not, therefore, account for particularly high Strontium values. A slate standard is included in the automatic correction, and this may account for the lack of correlation for Sr/Zr in Group II shale samples (see figure 1), which also have the lowest carbonate contents.

It was decided to correct the Zr data, for Sr Kβ. This was calculated using the gradient, of the line of correlation, between Zr and Sr (see figure 1 and table 1). The results of this recalculation of Zr results are given in table 1 and the Zr versus Sr graph is replotted and shown in figure 2. It is the recalculated data that has been used in the interpretation of XRF results found in Chapter 4.

Sample No.	Sr value (ppm)	x 0.0333	Zr value (ppm)	Zr (corr.)	Zr (ppm)
1	5131	171.0	102	-69.0	0
2	1365	45.5	127	81.5	82
3	3081	102.7	142	39.3	39
4	3887	129.6	153	23.4	23
5	6300	210.0	143	-67.0	0
6	2991	99.7	102	2.3	2
7	4432	147.7	164	16.3	16
8	3339	111.3	103	-8.3	0
9	2548	84.9	89	4.1	4
10	3591	119.7	233	113.3	113
11	2477	82.6	228	145.4	145
12	906	30.2	106	75.8	76
13	1108	36.9	29	-7.9	0
14	763	25.4	20	-5.4	0
15	2030	67.7	80	12.33	12
16	1525	50.8	46	-4.8	0
17	3270	109.0	114	5.0	5
18	2110	70.3	114	43.7	44
19	2041	68.0	39	-29.0	0
20	2228	74.3	52	-22.3	0
21	4190	139.7	136	-3.67	0
22	3834	127.8	129	1.2	1
23	1527	50.9	56	5.1	5
24	3941	131.4	161	29.6	30
25	1313	43.8	235	191.2	191
26	2582	86.1	110	23.9	24
27	2267	75.6	90	14.4	14
28	2271	75.7	51	-24.7	0
29	1350	45.0	30	-15.0	0
30	1138	37.9	35	-2.9	0
31	796	26.5	16	-10.5	0

Example of correction calculation.

Gradient of the line = 3000/100

correction factor = 3000/100 x 1/Sr
correction factor = 0.0333

Sample 1, Sr = 5131

5131 x 0.0333 = 171.0

Sample 1, Zr = 102

102 - 171.0 = -69.0

Therefore, for sample 1, the Zr result was below the detection limit of the XRF.

GEOPHYSICAL SURVEYS OF THE EAST KIRKTON LIMESTONE, LOWER CARBONIFEROUS, WEST LOTHIAN, SCOTLAND.

J. J. Doody, R. A. R. McGill, D. Darby and D. K. Smythe

Department of Geology & Applied Geology, University of Glasgow, Glasgow, G12 8QQ.

ABSTRACT.

Magnetic and resistivity geophysical surveys conducted across the only known exposure of the East Kirkton Limestone have produced new information upon its extent. This is important to determine because of its unique faunal assemblage and possible hot spring deposition, suggesting a potential for precious metal mineralisation. Magnetic anomalies are attributed to basalts within the Bathgate Hills Volcanic Formation. Modelling of the magnetic data demonstrates a general dip to the west of about 25°, and the presence of significant local faulting. Modelling of vertical electrical sounding data shows the East Kirkton sequence (the limestone and associated beds) to be a low resistivity layer within the more highly resistive volcanic sequence. The East Kirkton sequence is seen to deepen to the west, and also to the north probably by faulting. Therefore the present exposure is the only near surface occurrence of the East Kirkton Limestone locally, but within the area of the survey no lateral limits to the formation are observed.

KEY WORDS: Geophysics, hot springs, magnetic surveys, mineralisation, resistivity surveys, Visean.

The East Kirkton quarry at Bathgate (Fig. 1) is the only known exposure of the Lower Carboniferous East Kirkton Limestone, which occurs within the Bathgate Hills Volcanic Formation as part of a *ca.* 15 m thick largely sedimentary sequence observed within the quarry. Lithostratigraphically the East Kirkton sequence (EKS) can be divided broadly into three beds: the East Kirkton Limestone, forming over 50% of the sequence, overlain by the Little Cliff Shale and Geikie Tuff. Full details of the stratigraphy and location of the East Kirkton Limestone are given by Rolfe *et al.* (this volume). Overall, the sequence is a varied succession of thin, interbedded, lacustrine limestones, shales, sandstones, ironstones

and tuffs, thought to have formed in a hot spring environment (eg Hibbert 1836, Muir & Walton 1957). Current opinion is divided regarding the amount of geothermal input to the East Kirkton water body (McGill *et al.* 1993, Walkden *et al.* 1993).

Bedding planes seen at outcrop dip at 15-25° to the W. Various hypotheses exist regarding the extent of the East Kirkton Limestone beyond the quarry: (i) it continues N beneath a thin glacial cover as shown on the one-inch geological map (Scotland Sheet 31); (ii) subcrop to the N is limited due to faulting at the N end of the known exposure (Stephenson & Monro 1986); or (iii) the sequence was deposited in an isolated lagoon forming only a small lens of sediment (Geikie 1861).

Geophysical surveys were undertaken to determine the structure and extent of the EKS in the vicinity of the quarry. Exploration was undertaken mostly W (down dip) and to the N. Housing development prevented work to the S. The results are of use in future prospecting of the East Kirkton Limestone or precious metal mineralisation (Stephenson *et al.* 1983), or with regard to its rare fossil assemblage (Rolfe *et al.* 1990).

1. GEOPHYSICAL APPROACH.

Our aim was to determine the subsurface structure of the EKS using the East Kirkton quarry as a reference point. Given the presence of basaltic lavas and clastic volcanics above and below the sedimentary sequence, it was anticipated that there would be a strong contrast of magnetic and electrical resistivity properties between the EKS and volcanics. Borehole information was made available by the National Museums of Scotland, permitting calibration of the geophysical results but only to rather limited depths (typically 10 m, maximum 33 m).

2. MAGNETOMETER SURVEY.

The total magnetic field intensity was measured along 12 E-W traverses across the quarry and its projected continuation along strike to the N. The contoured results are plotted in Fig. 2. Large magnetic anomalies in the W of the survey area can be correlated with basalts at outcrop, and in the NE with a quartz dolerite sill. Low anomaly values are obtained within the East Kirkton quarry and to the N of the quarry, where

the anomaly trend coincides with the N-S strike of the strata. Although this suggests that the EKS may continue to the N at very shallow depth, it is absent from the line of boreholes GC3-6 (Fig. 3). A localised, high anomaly occurs immediately W of the quarry. This correlates with the basalt seen immediately above the EKS, but the limited extent of the anomaly suggests that there is local structure affecting the basalt.

Magnetic susceptibility measurements of borehole samples (Fig. 4) indicate that the largest susceptibility contrast is between basalt and other lithologies. Thus the distribution of basalts is the major control upon the local magnetic field. Remanent magnetisation of the highly magnetic basalts was measured; it showed a very low angle inclination. This would be expected for Lower Carboniferous lavas extruded in equatorial latitudes.

Using these values, a model profile across the East Kirkton quarry was determined using the GRAVMAG computer program. The model was constructed along line Z, a dip line crossing the anomaly immediately W of the quarry (Fig. 2) and passing near to BH1 (Fig. 3). The model (Fig. 5) shows two basaltic horizons. The upper one is the unit seen at outcrop W of the road. The lower one (7m thick) immediately overlies the EKS and is downfaulted by at least 7m near to the W side of the quarry. Other horizons cannot be distinguished magnetically. These results clearly demonstrate a general dip to the W of about 25°, and the presence of significant local faulting.

The one-inch geological map shows the EKS to be underlain by basalts (Fig. 1), which would be expected to generate a significant anomaly near to the subcrop of their contact with the EKS to the E of the quarry. This anomaly is clearly absent from our magnetic data (Fig. 2). We conclude that either the rocks beneath the EKS are not basalts but perhaps clastic volcanics, or that these basalts have lost their magnetic properties perhaps due to hydrothermal alteration. Our dataset does not permit us to distinguish between such models.

3. RESISTIVITY SURVEY.

Four electrical resistivity vertical soundings were conducted using expanding Wenner arrays (VES1-VES3 of Fig. 3) and an Offset Wenner array (VES4). Maximum electrode spacings were 40, 100, 64 and 64 m respectively. Computer modelling was undertaken for each sounding, assuming a 1-dimensional variation of ground electrical properties. Each

model is attributed to the centre point of the array. The field data and results of VES1 are shown in Fig. 6 to illustrate our data and the goodness of fit obtained in the modelling procedures. The models of all four soundings are shown in Fig. 7. A constant separation traverse (points 1 to 6 on Fig. 3) was carried out to determine changes in depth to the N of the quarry.

Resistivity of rock ranges over several orders of magnitude and is one of the most variable of rock physical properties. Most rock-forming minerals are insulators and electrical current is mainly carried through rock by the passage of ions in pore waters. Therefore porosity is the main control of resistivity, which generally increases as porosity decreases. Crystalline rocks may be conductive to some extent due to water-filled cracks and fissures. Identification of lithology is not possible on the basis of resistivity data alone, correlation with outcrop and/or boreholes is required.

At East Kirkton we attribute generally low, but highly variable, resistivities modelled at surface to soils and/or boulder clay. At depth the main resistivity contrast was expected to be between the highly resistive volcanics of the Bathgate Hills Volcanic Formation and the low resistivity of the mixed sedimentary EKS. Resistivities of much less than 100 ohm-m modelled at depth can be correlated with the EKS. High resistivities (480 ohm-m) above the EKS on VES1 and VES2 are correlated with the lower of the two basalts of the magnetic model. High resistivities (typically over 400 ohm-m) beneath the EKS are consistent with the presence of volcanic rocks. Fig. 7 is an attempt to correlate the results of VES1 to VES4. The lithological interpretations are based on modelled resistivity values and correlation with boreholes and the magnetic results. The correlation of units is entirely reasonable, particularly the contrast of the EKS and adjacent volcanic units. However, the assignment of lithologies to near surface layers and within the volcanics above the EKS must be treated with caution given the variability of resistivity values (see above).

The following points arise from the resistivity results:

1. Comparison of VES1 and VES2 confirms the significant westward deepening of the EKS shown by the magnetic interpretation.
2. VES1, VES3 and VES4 are located broadly along strike from each other, but show the sub-EKS volcanics to deepen northwards. This was confirmed by the constant separation traverse. Thus the EKS may thicken. The resolution of the resistivity data does not permit us to distinguish between a northward deepening due to folding or faulting.

4. DISCUSSION.

The geophysical techniques used have produced models of subsurface structure at East Kirkton based upon different rock physical properties. The resistivity survey has shown the EKS to be a low resistivity unit between volcanic units of higher resistivity. The magnetometer survey has provided a model of basalts within the overall sequence. Both techniques show the EKS to deepen to the SW. The magnetic model (Fig. 5) shows this deepening to be a function of dip. However, significant local structure is superimposed on this general trend.

The modelled E-W magnetic profile crosses the local anomaly immediately W of the quarry. A fault is modelled near to the W edge of this anomaly and it is suggested that the N edge of the anomaly is also associated with faulting, especially since the EKL also appears to be displaced at this point. Borehole BH2, drilled close to the NW edge of the quarry (Fig. 3), does not penetrate basalt. Good exposure of the base of the quarry sequence, at its northern end, indicates no displacement although it is possible that quarrying has assisted natural erosion processes and removed the basalt capping the succession; backfilling obscures these exposures.

Comparison of the magnetic and resistivity results regarding units below the EKS is revealing. High resistivity values are consistent with the basalt lavas shown on the one-inch geological map to underlie the EKS and subcrop to the E of the quarry. However, the absence of an associated magnetic signature indicates that either these lavas are no longer magnetic or that clastic volcanics underlie the EKS. Therefore we use the general term 'volcanics' for this unit on Fig. 7.

The resistivity modelling of the sub-EKS unit is also significant since it not only shows the top of the unit to deepen SW as expected, but also that its top (and so the base of the EKS) becomes deeper towards the N. The presence of local faulting seen at outcrop and in the magnetic model suggest that this deepening may be due to faulting.

It is seen to continue to the W and N, deepening and possibly thickening in both directions. Therefore, regarding the hypotheses outlined in our introduction, it would appear that locally the EKS occurs at surface only at the quarry, that Geikie's localised model is refuted at the scale of the survey, and that deepening to the N of the EKS could be fault

controlled. The presence of such faults could be an important factor in any precious metal mineralisation.

5. ACKNOWLEDGEMENTS.

This survey formed part of RARM's PhD research on the geochemistry and petrography of the East Kirkton Limestone, supervised by Dr. Allan Hall and Dr. Ian Rolfe. Both are thanked for discussions of these surveys. We are grateful for field assistance by a number of people including Peter Chung, Joe Crummy, Roger Hall, Chris McKeown and Susan Waldron. West Lothian District Council is thanked for access to the East Kirkton quarry. The staff from the National Museums of Scotland were most helpful with the provision of core samples and logged data from boreholes BH1-3 and GC1-6. Doyle Watts is thanked for assistance with magnetic susceptibility and remanent magnetisation measurements and for valuable discussion. We also thank Bob Cumberland and Sheila Hall for help with the figures.

6. BIBLIOGRAPHY.

Geikie, A. 1861. *In* Howell, H.H. & Geikie, A. (eds) *The geology of the neighbourhood of Edinburgh*: MEM GEOL SURV UK.

Hibbert, S. 1836. On the freshwater limestone of the Burdiehouse. TRANS SOC EDINBURGH, **13**, 169-182.

McGill, R.A.R., Hall, A.J. & Fallick, A.E. 1993. The East Kirkton palaeoenvironment: stable isotope evidence from silicates and sulphides. TRANS R SOC EDINBURGH EARTH SCI [this vol.]

Muir, R.O. & Walton, E.K. 1957. The East Kirkton Limestone. TRANS GEOL SOC GLASGOW, **12**, 157-168.

Rolfe, W.D.I., Durant, G.P., Fallick, A.E., Hall, A.J., Large, D.J., Scott, A.C., Smithson, T.R. & Walkden, G.M. 1990. An early terrestrial biota preserved by Visean vulcanicity in Scotland. *In* Lockley, M.G. & Rice, A. (eds). *Volcanism and fossil biotas,*, 13-24, GEOL SOC AM SPEC PAPER, **244**.

Rolfe, W.D.I., Durant, G.P., Baird, W.J., Chaplin, C., Paton, R.L. & Reekie, R.J. 1993. The East Kirkton Limestone, Lower Carboniferous, West Lothian, Scotland: introduction and stratigraphy. TRANS R SOC EDINBURGH EARTH SCI [this vol.]

Stephenson, D., Fortey, N.J. & Gallagher, M.J. 1983. Polymetallic mineralisation in Carboniferous rocks at Hilderston, near Bathgate, central Scotland. *Mineral Reconnaissance Programme Rep Inst Geol Sci*, 68.

Stephenson, D. & Monro, S.K. 1986. Bathgate Hills. *In* McAdam, A.D. & Clarkson, E. N. K., (eds.) *Lothian Geology: an excursion guide*, Edinburgh: Scottish Academic Press, 208-216.

Walkden, G., Irwin, R. & Fallick, A. 1993. Carbonate spherules and botryoids as lake floor sediments. TRANS R SOC EDINBURGH EARTH SCI [this vol.]

FIGURE CAPTIONS

Figure 1, Geological map of the East Kirkton quarry locality based on Scotland Sheet 31. EKL = non-marine East Kirkton Limestone; WKL = marine West Kirkton Limestone.

Figure 2, Detailed magnetic survey of the East Kirkton quarry locality. Data are contoured total magnetic field values in nT. Survey lines are indicated. Note that excavations at the Water Board Site exposed basaltic lavas.

Figure 3, Map of the resistivity profiles and boreholes used in this survey. VES1-4 are vertical electrical sounding profiles; the line marked 1-6 is a constant separation traverse profile. Boreholes are shown by labelled dots.

Figure 4, Magnetic susceptibility results for local lithologies determined from indicated boreholes. Note the logarithmic horizontal scale which is in SI units of susceptibility. Lst = Limestone. See Fig. 3 for location of boreholes.

Figure 5, Magnetic modelling results for survey line Z (see Fig. 2 for locality). Upper figure shows the observed and calculated profiles. The latter was computed from the model in the lower figure. Origin of the distance scale is at the W end of line Z (Fig. 2); the model profile is extended further W to include the upper basalt in the model. Both basalt horizons have a downward-pointing total magnetisation. The fault inferred at 90 m along the profile has the minimum throw required to account for the observed anomaly.

Figure 6, Comparison of the field data (crosses) of vertical electrical sounding profile VES1 (see Fig. 3) and final computed model curve (asterisks). The model is shown in the inset: depth in m, resistivities in ohm-m. EKS = East Kirkton sequence; Volc = Volcanics.

Figure 7, Correlation of the 1-dimensional depth models derived from the vertical electrical sounding profiles. Note: VES1 was sited immediately west of the East Kirkton quarry (see Fig. 3); boreholes GC5 and GC6, both located in the vicinity of VES3 and VES4, show a clay to weathered ash/tuff transition at depths of 5-10 m. EKS = East Kirkton sequence; Volc = Volcanics.

Figure 1

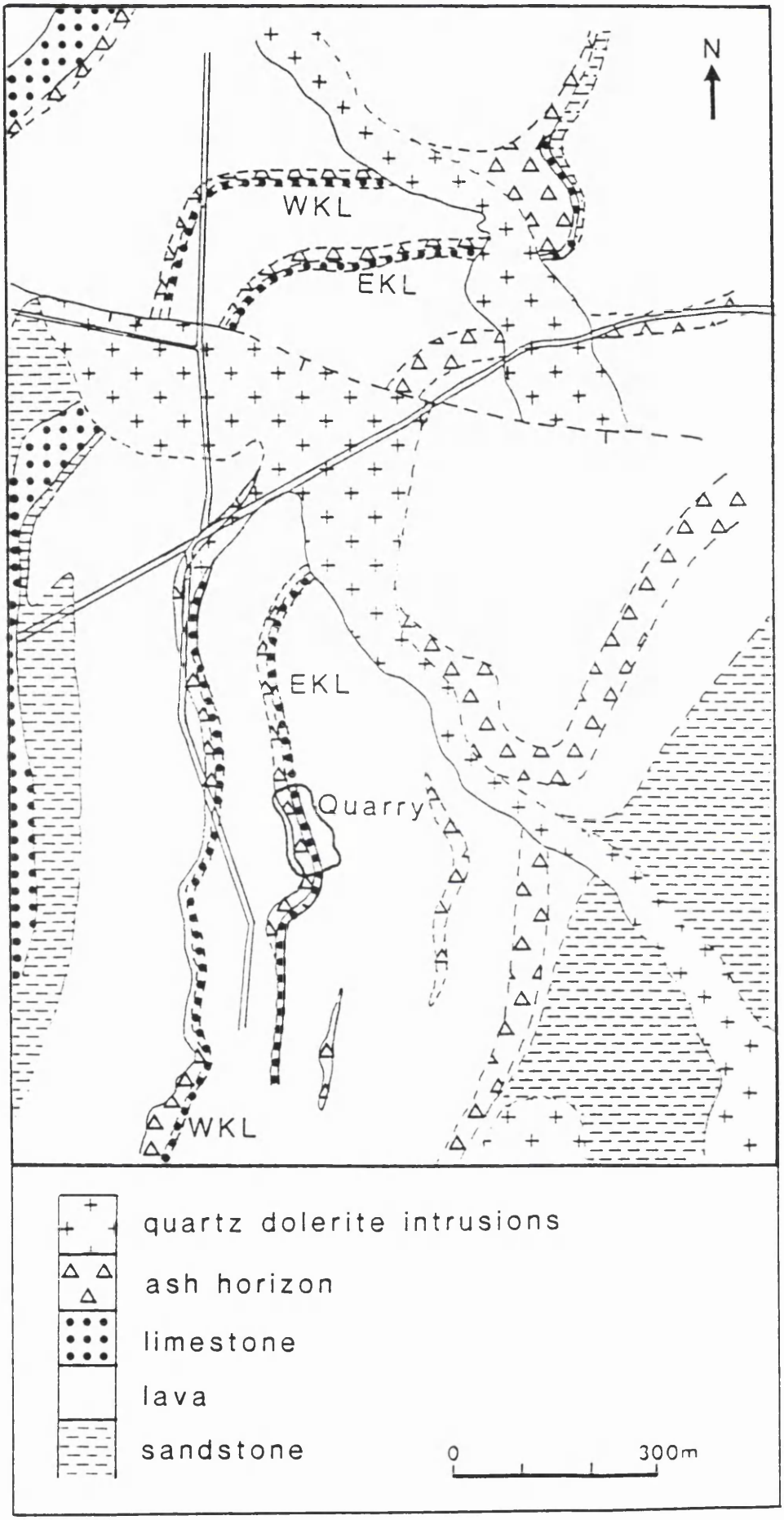
N
WKL
EKL
EKL
Quarry
WKL
quartz dolerite intrusions
ash horizon
limestone
lava
sandstone
0
300m

Figure 2

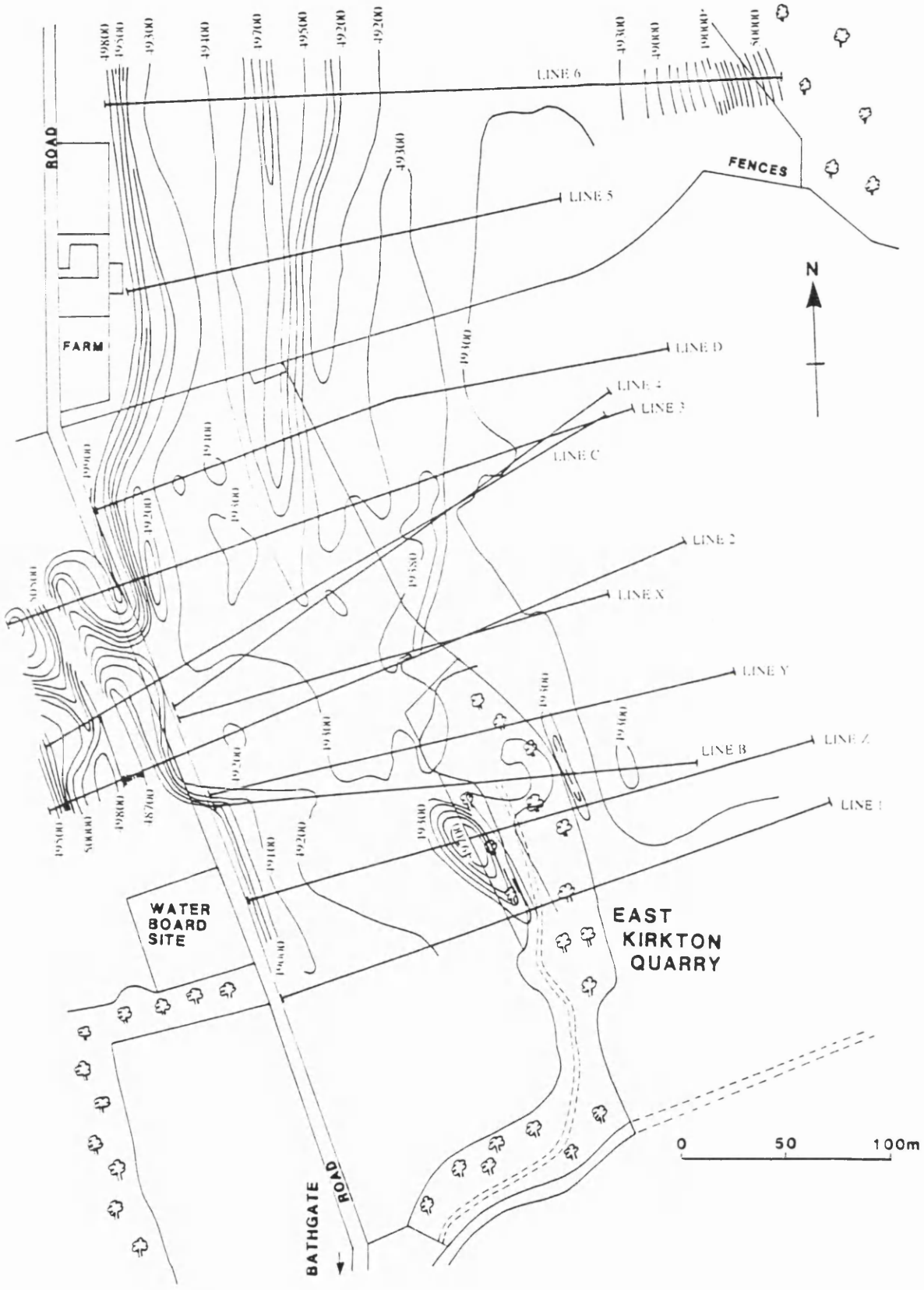
LINE 6
LINE 5
LINE D
LINE 4
LINE 3
LINE C
LINE 2
LINE X
LINE Y
LINE B
LINE Z
LINE 1
ROAD
FARM
FENCES
N
WATER BOARD SITE
EAST KIRKTON QUARRY
BATHGATE ROAD
0
50
100m

Figure 3

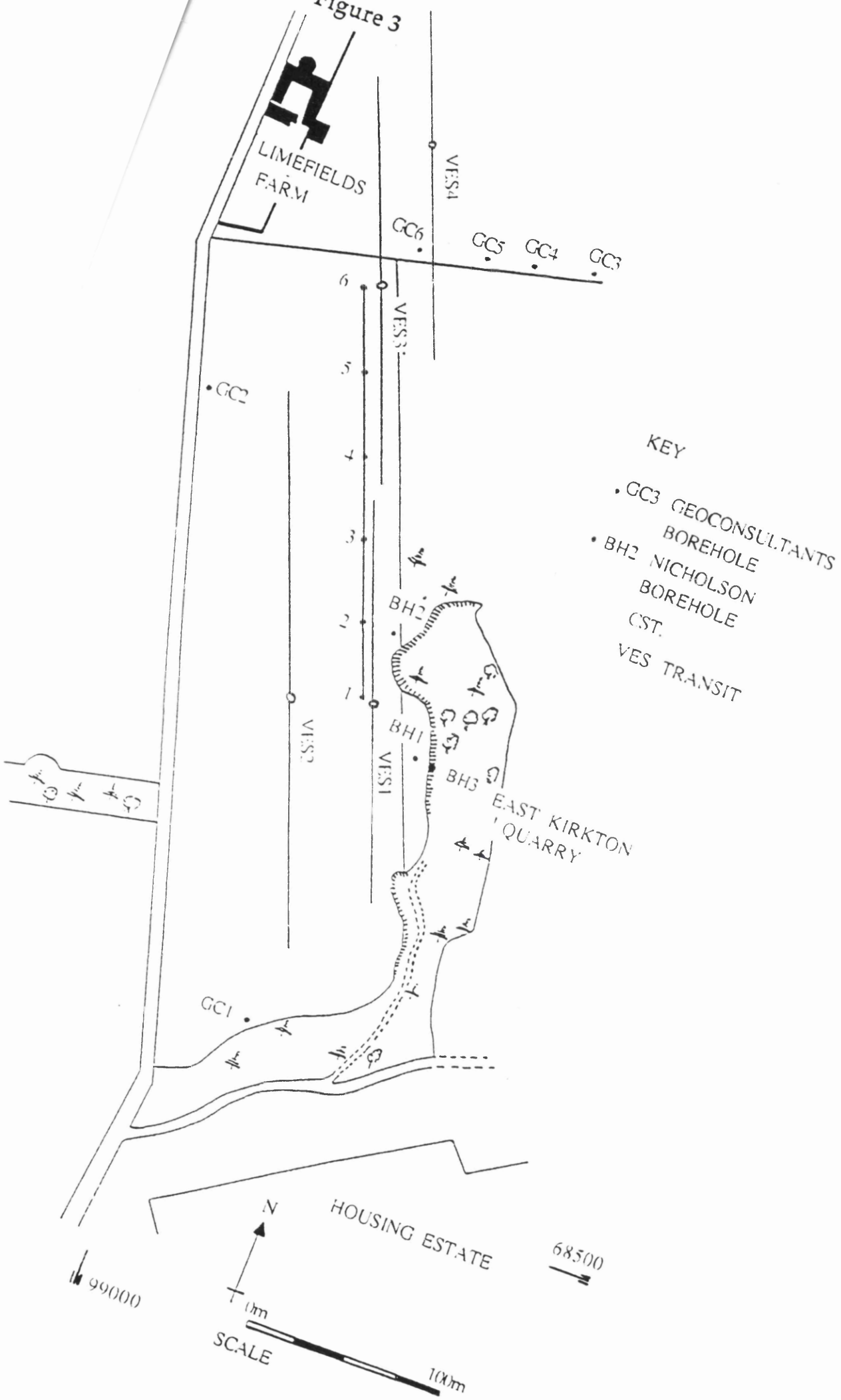
LIMEFIELDS FARM
VES4
GC6
GC5
GC4
GC3
6
VES3
5
GC2
4
3
BH2
2
1
BH1
VES2
VES1
BH3
EAST KIRKTON QUARRY
GC1
N
HOUSING ESTATE
99000
68500
0m
SCALE
100m
KEY
GC3 GEOCONSULTANTS BOREHOLE
BH2 NICHOLSON BOREHOLE
CST.
VES TRANSIT

Figure 4

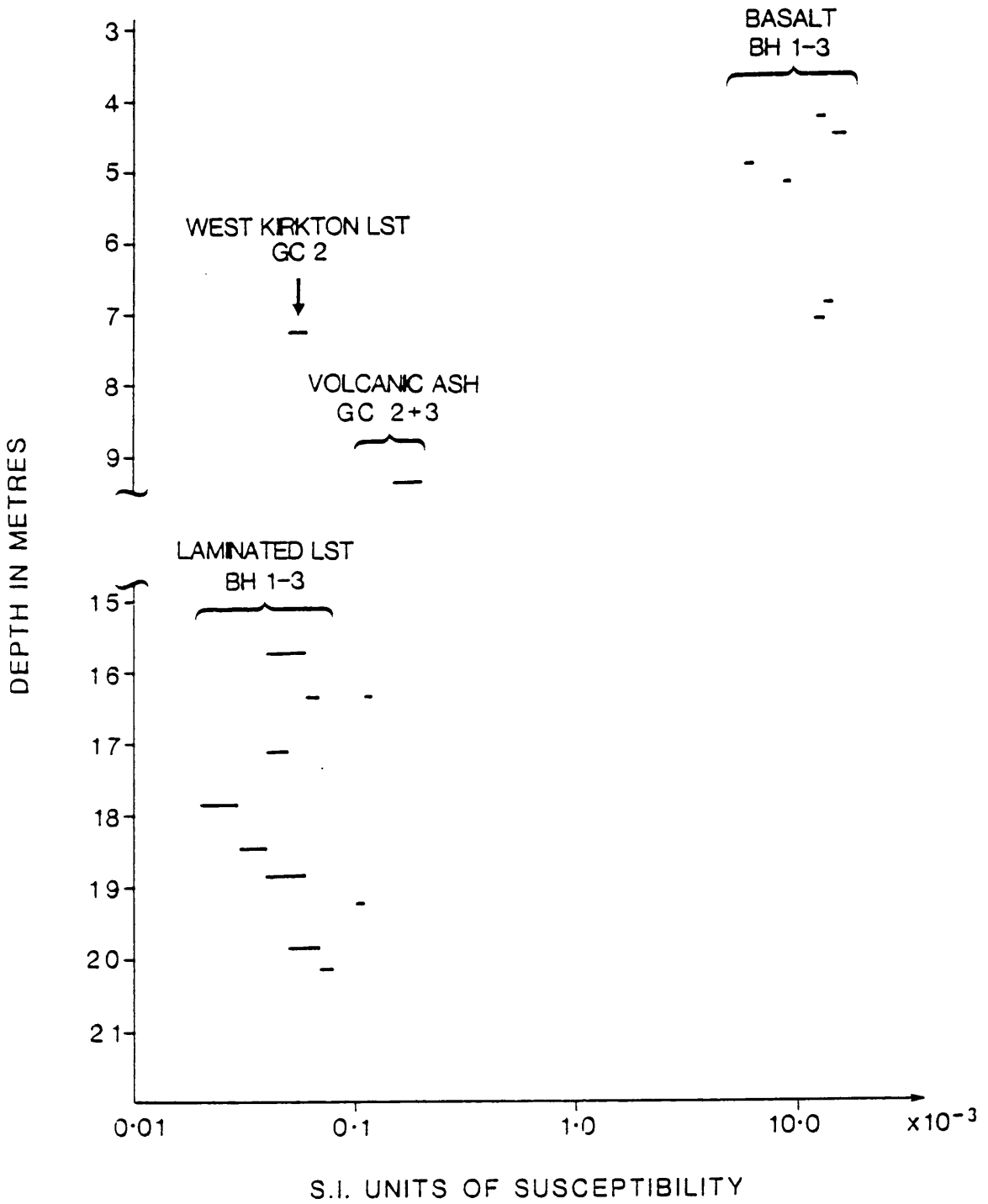
BASALT
BH 1-3
WEST KIRKTON LST
GC 2
VOLCANIC ASH
GC 2+3
LAMINATED LST
BH 1-3
DEPTH IN METRES
3
4
5
6
7
8
9
15
16
17
18
19
20
21
0·01
0·1
1·0
10·0
x10⁻³
S.I. UNITS OF SUSCEPTIBILITY

Figure 5

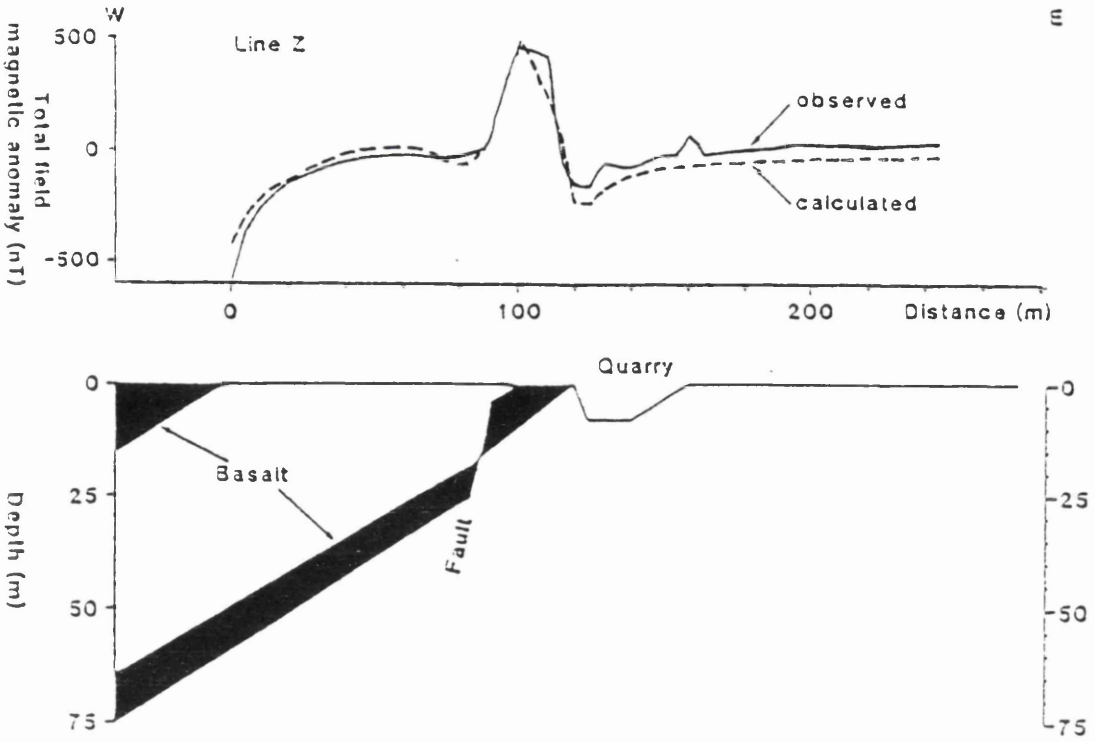

Figure 6

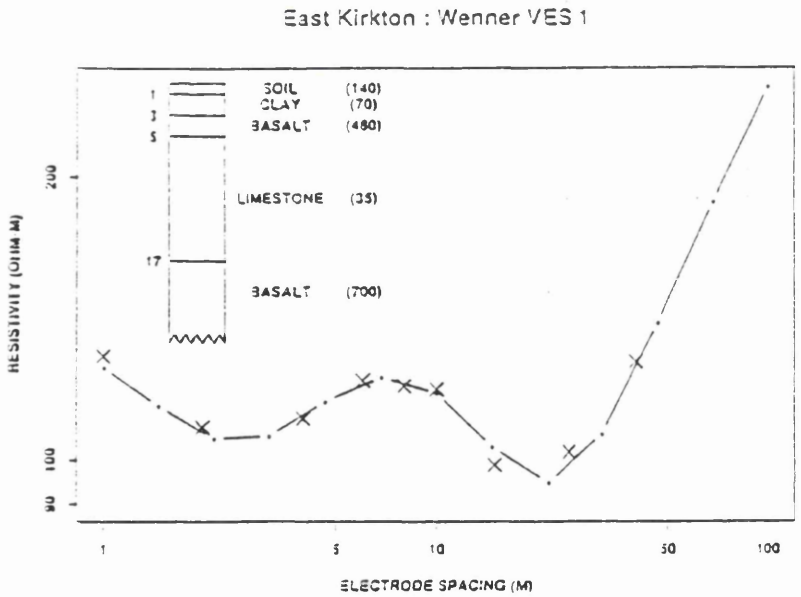

Figure 7

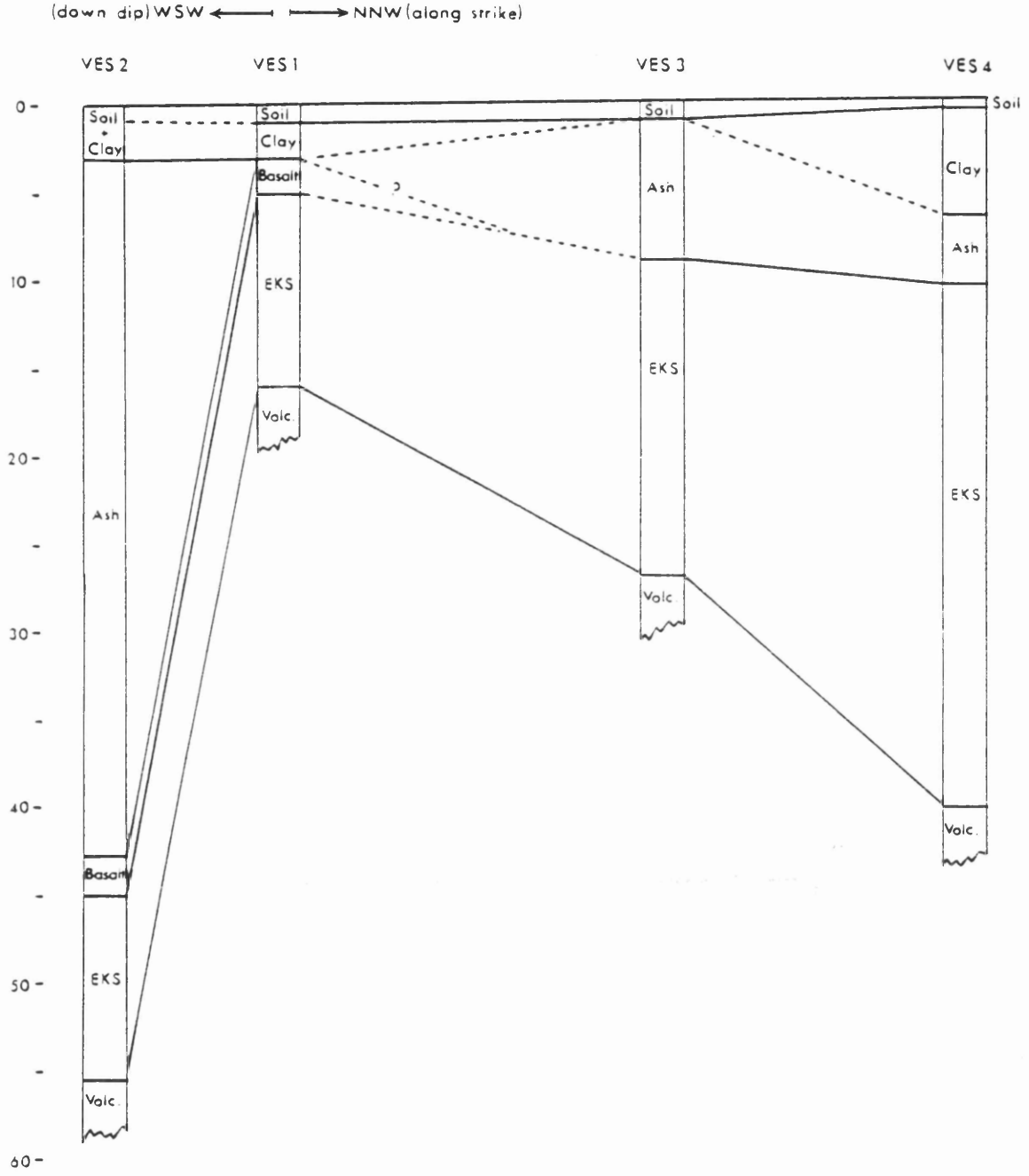

GLASGOW UNIVERSITY LIBRARY